

**DEVELOPMENT OF A MULTIPLEX PCR DETECTION SYSTEM  
AND IDENTIFICATION OF BINDING PEPTIDES  
FOR HUMAN *PLASMODIUM* SPECIES**

**CHEW CHING HOONG**

**FACULTY OF MEDICINE  
UNIVERSITY OF MALAYA  
KUALA LUMPUR**

**2014**

**DEVELOPMENT OF A MULTIPLEX PCR DETECTION SYSTEM  
AND IDENTIFICATION OF BINDING PEPTIDES  
FOR HUMAN *PLASMODIUM* SPECIES**

**CHEW CHING HOONG**

**THESIS SUBMITTED IN FULFILLMENT  
OF THE REQUIREMENTS FOR  
THE DEGREE OF DOCTOR OF PHILOSOPHY**

**FACULTY OF MEDICINE  
UNIVERSITY OF MALAYA  
KUALA LUMPUR**

**2014**

# UNIVERSITI MALAYA

## ORIGINAL LITERARY WORK DECLARATION

Name of Candidate: CHEW CHING HOONG (I.C/Passport No: 800406-11-5170 )

Registration/Matric No: MHA 080016

Name of Degree: DOCTOR OF PHILOSOPHY

Title of Project Paper/Research Report/Dissertation/Thesis ("this Work"):

DEVELOPMENT OF A MULTIPLEX PCR DETECTION SYSTEM AND IDENTIFICATION OF  
BINDING PEPTIDES FOR HUMAN *PLASMODIUM* SPECIES

Field of Study: MOLECULAR PARASITOLOGY

I do solemnly and sincerely declare that:

- (1) I am the sole author/writer of this Work;
- (2) This Work is original;
- (3) Any use of any work in which copyright exists was done by way of fair dealing and for permitted purposes and any excerpt or extract from, or reference to or reproduction of any copyright work has been disclosed expressly and sufficiently and the title of the Work and its authorship have been acknowledged in this Work;
- (4) I do not have any actual knowledge nor do I ought reasonably to know that the making of this work constitutes an infringement of any copyright work;
- (5) I hereby assign all and every rights in the copyright to this Work to the University of Malaya ("UM"), who henceforth shall be owner of the copyright in this Work and that any reproduction or use in any form or by any means whatsoever is prohibited without the written consent of UM having been first had and obtained;
- (6) I am fully aware that if in the course of making this Work I have infringed any copyright whether intentionally or otherwise, I may be subject to legal action or any other action as may be determined by UM.

Candidate's Signature

Date 21-01-2014



Subscribed and solemnly declared before,



Witness's Signature

Date 21-01-2014

Name: CHUA KEK HENG

Designation: PROFESSOR DR.

**ABSTRACT**

Malaria is one of the most serious global health challenges. Approximately 3.3 billion people live in malaria-endemic areas and the disease threatens the lives of more than one-third of the world's population. Malaria is caused by an eukaryotic protozoa *Plasmodium* and transmitted through the bite of female *Anopheles* mosquito. The known causative agents of human malaria include *Plasmodium vivax*, *P. falciparum*, *P. malariae*, *P. ovale*, and recently included *P. knowlesi* which is recognized as a zoonotic parasite. Malaria is a treatable disease, however the disease can become severe, leading to morbidity if untreated, especially for infections by two potential fatal species, i.e., *P. falciparum* and *P. knowlesi*. In the effort to improve the global health status, institution of control and surveillance of malaria, and subsequently enhancing the effectiveness of treatment management, it is critical to develop a rapid, accurate, species-specific/species-sensitive, and cost-efficient diagnostic tool for malaria detection. Therefore, a straightforward single-step multiplex polymerase chain reaction (PCR) targeting five human *Plasmodium* 18S small subunit ribosomal RNA (ssu rRNA) gene with an internal positive control was developed. This system is specific in detecting all five human malaria parasites with high sensitivity (i.e., 0.025 parasites/ $\mu$ l for *P. vivax*, 0.027 parasites/ $\mu$ l for *P. ovale*, 0.15 parasites/ $\mu$ l for *P. falciparum*, 0.25 parasites/ $\mu$ l for *P. knowlesi*, and 0.27 parasites/ $\mu$ l for *P. malariae*), and most significantly enables the simultaneous identification and differentiation of mixed infections at least up to the two-species level without any diagnostic constrains. In addition, the accuracy (sensitivity and specificity) of the detection system were also assured by random blind testing (n=50), clinical screening (n=246), and simulated mixed infections based on clinical samples (n=30) and clone DNA (n=60). All results were in agreement with the results from nested PCR which served as a molecular gold standard. Overall, this

multiplex system will definitely enhance the accuracy and accelerate the speed in the malaria diagnosis, and improve the efficacy of malaria treatment and control.

*Plasmodium* is an obligate intracellular parasite. Therefore, the understanding of how the parasites enter their host's cell is of great interest and this offers an attractive target for the development of novel therapeutics. Apical membrane antigen 1 (AMA1) is the most prominent and well characterized malarial surface antigen that is essential for parasite-host cell invasion, i.e., sporozoite into hepatocyte in liver stage and merozoite into erythrocyte in asexual stage. AMA1 has long served as a potent antimalarial drug target and pivotal vaccine candidate. In the present study, recombinant AMA1 proteins of *P. knowlesi* (rPkAMA1) as well as *P. vivax* (rPvAMA1) were expressed using *Escherichia coli* and the binding peptides were identified using a random dodecapeptide phage display library. Phage display is a powerful and cost-effective tool that can be used for assessing the protein-protein interactions. After third rounds of biopanning, two and three phage-displayed binding peptides with affinity to rPkAMA1 and rPvAMA1 respectively were identified and validated through peptide binding assays.

**ABSTRAK**

Malaria merupakan salah satu cabaran kesihatan global yang serius. Terdapat kira-kira 3.3 bilion orang menetap di kawasan endemik-malaria dan penyakit ini mengancam nyawa lebih daripada satu pertiga penduduk sedunia. Jangkitan malaria disebabkan oleh protozoa eukariotik *Plasmodium* dan ditularkan melalui gigitan nyamuk *Anopheles* betina. Agen-agen penyebab malaria manusia termasuk *Plasmodium vivax*, *P. falciparum*, *P. malariae*, *P. ovale* dan termasuk *P. knowlesi* yang diiktirafkan sebagai parasit zoonotik. Malaria adalah penyakit yang boleh dirawat, namun penyakit ini boleh menjadi teruk dan membawa morbiditi jika tidak dirawat, terutamanya bagi jangkitan oleh dua spesies yang berpotensi membawa maut, iaitu, *P. falciparum* dan *P. knowlesi*. Dalam usaha untuk meningkatkan status kesihatan global, institusi kawalan dan surveilans malaria, dan seterusnya peningkatan keberkesanan pengurusan rawatan, adalah kritikal untuk membangunkan alat diagnostik yang cepat, tepat, spesies-spesifik/spesies-sensitif, dan menjimatkan kos untuk pengesanan malaria. Oleh itu, PCR multipleks jelas satu langkah mensasarkan lima jenis gen 18S RNA ribosom subunit kecil (ssu rRNA) bagi *Plasmodium* manusia dengan satu kawalan positif dalaman telah dibangunkan. Sistem ini khusus untuk mengesan kesemua lima parasit malaria manusia dengan tahap sensitiviti yang tinggi (i.e., 0.025 parasit/ $\mu$ l untuk *P. vivax*, 0.027 parasit/ $\mu$ l untuk *P. ovale*, 0.15 parasit/ $\mu$ l untuk *P. falciparum*, 0.25 parasit/ $\mu$ l untuk *P. knowlesi*, dan 0.27 parasit/ $\mu$ l untuk *P. malariae*), dan paling ketara sekali membolehkan pengenalan dan pembezaan serentak jangkitan campuran sekurang-kurangnya sehingga ke tahap dua-spesies tanpa sekatan diagnostik. Di samping itu, ketepatan (sensitiviti dan spesifisiti) sistem pengesanan juga dijamin oleh ujian rawak buta (n=50), pemeriksaan klinikal (n=246), dan jangkitan campuran simulasi berdasarkan sampel klinikal (n=30) dan klon DNA (n=60). Kesemua keputusan adalah selaras dengan keputusan daripada PCR bersarang sebagai piawaian emas molekul. Keseluruhan, sistem multipleks ini

pasti akan meningkatkan ketepatan dan mempercepat jangkamasa diagnosis malaria, dan meningkatkan keberkesanan rawatan dan kawalan malaria.

*Plasmodium* adalah parasit intrasel obligat dan pemahaman tentang bagaimana parasit ini memasuki sel hos mereka menjadi tumpuan kerana ini menawarkan sasaran menarik bagi pembangunan terapeutik novel. Antigen membran apikal 1 (AMA1) adalah antigen permukaan malaria yang paling menonjol dan memainkan peranan penting bagi parasit memasuki sel hos, iaitu sporozoite ke dalam hepatosit di peringkat hati dan merozoite ke dalam eritosit di peringkat aseksual. AMA1 sudah lama dikenali sebagai sasaran tumpuan ubat antimalaria dan calon vaksin terpenting. Dalam kajian ini, protein AMA1 rekombinan bagi *P. knowlesi* (rPkAMA1) serta *P. vivax* (rPvAMA1) telah dihasilkan dengan menggunakan *Escherichia coli* dan peptida-peptida mengikat telah dikenal pasti dengan menggunakan perpustakaan paparan faj dodekapeptida. Faj paparan adalah suatu alat berkesan dan berkos efektif yang boleh digunakan untuk menilai interaksi protein-protein. Selepas pusingan ketiga biopanning, dua dan tiga faj-paparan peptida mengikat kepada rPkAMA1 dan rPvAMA1 telah masing-masing dikenal pasti dan disahkan melalui ujian-ujian mengikat peptida.

## ACKNOWLEDGEMENTS

The completion of this thesis would not have been possible without the assistance and support from many people. Therefore, I wish to express my deepest gratitude to the following people, who played a part in ensuring this thesis was completed.

First and foremost, I would like to express my earnest appreciation to my project supervisor, Prof. Dr. Chua Kek Heng, for his immeasurable guidance and dedication, have guided me through my most abstruse moments in attempt to complete my PhD research. A very special ‘thank you’ to him for enlightens. His expertise in molecular techniques improved my research skills and prepared me for future challenges.

My special ‘thank you’ is also extended to my benevolent co-supervisor, Assoc. Prof. Dr. Yvonne Lim Ai Lian, for her expert, sincere, and valuable guidance and encouragement extended to me. Her evermore advice have help me accomplished my task dutifully, especially during the thesis writing.

I would also wish to extend my gratitude to Prof. Dr. Rohela Mahmud and Assoc. Prof. Dr. Lee Ping Chin (Universiti Malaysia Sabah) for the blood samples collections.

I would like to express my gratitude to the UM/MOHE-HIR grant (E-000011-20001) as well as University of Malaya postgraduate research fund (PS155-2008C and PS251-2010A), and also Skim Latihan Akademik IPTA (SLAI) for providing me fellowship during the course of my PhD study.

Special thanks also extend to my friends and lab mates, Ms. Puah Suat Moi, Dr. Chai Hwa Chia, Dr. Kee Boon Pin, and Ms. Lau Tze Pheng for providing me assistance, support, and encouragement at all times.

Last but not least, an immense gratitude also goes out to my beloved family. Thanks for your unceasing encouragement and strong support.



---

**TABLE OF CONTENTS**

	<b><u>Page</u></b>
<b>ABSTRACT</b> .....	II
<b>ABSTRAK</b> .....	IV
<b>ACKNOWLEDGEMENTS</b> .....	VI
<b>TABLE OF CONTENTS</b> .....	VII
<b>LIST OF FIGURES</b> .....	XVI
<b>LIST OF TABLES</b> .....	XIX
<b>LIST OF APPENDICES</b> .....	XXI
<b>LIST OF SYMBOLS AND ABBREVIATIONS</b> .....	XXII
 <b>CHAPTER ONE: INTRODUCTION</b>	
1.1 Introduction .....	1
1.2 Objectives .....	7
 <b>CHAPTER TWO: LITERATURE REVIEW</b>	
2.1 Malaria disease .....	8
2.2 Vector of transmission .....	11
2.3 Global impacts of malaria .....	13
2.3.1 Global distribution of <i>Plasmodium</i> species .....	17
2.3.2 Malaria in Malaysia .....	22
2.4 Biology of <i>Plasmodium</i> species .....	26
2.4.1 Taxonomic classification of <i>Plasmodium</i> species .....	26
2.4.2 General life cycle .....	29

---

	<b><u>Page</u></b>
2.4.3 Characteristics of <i>Plasmodium</i> species infecting human .....	32
2.4.4 Blood stage morphologies .....	35
2.5 Signs, symptoms and complications of malaria .....	37
2.6 Diagnosis of malaria .....	40
2.6.1 Light microscopic examination .....	41
2.6.2 Rapid diagnostic tests (RDTs) .....	43
2.6.3 Molecular PCR diagnosis .....	44
2.7 Immune responses against <i>Plasmodium</i> species .....	47
2.8 Treatment and prevention .....	50
2.9 Malaria vaccine development .....	52
2.10 Genomes and proteome of <i>Plasmodium</i> species .....	55
2.11 <i>Plasmodium</i> merozoite .....	56
2.11.1 Apical membrane antigen 1 (AMA1) .....	59
2.12 Heterologous expression of the recombinant protein .....	62
2.12.1 Expression of protein in <i>E. coli</i> .....	63
2.12.2 Refolding of insoluble and incorrectly folded proteins .....	64
2.13 Protein-protein interactions .....	66
2.13.1 Phage display technology .....	67
2.13.2 Phage display technology and applications in malaria research .....	70
 <b>CHAPTER THREE: MATERIALS AND METHODS</b>	
3.1 Chemical agents and materials .....	72
3.2 Buffers, stock solutions, culture media, and other reagents .....	72
3.2.1 Buffers and solutions .....	72
3.2.2 Media, antibiotics, and enzyme substrates .....	72

---

	<b><u>Page</u></b>
3.2.3 PCR reagents and oligonucleotide primers .....	72
3.2.4 Restriction enzymes .....	73
3.3 General Methods .....	73
3.3.1 Sample collection .....	73
3.3.2 Parasitemia estimation .....	74
3.3.3 Malarial DNA extraction from blood sample .....	75
3.3.4 Preparation of <i>Escherichia coli</i> ( <i>E. coli</i> ) competent cells .....	77
3.3.5 Maintenance and recovery of bacteria .....	78
3.3.6 Plasmid extraction .....	78
3.3.7 Determination of DNA concentration .....	79
3.3.8 Gel electrophoresis .....	79
3.3.8.1 Agarose gel electrophoresis .....	79
3.3.8.2 SDS-polyacrylamide gel electrophoresis (SDS-PAGE) and Coomassie Blue protein staining .....	80
3.3.9 DNA purification from gel .....	81
3.3.10 PCR optimization .....	81
3.3.11 DNA sequencing .....	82
3.4 Development of a single-step multiplex PCR detection assay for five human <i>Plasmodium</i> species .....	82
3.4.1 Multiplex PCR primers design .....	82
3.4.2 <i>In silico</i> PCR .....	84
3.4.3 Multiplex PCR optimization .....	84
3.4.4 Positive control .....	85
3.4.5 Multiplex PCR amplification .....	86
3.4.6 Nested PCR amplification .....	87

---

	<b><u>Page</u></b>
3.4.7 <i>Plasmodium</i> 18S ssu rRNA clones construction .....	88
3.4.7.1 Screening of positive clones by colony PCR .....	89
3.4.7.2 Screening of positive clones by DNA sequencing .....	90
3.4.8 Sensitivity and specificity tests .....	91
3.4.8.1 Analytical sensitivity test .....	91
3.4.8.2 Analytical specificity test .....	92
3.4.8.3 Random blind test and clinical sample screening .....	92
3.4.8.4 Diagnostic sensitivity and specificity tests .....	93
3.4.9 Overview of the development of a multiplex PCR detection system for human <i>Plasmodium</i> species .....	94
3.5 Identification of binding peptides for PkAMA1 and PvAMA1 using a phage display library .....	95
3.5.1 Heterologous protein expression in prokaryotic system .....	95
3.5.1.1 Construction of PkAMA1 and PvAMA1 clones ...	95
3.5.1.2 Subcloning of <i>Plasmodium</i> AMA1 ectodomain ...	99
3.5.2 Protein induction .....	100
3.5.3 SDS-PAGE solubility screening .....	101
3.5.4 Western hybridization and colorimetric detection .....	102
3.5.5 Recombinant protein extraction from <i>E. coli</i> and insoluble inclusion body purification .....	104
3.5.5.1 Inclusion body solubilization .....	105
3.5.6 Affinity protein purification under denatured conditions and fusion-tag removal .....	106
3.5.7 Protein concentration determination using Bradford protein assay .....	107

---

	<b><u>Page</u></b>
3.5.8 Precipitation of recombinant protein and buffer exchange ....	108
3.5.9 Protein renaturation .....	109
3.5.9.1 Reduction of the target protein .....	109
3.5.9.2 Desalting and buffer exchange .....	109
3.5.9.3 Protein refolding by dialysis .....	110
3.5.9.4 Analysis of folding reactions .....	111
3.5.10 Protein identification by LC-MS/MS .....	112
3.5.11 Phage display and M13 general methods .....	112
3.5.11.1 Bacteria stain maintenance .....	112
3.5.11.2 Phage titering and plaques forming unit (pfu/ml) determination .....	113
3.5.11.3 Phage amplification and precipitation .....	114
3.5.11.4 Storage of phage .....	115
3.5.12 Biopanning of the phage display library .....	116
3.5.13 Post panning protocols: Mini preparation of phage amplification for sequencing and peptide binding assays .....	118
3.5.13.1 Phage single-stranded DNA (ssDNA) isolation and sequencing .....	119
3.5.13.2 Phage ELISA binding assay .....	120
3.5.13.3 Western blot binding assay .....	121
3.5.14 Protein sequence and bioinformatic analysis .....	122
3.5.15 Overview of the identification of binding peptides for PkAMA1 and PvAMA1 using a phage display library .....	123

---

	<u>Page</u>
<b>CHAPTER FOUR: RESULTS</b>	
4.1 Clinical samples collection and DNA extraction .....	124
4.2 Identification of malaria by microscopic examination .....	124
4.3 Nested PCR .....	126
4.4 18S ssu rRNA plasmids construction .....	128
4.5 Development of a single-step multiplex PCR detection assay for five human <i>Plasmodium</i> species .....	129
4.5.1 Multiplex PCR primers design and PCR optimization .....	129
4.5.2 Positive control .....	132
4.5.2.1 The pGEX4T1 plasmid DNA .....	132
4.5.2.2 The human and <i>Plasmodium</i> 18S ssu rRNA genes ..	134
4.5.2.3 The human $\beta$ -hemoglobin gene .....	136
4.5.3 Analytical sensitivity and specificity analyses .....	138
4.5.3.1 Sensitivity in single infection .....	138
4.5.3.2 Sensitivity in mixed infections .....	139
4.5.3.3 Simulated clinical mixed infections .....	143
4.5.3.4 Specificity analysis .....	144
4.5.4 Random blind test and clinical screening .....	145
4.5.5 Diagnostic sensitivity and specificity .....	147
4.6 Heterologous expression of PkAMA1 and PvAMA1 ectodomain proteins .....	148
4.6.1 <i>Plasmodium</i> strain used in plasmid construction .....	148
4.6.2 Construction of pPAL7-PkAMA1 and pPAL7-PvAMA1 plasmids .....	148
4.6.3 Sequencing and BLAST search of PkAMA1 and PvAMA1 ..	150

---

	<b><u>Page</u></b>
4.6.4 Protein sequence and bioinformatic analysis .....	153
4.6.5 Induction of protein expression .....	153
4.6.5.1 SDS-PAGE quick solubility screening .....	153
4.6.5.2 Detection of the expression by Western blot analysis .....	155
4.6.6 Recombinant protein extraction from <i>E. coli</i> and IB purification .....	156
4.6.6.1 Cell lysis and IB purification .....	156
4.6.6.2 Inclusion body solubilization .....	159
4.6.7 Affinity protein purification and fusion-tag removal .....	160
4.6.8 Analysis of folding reactions .....	163
4.6.8.1 Aggregation measurement .....	163
4.6.8.2 Reduced and non-reduced SDS-PAGE .....	164
4.6.9 Protein identification by LC-MS/MS .....	166
4.7 Identification of PkAMA1 and PvAMA1 binding peptides using a phage display library .....	167
4.7.1 Biopanning of phage library to PkAMA1 and PvAMA1 .....	169
4.7.2 Sequence analysis of phage clones selected from panning with PkAMA1 and PvAMA1 .....	169
4.7.3 Consensus sequence determination .....	172
4.7.4 Analysis of binding affinity of selected peptides to PkAMA1 and PvAMA1 .....	173
4.7.4.1 Phage ELISA binding assay .....	173
4.7.4.2 Western blot binding assay .....	176

---

	<u>Page</u>
<b>CHAPTER FIVE: DISCUSSION AND CONCLUSION</b>	
5.1    Diagnosis of malaria .....	177
5.1.1    Microscopic examination .....	178
5.1.2    Rapid diagnostic tests (RDTs) .....	180
5.1.3    Molecular PCR diagnosis .....	180
5.2    Multiplex PCR system for identification of five human <i>Plasmodium</i> species .....	183
5.2.1    The significant of 18S ssu rRNA gene in species determination .....	183
5.2.2    Clinical samples and negative controls .....	184
5.2.3    18S ssu rRNA plasmids construction .....	184
5.2.4    Primer design and multiplex PCR optimization .....	186
5.2.5    Positive control .....	187
5.2.6    Sensitivity and specificity analyses .....	190
5.2.6.1    Sensitivity and specificity in single infection .....	190
5.2.6.2    Sensitivity and specificity in mixed infections .....	191
5.2.6.3    Random blind test and clinical screening .....	192
5.2.6.4    Diagnostic sensitivity and specificity .....	193
5.2.7    Advantages of multiplex PCR over others molecular diagnostic assays .....	194
5.2.8    Future perspectives .....	196
5.2.9    Conclusion .....	197



	<b><u>Page</u></b>
5.3 Identification of binding peptides for human <i>Plasmodium</i> species .....	198
5.3.1 Merozoite surface antigens and host cell invasion .....	198
5.3.1.1 AMA1 as invasion property of <i>Plasmodium</i> species .....	198
5.3.1.2 AMA1 as a potent antimalarial drug target and pivotal malaria vaccine candidate .....	199
5.3.2 The significant of heterologous protein expression in <i>Plasmodium</i> studies .....	201
5.3.2.1 Heterologous expression of plasmodial proteins in prokaryotic system .....	202
5.3.3 Expression of recombinant PkAMA1 and PvAMA1 in <i>E. coli</i> .....	206
5.3.3.1 Construction of PkAMA1 and PvAMA1 protein expression clones .....	206
5.3.3.2 Induction of protein expression .....	208
5.3.3.3 Protein isolation and inclusion body purification ...	210
5.3.3.4 Affinity protein purification and fusion-tag removal .....	211
5.3.3.5 Renaturation of the rPkAMA1 and rPvAMA1 .....	212
5.3.4 Phage display technology and applications in <i>Plasmodium</i> AMA1 .....	216
5.3.5 Identification of peptides affinity for PkAMA1 and PvAMA1 .....	218
5.3.6 Future perspectives .....	222
5.3.7 Conclusion .....	224
<b>REFERENCES</b> .....	226
<b>APPENDICES</b> .....	244
<b>RESEARCH OUTCOMES</b> .....	282

## LIST OF FIGURES

<b><u>Figure</u></b>	<b><u>Description</u></b>	<b><u>Page</u></b>
Figure 2.1:	Countries and territories affected by Malaria in 2010. ....	10
Figure 2.2:	Cumulative probability of globally malaria deaths by regions and age categories in 2010. ....	15
Figure 2.3:	Distribution of human <i>P. knowlesi</i> cases. ....	21
Figure 2.4:	Distribution of malaria cases in Malaysia in year 2009. ....	23
Figure 2.5:	The distributions of three most common infectious species in Malaysia, 2010. ....	25
Figure 2.6:	Phylogenetic tree of <i>Plasmodium</i> species. ....	27
Figure 2.7:	General life cycle of human <i>Plasmodium</i> species. ....	31
Figure 2.8:	Atlas of human malaria. ....	35
Figure 2.9:	Principle of immunochromatographic RDT. ....	43
Figure 2.10:	Schematic representation of immune responses against <i>Plasmodium</i> parasites. ....	49
Figure 2.11:	Sites in the malaria life cycle that could be interrupted by vaccines. ....	53
Figure 2.12:	The malaria life cycle, parasites, and parasite targets (major antigens) used for vaccine development. ....	54
Figure 2.13:	Structure of <i>Plasmodium</i> merozoite and mechanisms of merozoite invasion. ....	58
Figure 2.14:	Structure of AMA1. ....	60
Figure 2.15:	Phage display. ....	69
Figure 4.1:	Nested PCR results. ....	127
Figure 4.2:	Pentaplex PCR results. ....	131
Figure 4.3:	Multiplex PCR results with an external positive control, pGEX4T plasmid DNA. ....	133

## LIST OF FIGURES (continued)

<b><u>Figure</u></b>	<b><u>Description</u></b>	<b><u>Page</u></b>
Figure 4.4:	Multiplex PCR results with human internal positive control, <i>Plasmodium</i> genus-, and species-specific primers are both targeting 18S ssu rRNA gene. ....	135
Figure 4.5:	Hexaplex PCR results with a human internal positive control targeting $\beta$ -hemoglobin gene. ....	137
Figure 4.6:	Detection limits of the hexaplex PCR system to five human <i>Plasmodium</i> species. ....	138
Figure 4.7:	Sensitivity assay of the hexaplex PCR system in two species mixed infections based on cloned DNA. ....	141
Figure 4.8:	Hexaplex PCR results based on simulated mixture of clone DNAs. ....	142
Figure 4.9:	Hexaplex PCR results based on simulated clinical mixed infections. ....	143
Figure 4.10:	Confirmation of pPAL7-PvAMA1 construct by restriction enzyme digestion and colony PCR. ....	149
Figure 4.11:	<i>Plasmodium</i> AMA1 coding DNA inserted into pPAL7 vector. ...	151
Figure 4.12:	Protein sequences of the construct for rPkAMA1 and rPvAMA1 comprised 446 amino acids residues. ....	152
Figure 4.13:	Fractionation profile of the supernatant and pellet after centrifugation, on reduced 12 % SDS-PAGE. ....	154
Figure 4.14:	Western blot analyzed the expression level of pPAL7-PkAMA1 and pPAL7-PvAMA1 using anti-Profinity eXact monoclonal antibody. ....	155
Figure 4.15:	Profinity eXact-tagged PkAMA1 protein expression and IB purification. ....	157
Figure 4.16:	Profinity eXact-tagged PvAMA1 protein expression and IB purification. ....	158

## LIST OF FIGURES (continued)

<b><u>Figure</u></b>	<b><u>Description</u></b>	<b><u>Page</u></b>
Figure 4.17:	Optimization of concentrations of urea (2 M to 8 M) used in IB solubilization buffer.....	159
Figure 4.18:	Profinity eXact tag-free rPkAMA1 purified and eluted using a 1 ml Bio-Scale Mini <sup>TM</sup> Profinity eXact cartridge under denatured and reduced conditions. ....	161
Figure 4.19:	Profinity eXact tag-free rPvAMA1 purified and eluted using a 5 ml Bio-Scale Mini <sup>TM</sup> Profinity eXact cartridge under denatured and reduced conditions. ....	162
Figure 4.20:	Reduced and non-reduced SDS-PAGE analysis of refolding of rPkAMA1 and rPvAMA1 ectodomain proteins. ....	165
Figure 4.21:	Phage titering. ....	168
Figure 4.22:	Amplification and sequencing of phage clone selected from biopanning of rPkAMA1. ....	170
Figure 4.23:	Amino acid sequences alignment of selected dodecapeptides obtained after three rounds of biopanning against rPkAMA1 and rPvAMA1. ....	172
Figure 4.24:	Phage ELISA binding assay for peptides selected from biopanning against rPkAMA1. ....	174
Figure 4.25:	Phage ELISA binding assay for peptides selected from biopanning against rPvAMA1. ....	175
Figure 4.26:	Western blot assay for peptides binding to rPkAMA1 and rPvAMA1. ....	176
Figure 5.1:	Schematic of the multiplex PCR amplification for identification of five human <i>Plasmodium</i> species with a positive control. ....	189
Figure 5.2:	Consensus motif aligned using ClustalW. ....	220

## LIST OF TABLES

<b><u>Table</u></b>	<b><u>Description</u></b>	<b><u>Page</u></b>
Table 2.1:	Reported malarial cases and deaths in the year 2008, 2009, and 2010. ....	13
Table 2.2:	Geographical distribution of the different species of <i>Plasmodium</i> in the tropics. ....	17
Table 2.3:	Global distribution of malaria cases by species. ....	18
Table 2.4:	Reported malaria cases and deaths in Malaysia, 2008-2010. ....	23
Table 2.5:	Scientific classification of human protozoa of the genus <i>Plasmodium</i> . ....	28
Table 2.6:	Characteristics of infection with the five human <i>Plasmodium</i> species. ....	34
Table 2.7:	Morphological features of the parasitized red blood cell and five <i>Plasmodium</i> species in different stages. ....	36
Table 2.8:	Comparison of diagnostic methods for diagnosing <i>Plasmodium</i> infection in blood. ....	46
Table 2.9:	The pharmacology of antimalarials. ....	50
Table 2.10:	Protein Data Bank entries of three-dimensional structure of <i>Plasmodium</i> AMA1. ....	62
Table 3.1:	<i>Plasmodium</i> species and GenBank accession numbers for the ssu rRNA sequence. ....	83
Table 3.2:	Formulas used in diagnostic specificity and sensitivity tests. ....	93
Table 3.3:	Primer pairs used in protein expression of PkAMA1 and PvAMA1. ....	96
Table 4.1:	Distribution of <i>Plasmodium</i> species and parasitemia obtained from microscopic examination. ....	125
Table 4.2:	Validation of sensitivity in simulated mixed infections using clone DNA. ....	140

## LIST OF TABLES (continued)

<b><u>Table</u></b>	<b><u>Description</u></b>	<b><u>Page</u></b>
Table 4.3:	Comparison of results for detection of <i>Plasmodium</i> species by hexaplex PCR and microscopy. ....	146
Table 4.4:	The sensitivity, specificity, positive predictive value (PPV), and negative predictive value (NPV) of the hexaplex PCR and microscopy were compared to a standard nested PCR. ....	147
Table 4.5:	LC-MS/MS spectrum mill analysis of PkAMA1 and PvAMA1. ...	166
Table 4.6:	Phage titers obtained following each round of biopanning of rPkAMA1 and rPvAMA1. ....	169
Table 4.7:	Peptide sequences obtained in the third round of each biopanning against PkAMA1 and PvAMA1. ....	171
Table 5.1:	Binding peptides for rPkAMA1 and rPvAMA1 in the present study and rPfAMA1 in the previous studies. ....	220

---

**LIST OF APPENDICES**

<b><u>Appendix</u></b>	<b><u>Description</u></b>	<b><u>Page</u></b>
Appendix 1:	Chemical agents and materials. ....	244
Appendix 2:	Preparation of buffers, media, and stock solutions. ....	247
Appendix 3:	PCR reagents and oligonucleotide primers. ....	269
Appendix 4:	Overview of recombinant protein production using Profinity eXact™ system. ....	271
Appendix 5.1:	BLASTN search of recombinant PkAMA1. ....	272
Appendix 5.2:	BLASTN search of recombinant PvAMA1. ....	273
Appendix 5.3:	BLASTP search of recombinant PkAMA1. ....	274
Appendix 5.4:	BLASTP search of recombinant PvAMA1. ....	275
Appendix 6:	LC-MS/MS results and analysis. ....	276
Appendix 7:	Protein expression and refolding records for <i>Plasmodium</i> AMA1 deposited in REFOLD database. ....	277
Appendix 8:	Identification of binding peptides for PkAMA1. ....	278
Appendix 9:	Identification of binding peptides for PvAMA1. ....	279
Appendix 10:	Ethics approval letter. ....	280
Appendix 11:	Inform consent form. ....	281

**LIST OF SYMBOLS AND ABBREVIATIONS**

~	approximately
95 % CI	95 % confidence interval
AMA1	apical membrane antigen 1
AT	adenine thymine
BLASTN	nucleotide basic local alignment search tool
BLASTP	protein basic local alignment search tool
BSA	bovine serum albumin
CDC	Centers for Disease Control and Prevention
C-terminal	carboxyl terminal
Cys	cysteine
DNA	deoxyribonucleic acid
dNTP	deoxyribonucleoside triphosphate
DTT	dithiothreitol
<i>E. coli</i>	<i>Escherichia coli</i>
e.g.	for example
EDTA	ethylenediamine tetraacetic acid
ELISA	enzyme-linked immunosorbent assay
et al.	et alia or and others
EtBr	ethidium bromide
etc.	et cetera
GC	guanine cytosine
HRP	horseradish peroxidase
i.e.	id est or that is or other words
IB(s)	inclusion body(bodies)
ICT	immunochromatographic test
IPTG	isopropyl- $\beta$ -D-thiogalactoside
iRBC(s)	infected red blood cell(s)



**LIST OF SYMBOLS AND ABBREVIATIONS** (continued)

18S ssu rRNA	18 Svedberg small subunit ribosomal RNA
LB	Luria Bertani
LMW	low molecular weight
N-terminal	amino terminal
NMR	nuclear magnetic resonance
PAGE	polyacrylamide gel electrophoresis
PBS	phosphate buffered saline
PCR	polymerase chain reaction
PEG	polyethylene glycol
PFU	plaque forming units
RBCs	red blood cells
RDT	rapid diagnostic test
RE(s)	restriction endonuclease(s)
rPkAMA1	recombinant PkAMA1
rPvAMA1	recombinant PvAMA1
sdH <sub>2</sub> O	sterile distilled water
SDS	sodium dodecyl sulphate
S-S	disulfide bonds
<i>Taq</i>	<i>Thermus aquaticus</i>
TBE	Tris-borate-EDTA
TBS	Tris-buffered saline
TEMED	N,N,N',N'-tetramethyl-ethylenediamine
UMMC	University Malaya Medical Centre
UV	ultraviolet
WHO	World Health Organization
Xgal	5-bromo-4-chloro-3-indolyl- $\beta$ -D-galactoside

---

**UNITS OF MEASUREMENT**

$A_{260}$	absorbance at wavelength 260 nm
mA	milliampere
bp	base pair
kb	kilobase pair
kDa	kiloDalton
°C	degree Celsius
g	gram
fg	femtogram
kg	kilogram
μg	microgram
mg	milligram
pg	picogram
× g	units of gravity (relative centrifugal force)
L	liter
μl	microliter
ml	milliliter
M	mole per liter or molar
μM	micromolar
mM	millimolar
nm	nanometer
OD	optical density
%	percentage
rpm	revolutions per minute
×	times
U	unit
V	volt
v/v	volume per volume
w/v	weight per volume

## CHAPTER ONE: INTRODUCTION

### 1.1 Introduction

Malaria is a mosquito-borne parasitic disease caused by the unicellular, eukaryotic protozoa of the genus *Plasmodium* and *Anopheles* mosquitoes are vectors of transmission. Malaria continues to be one of the most severe worldwide public health problems that affects many of the poorest nations, especially in the African regions. Malaria is a devastating disease, killing one to two child/children every minute in Africa, representing a serious threat to travelers. Almost half of the world populations are live in areas at risk of malaria transmission and World Health Organization (WHO) main focal regions include most of African regions, many parts of Southeast Asia, Eastern Mediterranean, Western Pacific, and areas of Americas.

Thus far, five causative *Plasmodium* parasites namely *Plasmodium falciparum*, *Plasmodium vivax*, *Plasmodium malariae*, *Plasmodium ovale*, and *Plasmodium knowlesi* have been recognized by WHO as able to infect humans. All parasites that cause human malaria develop through a general life cycle, which alternates between human host (liver and erythrocytic stages for asexual reproduction) and anopheline mosquito (sporogonic stage for sexual reproduction). In human host, there is a clinically silent replication during the liver stage (asymptomatic); while parasites density expands exponentially as a consequence of repetitive rounds of invasion, growth, and replication during erythrocytic stage, and thus leading to the symptoms and complications of malaria due to intensive rupture of infected erythrocytes and release of huge amounts of infective asexual merozoites into blood stream. Therefore, erythrocytic cycle always served as an importance diagnostic and therapeutic stage during human infections. This cyclical accumulation of parasites in blood causes a recurring flu-like illness characterized by fevers, headaches, chills, and sweating with periodicity cycle, i.e., quotidian (24 hours) for *P. knowlesi*, tertian (48 hours) for *P. vivax*, *P. falciparum*, and

*P. ovale*, and quartan (72 hours) for *P. malariae* infections. The present studies also mainly focus on this stage.

In terms of disease severity by species, *P. falciparum* and *P. knowlesi* are the two most virulent species and are potentially fatal. Falciparum malaria also known as malignant and fatalistic malaria accounts for approximately 15 % global malaria cases and more than 90 % of global malaria deaths annually, mainly in African region and threaten the majority of young children below 5 year of ages. Sequestrating characteristic to vital organs of falciparum infection is the pathogenesis of this deadly disease (Hay, et al., 2009). Knowlesi malaria is a zoonotic parasite and recently recognized as the fifth human malaria that is widespread in the forested areas of Southeast Asia especially in Malaysian Borneo and extends to Peninsular Malaysia and neighboring countries (Cox-Singh, et al., 2008; White, 2008). Severe complications are common in knowlesi infection and potentially lethal associated with hyperparasitemic and developed marked hepatorenal dysfunction. Thus far, 19 knowlesi deaths have been reported in Malaysia (Cox-Singh, et al., 2008; Cox-Singh, et al., 2010; Daneshvar, et al., 2009; Rajahram, et al., 2012; William, et al., 2011). *Plasmodium vivax* has the widest global distribution, contributing to more than 80 % of global malaria cases. Even though *P. vivax* infection is known as benign malaria in many cases, however the surge of drug resistance strain, which is potentially fatal has weaken the malaria treatment and control (Mueller, et al., 2009). Malaria cause by *P. malariae* and *P. ovale* infections are relatively rare, account for less than 5 % of malaria cases worldwide and have mild disease outcomes (Collins & Jeffery, 2005; Collins & Jeffery, 2007).

Malaria is actually a curable disease; however disease can become severe if left untreated, especially in *P. falciparum* and *P. knowlesi* infections. Therefore, the accuracy of malaria diagnosis plays a crucial role for the institution of effectiveness of treatment management and malaria control. Generally, cost effectiveness, rapidity of

test results, ease of diagnostic procedure and result interpretations, as well as personnel training are the major considerations in malaria diagnosis. Currently, available malaria diagnostic tools mainly targeting erythrocytic cycle, including microscopic discriminations, immunochromatographic tests and molecular PCR assays.

Despite low sensitivity and specificity, especially in the diagnosis of low parasitemia and mixed infections, conventional light microscopic examination of Giemsa stained thin/thick blood smears remain the gold standard procedure in the routine diagnosis of malaria. Microscopic examination is based on the morphology appearances of asexual *Plasmodium* species in the blood circulation and the diagnostic accuracy greatly depends on the experience and skill of microscopists. Overall, microscopy approach is only accurate when the parasitemia exceed 50 parasites/ $\mu$ l of blood sample; however, it enables the identification and quantification of *Plasmodium* parasites, both of which are significant in accessing the disease severity and monitoring the prescription of adequate therapy. Generally, confusion due to morphological similarities of blood stages of some *Plasmodium* species to others is one of the major challenges in microscopic identification. For instance, *P. knowlesi* is undistinguished from *P. falciparum* in early blood ring stage and *P. malariae* in other stages.

Immunochromatographic dipstick tests (ICTs) or rather rapid diagnostic tests (RDTs) that are based on detection of *Plasmodium* antigen are adjuncts to microscopic examination and widely used in many diagnostic laboratories. This rapid malaria detection assay requires only 15 to 20 minutes to obtain results and demands less technical interpretation. Nonetheless, factors such as low sensitivity (required 100 to 200 parasites/ $\mu$ l), variable detection thresholds and field stability, and most importantly the inability to distinguish the parasites at species level limit the usage of available commercial kits in some cases.

The advent of molecular tools such as PCR based diagnostics in many cases has shown the highest specificity and sensitivity in the identification of all five human malaria parasites. Overall, PCR is able to detect parasites at low titer of 5 parasites/ $\mu$ l of blood and most recent study attained a detection limit of 0.5 parasites/ $\mu$ l in the latent and recrudescence stage of malaria disease (malERA Consultative Group on Diagnoses and Diagnostics, 2011). Conventional PCR assays (i.e., nested PCR, semi-nested PCR, and multiplex PCR), real-time or quantitative PCR (qPCR) assays, and loop-mediated isothermal amplification (LAMP) assay have been developed to identify and differentiate malaria parasites up to species levels. In general, nested PCR (Singh, et al., 1999; Singh, et al., 2004; Snounou, et al., 1993) has been considered the molecular gold standard for malaria detection. If compared with microscopy and RDTs, conventional PCR-based assays certainly are more time-consuming, especially in semi-nested PCR that require at least two PCRs (6 hours) and nested PCR that require six PCR procedures (20 hours) to test for the five human parasites up to species levels. To date, the published descriptions of semi-nested PCR (Rubio, et al., 1999) and single-step multiplex PCR (Kho, et al., 2003; Padley, et al., 2003; Patsoula, et al., 2003) could only differentiate from two (mainly focused on *P. falciparum* and *P. vivax*) to four species (excluding *P. knowlesi*). On the other hand, qPCR is a rapid assay and the result is obtained in a more straightforward manner based on completion of amplification without any downstream analysis through gel electrophoresis (Mangold, et al., 2005; Perandin, et al., 2004; Rougemont, et al., 2004; Safeukui, et al., 2008). The qPCR assay also allows parasite quantification, which cannot be achieved by conventional PCR approaches; however, the cost and reagents and equipment are much higher than for any conventional PCR assays. More recently, LAMP assay has claimed to be the most simple and less technically demanding approach that involves an isothermal amplification of targeted DNA for identification of each *Plasmodium* species (Han, et

---

al., 2007). LAMP results can be either detected by agarose gel electrophoresis or turbidity assessment by naked eye or a turbidimeter. However, the result obtained by using LAMP is qualitative and there is no specific indicator to determine whether it is a true positive or false positive result due to contamination. Furthermore, large scale screening using LAMP is still under assessment and the development of multiplex LAMP that involves many primers could also be challenging.

To overcome these limitations and challenges, therefore the present study aimed to develop and establish a straightforward single-step multiplex PCR based detection assay, which enables the simultaneous identification and differentiation of all five human *Plasmodium* parasites in a single tube reaction. This is an attractive option for routine malaria diagnosis, since mixed infections can be detected in a single round PCR. Furthermore, multiplex PCR could shorten the time and cut down the costs for reagents and disposable consumables in molecular diagnosis of human malaria.

Besides the urgency to develop a diagnostic method for the detection of all five human *Plasmodium* species, it is also important to study the protein that appears to be essential during the invasion of host cells by the malaria parasite. *Plasmodium* is an obligate intracellular parasite and the appearance of parasite in merozoite form is the most infective stage during human infection. The survivors of these parasites rely on the ability of these parasites in host cell penetration and replication. Nowadays, a number of proteins have been implicated in the invasion process, but their precise functions remain unknown in most cases. Apical membrane antigen (AMA1) is one the most well characterized malaria surface antigen that is crucial for host cell invasion. AMA1 is type I integral membrane protein, build up of a prosequence domain, an ectodomain (ectoplasmic region), a single transmembrane domain, and a small C-terminal cytoplasmic domain. Ectoplasmic region of AMA1 comprises of 16 invariant cysteine residues that are cross linked and folded into eight pairs of conserved disulfide bonds,

which are dispersed and defined the ectodomain into three distinct subdomains, i.e., domain I (DI), domain II (DII), and domain III (DIII). The disulfide bonds are essential for structure stability and functionality of the AMA1 protein (Hodder, et al., 1996). Despite AMA1 being a low abundance malaria surface antigen; it represents the most prominent immunogen that is able to stimulate strong immune response in both human and animal models, therefore widely regarded as a potent target of antimalarial drugs and pivotal malaria vaccine candidate (Macrailld, et al., 2011; Remarque, et al., 2008). AMA1 is expressed abundantly in sporozoites (pre-erythrocytic stage) as well as merozoites at the end of the tissue schizogony (pre-erythrocytic stage) and erythrocytic schizogony (erythrocytic stage), therefore offers the potential for the development of therapeutics or vaccines acting against these two critical stages. Numerous studies have confirmed that monoclonal and polyclonal antibodies against AMA1 block the entry of parasite into host cell *in vitro* or protect against blood stage growth *in vivo*. Besides the anti-AMA1 antibodies, there is evidence of peptides derived from or with affinity for AMA1 of *P. falciparum* that can also inhibit invasion of erythrocyte by parasite *in vitro*.

Although AMA1 is long thought to be a target of natural immune response that can inhibit invasion, little is known about the molecular mechanisms by which immunologically relevant portions of AMA1 could facilitate the invasion process, therefore, characterization and identification of peptide ligands as well as ligand- or receptor-binding sites that specifically interact with, and block the function of AMA1 is essentially important.

Phage display technique is a cost-effective and powerful tool that is widely applied in the study of protein-protein interactions. Studies in protein-protein interactions might contribute to some exploration of biological/molecular function of plasmodia proteins thus enhance the development of novel therapeutics. The phage display library is an assembly of peptides library which consists of billion of short and

---



variable amino acid sequences displayed on the surfaces of bacteriophage M13. The peptide library allows the selection of peptides, which have high binding affinity to the immobilized target protein. Previous phage display studies on AMA1 protein are mainly focused on *P. falciparum*, there is a vital need to include studies based on two other significant *Plasmodium* species, i.e., *P. vivax* and *P. knowlesi*.

The present study was aimed to investigate and identify the possible binding peptides, which are highly bond to recombinant AMA1 ectodomain proteins of *P. knowlesi* (rPkAMA1) and *P. vivax* (rPvAMA1) using a phage display random dodecapeptide library. The study was initiated with heterologous recombinant protein expression using *E. coli* to produce sufficient starting material for latter used in biopanning against rPkAMA1 and rPvAMA1 in phage display study. The correct folding of eight disulfide bonds within AMA1 ectodmain has been shown to be crucial for its immunological activity. Irreversibly reduced AMA1 is not recognized by antibodies raised against the native AMA1. Furthermore, immunization with reduced and alkylated AMA1 was failed to induce protective immune response, therefore the present study also include the protein renaturation step that is aimed to restore the function of rPkAMA1 and rPvAMA1, which were expressed in forms of insoluble inclusion body and purified under denatured conditions.

## **1.2 Objectives**

1. To develop a more accurate, species-sensitive/species-specific, cost-effective, as well as rapid single step multiplex PCR method for the diagnosis of five main human malaria parasites, *P. falciparum*, *P. vivax*, *P. malariae*, *P. ovale* (*P. ovale curtisi* and *P. ovale wallikeri*), and *P. knowlesi*.
2. To identify the binding peptides for refolded recombinant apical membrane antigen 1 (AMA1) ectodomain of *P. knowlesi* (rPkAMA1) and *P. vivax* (rPvAMA1).

## CHAPTER TWO: LITERATURE REVIEW

The global impact of malaria, a parasitic disease transmitted through the bite of an infective female *Anopheles* species mosquito is still serious. Malaria in humans is caused by intracellular protozoa of the genus *Plasmodium*. The known causative agents of human malaria include *Plasmodium vivax*, *Plasmodium falciparum*, *Plasmodium malariae*, *Plasmodium ovale* (exist in two forms, i.e., *P. ovale curtisi* and *P. ovale wallikeri*), and most recently *Plasmodium knowlesi* which is a zoonotic species.

### 2.1 Malaria disease

Malaria remains one of the major killers of humankind worldwide and threatens the lives of more than one-third of the world's population, provoking public health challenges in global malaria control. Each year, there are at least 250-600 million clinical cases of malaria being reported worldwide with more than a million (1.5-2.7 million) deaths, occurring mostly among African children (Greenwood, Bojang, Whitty, & Targett, 2005; Wellems, Hayton, & Fairhurst, 2009). Globally, malaria ranks as the fifth cause of death from infectious diseases, after respiratory infections, diarrhoeal diseases, HIV/AIDS, and tuberculosis; while in Africa, malaria is the second leading cause of death after HIV/AIDS (WHO, 2013a). Besides that, malaria is re-emerging as the first infectious killer and it is the number one priority tropical disease of the WHO (Malaria Site, 2012).

The latest malaria statistics reported that almost half of the world's population (approximately 3.3 billion people) lives in malaria-endemic areas including 104 countries and territories of the tropical and subtropical areas, encompassing Africa region; Amazon, Central, and Southern of Americas; Mediterranean region; Central, South, and Southeast Asia; as well as Pacific region (WHO, 2012).

Generally, the transmission of malaria is more intense in warmer regions closer to the equator, such as in areas of the Americas, many parts of Asia, and much of Africa. The prevalence of malaria in tropical regions is due to the significant amounts of rainfall with consistent high temperatures and humidity, along with stagnant waters, which allow the *Anopheles* mosquito to thrive and breed. In contrast, malaria transmission is unstable with a low incidence rate (limited cases) at the high altitude areas over elevations of 1,500 m, desert areas (excluding oases), as well as during dry and colder seasons even in some parts of malaria-endemic countries. Figure 2.1 shows the geographic distribution of malaria worldwide in the year 2010 (Arguin & Mali, 2012).

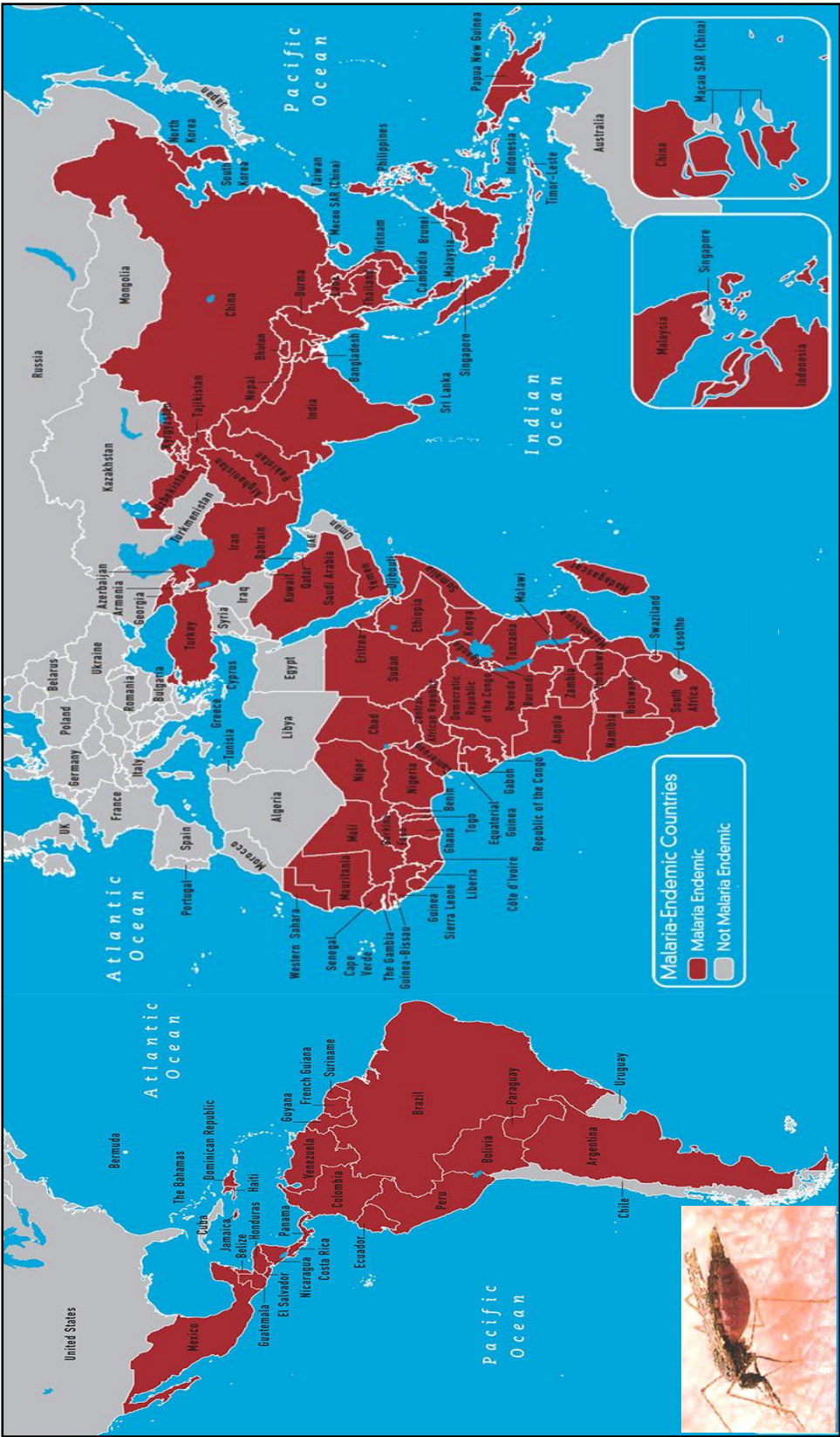


Figure 2.1: Countries and territories affected by Malaria in 2010 (adapted from (Arguin & Mali, 2012)).

## 2.2 Vector of transmission

Female *Anopheles* mosquitoes are the exclusive vector of malaria disease. Generally, malaria parasites are transmitted from human to human through the bites of infected female *Anopheles* mosquito, typically at night time. Currently, there are approximately 530 *Anopheles* species found around the world, only 70 to 80 *Anopheles* species transmit malaria in nature, with diverse breeding and feeding habits, and thus result in vast disease spectra in different population target groups and epidemiological settings. The intensity of malaria transmission depends on factors related to the vector, the parasite, the human host, and the environment [Alonso, et al., 2011; Centers for Disease Control and Prevention (CDC), 2012; Choochote & Saeung, 2013; Manguin, Bangs, Pothikasikorn, & Chareonviriyaphap, 2010; Manguin, Garros, Dusfour, Harbach, & Coosemans, 2008].

The parasites require the mosquito host to complete their sexually development. Once a mosquito is infected, it is infected for life and continues to transmit infections, therefore the lifespan of mosquito also play a crucial role in disease transmission. Only female mosquitoes feed on blood as they require high protein diets in order to reproduce rafts of eggs. Even though *Anopheles* mosquitoes breed in water, each of the *Anopheles* species has its own breeding preference, for example some prefer shallow collections of fresh water, such as puddles, paddy fields, tire tracks, as well as irrigation water. The areas of distribution also differ, for instance, *Anopheles gambiae* is the major vector in Africa that can breed in diverse habitats, *Anopheles fluviatilis* and *Anopheles minimus* are found in the foothill regions, whereas *Anopheles philippinensis* and *Anopheles culicifacies* are found in the plains, *Anopheles stephensi* and *Anopheles sundaicus* are found in the coastal regions. Species like *An. stephensi* are highly adaptable and are found to be potent vectors of human malaria (CDC, 2012; WHO, 2013a).

Generally, *Anopheles* mosquitoes are found worldwide except Antarctica. Environmental factors including climate conditions, such as temperature, humidity, rainfall pattern, etc. play a larger role in malaria transmission, since wet, tropical areas are conducive for mosquito breeding. For instance, in many places, transmission of malaria is seasonal, surging during and just after the rainy season. Besides that, the urbanization and land use might also bring changes to the ecosystem, which contribute to the changing pattern of malaria transmission (Gallup & Sachs, 2001; WHO, 2013a).

Vector control measures, such as the use of insecticides and larva controls play a critical role in malarial elimination and eradication, however some of the mosquitoes may shift resistance to that insecticide after prolong exposure over several generations, thus impairing the successful in vector controls (Alonso, et al., 2011).

### 2.3 Global impacts of malaria

In 2010, there were an estimated 219 million of malaria cases (with an uncertainty range of 154 million to 289 million) and 660,000 malaria deaths worldwide (with an uncertainty range of 490,000 to 836,000) being reported, and the WHO main focal regions include Africa, Southeast Asia, and Eastern Mediterranean regions (WHO, 2012). Generally, people living in the poorest countries are more vulnerable to malaria. There were approximately 80 % of global malaria cases and more than 90 % deaths that have occurred in the African region (between the years 2008 to 2010). This was followed by Southeast Asia region that attributed to approximately 14 % of clinical cases and 6 % of global deaths, as well as Eastern Mediterranean region with approximately 5 % of clinical cases and 2 % of deaths (Table 2.1).

Table 2.1: Reported malarial cases and deaths in the year 2008, 2009, and 2010 (WHO, 2012).

		2008	2009	2010
<b>World population</b> (in billions)		<b>6.7</b>	<b>6.8</b>	<b>6.9</b>
<b>Malaria cases</b> (in millions)	<b>World</b>	<b>225</b>	<b>222</b>	<b>219</b>
	Africa	182 (81 %)	179 (81 %)	174 (79 %)
	Southeast Asia	29 (13 %)	30 (14 %)	32 (15 %)
	Eastern Mediterranean	11 (5 %)	11 (5 %)	10 (5 %)
	Western Pacific	2 (< 1 %)	2 (< 1 %)	2 (< 1 %)
	Americas	1 (< 1 %)	2 (< 1 %)	1 (< 1 %)
<b>Malaria deaths</b>	<b>World</b>	<b>711,000</b>	<b>691,000</b>	<b>660,000</b>
	Africa	654,000 (92 %)	630,000 (91 %)	596,000 (90 %)
	Southeast Asia	37,000 (5 %)	39,000 (6 %)	43,000 (7 %)
	Eastern Mediterranean	15,000 (2 %)	16,000 (2 %)	15,000 (2 %)
	Western Pacific	4,200 (< 1 %)	4,700 (< 1 %)	4,000 (< 1 %)
	Americas	1,000 (< 1 %)	1,200 (< 1 %)	1,100 (< 1 %)

Young children, pregnant women, and immunocompromised individual, i.e., HIV/AIDS carrier are the three most vulnerable groups to malaria (Shetty, 2012). Of these malaria-related deaths, overwhelming majority are children under 5 years of age because their immune systems have not developed enough to fend off the parasites attack (Figure 2.2). In 2010, approximately 86 % deaths globally were found among child < 5 years of age, making this disease one of the major causes of infant and juvenile mortality (WHO, 2012). Malaria kills one to two African child in every minute (Shetty, 2012). For those children who survive, malaria also drains vital nutrients from children, impairing their physical and intellectual developments. Malarial sickness is also one of the principal reasons for poor school attendance (Girard, Reed, Friede, & Kieny, 2007; Rogerson & Carter, 2008).

Pregnant women living in malaria endemic areas are 4-times more likely than non-pregnant women to get severe malaria and twice as likely to die of disease because her immune system is partially suppressed during pregnancy (Shetty, 2012). Besides, malaria attack during pregnancy can be more severe and they have an increase risk of serious pregnancy outcomes, including prematurity, miscarriage, stillbirth, and death. Infected mother can transmit malaria to her infant before or during delivery. There were an estimated 10,000 maternal deaths and up to 200,000 newborn deaths annually due to malaria during pregnancy (Desai, et al., 2007; Steketee, Nahlen, Parise, & Menendez, 2001).

HIV infection weakens the immune system, thus making people living with HIV more vulnerable to malaria. Malaria infection causes HIV viral loads to shoot up, which could increase its transmission (Shetty, 2012).



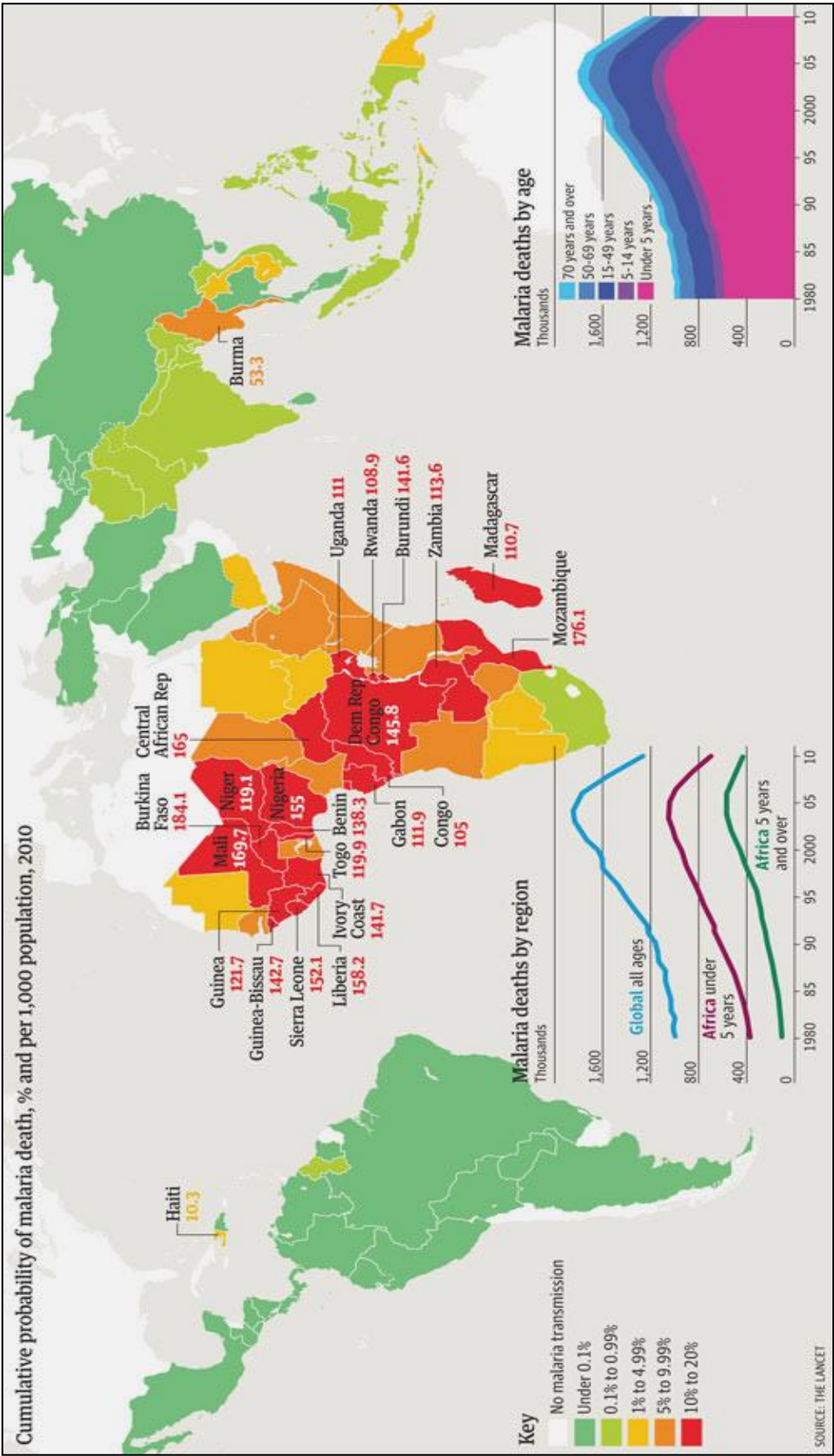


Figure 2.2: Cumulative probability of globally malaria deaths by regions and age categories in 2010 (adapted from <http://www.guardian.co.uk/news/datablog/2012/feb/03/malaria-deaths-mortality>).

Malaria can also be transmitted through a blood transfusion although this is very rare. The asexual parasites are directly inoculated into the blood without pre-erythrocytic replication, therefore has a shorter incubation period and relapses do not occur (Chauhan, Negi, Verma, & Thakur, 2009).

The fact that the local community had reduced natural immunity to malaria may also have contributed to the high mortality rate. For instance, non-immunized travelers, refugees, displaced persons, immigrants, and laborers from malaria-free areas are more likely to become very sick and die when they get infected (Erdman & Kain, 2008). In addition, mortality rates were high as the area has poor health infrastructures and services. Poor people and indigenous living in rural areas, who lack the knowledge, money, or access to health care are at greater risk of getting this disease.

Malaria is commonly associated with poverty and may also be a major hindrance to the social-economic development. Malaria not only causes illness and lives lost, but also a great drain on many national economies. The breakdown of the public health system and high expenditure on health care and malarial treatment cause the consequence of poverty of a community or country (Sachs & Malaney, 2002). People with malaria are less productive resulting in loss of income due to the sickness, and thus cause reduction in economic output (Greenwood, et al., 2005; Wellems, et al., 2009). Other economic impacts include loss of foreign investment and tourism. According to WHO, the annual costs (direct or indirect) related to malaria in Africa are estimated to be more than US\$ 12 billion every year (Shetty, 2012).

### 2.3.1 Global distribution of *Plasmodium* species

*Plasmodium* is a parasite which is widely distributed all over the world. Each of the *Plasmodium* species has a defined area of endemicity, although geographic overlap is common. *Plasmodium* species causing human malaria are generally restricted to tropical and subtropical regions. However, global warming and population migrations do have a bearing on the distribution of these parasites. Table 2.2 and Table 2.3 show the global distribution of five human *Plasmodium* species.

Table 2.2: Geographical distribution of the different species of *Plasmodium* in the tropics.

	<i>P. falciparum</i>	<i>P. vivax</i>	<i>P. ovale</i>	<i>P. malariae</i>	<i>P. knowlesi</i>
<b>North Africa</b>	frequent	predominant	absent	frequent	none
<b>West Africa</b>	predominant	very rare	frequent	rare	none
<b>Central Africa</b>	predominant	very rare	rare	frequent	none
<b>East Africa</b>	predominant	rare	rare	frequent	none
<b>Indian Ocean</b>	predominant	rare	rare	frequent	none
<b>Central America</b>	frequent	frequent	absent	rare	none
<b>South America</b>	frequent	predominant	absent	rare	none
<b>Indian subcontinent</b>	frequent	predominant	very rare	rare	none
<b>Southeast Asia</b>	predominant	frequent	rare	rare	frequent
<b>Pacific Islands</b>	frequent	frequent	rare	rare	none

Table 2.3: Global distribution of malaria cases by species.

<i>Plasmodium</i> species	Global distribution	References
<i>P. vivax</i> *	Contribution to > 80 % of global cases and widespread throughout the subtropical and temperate regions with low rate of infection in West and Central Africa (high prevalence of Duffy negativity population that naturally resistant to <i>P. vivax</i> infection).	Mueller, et al., 2009
<i>P. falciparum</i> *	Contributed to ~ 15 % global malaria cases and > 90 % global deaths. Concentrated in tropical and subtropical region and most prevalent at Africa region (~ 60 % of the global total falciparum malaria) with the highest burden in Nigeria and Democratic Republic of Congo as well as 19 countries of Central, South, and East Asia (39 %) with the highest burden in India and Myanmar.	Hay, et al., 2009
<i>P. malariae</i>	Restricted to subtropical area. Most common in sub-Saharan Africa and Southwest Pacific. Less frequently encountered in Asia, Middle East, Central and South America.	Collins & Jeffery, 2007
<i>P. ovale curtisi</i> (classic type) <i>P. ovale wallikeri</i> (variant type)	Distributed in sub-Saharan Africa, South-East Asia (Philippines, Cambodia, Myanmar, Vietnam, and Thailand), Middle East, India subcontinent, Papua New Guinea, Irian Jaya, and East Timor in Indonesia.	Collins & Jeffery, 2005; Sutherland, et al., 2010
<i>P. knowlesi</i>	Widespread in forested areas of Southeast Asia and most prevalent in Malaysia. Cases also have been reported in Philippines, Thailand, Indonesia, Vietnam, Myanmar, and Singapore.	Singh, et al., 2004; Antinori, Galimberti, Milazzo, & Corbellino, 2013

\* Drug resistant strains present in most species of endemic regions (Karyana, et al., 2008; Tjitra, et al., 2008).

Generally, *P. vivax* infections have the widest global distribution and prevalent in subtropical and temperate regions, with 2.5 billion people at risk and 80-300 million cases reported annually (Mueller, et al., 2009). *Plasmodium vivax* is more tolerant to lower ambient temperature, thus the transmission is not restricted to cooler regions (Carlton, et al., 2008). *Plasmodium falciparum* is the second most prevalent, but the most lethal species, being responsible for more than 90 % of malaria mortality annually. *Plasmodium falciparum* infections are concentrated in the tropical and subtropical regions such as Africa, Central and Southeast Asia, and America (Hay, et al., 2009). Infections caused by other species are relatively scanty; with *P. malariae* being limited to subtropical area (Collins & Jeffery, 2007) as well as *P. ovale* being restricted to Sub-Saharan Africa (Collins & Jeffery, 2005).

The newcomer fifth human malaria parasite, *P. knowlesi*, which formerly cause malaria only in macaques, is now widespread in forested areas of Southeast Asia countries (White, 2008). So far, human *P. knowlesi* infections have been described in high numbers only in Malaysia with a great majority of cases originating from Malaysia Borneo, i.e., Sabah and Sarawak states (Barber, et al., 2011; Cox-Singh, et al., 2008; Cox-Singh & Singh, 2008; Daneshvar, et al., 2009; Singh, et al., 2004; William, et al., 2011). Numerous cases have also been described in Peninsular Malaysia (Cox-Singh, et al., 2008; Lee, Adeeba, & Freigang, 2010; Vythilingam, et al., 2008). Since the availability of *P. knowlesi* species-specific nested PCR in the year 2004 (Singh, et al., 2004), several *P. knowlesi* cases have been reported in other Southeast Asian countries, including Thailand (Jongwutiwes, Putaporntip, Iwasaki, Sata, & Kanbara, 2004; Putaporntip, et al., 2009; Sermwittayawong, Singh, Nishibuchi, Sawangjaroen, & Vuddhakul, 2012), Myanmar (Jiang, et al., 2010; Zhu, Li, & Zheng, 2006), Indonesia (Figtree, et al., 2010; Sulistyaningsih, Fitri, Loscher, & Berens-Riha, 2010), Philippines (Luchavez, et al., 2008), Singapore (Berry, et al., 2011; Jeslyn, et al., 2011; Ng, et al.,

---

2008; Ong, Lee, Koh, Ooi, & Tambyah, 2009), and Vietnam (Van den Eede, et al., 2009; Van den Eede, et al., 2010) (Figure 2.3A); only limited traveler's cases were reported in Europe countries (Berry, et al., 2011; Bronner, Divis, Farnert, & Singh, 2009; Chin, Contacos, Coatney, & Kimball, 1965; Ennis, et al., 2009; Hoosen & Shaw, 2011; Kantele, Marti, Felger, Muller, & Jokiranta, 2008; Ta, et al., 2010; Van Hellemond, et al., 2009), Taiwan (Kuo, Chiang, Chan, Tsai, & Ji, 2009; Link, et al., 2012), and Japan (Tanizaki, et al., 2013) after returning from forested areas of Southeast Asia (Figure 2.3B).

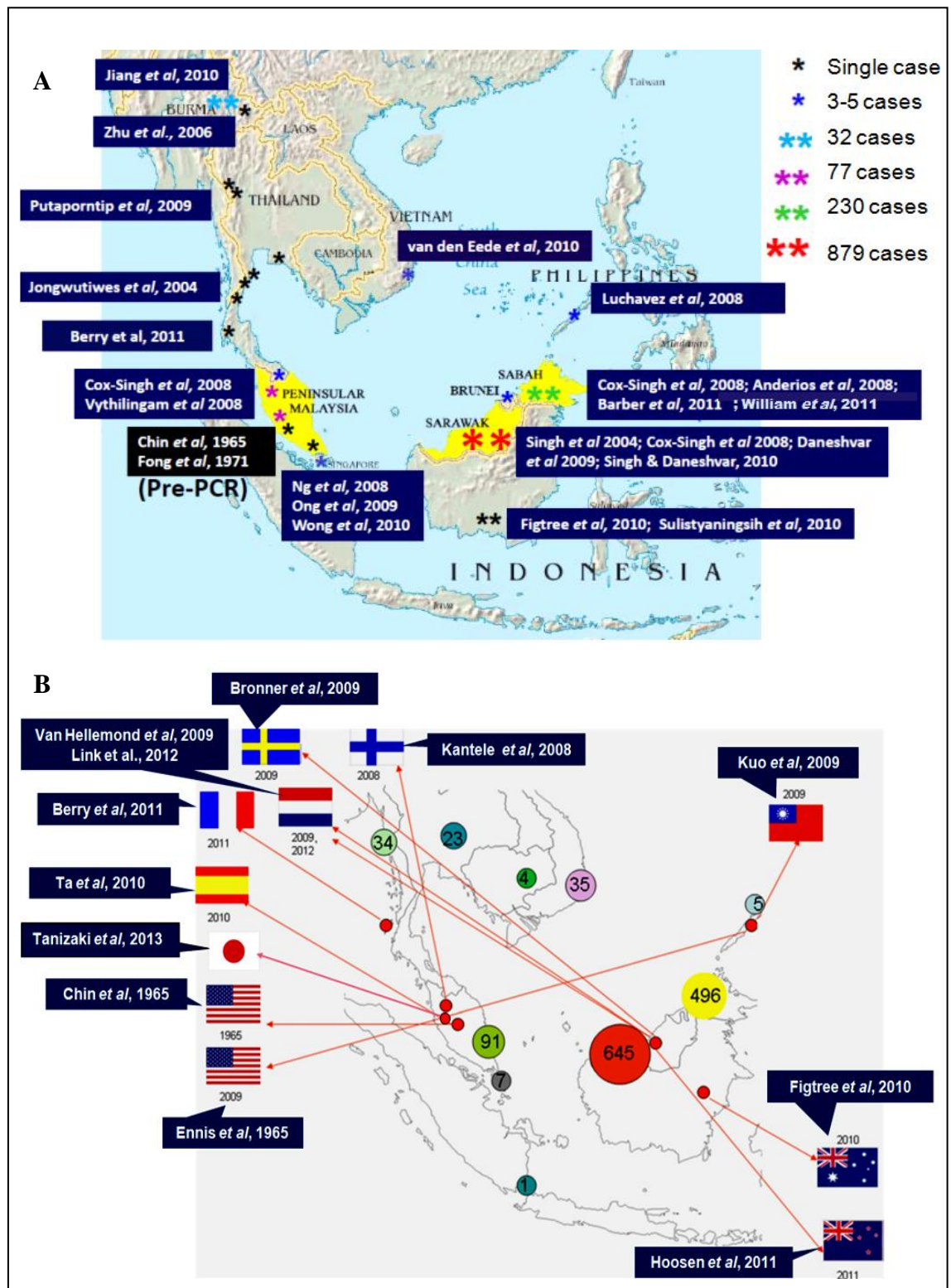


Figure 2.3: Distribution of human *P. knowlesi* cases. (A) Human *P. knowlesi* cases have been reported nearly in all countries in Southeast Asia (adapted from Singh, 2011). (B) Traveller's cases of *P. knowlesi*, whereby red dot indicate where travellers probably acquired their infection, while flags indicate the countries where infection was diagnosed (adapted from Antinori, et al., 2013).

### **2.3.2 Malaria in Malaysia**

Malaysia is situated in the hot, humid equatorial region and therefore is receptive and vulnerable to the transmission of malaria. Malaysia consists of West Malaysia or known as Peninsular Malaysia as well as East Malaysia separated by the South China Sea. East Malaysia also known as Malaysian Borneo located on the island of Borneo consists of the two Malaysian states, Sabah and Sarawak. East Malaysia is less populated and less developed compared to West Malaysia and its landmass is larger and mainly surrounded by natural forested areas.

Malaysia has been characterized as in the pre-elimination stage by WHO, with only 3 % of the population at risk of malaria. The target to achieve elimination of malaria in Peninsular Malaysia is by 2015 and Malaysian Borneo by 2020 (Ministry of Health Malaysia, 2012; WHO, 2012).

According to the Ministry of Health Malaysia and Malaria World Report 2012, the reported malaria cases in Malaysia were 7,390 in 2008 but decreased to 7,010 cases in 2009 and 6,650 in 2010. The numbers of malaria deaths have remained steady at between 20-40 deaths per year over the last decade. There were slight increases in malaria deaths from 26 cases in year 2009 to 33 cases in year 2010 (Ministry of Health Malaysia, 2012; WHO, 2012).

In Malaysia, the majority of malaria cases were reported in Sabah state, followed by Sarawak state, and the rest were distributed in Peninsular Malaysia with a majority of cases in the central, southeastern and northern coastal regions (Kheong, 2010).

Table 2.4 shows the reported malaria cases and deaths in years 2008 to 2010, whereas Figure 2.4 indicates the distribution of cases in Malaysia in year 2009.



Table 2.4: Reported malaria cases and deaths in Malaysia, 2008-2010.

Malaysia		2008	2009	2010
Population (million)		27.0	27.5	28.9
Total malaria cases		7,390	7,010	6,650
Malaria deaths		30	26	33
Cases distribution	Peninsular	1,342 (18.2 %)	1,178 (16.8 %)	N/A (20 %)
	Sarawak	1,909 (25.8 %)	1,823 (26.0 %)	N/A (22 %)
	Sabah	4,135 (56.0 %)	4,009 (57.2 %)	N/A (58 %)
Prevalence by species (%)	<i>P. falciparum</i>	31	27	25
	<i>P. vivax</i>	51	48	57
	<i>P. ovale</i>	-	-	-
	<i>P. malariae</i>	6	8	7
	<i>P. knowlesi</i>	8	13	8
	Mixed infection	4	4	3

N/A indicates not available.

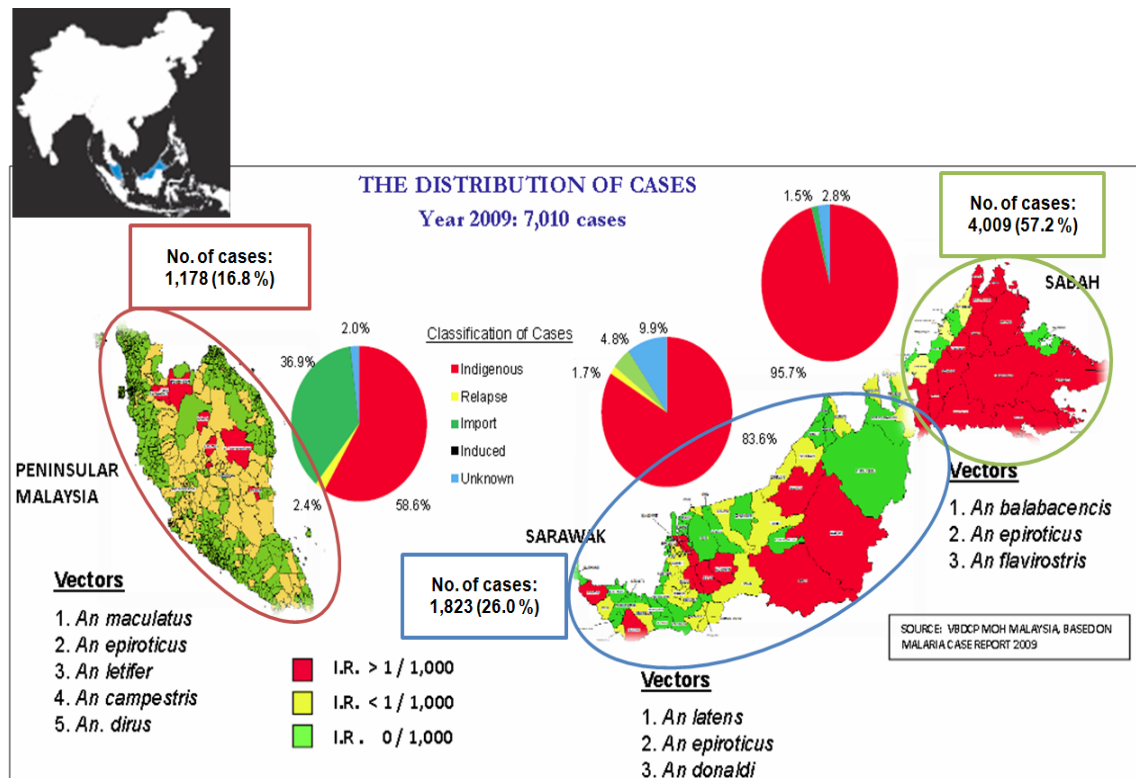


Figure 2.4: Distribution of malaria cases in Malaysia in year 2009 (adapted from Kheong, 2010).

The pie charts in Figure 2.4 show the classification of the cases in year 2009. Malaria cases were commonly reported in rural areas, which have high density of indigenous tribal groups, who live within the remote forested or forest-fringe areas. Other high-risk groups include outdoor laborers such as agriculture, logging camp, and jungle workers. These occupations may predispose them to high risk of exposure to malaria vector. However, with regards to malaria cases in urban areas, it has been noted that malaria imported by immigrant and foreign workers from endemic countries have surged in urban district, i.e., Selangor state (Lee, et al., 2010; Masitah, Aini, & AyuSaid, 2008). In 2010, 12 % of malaria cases are attributed to the imported cases from malaria-endemic neighboring countries, primarily from Indonesian and Filipino workers, while the multi-drug resistance infections are from Indonesia, Myanmar, and Thailand (Ministry of Health Malaysia, 2012; Shetty, 2012).

With regards to malaria cases by species in Malaysia, *P. vivax* remains the most common cause of infection, followed by *P. falciparum*, and *P. knowlesi* infections (Table 2.4). Even though *P. knowlesi* ranked the third most common infectious agent, the incidence rate is relatively high in Malaysian Borneo if compared to Peninsular Malaysia (Kantele & Jokiranta, 2011) (Figure 2.5). *Plasmodium knowlesi* can cause severe malaria complications with a rate of 6 to 9 % (e.g., respiratory distress, acute renal impairment, shock, and hyperbilirubinemia, etc.) and with a case fatality rate of 3 % (Antinori, et al., 2013). Severe disease cause by *P. knowlesi* infection has been reported in Sarawak (Cox-Singh, et al., 2008; Cox-Singh, et al., 2010; Cox-Singh & Singh, 2008), Sabah (Barber, et al., 2011; Cox-Singh, et al., 2010; Joveen-Neoh, Chong, Wong, & Lau, 2011; Rajahram, et al., 2012; William, et al., 2011), and Peninsular Malaysia (Cox-Singh, et al., 2008; Lee, et al., 2010; Vythilingam, et al., 2008), including 19 fatal cases, in where 12 knowlesi deaths were in Sabah state and seven in Sarawak state (Cox-Singh, et al., 2008; Cox-Singh, et al., 2010; Daneshvar, et al., 2009; Rajahram, et al., 2012;

William, et al., 2011).

Cases with *P. malariae* infection as well as mixed infections are occasionally reported, whereas *P. ovale* infection is very rare in Malaysia (Ministry of Health Malaysia, 2012). However, recently the first imported case of *P. ovale* from a 20-year-old Nigerian male student was reported in Malaysia (Lim, et al., 2010). Figure 2.5 show the distribution of the three most common *Plasmodium* species in Malaysia.

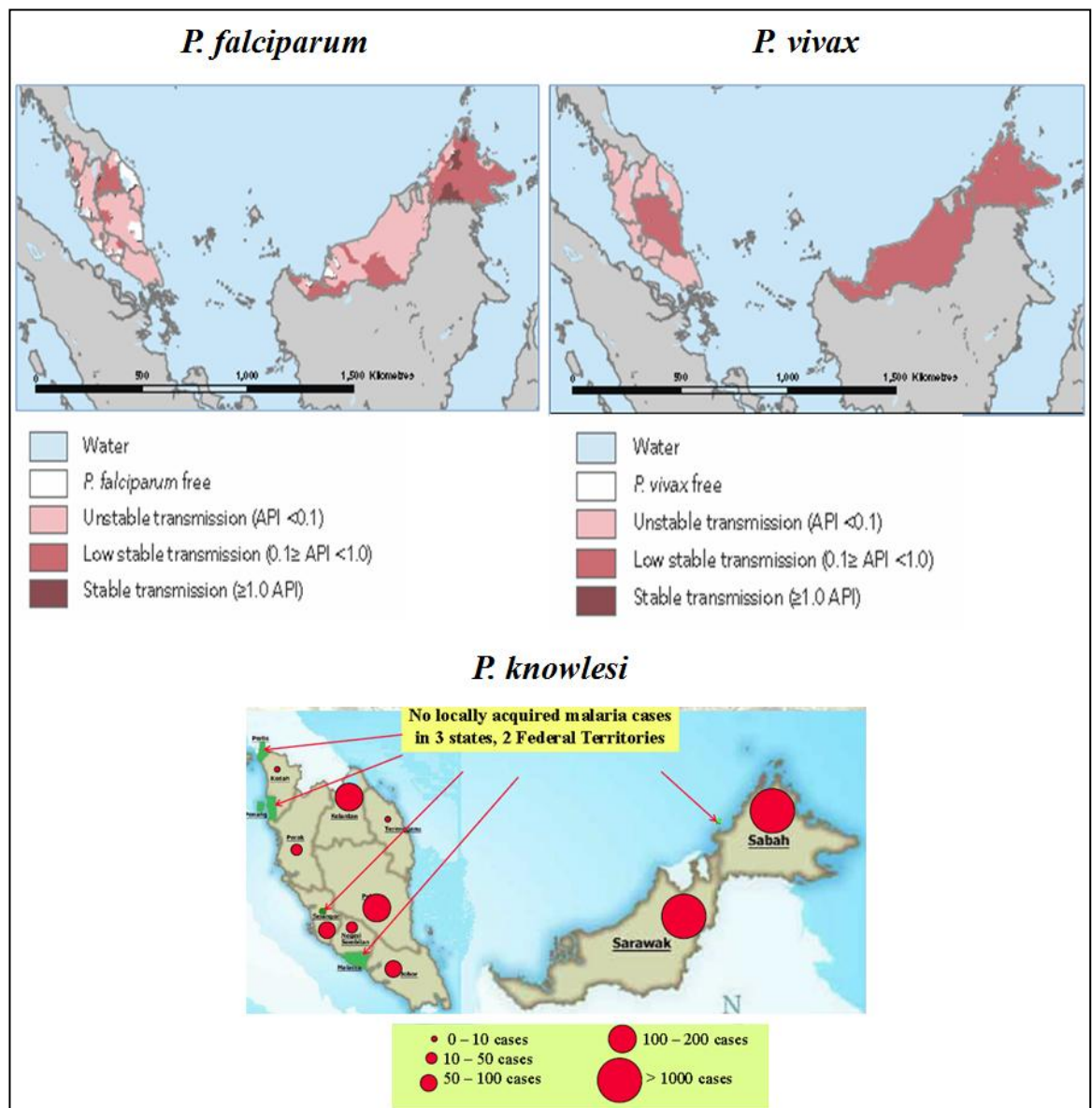


Figure 2.5: The distributions of three most common infectious species in Malaysia, 2010 (adapted from Ministry of Health Malaysia, 2012; Rundi, 2011).

## 2.4 Biology of *Plasmodium* species

Malaria is an infectious disease caused by protozoan single-celled (unicellular eukaryotic) parasite from the genus called *Plasmodium*. There are over 200 different species of *Plasmodium* that produce disease in non-human primates, rodents, reptiles, and birds, in addition to humans. Thus far, about 30 species naturally infect non-human primates (monkeys, great apes, and others), whilst only five identified species, i.e., *P. vivax*, *P. falciparum*, *P. malariae*, *P. ovale*, and *P. knowlesi* cause malaria in humans. The most recent evidence indicates that *P. ovale* is composed of two subspecies, i.e., *P. ovale curtisi* (classic type) and *P. ovale wallikeri* (variant type) (Sutherland, et al., 2010).

### 2.4.1 Taxonomic classification of *Plasmodium* species

In 1885, the genus *Plasmodium* was first created by Ettore Marchiafava and Angelo Celli. They used unstained blood smears and the new Zeiss oil-immersion lenses to describe a blood-borne parasites first observed by Charles Louis Alphonse Laveran in 1880 from blood of a malaria victim. Marchiafava and Celli confirmed that, the parasite can inhibit erythrocytes and cause an infectious disease called malaria. The nomenclature of *Plasmodium* is derived due to these protozoa took the form of a plasmodium, a cell with multiple nuclei and an amorphous shape. After that, Ronald Ross identified the mosquito vector in 1897, whereas Henry Shortt and Cyril Garnham identified the hepatic stages in 1947 (McFadden, 2012).

*Plasmodium* belongs to the family *Plasmodiidae*, order Haemosporidia and phylum Apicomplexa. Unusual characteristics of this organism in comparison to general eukaryotes include the presence of rhoptry, micronemes, and polar rings near the apical end. Figure 2.6 is a general phylogenetic tree of *Plasmodium* species and Table 2.5 shows the scientific classification of the five human protozoa of the genus *Plasmodium*.

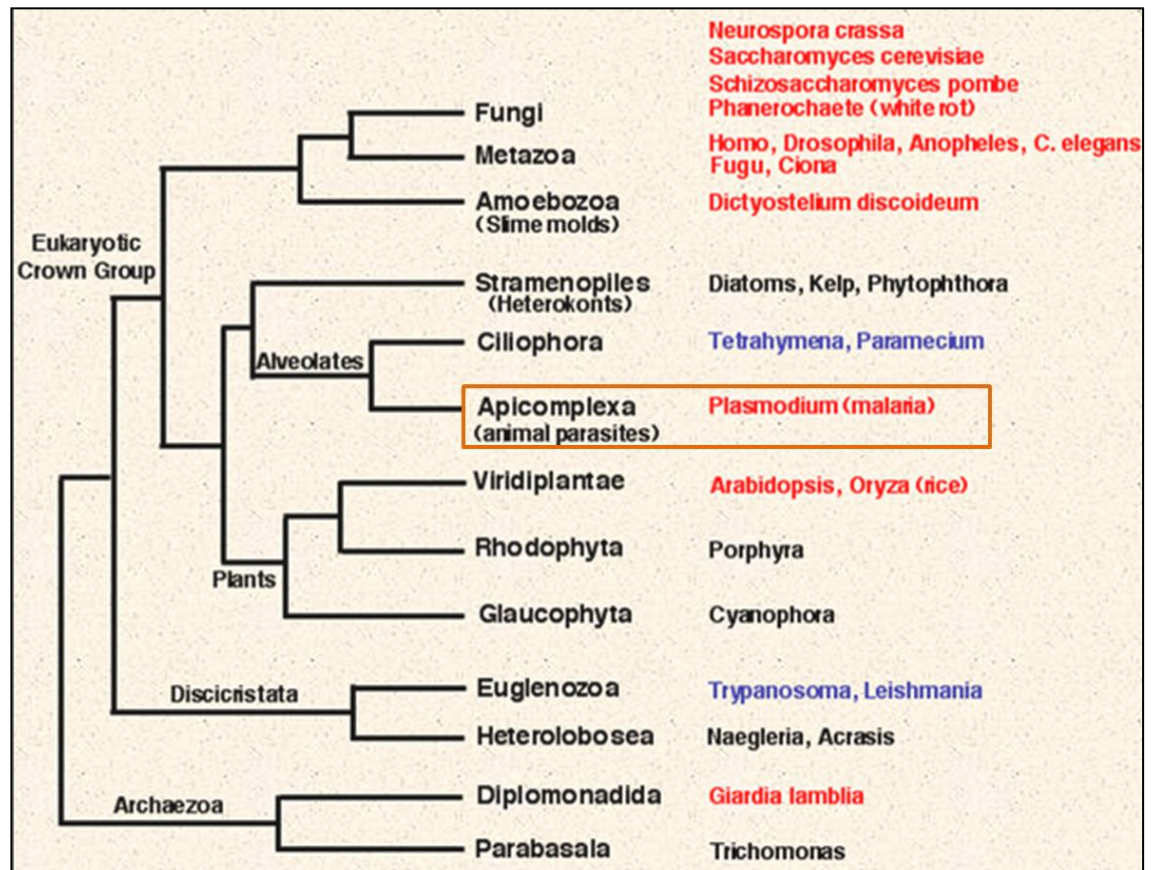


Figure 2.6: Phylogenetic tree of *Plasmodium* species (obtained from [http://bioweb.uwlax.edu/bio203/s2007/augustin\\_laur/family\\_tree.htm](http://bioweb.uwlax.edu/bio203/s2007/augustin_laur/family_tree.htm)).

Table 2.5: Scientific classification of human protozoa of the genus *Plasmodium* (adapted from Antinori, Galimberti, Milazzo, & Corbellino, 2012).

Scientific classification		Reason of classification
<b>Domain</b>	Eukaryota	Cellular structure containing organelle.
<b>Kingdom</b>	Chromalveolata	Contains protists (cellular organism without specialized tissue).
<b>Superphylum</b>	Alveolata	
<b>Phylum</b>	Apicomplexa	Contains organisms that have no individual form of motion, except for their gametes. (cells with cluster of organelles known as apical complex).
<b>Class</b>	Aconoidasida	Have a tip at the end of their form which allows them to enter/penetrating the other organisms/species.
<b>Order</b>	Haemosporida	Haemosporidia literally means blood spores. All members of this phylum are parasitic in vertebrate hosts and share similar life cycle.
<b>Sub-order</b>	Haemosporidiidea	
<b>Family</b>	<i>Plasmodiidae</i>	Exhibits asexual reproduction in a vertebrate host and sexual reproduction in a definitive host (a mosquito, in the case of the <i>Plasmodium</i> species that infect all mammals, including humans).
<b>Genus</b>	<i>Plasmodium</i> ; <i>Laverania</i>	Laverania was the old generic name for malaria causing Haemosporidia protozoa.
<b>Species</b>	<i>P. falciparum</i>	Malignant malaria
	<i>P. vivax</i>	<i>Plasmodium vivax</i> is divided into two subtypes, a dominant form, VK210 and a variant form, VK247. This division is dependent on the amino acid composition of the circumsporozoite (CS) protein (Kim, et al., 2010).
	<i>P. malariae</i>	Benign malaria
	<i>P. ovale</i>	<i>P. ovale</i> has been found to exist in two forms, <i>P. ovale curtisi</i> (classic type) and <i>P. ovale wallikeri</i> (variant type) (Sutherland, et al., 2011).
	<i>P. knowlesi</i>	Simian malaria

### 2.4.2 General life cycle

The life cycle of *Plasmodium* species is extraordinarily complex and specific for the particular parasite species (Florens, et al., 2002). In general, the *Plasmodium* parasites live part of its life in human and part in female mosquitoes (exclusively of the genus *Anopheles*) (Figure 2.7). Infected female *Anopheles* plays a role as vector in human-human transmission. Basically, it can be distinguished into three main stage-cycles, i.e., pre-erythrocytic and erythrocytic cycles in human host, and sporogonic cycle in mosquito.

In human host, infection starts after the inoculation of few sporozoites into the blood stream during the blood meal of an infected mosquito. Within minutes after entering the blood circulation, sporozoites are able to travel quickly to liver and invade hepatocytes, whereby they replicate and developed into liver schizonts. The liver stage development also known as pre-erythrocytic or tissue schizogony. The sporozoite will initially undergo the early liver stage to form trophozoite and then mature into tissue schizont during the next 5-15 days. For some instance, the sporozoites of *P. vivax* and *P. ovale* will keep dormancy or persists in hepatocytes as hypnozoites, which may remain for years and are responsible for new attacks of the disease if re-activated; probably relapse is due to incomplete treatment. Basically, the rupture of tissue schizonts will subsequently release several thousands of infectious merozoites into blood stream, whereby they invade the red blood cells (RBCs) and thus initiating the erythrocytic cycle.

In erythrocytic cycle, parasites can either undergo asexual multiplication (erythrocytic schizogony) or sexually differentiated into either macro- or micro-gametocytes, which will eventually be ingested by female *Anopheles* mosquito during a blood meal. In general, the erythrocytic schizogony process is similar to the tissue schizogony in liver stage, whereby parasite also multiplies to form trophozoite within

RBC, and then mature into schizont that carries 6-36 infectious merozoites. The trophozoites mature over the course of 24-72 hours and the rupture of erythrocytes releases a new wave of merozoites that are able to infect other erythrocytes into the blood stream.

The parasites multiplication in the midgut of the female *Anopheles* mosquito is known as sporogonic cycle, which starts after ingestion of both female and male gametocytes from human host during blood meal acquisition. The sporogonic cycle involves the fertilization of those mature microgametocyte and macrogametocyte to form zygote that may subsequently develop into ookinate and then multiply to form oocysts. Upon maturation, one oocyst contains thousands of sporozoites. The life cycle in mosquito ends up with the rupture of matured oocysts and release of infectious sporozoites into mosquito salivary gland (Greenwood, et al., 2005). The duration of the sexual life cycle takes about 9-16 days, being largely dependent on temperature conditions. Figure 2.7 shows the overview of the general life cycle of human *Plasmodium* species.



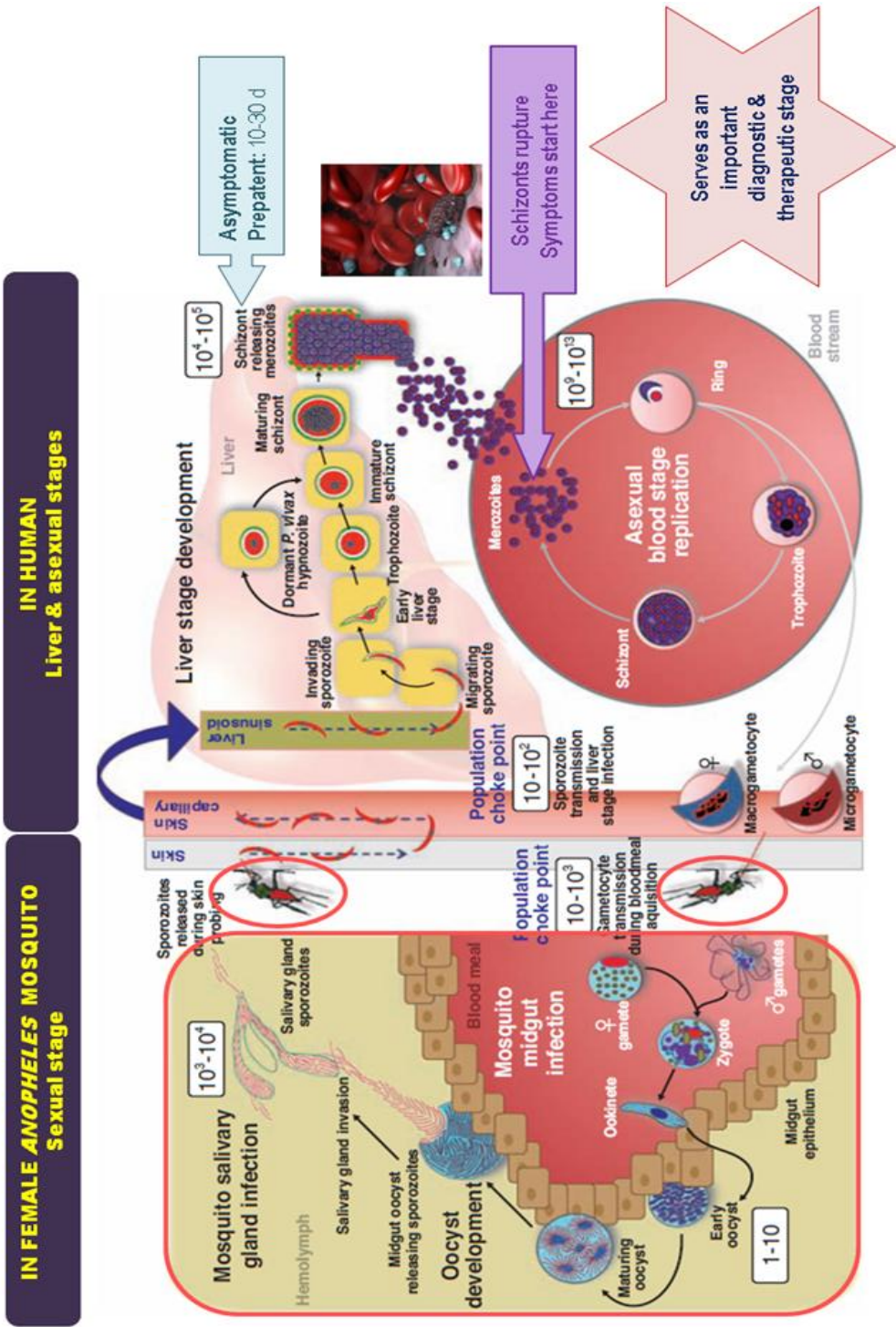


Figure 2.7: General life cycle of human *Plasmodium* species (adapted from Kappe, Vaughan, Boddey, & Cowman, 2010).

### 2.4.3 Characteristics of *Plasmodium* species infecting human

Even though, five human *Plasmodium* parasites have to share a common life cycle in human host, however the details in life cycle, such as host erythrocyte cells preference, prepatent period, length of tissue and erythrocytic schizogony (including number of merozoites produced in each schizogony), as well as the presence or absence of the dormant liver stage are species dependent. Each species also differs with regard to their blood-stage morphology, clinical manifestations, and disease severity.

In the human liver, the sporozoites undergo their replication becoming a tissue schizont that contains thousands of merozoites (can up to 40, 000 in *P. falciparum*), and the pre-erythrocytic schizogony takes a minimum maturation time of 6 days in *P. falciparum* and a maximum of 16 days in *P. malariae*. The rupture of mature tissue schizonts and releasing of merozoites will be subsequently followed by blood stage infection. For some exception, *P. vivax* and *P. ovale* are able to persist in liver as hypnozoites that are eventually responsible of the phenomenon of late relapse of infection. The period of time between sporozoites inoculation to the appearance of first merozoites in the peripheral blood, is known as prepatent period. The incubation period is somewhat longer because signs and symptoms do not appear until the parasitemia is sufficiently advanced.

In contrast to tissue schizogony, erythrocytic trophozoites mature over the course of 24-72 hours to form blood schizonts, each composed of 6-36 merozoites (Table 2.6). The rupture of blood schizonts and releasing of infectious merozoites are responsible for the appearance of cycle similar to periodicity of febrile paroxysm, i.e., quotidian (fever spikes every 24 hours) for *P. knowlesi*, tertian (fever every 48 hours) for *P. falciparum*, *P. vivax*, and *P. ovale*, as well as quartan (fever every 72 hours) for *P. malariae* infections. Therefore, erythrocytic cycle always serves as an important diagnostic and therapeutic stage in malaria.

In general, *P. falciparum* and *P. knowlesi* are able to infect RBCs of all ages, resulting in high levels of parasitemia (hyperparasitemia; more than 5 % RBCs infected or 250,000 parasites/ $\mu$ l). In contrast, *P. vivax* and *P. ovale* infect only young RBCs and thus cause a lower level of parasitemia (maximum parasitemia is 2 % or 100,000 parasites/ $\mu$ l). Whereas, *P. malariae* infection is responsible of chronic low parasitemia (rarely exceeding 30,000 parasites/ $\mu$ l) due to the preference of the parasite to develop in older erythrocytes, reduced growth rate, i.e., long development cycles (pre-erythrocytic and erythrocytic cycles with 14-16 hours and 72 hours, respectively), and also the low number of merozoites produced per erythrocytic cycle (Gaur, Mayer, & Miller, 2004).

The characteristics of infection with the five *Plasmodium* species have consequently influence the clinical outcome of malaria infection. Table 2.6 summarizes all the characteristics of infection with the five species of *Plasmodium* infecting human.

Table 2.6: Characteristics of infection with the five human *Plasmodium* species (modified from Antinori, et al., 2012).

Characteristics	<i>P. falciparum</i>	<i>P. vivax</i>	<i>P. ovale</i>	<i>P. malariae</i>	<i>P. knowlesi</i>
Incubation period (days)	7-14	12-17	10-14	15-18	N/A
Pre-erythrocytic stage (days)	5-7	6-8	9	14-16	8-9
Prepatent period (days)	9-10	11-13	12-20	15-16	9-12
Erythrocytic cycle (hours)	48	48	49-50	72	24
Febrile paroxysm	Tertian or sub-tertian	Tertian	Tertian	Quartan	Quotidian
Erythrocytes preference	All	Reticulocytes	Reticulocytes	Mature erythrocytes	All
Merozoites/tissue schizogony	40,000	> 10,000	15,000	2,000	N/A
Merozoites/RBC schizogony	8-24	12-24	6-14	6-12 (usually 8)	10-16
Parasitemia/μl					
Average	20,000-500,000	20,000	9,000	6,000	600-10,000
Maximum	2,000,000	100,000	30,000	20,000	236,000
Febrile paroxysm (hours)	16-36 or longer	8-12	8-12	8-10	8-12
Symptom duration (untreated)	2-3 weeks	3-8+ weeks	2-3 weeks	3-24 weeks	N/A
Maximum	6-17 months	5-8 years	12-20 months	20-50+ years	N/A
Severe malaria	Yes	Yes	No	No	Yes
Relapses from hypnozoites	No	Yes	Yes	No	No
Recurrences	Yes (treatment failure)	Yes (treatment failure)	No	Yes (can persists in blood up to 30 years)	Yes
Initial clinical manifestations and severity	Severe/life threatening/lethal/maglinant/fatalistic	Moderate to severe	Mild	Mild/chronic/asymptomatic	Potentially life threatening
Severe malaria	Up to 24 %	Up to 22 %	Very rare	Very rare	6-10 %
Drug resistance	Yes**	Yes**	No	No	No
References	-	-	Collins & Jeffery, 2005	Collins & Jeffery, 2007	Lee, Cox-Singh, & Singh, 2009

\* N/A indicates not available.

\*\* Chloroquine resistance *P. falciparum* and *P. vivax* (Tjitra, et al., 2008).

#### 2.4.4 Blood stage morphologies

Each of the five causative agents of human malaria has a distinctive appearance under microscope observation. Two or more species can simultaneously infect a single person causing mixed infections. Complete knowledge of the morphological features of the different blood stages of the different *Plasmodium* species represents the essential basis of a correct laboratory diagnosis confirmation of malaria infection. Generally, Atlas of Human Malaria (Figure 2.8) is used as a major guideline for *Plasmodium* identification. Table 2.7 summarizes the appearances of parasitized RBCs as well as morphological features of five human *Plasmodium* species in stained thin blood films.

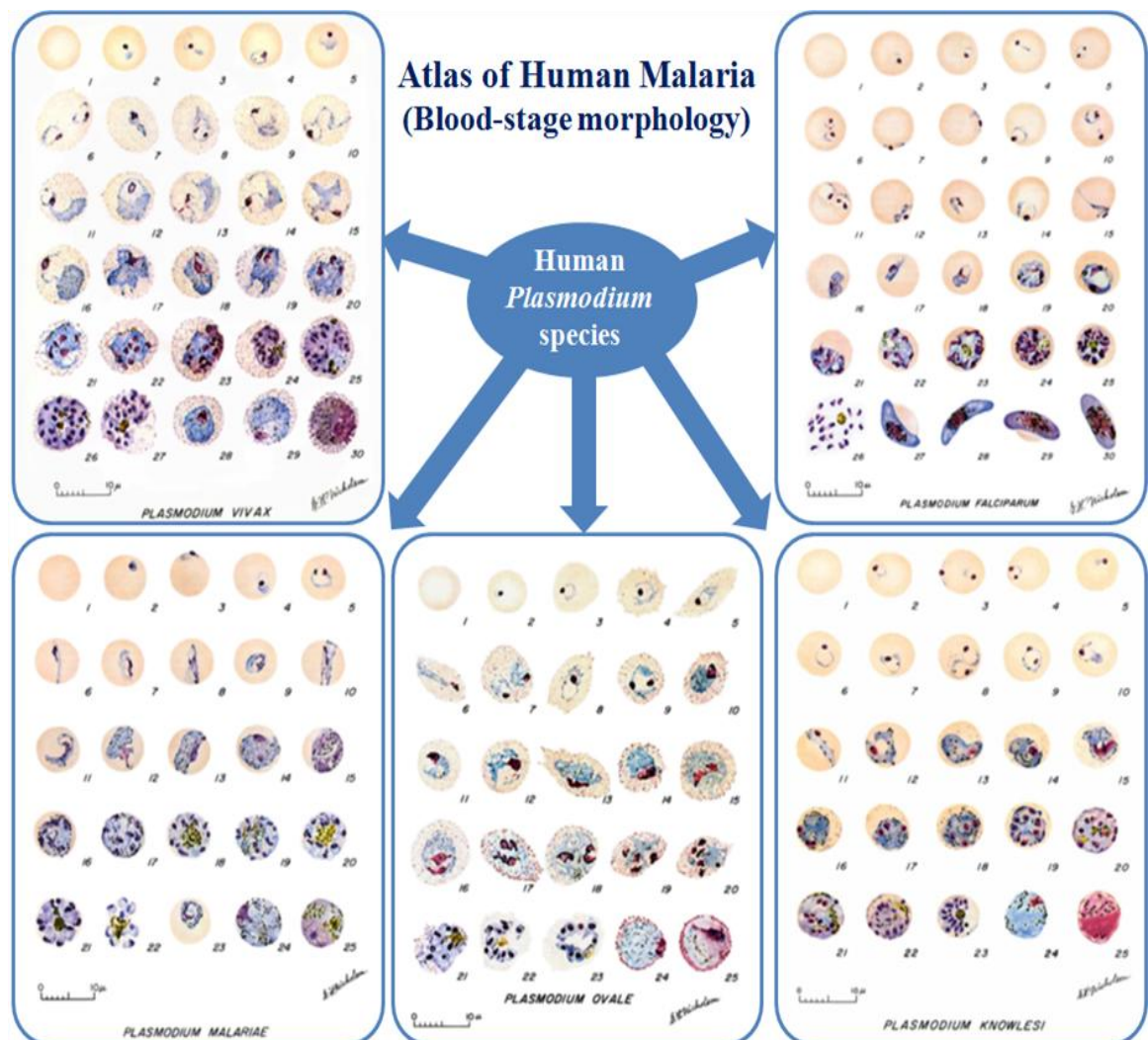


Figure 2.8: Atlas of human malaria (illustrations adapted from Coatney, Collins, Warren, & Contacos, 1971).

Table 2.7: Morphological features of the parasitized red blood cell and five *Plasmodium* species in different stages (adapted from CDC, 2009).

Species	Stages	Appearance of RBCs	Appearance of Parasites
<i>P. falciparum</i>	Ring	Normal; multiple infection of RBC more common than in other species, Maurer's clefts under certain staining conditions	Delicate cytoplasm; 1 to 2 small chromatin dots; occasional appliqué (accollé) forms
	Trophozoite	Normal; rarely, Maurer's clefts under certain staining conditions	Seldom seen in peripheral blood; compact cytoplasm; dark pigment
	Schizont		Seldom seen in peripheral blood; contains 8-24 small merozoites; dark pigment, clumped in one mass
	Gametocyte	Distorted by parasite	Crescent or sausage shape; chromatin in a single mass (macrogametocyte) or diffuse (microgametocyte); dark pigment mass
<i>P. vivax</i>	Ring	Normal to 1.25×, round; occasionally fine Schüffner's dots; multiple infection of RBC not uncommon	Large cytoplasm with occasional pseudopods; large chromatin dot
	Trophozoite	Enlarged 1.5-2×; may be distorted; fine Schüffner's dots	Large amoeboid cytoplasm; large chromatin; fine, yellowish-brown pigment
	Schizont		Large, may almost fill RBC; contains 12 to 24 merozoites; yellowish-brown, coalesced pigment
	Gametocyte		Round to oval; compact; may almost fill RBC; chromatin compact, eccentric (macrogametocyte) or diffuse (microgametocyte); scattered brown pigment
<i>P. ovale</i>	Ring	Normal to 1.25×, round to oval; occasionally fine Schüffner's dots; occasionally fimbriated; multiple infection of RBC not uncommon	Sturdy cytoplasm; large chromatin
	Trophozoite	Normal to 1.25×; round to oval; some fimbriated; Schüffner's dots	Compact with large chromatin; dark-brown pigment
	Schizont		Contains 6 to 14 merozoites with large nuclei, clustered around mass of dark-brown pigment
	Gametocyte		Round to oval; compact; may almost fill RBC; chromatin compact, eccentric (macrogametocyte) or more diffuse (microgametocyte); scattered brown pigment
<i>P. malariae</i>	Ring	Normal to 0.75×	Sturdy cytoplasm; single large chromatin
	Trophozoite	Normal to 0.75×; rarely, Ziemann's stippling under certain staining conditions	Compact cytoplasm; large chromatin; occasional band forms; coarse, dark-brown pigment
	Schizont		Contains 6 to 12 (usually 8) merozoites with large nuclei, clustered around mass of coarse, dark-brown pigment ; occasional rosettes
	Gametocyte		Round to oval; compact; may almost fill RBC; chromatin compact, eccentric (macrogametocyte) or more diffuse (microgametocyte); scattered brown pigment
<i>P. knowlesi</i>	Ring	Normal to 0.75×; multiple infection of RBC not uncommon	Delicate cytoplasm; 1 to 2 prominent chromatin dots; occasional appliqué (accollé) forms
	Trophozoite	Normal to 0.75×; rarely, Sinton and Mulligan's stippling (under certain staining conditions)	Compact cytoplasm; large chromatin; occasional band forms; coarse, dark-brown pigment
	Schizont		Contains up to 16 merozoites with nuclei, clustered around mass of coarse, dark-brown pigment; merozoites irregularly scattered or grape-like cluster; mature merozoites appear segmented
	Gametocyte		Round to oval, compact; may almost fills RBC; chromatin compact, eccentric (macrogametocyte) or more diffuse (microgametocyte); scattered brown pigment

## 2.5 Signs, symptoms and complications of malaria

Malaria infection is asymptomatic during maturation in liver. Clinical malaria disease will be apparent during the erythrocytic cycle of infection and can present in a wide range of symptoms. The common symptom is characterized by a cycle similar to periodicity of the paroxysm fever and chill, and this febrile paroxysm typically lasting 8-12 hours and characterized by three main stages, i.e., the cold stage (rapid rise of the temperature associated with chill) followed by hot stage (temperature peak, skin vasodilatation, headache, and myalgias) and lastly the sweat stage (defervescence).

World Health Organization has classified malaria into two categories, chronic (uncompleted) malaria and severe (complicated) malaria (WHO, 2000). Uncomplicated malaria is defined as symptomatic malaria without signs of severity or evidence of vital organ dysfunction. The common manifestations of uncomplicated malaria may be the classical flu-like symptoms such as fever, shaking chill, headache, and body pain, but a wide spectrum of symptoms are possible. In severe malaria, multi-organs failure, coma, and death are typical, especially in non-immune individual, children, and pregnant women. Malaria infection is usually associated with a reduction of hemoglobin levels due to hemolysis of parasitized RBCs and this largely contributed to severe anemia accompanied with jaundice in young children and pregnant women living in highly malaria endemic region. Some malaria infections can turned severe and lead to death very rapidly if untreated, especially in two fatalistic infections, i.e., *P. falciparum* and *P. knowlesi*. The emergence of multi-drug resistant strains of *P. falciparum* and *P. vivax* is also exacerbating the situation (Conway, 2007; Rubio, et al., 1999; Tjitra, et al., 2008).

*Plasmodium falciparum* is the most lethal malaria worldwide and can evolve rapidly to severe illness and deaths due to the cytoadherence property shown by the infected erythrocytes to host epithelium, which allows the parasites to escape from clearance by the spleen. The sequestration pathogenesis also allows this parasite hidden

away in the deep organs of the body; therefore in most of the blood stages, i.e. late trophozoite, schizont and gametocytes stages of *P. falciparum* are not seen in the peripheral blood except in heavy infection (Zimmerman, Mehlotra, Kasehagen, & Kazura, 2004). In addition, falciparum infected erythrocytes can clump together or form rosette by sticking to other uninfected erythrocytes, thus causing blockages in blood capillaries that can consequently lead to malaria death. The main complications linked to falciparum death are severe malaria (leading to profound hypoxia and congestive cardiac failure), cerebral malaria (leading to coma, altered mental status, multiple seizures with *P. falciparum* in the blood, and other cerebral symptoms) and respiratory distress syndrome. The complications in falciparum malaria is lethal if left untreated and even with treatment, 15 % of children and 20 % of adults developed cerebral malaria die (WHO, 2008).

In addition to *P. falciparum* infection, the newly recognized human *P. knowlesi* infections can also result in severe disease and potentially fatal. Currently, increasing epidemiology studies based on knowlesi malaria in Malaysian Borneo are being published with improved information on the disease severity and clinical complications (Cox-Singh, et al., 2008; Cox-Singh, et al., 2010; Daneshvar, et al., 2009; Rajahram, et al., 2012; William, et al., 2011). The shortest erythrocytic replication period (24 hours) and high parasite loads (hyperparasitemia) have been concluded as the two key features that lead to severe malaria and malaria death in *P. knowlesi* infections. Acute respiratory distress, acute renal failure, shock and hyperbilirubinemia are most common complications noted in patients with severe disease (Antinori, et al., 2013; William, et al., 2011). Thus far, 19 knowlesi deaths have been reported, seven cases were in Sarawak state (Cox-Singh, et al., 2008; Cox-Singh, et al., 2010; Daneshvar, et al., 2009) and 12 in Sabah state (Rajahram, et al., 2012; William, et al., 2011).



In contrast to the above two potentially fatal infections, *P. vivax*, *P. ovale*, and *P. malariae* infections always exhibit less severe disease outcome restricting to fever with rare complication. *Plasmodium vivax* and *P. ovale* exhibit the hypnozoite stage and can cause true relapses several months after the primary infection (Collins & Jeffery, 2005). *Plasmodium malariae* does not relapse from persistent liver stage parasites, but the parasite is able to persist in the blood at very low density for extremely long period, perhaps for entire life of human host causing recrudescence even after more than 40 years or longer (Collins & Jeffery, 2007).

Recrudescence, re-infection and relapse are the three main causes of the recurrence of malaria after treatment. Recrudescence occurs when parasites are not properly cleared by treatment. For instant, *P. falciparum* that are resistant to antimalarial drug and *P. malariae* can remain in the blood for months or even years and cause recurrent symptoms from time to time. Re-infection indicates complete clearance of parasites in the previous infection and the new infection is actually established from a separate infective mosquito bite and the infection can occur with any malaria parasites. On the other hand, relapse infection is a unique characteristic of *P. vivax* and *P. ovale* infections that involves re-emergence of blood-stage parasites from hynozoites in the liver. This can occur any time after several weeks or months of the primary attack.

## **2.6 Diagnosis of malaria**

The empirical clinical diagnosis remains the most common method to diagnose malaria that is based on the observation of the clinical features of the disease. However, the accuracy of this clinical presumptive diagnosis is poor due to the extremely wide spectrum of clinical signs and symptoms ranging from mild to severe malaria. Furthermore, the flu-like symptoms (e.g., fever, headache, myalgias, etc.) and other severe signs (e.g., acute anemia, coma, renal failure, etc.) are extremely non-specific, mimicking a large series of other clinical conditions of many other febrile type tropical diseases (WHO, 2000). Moreover, the efficacy of the clinical diagnosis is also subjected to many other factors, such as the endemicity of different species; the population movements; the inter-relation between the levels of transmission, immunity, parasitemia, and symptoms; the problems of recurrent-malaria and/or drug resistance; and the previous anti-malaria medication or used of chemoprophylaxis etc. (Karyana, et al., 2008; Rogerson & Carter, 2008; Shetty, 2012). Therefore, once malaria is suspected on clinical grounds, it is mandatory to obtain the parasitological laboratory confirmation of the presence of malaria parasites or its antigens/products in the patient blood prior treatment is given.

The availability of prompt and accurate diagnostic method is paramount in effective management of malaria. In general, financial resources, uncomplicated diagnostic procedure, personnel training, as well as rapid availability of the results, are the major considerations in malaria diagnosis (malERA Consultative Group on Diagnoses and Diagnostics, 2011; Moody, 2002). Basically, the erythrocytic cycle of infection is responsible for symptoms and signs of infection, thus current malaria diagnostic methods are targeting the parasites in peripheral blood. Nowadays, microscopic examination (parasite identification), immunochromatographic dipstick tests (ICTs) or rapid diagnostic tests (RDTs) (antigen detection), and molecular PCR

assays (parasite nucleic acid detection) are the three most common laboratory diagnostic methods.

### **2.6.1 Light microscopic examination**

Conventional light microscopic examination of Giemsa-stained thin and/or thick smear films remains the gold standard for routine laboratory diagnosis of malaria and this can be attributed to the rapidity of result, low cost, simplicity, reliability in most settings even though in many cases this assay has shown to have low sensitivity and specificity, especially in cases of low parasitemia, sequestered parasites, as well as mixed-infection (malERA Consultative Group on Diagnoses and Diagnostics, 2011; Moody, 2002). The microscopy approach is only accurate when the minimum parasite titer in the blood sample is 50 parasites/ $\mu$ l; however, it is able to identify and further quantify the parasite numbers in the patient samples, both of which are significant in assessing the disease severity and prescription of adequate therapy. Overall, the accuracy of results varies depending on the experience and skill of laboratory technicians (Moody, 2002; Zimmerman, et al., 2004).

In thin films, the red blood cells (1.5  $\mu$ l blood) are fixed so that the morphology of the parasitized cells can be seen. Species identification can be made based upon the size and shape of the various stages of the parasite (Figure 2.8 and Table 2.7; Session 2.4.4). Generally, thin and thick blood smears have a difference in sensitivity, with 100-200 parasites/ $\mu$ l and  $\sim$  10 parasites/ $\mu$ l, respectively. Therefore, examination of a thick blood film is recommended when there is low parasitemia. The red cells are approximately 6-20 layers thick (3-4  $\mu$ l blood), which results in a larger volume of blood being examined. In thick films, the red blood cells are lysed, so diagnosis is based on the appearance of the parasite and the parasites tend to be more compact and denser than in thin films.

Despite these strengths, microscopic examination has created diagnostic problem in cases whereby there are changes in the morphological appearances of parasites due to drug pressure, genetic variation and also approaches of blood collection. Besides that, morphological similarities of blood stages of some *Plasmodium* species to others also leads to misdiagnosis of *Plasmodium* to species level and the overlooking of fatal species, which will consequently weaken the effectiveness of treatments and malaria management (Mayxay, Pukrittayakamee, Newton, & White, 2004; Moody, 2002). For instance, microscopic diagnosis of *P. knowlesi* infection is quiet challenging especially for inexperienced microscopist as the morphology of *P. knowlesi* is always undistinguishable from *P. falciparum* during the early ring stage and *P. malariae* during the other blood stages, i.e., trophozoite, schizont, and gametocyte (Lee, et al., 2009; Singh, et al., 2004). Mixed infections are often missed (Mayxay, et al., 2004); especially when *P. malariae* and *P. ovale* coexist with other species, as their densities are often low in comparison to that of *P. falciparum* (Conway, 2007; Zimmerman, et al., 2004). Furthermore, in *P. falciparum* infection, usually only very young forms (ring forms) can be observed in the peripheral blood because older parasites are being adhere to the endothelium of blood vessels in deep organs (e.g. the brain) (Zimmerman, et al., 2004). Regardless of some limitations in microscopy technique, there is no alternative method that could be established to replace this universally accepted gold standard method.

### 2.6.2 Rapid diagnostic tests (RDTs)

Various RDTs are commercially available to detect antigens derived from malaria parasites. Such immunologic (immunochromatographic) tests are most often designed in a dipstick or cassette format, which require only 15 to 20 minutes to obtain results and need less technical interpretation. The limitations of RDTs include having variable detection thresholds and field stability, low sensitivity (100-200 parasites/ $\mu$ l), and that most of the kits are unable to distinguish the parasites up to species level (malERA Consultative Group on Diagnoses and Diagnostics, 2011; Moody, 2002). For instance, the currently approved RDTs could only detect two different malaria antigens, i.e., one is specific for *P. falciparum* (histidine-rich protein 2) and the other is conserved across the human malaria (*Plasmodium* lactate dehydrogenase or aldolase enzymes), thus further microscopy confirmation is still needed to determine the species that is detected by the RDTs (Murray, Gasser, Magill, & Miller, 2008). Figure 2.9 show the principle and result interpretation of RDTs.

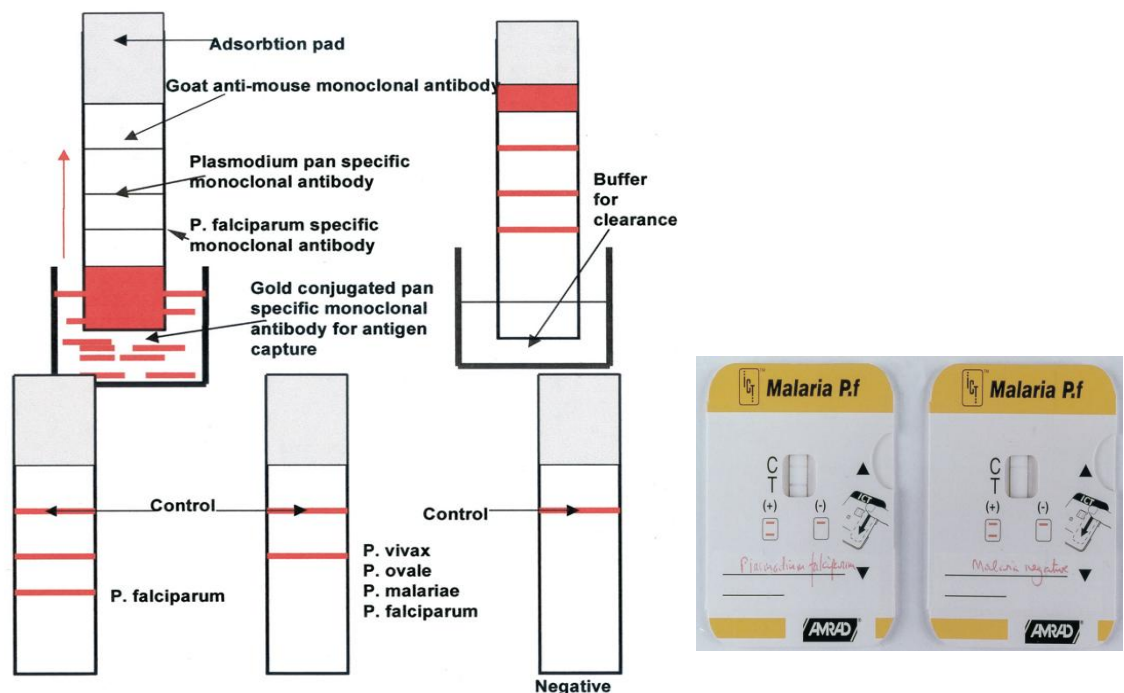


Figure 2.9: Principle of immunochromatographic RDT (adapted from Moody, 2002).

### 2.6.3 Molecular PCR diagnosis

The advent of molecular tools such as PCR has provided more specific, sensitive, and reliable molecular techniques for the diagnosis of malaria based on the detection of parasite nucleic acid (Conway, 2007; malERA Consultative Group on Diagnoses and Diagnostics, 2011). *Plasmodium vivax* and *P. ovale* as well as *P. malariae* and *P. knowlesi* are not always distinguishable on the basis of morphologic characteristics alone, and the use of molecular tools will help clarify their diagnosis. The principle of PCR is based on the amplification of a selected region of the malarial genome. Genus-specific and species-specific sequences of the asexual stage-expressed 18S small subunit ribosomal RNA (ssu rRNA), circumsporozoite surface protein (*csp*), a nuclear gene encoding a cysteine protease, and the cytochrome b (*Cytb*) gene have comprised several common targets in molecular studies of malaria (Conway, 2007; Moody, 2002).

In general, PCR enables the detection of parasites at low titer of 5 parasites/ $\mu$ l (Moody, 2002), and the most recent study attained a detection limit of 0.5 parasite/ $\mu$ l in the latent or recrudescence stage of malaria disease (malERA Consultative Group on Diagnoses and Diagnostics, 2011). Although PCR assays have shown in many cases to have improved the sensitivity and specificity for the diagnosis of malaria over microscopy or RDTs, in many cases the time duration required to obtain results is much longer, with at least three hours to one day for sample processing (malERA Consultative Group on Diagnoses and Diagnostics, 2011; Moody, 2002; Tangpukdee, Duangdee, Wilairatana, & Krudsood, 2009).

PCR-based amplification assays, including nested PCR (Singh, et al., 1999; Singh, et al., 2004; Snounou, et al., 1993), semi-nested PCR (Rubio, et al., 1999), multiplex PCR (Padley, Moody, Chiodini, & Saldanha, 2003; Patsoula, Spanakos, Sofianatou, Parara, & Vakalis, 2003), real-time or quantitative PCR (qPCR) (Mangold, et al., 2005; Perandin, et al., 2004; Rougemont, et al., 2004; Safeukui, et al., 2008), and

a more recently approach, loop-mediated isothermal amplification (LAMP) have been developed to identify malaria parasites to species level (Han, et al., 2007).

In general, nested PCR has been considered as the molecular gold standard for malaria identification in clinical diagnosis, sub-clinical (asymptomatic) screening, and epidemiology studies (Moody, 2002; Singh, et al., 1999; Singh, et al., 2004; Snounou, et al., 1993; Zimmerman, et al., 2004). Nested PCR has been established not only as the molecular parameters for the sensitivity and specificity of other PCRs, but also for the other diagnostic assays, i.e., microscopy and RDTs. However, this assay is time-consuming and labor-intensive among conventional PCR assays, as it requires a large number of reagents and disposable consumables, given that at least six separate PCRs (one round of genus-specific PCR followed by five separate rounds of species-specific PCRs) and agarose gel electrophoresis are needed to test for the five human malaria infection species. The semi-nested PCR (Rubio, et al., 1999) is based on a combination of techniques of nested PCR and multiplex PCR, which involve two rounds of PCR, i.e., a genus-specific PCR followed by a species-specific multiplex PCR (able to detect four species excluding *P. knowlesi*). Multiplex PCR on the other hands can simultaneously detect more than two plasmodia species in a single tube reaction. To the best of our knowledge, the currently available single round multiplex PCR assays could only differentiate up to two *Plasmodium* species that focused on *P. falciparum* and *P. vivax* (Kho, et al., 2003; Patsoula, et al., 2003) and four species excluding *P. knowlesi* (Padley, et al., 2003).

The real-time PCR or qPCR enables the detection of parasite nucleic acid based on the quantification of the intensity/signal of fluorescence probes [TaqMan and fluorescence resonance energy transfer (FRET) probes] and dyes [SYBR Green and high-resolution melt (HRM) dyes] using a high end real-time thermocycler, thus also allows the parasite quantification, which cannot be achieved by other conventional PCR

---

approaches (de Monbrison, Angei, Staal, Kaiser, & Picot, 2003; Gan & Loh, 2010; Mangold, et al., 2005; Perandin, et al., 2004; Rougemont, et al., 2004; Safeukui, et al., 2008; Shokoples, Ndao, Kowalewska-Grochowska, & Yanow, 2009).

In contrast to conventional and real-time PCRs, the LAMP is a simple and less technically demanding approach that involves isothermal amplification of targeted DNA for identification of each *Plasmodium* species. LAMP results can be detected either by agarose gel electrophoresis or turbidity assessment by the naked eye or with a real-time turbidimeter (Han, et al., 2007). The combination of real-time turbidimeter in the results interpretation allows parasite quantification.

Table 2.8 shows the overview of the three currently available methods in diagnosis of malaria.

Table 2.8: Comparison of diagnostic methods for diagnosing *Plasmodium* infection in blood (adapted from Moody, 2002).

Parameter	Microscopy	RDT	Conventional PCR
Format	Slides with blood smears	Dipstick	PCR reagents
Equipment	Microscope	Kit only	PCR apparatus
Sensitivity (parasites/ $\mu$ l)	Expert ~5-10 Routinely > 50	100-200	< 5
Specificity	All species, except <i>P. knowlesi</i>	<i>P. falciparum</i> only	All species
Parasite density or parasitemia	Yes	Crude estimation	No
Time for result	30-60 minutes	20-30 minutes	Within 24 hours
Test result	Direct visualization of the parasites	Colour changes on antibody coated lines	Agarose gel electrophoresis
Skill level	High	Low	High
Cost/test	Low	Moderate	High
Remarks	Gold standard for routine laboratory	Alternative assay	Nested PCR as molecular gold standard



## 2.7 Immune responses against *Plasmodium* species

In areas of moderate to intense transmission conditions, repeated plasmodial infections (over years of exposure) result in the development of acquired immunity, which is both species- and stage-specific. This partially protective immunity gradually develops with age, thus giving protective effect to older children and adult rather than young children. Therefore, most malaria deaths in Africa occur in young children, whereas in areas with less transmission and low immunity, all age groups are at risk. Acquired immunity is rarely sterile, but rather associated with low-grade parasitemia and episodes of clinical disease throughout life. While acquired immunity never provide complete protection, but it does reduce the risk to severe malaria (Doolan, Dobano, & Baird, 2009). Generally, children born to immune mothers are protected against disease during first six months of their life by maternal antibodies before acquisition of an adequate active immunity. However, acquisition of active immunity to malaria is slow and requires repeated parasite exposure to be maintained. As a result, mortality due to malaria is mainly restricted to early childhood. Furthermore, genetic variability of both the human host and the parasite, parasite-induced immune-suppression and other reasons also account for this instability (Doolan, et al., 2009).

Malaria infection gives rise to host responses which are regulated by both the innate and adaptive immunity as well as establishment of memory (Doolan & Martinez-Alier, 2006; Douradinha & Doolan, 2011). The mechanisms of immune response against malaria parasites are being summarized (Douradinha & Doolan, 2011) in Figure 2.10. Parasites were injected into human peripheral circulation by infected mosquito bite. Some sporozoites enter the hepatocytes initiating liver stage replication. There is evidence that specific antibodies generated by previous exposure or immunization could inhibit subsequent sporozoite invasion of the hepatocyte. Other sporozoites remains in the skin are drained to the nearest lymph node and eventually degraded. Antigen

presenting cells, including dendritic cells, uptake parasite remnants from lymph node and apoptotic bodies of infected hepatocytes and then present the parasite antigens to naive T cells for subsequent immune responses. Malaria-induced cell-mediated immune responses may be protective against both extra- and intra-erythrocytic parasites. Generally, T-cells play a major role in the acquisition and maintenance of protective immunity to malaria. CD4<sup>+</sup> T-cells regulate immune responses to the asexual blood stages of the parasite by cytokine production and providing help for B-cells to produce specific antibodies, whereas CD8<sup>+</sup> T-cells has an important role in the pre-erythrocytic immunity as well as protection against severe malaria. There is also evidence that macrophages, dendritic cells, and NK cells are important effectors of immunity against malaria. The T-cells and B- cells will eventually develop into a memory populations and the process occurs over time, which may induce a stronger response against subsequent infection with same pathogen.

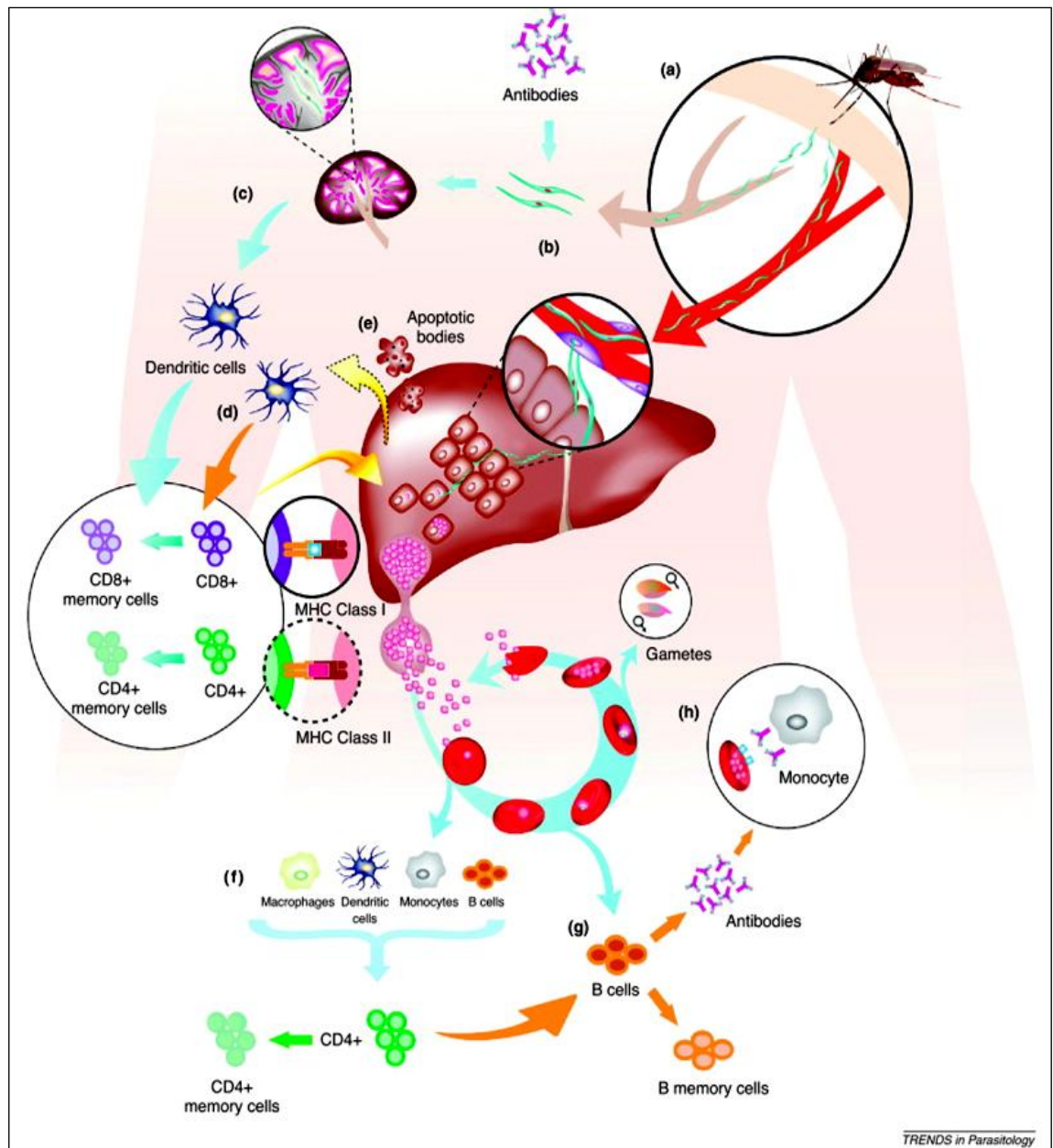


Figure 2.10: Schematic representation of immune responses against *Plasmodium* parasites (adapted from Douradinha & Doolan, 2011).

## 2.8 Treatment and prevention

Malaria is actually a preventable and treatable disease. A variety of drugs have been developed for therapeutic (treatment) and prophylactic (preventive) purposes (Table 2.9). Malaria is currently treated using drugs that kill the parasites and many are derivatives of quinine compound.

Table 2.9: The pharmacology of antimalarials (adapted from WHO, 2010a).

Antimalarial drug	Target of therapy	Examples
Blood schizonticidal drugs	Act on erythrocytic stage of the parasites thereby terminating clinical illness.	Quinine, artemisinins, amodiaquine, chloroquine, lumefantrine, tetracycline, atovaquone, sulphadoxine, clindamycin, proguanil
Liver/tissue schizonticidal drugs	Act on primary tissue forms of plasmodia which initiate the erythrocytic stage. Block further development of the infection.	Primaquine, pyrimethamine, proguanil, tetracycline
Gametocytocidal drugs	Destroy sexual forms of the parasites thereby preventing transmission of infection to mosquitoes.	Primaquine, artemisinins, quinine
Hypnozoitocidal drugs	Act on persistent liver stages of <i>P. vivax</i> and <i>P. ovale</i> , which cause recurrent illness.	Primaquine, tafenoquine
Sporozontocidal drugs	Act by affecting further development of gametocytes into oocytes within the mosquito thus abating transmission.	Primaquine, proguanil, chlorguanil
Chemoprophylaxis	Preventive medications. The choice of chemoprophylaxis varies depending on the species and drug resistance prevalent in a country.	Combination of antimalarial drugs. Use of anti-malarial drugs to prevent the development of malaria.

Prompt and effective treatment of malaria requires a rapid and precise laboratory diagnosis. Over-diagnosis of malaria may lead to improper treatment, wastage of drugs, and also causes the widespread problems with drug resistance amongst the parasites to the currently available drugs. Generally, the effectiveness of antimalarial drugs is varying with different species of the parasite as well as the stages of the parasite's life cycle (Table 2.9). For instance, rapid diagnosis and prompt treatment is paramount for two fatal species, i.e., *P. falciparum* and *P. knowlesi*; whereas, treatment of *P. vivax* and *P. ovale* infections with hypnozoitocidal drugs is essential to eliminate persistent liver stage.

Thus far, effective malaria vaccines are still not available; all currently recommended primary chemoprophylaxis regimens involve continuously taking of the medicine before travel, during travel, and until a period of time after leaving the malaria endemic area. Beginning the prophylactic before travel allows the antimalarial agent to be in the blood before the traveler is exposed to malaria parasites.

Other preventive measures including vector control programmes, such as using of dichlorodiphenyltrichloroethane (DDT) has successfully reduced the malaria transmission; unfortunately, the rapid emergence of insecticide resistance mosquitoes, particularly in Africa have lead to the resurgence of malaria in many countries. Therefore, the best protection is the avoidance of mosquito bites such as remaining in well-screened areas using bed nets, insect repellants, and residual insecticide sprays.

## **2.9 Malaria vaccine development**

Currently, there are still no effective malaria vaccines available. The complexity and multiple life cycle stages as well as a myriad of potential vaccine antigens to each stage are the major challenges in the progression towards efficient malaria vaccine development (Beeson & Crabb, 2007; Todryk & Hill, 2007).

Generally, there are several sites in the malaria life cycle that could be interrupted by vaccine: (i) pre-erythrocytic vaccines in liver stage are directed against schizonts-infected liver cells, thus preventing merozoites release and infection to the vaccinated individual (infection blocking), (ii) erythrocytic vaccines in the asexual blood stage are aim to reduce or eradicate the parasites in the blood-borne forms, thus reduce the severity of malaria infections (antidisease), and (iii) transmission-blocking vaccine inside the mosquito do not protect an individual but rather the community at large based on the fact that the proteins expressed during the sexual stage did not evolve to circumvent the human immune system. As such, antibodies taken up by mosquito during a blood meal can act against these parasites, thereby preventing re-infection of the population. Figure 2.11 show the three strategies for malaria vaccines development.

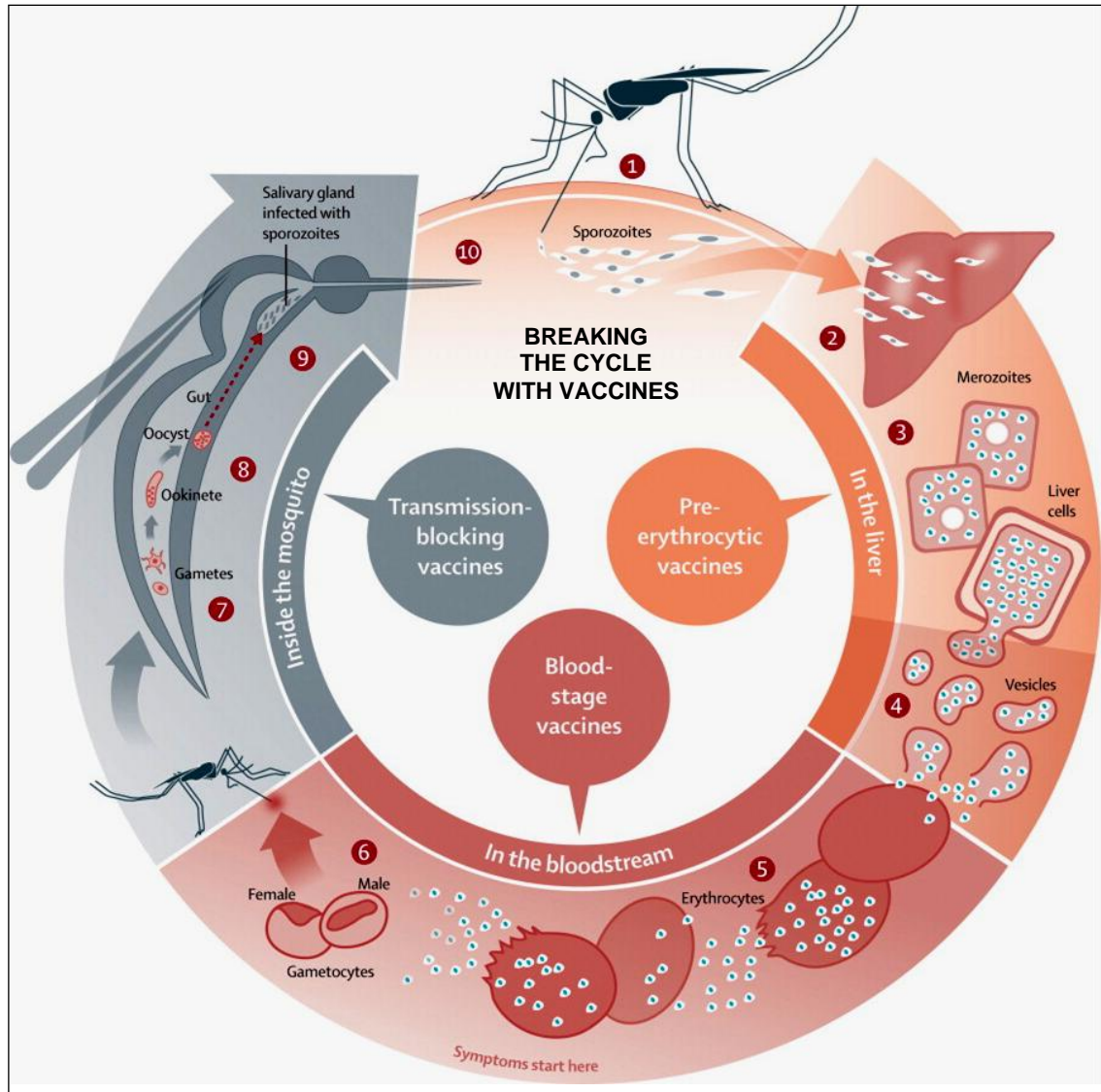


Figure 2.11: Sites in the malaria life cycle that could be interrupted by vaccines (adapted from <http://www.malariavaccine.org/malvac-lifecycle.php>).

Currently, the attenuated whole parasites (sporozoite) immunization and subunit vaccines (recombinant or genetically engineered proteins or antigens from the surface of the parasite) are the two main strategies in malaria vaccine development, both of which show promising results in clinical trials (Vaughan & Kappe, 2012). Figure 2.12 show some of the most potent vaccine candidate antigens that have undergone clinical trials, of which effectively stimulate the host immune responses to destroy or arrest the malaria parasite.

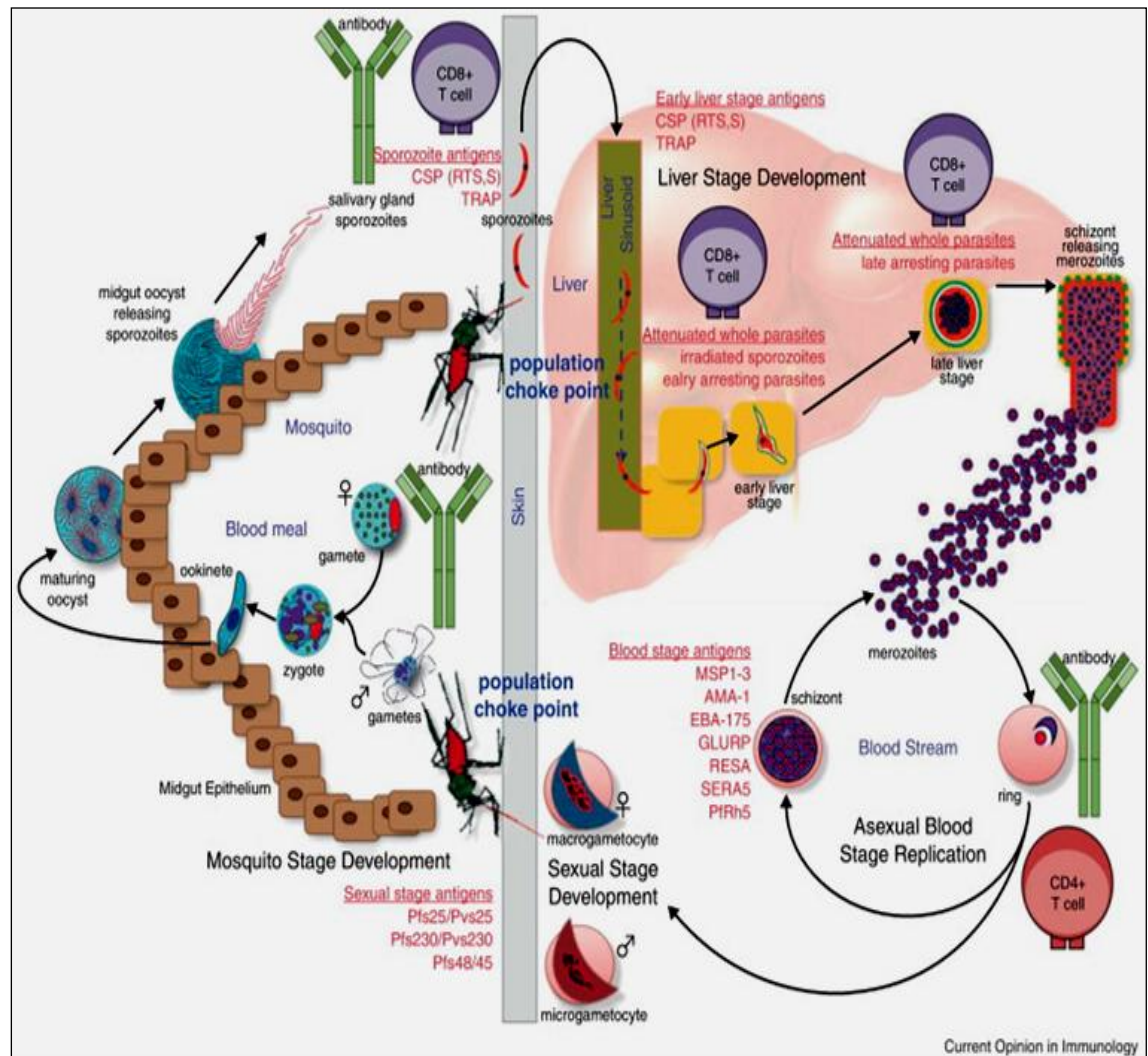


Figure 2.12: The malaria life cycle, parasites, and parasite targets (major antigens) used for vaccine development (adapted from Vaughan & Kappe, 2012).



## 2.10 Genomes and proteome of *Plasmodium* species

The completion of whole genome sequencing of *Plasmodium* species may allow study of the evolution and population biology of the parasite, allow parasite transmission patterns to be characterized, and meantime facilitate the identification of new drug resistance genes, thus opens up new approaches in the development of antimalarial drugs as well as vaccines in order to intervene malaria transmission.

Thus far, three of the most vital human malaria parasites, i.e., *P. falciparum* (Gardner, et al., 2002), *P. vivax* (Carlton, et al., 2008), and *P. knowlesi* (Pain, et al., 2008) nuclear DNA were fully sequenced with the total genome size of 23.3 million bases (Mb), 26.8 Mb, and 23.5 Mb, respectively, that split into 14 linear chromosomes with an overall of more than 50 % of A+T content (81 % in *P. falciparum*, 58 % in *P. vivax*, and 63 % in *P. knowlesi*). Malaria parasites are highly complex, containing over 5,000 coding genes, i.e., 5,403 genes in *P. falciparum*, 5,433 genes in *P. vivax*, and 5,188 genes in *P. knowlesi* (Carlton, et al., 2008; Gardner, et al., 2002; Pain, et al., 2008), most of which encoding surface proteins or antigens expressed throughout several antigenically distinct life cycle forms (Pain, et al., 2008).

Proteome analysis throughout the life cycle within human host of *P. falciparum* (Florens, et al., 2002; Lasonder, et al., 2002) and *P. vivax* (Roobsoong, et al., 2011) have been studied based on conventional 2D gel and mass spectrometry analyses. Differential and stage-specific patterns of gene expression and its products in both host and parasite have been identified, which might open up an insight into the pathogenesis of the parasites and thus provide potential targets for therapeutic and vaccine developments.

### 2.11 *Plasmodium* merozoite

Merozoite stage was characterized by the expression of surface proteins that mediate invasion and immune evasion (Florens, et al., 2002). It is important to understand the molecular details of this process, as this machinery can be a target for both vaccine and drug developments. The merozoite is the infective forms of *Plasmodium* parasite in human host, release at the final stage of pre-erythrocytic and erythrocytic developments due to the rupture of mature liver schizonts as well as erythrocyte schizonts, respectively, and after a short period in the blood stream, they are bind to and invade new erythrocytes. Therefore, the invasive ability of the merozoite into RBC plays a pivotal role in malaria pathogenesis.

In general, antigens of *Plasmodium* are not only presented on the surface of merozoites, some are stored in the apical organelles located at the leading-end of merozoite, which plays a central role in host cell invasion and are responsible for antigenic diversity in these organisms. Merozoites are protected from host immune attack during replication in erythrocytes, however, once release into blood stream at the end of replication cycles; it will consequently stimulate the host immune response (Cowman & Crabb, 2006).

The malaria parasite is the most prominent member of the phylum of Apicomplexa that exhibits an apical complex. Apical complex is make-up of a set of structural components, which have functionally homologous for host cell invasion and mainly located at the anterior end of merozoite, displacing the nucleus and mitochondria towards the posterior end (Figure 2.13). Three distinct types of secretory organelles, i.e., rhoptries, micronemes, and dense granules are found at the apical end of the invasive stages. The conoid, polar rings, and sub-pellicular microtubules are the main cytoskeletal components. Other organelles including nucleus, endoplasmic reticulum, Golgi apparatus, ribosomes, mitochondrion, and apicoplast are all enclosed by a pellicle

(inner membranous structure) (Figure 2.13).

The host cell invasion process is characterized by the initial random attachment of parasite with the target cell, followed by intimate association between the apical end of the parasite and the host plasma membrane, and ultimately parasite forced entry into a host cell (Cowman & Crabb, 2006; Tyler, Treeck, & Boothroyd, 2011) (Figure 2.13). Invasion process is complex, involving sequentially secretion of proteins from specialized secretory organelles that are necessary to aid entry of a host cell (Macraill, Anders, Foley, & Norton, 2011; Tyler, et al., 2011). During invasion, tight junction or so-called moving junction (MJ) is formed due to interaction of a number of parasite proteins and host surface receptors that is visible as a ring of contact under electron micrographs. Parasite entry into parasitophorous vacuole by movement of the junction, followed by the resealing of the parasitophorous vacuole and erythrocytic membranes, while the surface coat remained outside is shedding off (Tyler, et al., 2011).

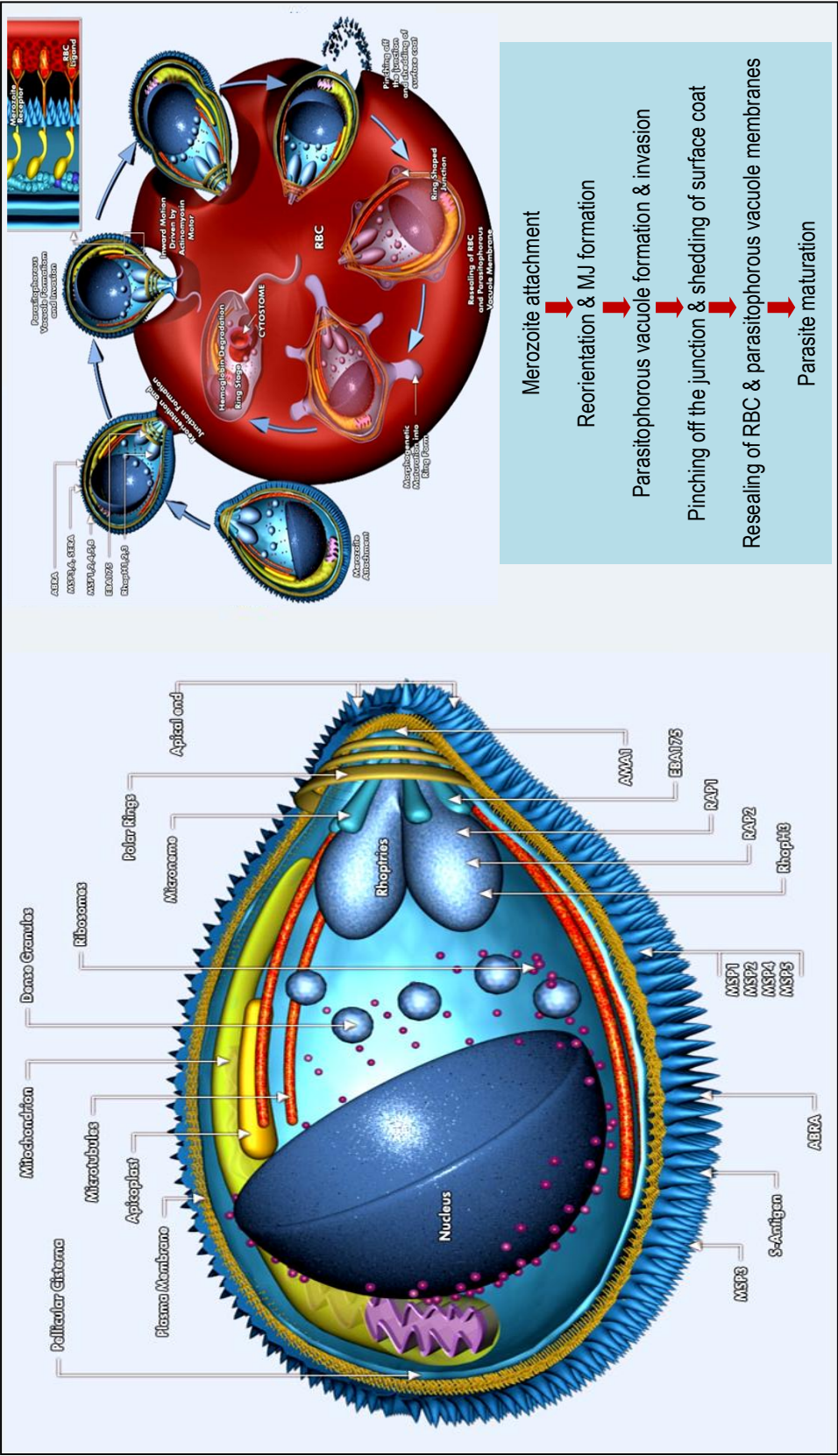


Figure 2.13: Structure of *Plasmodium* merozoite (left) and mechanisms of merozoite invasion (right) (adapted from <http://www.qiagen.com/products/genes%20and%20pathways/Pathway%20Details.aspx?pwdid=423>; <http://www.qiagen.com/products/genes%20and%20pathways/Pathway%20Details.aspx?pwdid=164>).

### 2.11.1 Apical membrane antigen 1 (AMA1)

Numerous molecules that are implicated in the invasion process have been identified in the apical organelles (rhoptry and micronemes) as well as on both merozoite and erythrocyte surfaces. However, only a handful of the molecules are well characterized and the molecular mechanisms involved at each step of invasion are not well understood. Among these molecules, apical membrane antigen 1 (AMA1) was first identified in *P. knowlesi* as an invariant merozoite surface antigen since 30 years ago (Deans, et al., 1982) and is long thought to be involved in RBC invasion by *Plasmodium* merozoites. The AMA1 is well known as a prime malaria vaccine candidate on challenge with blood-stage parasites (Anders, Adda, Foley, & Norton, 2010).

AMA1 protein is encoded by a single essential *ama1* gene present in all *Plasmodium* species. *Ama1* gene encodes this protein in varying length ranged between 556 to 563 amino acids in most *Plasmodium* species, exclusion of *P. falciparum* with approximately 622 amino acids. AMA1 is a microneme protein as where it is located and the expression is abundance in the late schizont stage of the asexual life cycle of the *Plasmodium* parasite. In general, mature AMA1 is a globular, low-abundance, structurally conserved type I integral membrane (transmembrane) protein (Hodder, et al., 1996). The AMA1 protein comprises of several regions including a prosequence, an ectodomain (extracellular domain) that build up by three distinct domains (a relatively N-terminal domain I, a central domain II, and a C-terminal domain III), a single transmembrane region, and a small C-terminal cytoplasmic domain. The ectodomain has 16 interspecies conserved cysteine residues that linked to form eight intramolecular disulfide bonds, in where three are located in domain I and domain III, and two in domain II, which are crucial for structural stabilization and domains discrimination (Bentley, 2006; Cowman & Crabb, 2006; Hodder, et al., 1996) (Figure 2.14).

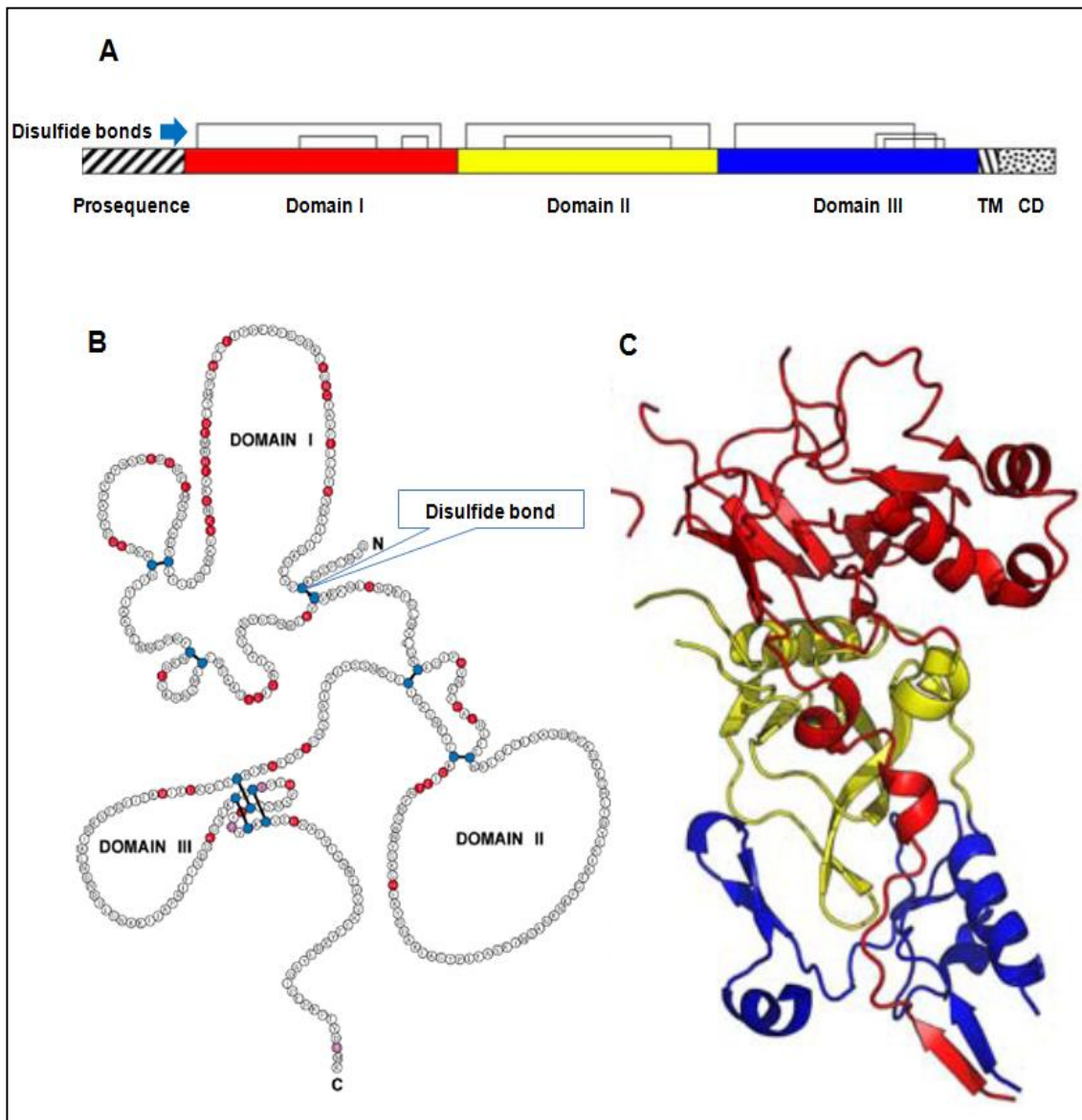


Figure 2.14: Structure of AMA1. (A) The primary structure of AMA1. TM indicates transmembrane region and CD indicates C-terminal cytoplasmic domain. (B) The primary sequence of *Plasmodium* AMA1 ectodomain, showing the three putative domains, I, II, and III, and the location of the eight disulphide bridges. (C) Three-dimension crystal structure of the PvAMA1 ectodomain (1W8K), showing the organization of domains I, II, and III shaded as A (modified from Hodder, et al., 1996 and MacRaild, et al., 2011).

The PfAMA1 molecule is synthesized as a 83-kDa precursor and shortly after synthesis, the N-terminal prosequence is cleaved to form 66-kDa polypeptide (Narum & Thomas, 1994), whereas other *Plasmodium* species is synthesized as a 66 kDa protein, which is translocated to the merozoite surface via the rhoptry neck prior to the initiation of invasion. At or around the point of invasion, AMA1 molecule is then proteolytically processed into small fragments in the form of entire AMA1 ectodomain with the size of 44-48 kDa by a single cleavage of 29 residues distal to the transmembrane domain (Collins, et al., 2007).

Basically, AMA1 in *Plasmodium* species is expressed in two critical life-cycle forms, the sporozoites and the merozoite, both of which invade human hepatocytes and erythrocytes, respectively (Triglia, et al., 2000; Silvie, et al., 2004). The role of AMA1 in sporozoites has not been well studied. In contrast, AMA1 in merozoites is one of the well-characterized and functionally important amongst the merozoites membrane proteins that responsible for erythrocytes invasion. The AMA1 knockout strains are not viable, implying that AMA1 is crucial in the parasite life cycle (Triglia, et al., 2000).

Despite its low abundance compared with other merozoite proteins, AMA1 is a high immunogenic protein in natural human infections. Although merozoites are extracellular for only a short time, surface antigens are subjected to immune attack and antibodies against AMA1 blocking the invasion of both hepatocytes by sporozoites (Silvie, et al., 2004) as well as erythrocytes by merozoites (Boyle, et al., 2010).

The three-dimensional structure of AMA1 obtained either by X-ray crystallography or nuclear magnetic resonance (NMR) spectroscopy based on complete or truncated forms of AMA1 extracellular domains from *P. vivax* (Pizarro, et al., 2005) and *P. falciparum* (Bai, et al., 2005; Feng, et al., 2005; Nair, et al., 2002) are currently available in Protein Data Bank (PDB) (Table 2.10).

Table 2.10: Protein Data Bank entries of three-dimensional structure of *Plasmodium* AMA1.

Recombinant AMA1	Domain/s	Method	PDB entry	Year	References
PfAMA1	III	NMR	1HN6	2000	Nair, et al., 2002
PfAMA1	II	NMR	1YXE	2005	Feng, et al., 2005
PfAMA1	I-II	X-ray	1Z40	2005	Bai, et al., 2005
PvAMA1	I-III	X-ray	1W8K and 1W81	2005	Chesne-Seck, et al., 2005; Pizarro, et al., 2005

Protein Data Bank (PDB): <http://www.wwpdb.org/>

## 2.12 Heterologous expression of the recombinant protein

Generally, protein expression applied the principle of recombinant DNA technology by cloning a fragment of target coding DNA (cDNA) into a plasmid vector, followed by transformation or transfection and recombinant expression of the target protein into a heterologous host cell in the form of fusion protein with specific ‘tag’ sequences that can further be retrieved by affinity chromatography. Nowadays, heterologous expression of proteins has been widely exploited for the bioproduction of many therapeutic proteins as well as antigens for molecular biological assays. There are several different types of expression host systems, e.g., prokaryotic system mainly focused on *Escherichia coli* (*E. coli*) cells, baculovirus system based on insect cells, yeast system i.e., *Pichia pastoris* and *Saccharomyces cerevisiae*, etc. Heterologous expression of plasmodial protein is principally carried out for preparative purposes, for example, crystallization and structure studies, preparation for recombinant vaccines, drug screening, antigen preparation, enzymatic and other *in vitro* functional assay, etc (Birkholtz, et al., 2008; Fernandez-Robledo & Vasta, 2010). The expression systems applied in plasmodial studies have been reviewed elsewhere (Birkholtz, et al., 2008; Fernandez-Robledo & Vasta, 2010).



### 2.12.1 Expression of protein in *E. coli*

In general, *E. coli* remains as a predominant host for the heterologous expression of recombinant proteins in many research, diagnostic, and pharmaceutical studies. Bacterial system is the most preferable system due to simple operations control without sophisticated laboratory equipment, low costs, high protein yield, short growth time, and convenient expression. Furthermore, there is a large selection of vectors and host strains that are currently available.

The limitation of bacterial system is in its inability to perform post-translational modifications. Moreover, most overexpressed proteins are frequently found in an insoluble form called inclusion body (IB) that lack in biological activity. IB is aggregates form of partially folded or misfolded proteins, which have hydrophobic or sticky regions exposed that can interact with other similar proteins. The IB is dense and usually deposited as dark intracellular particles with 0.2 - 0.5  $\mu\text{m}$  in diameter under microscopy observation. The main component of IB is recombinant protein and this aggregated protein is usually protected from proteolytic attack. In some circumstance, IB also allows expression of toxic proteins that might be harmful to host cells. Since the target protein is relatively pure in washed IB, the challenge is not so much to purify the target, but rather to solubilize an IB (Burgess, 2009). Nowadays, there has been an increase in products and protocols, i.e., expression, cell disruption, IB isolation and purification, and IB solubilization, which are generally applicable to the IB issue. The downstream process to recover the recombinant protein into its native structure is known as refolding.

### **2.12.2 Refolding of insoluble and incorrectly folded proteins**

Following the solubilization of IB with denaturing agent (either 4-8 M urea or 4-6 M guanidinium hydrochloride) and reducing agent (1-10 mM DTT; if protein contains disulphide bonds), recombinant protein can be refolded to regain full biological function by slowly removing denaturing agents that allow folding of protein and formation of the correct intramolecular associations. Refolding can be straightforward for small proteins and for proteins that do not contain disulfide bridges, however, it is challenging in many cases. Optimal conditions for refolding are protein dependent and unpredictable. However, much refolding data is available through the literatures and has been compiled in databases, e.g., REFOLD database (<http://refold.med.monash.edu.au/>). Successful refolding is often dependent on the careful optimization of a number of parameters such as protein concentration, temperature, reaction time, disulfide exchange reagents as well as buffer additives. Dialysis, dilution, on-column refolding are several refolding techniques (Burgess, 2009; Cabrita & Bottomley, 2004).

Protein aggregation is often clearly visible when refolding conditions are not optimized. Therefore, virtual inspection can be used to quickly determine which samples warrant further analysis. Turbidity measurements at 390 nm may also be performed to quantitatively measure aggregation (Tresaugues, et al., 2004; Vincentelli, et al., 2004). The most reliable and informative way to assess the quality of protein is by using a known activity assay. However, most proteins being studied have no known function and structure or have very difficult biological assay. Therefore, the samples can also be analyzed using size-exclusion chromatography as well as circular dichroism or fluorescence techniques, which the spectrum will provide significant information about a protein's secondary and tertiary structures. However, the latter methods can be labor-intensive and difficult to interpret, and the protein sample should be > 90 % pure in a compatible buffer. The nature of disulphide bonds can be achieved by the most

straightforward method using reducing and non-reducing SDS-polyacrylamide gel electrophoresis (PAGE). The used of thiol specific dyes (Ellman's reagent) and mass spectrometry are all other techniques that were also employed (Cabrita & Bottomley, 2004).

### 2.13 Protein-protein interactions

The erythrocytic stages of the malaria parasite are responsible for the clinical symptoms associated with the infection. Therefore, drugs and vaccine against these stages would act therapeutically by reducing the severity of the clinical symptoms (Richards & Beeson, 2009). Currently, it is increasingly clear that a greater understanding of the molecular interaction between the parasite and its host would assist in the development of new therapeutics and most importantly, a vaccine for long term sustainable reduction in the global burden of malaria.

There are several methods available for studying the protein-protein interactions and the X-ray crystallography is a gold standard method, which allows direct three-dimensional (3D) view of the interaction between the two compounds such as antigen and antibody. However, this method is time-consuming, expensive, and technically challenging that requires large amount of homologous and highly purified native protein. Three-dimensional structures of *Plasmodium* surface proteins, such as AMA1, merozoite surface antigen 1 (MSP1), erythrocyte-binding antigen 75 (EBA175), duffy-binding-like (DBL), and surface protein 25 (P25) created either by X-ray crystallography or NMR spectroscopy in structural studies are currently available in Protein Data Bank (<http://www.wwpdb.org/>) (Bentley, 2006). Phage display technique is an alternative approach that allows large scale screening and identifying protein-protein, protein-peptide, and protein-DNA interactions. Phage display technology is comparably faster and relatively inexpensive interaction assay compared with 3D structuring technology.

### 2.13.1 Phage display technology

*In vitro* displaying random peptides on the surface of phage was an idea derived from George Smith in the year 1985, when he demonstrated the display of foreign peptides on filamentous phage by fusing the peptide of interest onto gene III of filamentous phage (Smith, 1985). Phage display is a simple functional genomic methodology for screening and identifying protein-protein interaction that involves the construction of a phage library by inserting DNA fragments into phage or phagemid genomes, followed by assembly of peptide libraries, which contains billion of short, variable amino acid sequences that are displayed on the surface of phage particles, which can then be panned for by enabling the phage to interact with selected immobilized targets that have been identified, i.e., recombinant protein (that has interest as drug target) and/or antibodies (Mullen, Nair, Ward, Rycroft, & Henderson, 2006). This creates a direct physically linked between the single-stranded DNA (ssDNA) sequences in the phage genome and their encoding peptide sequence displayed on the surface (Wang & Yu, 2004).

With the further improvement and adaptation of this technology, thus far, there is arrays of peptide libraries that have been established (Figure 2.15A). Random peptide libraries are the most common and created from synthetic random degenerate oligonucleotide inserts. Those libraries are universal in nature and suitable for various applications and field of studies on protein-protein interactions, especially to identify linear antigenic epitopes (Mullen, et al., 2006). The only limitation is that the peptide sequences discovery from this type of libraries might not representative to or found within the antigen or intact pathogen (Mullen, et al., 2006). Antibody libraries are created from immunoglobulins and express commonly as scFv or Fab fragments (Barbas, Burton, Scott, & Silverman, 2001). Whereas, natural peptide libraries display natural peptides and proteins created from randomly fragmented DNA from the

genomes of selected organisms (Lanzillotti & Coetzer, 2008). The peptides or proteins selected from natural peptide libraries are more significant in the stimulation of immunity response that cross-reacts with native pathogens and thus can be serve as promising subunit vaccines (Matthews, Davis, & Smith, 2002; Mullen, et al., 2006). For instance, the *Plasmodium* cDNA library (Lauterbach, Lanzillotti, & Coetzer, 2003) and AMA1 peptide library (Coley, et al., 2001) are two examples of natural peptide libraries constructed from *P. falciparum*.

The phage display cycle is simple as shown in Figure 2.15B and 2.15C: (i) A library of variant DNA sequence encoding short peptides is created, cloned into phage or phagemid genomes as fusions to coat protein gene, and phage particles are produced. (ii) The phage library displaying variant peptides is exposed to a target molecule immobilized onto plate and phages with appropriate specificity are captured. (iii) Non-binding phages are then washed away. (iv) Bound phages are eluted by conditions that disrupt the interaction between the displayed peptides and the target. (v) Eluted phages are infected into host bacterial cells and thereby amplified. (vi) Amplified phage library is then used for subsequence biopanning cycle, usually repeated between three to five rounds to generate a library that is greatly enriched in the number of phage with binding affinity to the immobilized protein. (vii) Phage populations may be selected and analyzed individually (Willats, 2002). The possibility of individual phage binds either to target protein or background can be further confirmed by established phage ELISA as well as phage Western blotting assays. The interactions between two proteins can be predicted through various computer program and databases of native sequences, e.g., mimox (Huang, Gutteridge, Honda, & Kanehisa, 2006) and mimoDB (Huang, et al., 2012) in mimotope mapping, and 3D-Epitope-Explorer (3DEX) (Schreiber, Humbert, Benz, & Dietrich, 2005) in epitope mapping etc.

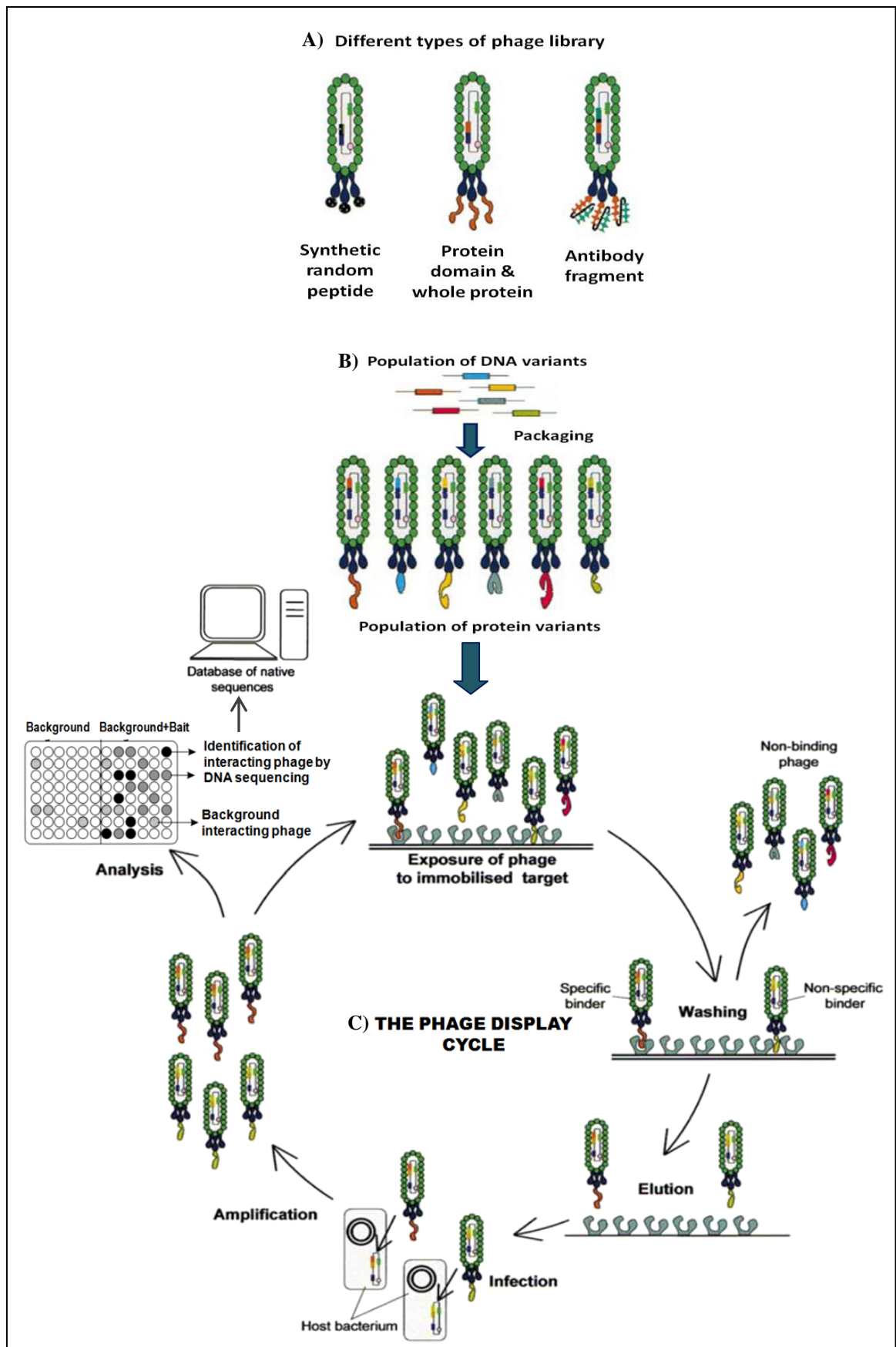


Figure 2.15: Phage display. (A) Different types of phage library. (B) Construction of phage library. (C) The phage display cycle (adapted from Willats, 2002).

Phage display is a powerful and cost effective tool, which is widely used for the investigation of protein-protein interactions, immunoassay development, identification of peptide agonists and antagonists for receptors, identification of targets for the inhibition, elucidation of neutralizing sites, investigation into pathogenesis of disease, identification of peptide drug and vaccine candidates, and the isolation and engineering of recombinant antibodies (Mullen, et al., 2006; Wang & Yu, 2004).

### **2.13.2 Phage display technology and applications in malaria research**

Phage display is a widely applicable technique used in studies of protein functions and biological process in malaria especially for probing and characterizing the molecular host-parasite interactions, and thus helps to aid in the identification of peptide ligands as well as mapping of the epitope and/or mimotope of monoclonal and polyclonal antibodies, which could potentially improve diagnostic and therapeutic value.

Generally, ligand is refer to a substance, usually small molecule that reacts to form a complex with another biomolecule to serve a biological purpose or rather it is a signal triggering molecule, binding to a site of a target protein. Ligands include substrates, inhibitors and activators. Ligand binding to a receptor alters its chemical conformation (3D shape) and the conformational state of a receptor protein determines its functional state. The tendency of binding is so-called affinity. Epitope is defined as contracting points of any molecular interaction in biological system and is more often used to describe the region of antigen that involve in specific binding to an antibody (B- or T-cell epitopes) (Lanzillotti & Coetzer, 2008; Mullen, Nair, Ward, Rycroft, & Henderson, 2006; Wang & Yu, 2004). Epitope mapping is initially termed to describe all activity on determination of the sequence or structure of a given epitope towards antibodies. Nowadays, epitope mapping is no longer limit to immunology study, and is instead being applied in all fields of biology (Wang & Yu, 2004).



In an attempt to provide insight into the biological function and immunological properties which lie behind the targeted *Plasmodium* proteins, many studies have been done utilizing phage display libraries and have been reviewed and summarized (Lanzillotti & Coetzer, 2008). The large repertoire of possible applications of phage display has led to it being utilized in the combat against malaria in several ways. Phage display human antibodies library was used to identify the antibodies against *P. falciparum* MSP1 and thus inhibit the parasite growth (Sowa, et al., 2001), to identify antibody that recognizes parasitized erythrocytes (Wajanarogana, Prasomrothanakul, Udomsangpetch, & Tungpradabkul, 2006), to elucidate human antibody response to sporozoites protein (Chappel, Rogers, Hoffman, & Kang, 2004), and peptides derived from human antibodies library that bind to mosquito midgut antigens have great value as transmission-blocking agents (Foy, et al., 2002). Random peptides libraries were used to identify peptides that block the invasion and development of *P. falciparum* in *Anopheles gambiae* (Ghosh, Moreira, & Jacobs-Lorena, 2002; Ghosh, Ribolla, & Jacobs-Lorena, 2001), or merozoite invasion of human erythrocyte (Harris, et al., 2005; Keizer, et al., 2003; Li, et al., 2002), as well as those targets infected erythrocytes (Eda, Eda, & Sherman, 2004). The only study on biopanning of a *P. falciparum* cDNA library against human erythrocyte-membrane proteins successfully identified seven malaria proteins that are potentially involved in the entry into or exist from human erythrocyte by *P. falciparum* and such proteins could become vaccine targets (Lauterbach, et al., 2003).

## **CHAPTER THREE: MATERIALS AND METHODS**

### **3.1 Chemical agents and materials**

All chemical agents used in this study were analytical grade or highest grade obtained from various companies. Disposable materials, commercial kits, and equipments were listed in Appendix 1.

### **3.2 Buffers, stock solutions, culture media, and other reagents**

#### **3.2.1 Buffers and stock solutions**

Water was purified by a Milli-Q apparatus (Millipore). Buffers and stock solutions were prepared as described in Appendix 2.

#### **3.2.2 Culture media, antibiotics, and enzyme substrates**

In general, all culture media (agar or broth) used in bacteria cultivation and phage amplification were made as described in Appendix 2N. All culture media were autoclaved sterilized prior used. The antibiotics and enzymes substrates are heat labile, thus were filter-sterilized through 0.25  $\mu$ M syringe filter.

#### **3.2.3 PCR reagents and oligonucleotide primers**

The reaction buffers supplied together with DNA polymerase were listed in Appendix 3. All oligonucleotide primers with TOP purified PCR grade used in colony PCR, multiplex PCR, nested PCR, sequencing, and protein expression were synthesized from 1<sup>st</sup> Base Sdn Bhd (Malaysia). All primers were dissolved in TE buffer (10 mM Tris-HCl, 1 mM EDTA, pH 8) to a final concentration of 400  $\mu$ M as stock solution and further diluted into 50  $\mu$ M as working solution. All PCR reagents and primer solutions were stored at -20 °C.

### **3.2.4 Restriction enzymes**

Restriction enzymes (*Bam*HI and *Spe* I) together with reaction buffers were purchased from Fermentas (USA). All REs and reaction buffers were stored at -20°.

## **3.3 General Methods**

### **3.3.1 Sample collection**

A total of 226 whole blood samples were collected from patients suspected with malaria and admitted to University of Malaya Medical Center (UMMC), Kuala Lumpur (n=54) and Telupid Health Clinic, Sabah (n=172) from 2008 to 2010. An aliquot of each sample was used for routine biological diagnostic in the laboratories and the remaining was extracted to obtain the total genomic DNA. Another 20 whole blood samples were also collected from healthy individuals as negative controls. Written informed consent was obtained from each patient and healthy donor before blood sample was taken (Appendix 11). The study was approved by the Ethics Committee reviewer board of University Malaya Medical Centre (UMMC), Malaysia (MEC reference number: 709.2) (Appendix 10).

### 3.3.2 Parasitemia estimation

For suspected malaria patients, thin and thick blood films were prepared at the time of admission prior to anti-malaria treatment. Thin/thick films were stained with 10 % Giemsa solution and examined at  $\times 1,000$  under oil immersion by experienced microscopists at each hospital and the levels of parasitemia were estimated, whereby,

+ = 1-10 parasites per 100 thick film fields,

++ = 11-100 parasites per 100 thick film fields,

+++ = 1-10 parasites per single thick film field, and

++++ =  $> 10$  parasites per single oil-immersion thick film field.

In present study, the parasite counts were estimated with a slightly modification, whereby,

+ = 4-40 parasites/ $\mu\text{l}$ ,

++ = 41-400 parasites/ $\mu\text{l}$ ,

+++ = 401-4000 parasites/ $\mu\text{l}$ , and

++++ =  $> 4000$  parasites/ $\mu\text{l}$  of blood.

Blood films were defined as negative if no parasite was observed in 300 microscopic fields. The data from microscopy (species and parasite counts) was retained for subsequent comparative analysis.

In the PCR sensitivity validation, the parasitemia was counted in at least 25 microscopic fields of thin blood smear (WHO, 2010b). The total parasite count/ $\mu\text{l}$  of blood was calculated as follows:

$$\frac{\text{number of observed asexual parasites} \times \text{total RBC count}/\mu\text{l}}{\text{total number of RBC scanned in 25 microscopic fields}} = \text{parasite}/\mu\text{l of blood}$$

### 3.3.3 Malarial DNA extraction from blood sample

Whole blood samples were equilibrated to room temperature and centrifuged at  $800 \times g$  for 15 minutes. A total of 200  $\mu$ l infected red blood cells (iRBCs) was drawn from the bottom of EDTA-coated blood tube into a 1.5 ml microcentrifuge tube. Parasites were isolated by saponin lysis of iRBCs according to Goman, et al. (1982). With saponin, the membrane of erythrocytes is selectively lysed, whereas the parasitophorous vacuole with the parasite inside remains undamaged. In general, iRBCs sample was centrifuged for 10 min at  $6,000 \times g$  and the supernatant was discarded. Then, the pellet was washed once in 1 ml of cold PBS (pH 7.2) and centrifuge at  $6,000 \times g$  for 10 minutes. The pellet was resuspended in 1 ml of PBS and 10  $\mu$ l of 5 % (w/v) saponin was added at a final concentration of 0.05 % and gently mixed. After that, tube was incubated at room temperature for 10 minutes and immediately centrifuged at  $6,000 \times g$ . The malarial pellet was then washed twice with PBS buffer followed by centrifugation at  $6,000 \times g$  for 15 minutes to remove the excessive saponin. Washed pellet was then dissolved in 200  $\mu$ l PBS and DNA was extracted using QIAamp<sup>®</sup> DNA Mini kit (Qiagen, Germany), according to the manufacturer's protocol.

In general, 20  $\mu$ l of proteinase K ( $> 600$  mAU/ml) and 4  $\mu$ l of RNase (100 mg/ml, Invitrogen) were added into the pellet and mixed by pipetting. After that, 200  $\mu$ l of lysis AL buffer was added to the sample and immediately mixed by vortex for 15 seconds. The solution was then incubated at  $65^\circ\text{C}$  for 10 minutes using heat block (Major Science). Then, the tube was centrifuged and 200  $\mu$ l of absolute ethanol was added to the sample and mixed again by brief vortex for 15 seconds. The mixture was applied to the QIAamp mini spin column, which placed in a 2 ml collection tube and centrifuged at  $6,000 \times g$  for 1 minute. The spin column was placed in a clean 2 ml collection tube and 500  $\mu$ l of AW1 buffer was added, followed by centrifugation at  $6,000 \times g$  for 1 minute. Again, the spin column was placed into clean collection tube

and 500  $\mu\text{l}$  of AW2 buffer was added followed by centrifugation at  $20,000 \times g$  for 3 minute. The QIAamp spin column was placed in a clean 1.5 ml microcentrifuge tube for DNA elution. All collection tubes containing the filtrate were discarded. Then, 100  $\mu\text{l}$  of AE buffer or  $\text{dsH}_2\text{O}$  was added to the column and incubated at room temperature for 5 minute, followed by centrifugation at  $6,000 \times g$  for 1 minute. On the other hand, DNA from 20 healthy controls was extracted directly from 200  $\mu\text{l}$  whole blood sample utilizing the same kit without saponin adding.

The DNA sample was eluted in 100  $\mu\text{l}$  of AE buffer, thus corresponding to approximately 2  $\mu\text{l}$  of blood per  $\mu\text{l}$  of DNA. The concentration and purity of DNA were determined using NanoPhotometer<sup>TM</sup> (IMPLEN, Germany). DNA was stored at  $-20\text{ }^{\circ}\text{C}$  and 1.5  $\mu\text{l}$  was used for each PCR assay.

### 3.3.4 Preparation of *Escherichia coli* (*E. coli*) competent cells

Chemically-treated competent *E. coli* cells, Top 10 and C-Max- $\alpha$  used in general DNA cloning and BL21-CodonPlus (DE3)-RIL that contains supplementary rare tRNA expression plasmid pRIL (Stratagene) used in protein expression were prepared freshly prior to DNA cloning.

In general, a single colony of either Top 10 or C-Max- $\alpha$  *E. coli* was inoculated into 10 ml of LB broth. Whereas BL21-CodonPlus (DE3)-RIL *E. coli* was inoculated into 10 ml LB broth containing 34  $\mu$ g/ml of chloramphenicol for pRIL selection. The culture was grown overnight at 37 °C.

Then, 1 ml of the overnight culture was inoculated into 100 ml of LB broth and incubated at 37 °C with shaking at 200 rpm for two hours until the culture reach the exponential phase ( $OD_{600}$  reached 0.5), determined by NanoPhotometer<sup>TM</sup> (IMPLEN, Germany). The culture was transferred to 50 ml Falcon tube and centrifuged at  $3,000 \times g$  for 10 minutes. Supernatant was discarded and the cell pellet was subsequently incubated on ice for 10 minutes. The chilled cell pellet was then resuspended in 30 ml ice-cold 0.1 M  $CaCl_2$  and incubated on ice for one hour followed by centrifugation at  $3,000 \times g$  for 10 minutes. Competent cells are very fragile, thus resuspension in 1 ml of ice-cold 0.1 M  $CaCl_2$  using disposable Pasteur pipette has to be done gently. The competent cells could be used immediately or stored at -80 °C with 15 % (v/v) glycerol for further experiment. For -80 °C storage, the competent cells were aliquoted into 100  $\mu$ l working volume in microcentrifuge tubes and immediately frozen with chilled absolute ethanol (kept at -80 °C) prior to transfer to -80 °C freezer.

### 3.3.5 Maintenance and recovery of bacteria

In general, various strains of *E. coli* were grown overnight in 10 ml of LB broth [1 % (w/v) Tryptone, 0.5 % (w/v) Yeast extract, 0.17 M NaCl] at 37 °C. The cell culture was centrifuged at  $1,000 \times g$  for 1 minute and pelleted cells was resuspended in 2 ml of LB broth containing 15 % (v/v) glycerol and stored at -80 °C in two aliquots. Culture was recovered by scraping off some frozen cells with a sterile loop to subculture the bacteria into either a liquid broth or streaked on an agar plate from the stock culture.

### 3.3.6 Plasmid extraction

Bacteria containing plasmid DNA was inoculated in 10 ml of LB containing appropriate antibiotic. Culture was incubated overnight at 37 °C with shaking at 200 rpm. Plasmid DNA was isolated from *E. coli* culture using HiYield Plasmid Mini Kit (Yestern Biotech, Taiwan) according to manufacturer's instructions. In general, 1.5 ml of overnight culture was transferred into a microcentrifuge tube and centrifuged at  $14,000 \times g$  for 1 minute and supernatant was discarded. Pellet was resuspended in 200  $\mu$ l of PD1 buffer by vortex. Then, 200  $\mu$ l of PD2 buffer was added to the suspension and mixed gently by inverting the tube 10 times followed by incubation at room temperature for 2 minutes until the lysate was clear. Three hundred  $\mu$ l of PD3 buffer was added to neutralize the lysate and mixed by inverted the tube 10 times, followed by centrifugation at  $14,000 \times g$  for 3 minutes. Less than 800  $\mu$ l of supernatant of the clear lysate was aspirated using pipette tip without disturbing the pellet and was then applied to the PD column placed in 2 ml collection tube. The spin column was centrifuged at  $6,000 \times g$  for 30 seconds. The flow through in the collection tube was discarded and the spin column was placed back in the collection tube. Four hundred  $\mu$ l of W1 buffer was added to the PD column and centrifuged at  $6,000 \times g$  for 30 seconds. The flow through was discarded and 600  $\mu$ l of W2 buffer was added to PD column and centrifuged at



6,000 × g for 30 seconds. The flow through was discarded and centrifuged at 14,000 × g for extra 2 minutes to dry the column matrix. Dried PD column was placed in a clean microcentrifuge tube and 50 µl of Elution buffer or sdH<sub>2</sub>O was added to the center of column matrix and let it stand for 2 minutes until Elution buffer or sdH<sub>2</sub>O was fully absorbed by the matrix. The plasmid DNA was then eluted by centrifugation at 14,000 × g for 2 minutes. The plasmid concentration and purity were determined using a nanospectrometer (IMPLEN, Germany). Plasmid DNA was then stored at -20 °C.

### **3.3.7 Determination of DNA concentration**

The concentration of extracted DNA was determined by using a nanospectrometer (IMPLEN, Germany). Concentration of double-stranded DNA (ng/µl) and single-stranded DNA (ng/µl) were calculated from the absorbance at 260 nm ( $A_{260}$ ), using the following equation (Sambrook & Russell, 2001):

$$\text{Concentration} = A_{260} \times 1 \text{ absorption unit at } A_{260} \times \text{dilution factor}$$

One absorbance unit at 260 nm is equal to 50 ng/µl of double stranded DNA and 38 ng/µl of single stranded DNA. Purity of DNA was determined by calculation the ratio of  $A_{260}$  to  $A_{280}$ , and pure DNA has an  $A_{260}/A_{280}$  ratio of 1.7-1.9.

### **3.3.8 Gel electrophoresis**

#### **3.3.8.1 Agarose gel electrophoresis**

Plasmid DNA, PCR products, and RE digested samples were electrophoresed on agarose gel (1 to 3 % w/v) stained with EtBr in 1× TBE buffer [90 mM Tris-borate, 2 mM EDTA (pH 8)]. The DNA fragments were visualized under UV transilluminator and photographed using a gel documentary system (Major Science).

### 3.3.8.2 SDS-polyacrylamide gel electrophoresis (SDS-PAGE) and Coomassie Blue protein staining

SDS-PAGE was carried out using MiniProtean II apparatus (Bio-Rad). In general, protein sample was mixed with equal volume of 2× Laemmli sample buffer [0.125 M Tris-HCl, 4 % (w/v) SDS, 20 % (v/v) Glycerol, 0.02 % (w/v) Bromophenol Blue, pH 6.8]. There were two types of SDS-PAGE, i.e., reduced and non-reduced with presence or absence of reducing agent ( $\beta$ -mercaptoethanol) in sample buffer, respectively. The reduced sample was pre-heated at 95 °C for 10 minutes and then cooled on ice immediately before loading, whereas, non-reduced sample was loaded directly into gel without pre-heat step.

Generally, 10  $\mu$ l of sample mixture was loaded per lane. The samples were electrophoresed on 12 % SDS-polyacrylamide separating gel [12 % (v/v) polyacrylamide ready-mix solution, 375 mM Tris-HCl (pH 8.8), 0.1 % (w/v) SDS, 0.08 % (w/v) APS, 0.8 % (v/v) TEMED] with upper stacking gel [4.5 % (v/v) polyacrylamide ready-mix solution, 125 mM Tris-HCl (pH 6.8), 0.1 % (w/v) SDS, 0.1 % (w/v) APS, 0.001 % (v/v) TEMED] in 1× SDS electrophoresis buffer [50 mM Tris-base (pH 8.3), 50 mM glycine, 0.02 % (w/v) SDS] at 150 V for 80 minutes. Spectra™ Multicolor Broad Range Protein Ladder (10 – 260 kDa) (Fermentas) was used as the molecular weight.

Coomassie Blue staining process was performed in a small plastic container with gentle shaking on an orbital rotary (Major Sciences). The resolved polyacrylamide gel was rinsed three times in distilled water for 5 minutes to remove the excessive SDS and stained with Bio-Safe™ Coomassie G-250 stain (Bio-Rad) for 1 hour, and then the stain was discarded. This was followed by destaining with distilled water for 30-60 minutes until the resolving protein bands on gel were clearly visible. The result was then documented using ImageScanner III (GE Healthcare).

### **3.3.9 DNA purification from gel**

The QIAquick gel extraction kit (Qiagen, Germany) was used to purify PCR amplified DNA. All reactions were performed as described by the manufacturer's instructions.

PCR amplified band of expected size was excised from the 1.5 % (w/v) agarose gel with a clean and sharp scalpel and the gel slice was weighed. Three volumes of QG buffer was added to one volume of gel excised (100 mg = ~ 100 µl) and incubated at 50 °C for 10 minutes accompanied with brief vortexing every 2 minutes to dissolve the gel. One volume of absolute isopropanol was added to the sample and mixed. The sample was then applied to the column that placed in a 2 ml collection tube and centrifuged at  $17,900 \times g$  for 1 minute. The flow-through was discarded. An additional 0.5 ml of QG buffer was added and centrifuged for another 1 minute and the flow-through was discarded. A 0.75 ml of PE buffer was added to wash the column, centrifuged for 1 minute and flow-through was then discarded. This was followed by centrifugation for 1 minute to remove the residual of ethanol from buffer PE. Later, the column was placed into a clean 1.5 ml microfuge tube. Thirty µl of EB buffer (10 mM Tris-Cl, pH 8.5) was added to the center of the column and the column was left standing for 1 minute followed by centrifugation for 1 minute to elute the DNA. The purified DNA was then used in DNA cloning or stored at -20 °C.

### **3.3.10 PCR optimization**

PCR conditions were optimized with various modifications of reaction mixtures (MgCl<sub>2</sub> concentration, dNTP mixture, primers concentration) and thermal cycling steps (denaturation, annealing, and extension times and temperatures). The PCR protocols (multiplex PCR, nested PCR, colony PCR etc.) were described in more detail in the related session.

### **3.3.11 DNA sequencing**

Purified DNA sample for sequence confirmation was prepared and sent out for sequencing service (First BASE Laboratories, Malaysia). DNA sequencing was performed using a Big Dye<sup>®</sup> Terminator (version 3.1) Cycle Sequencing Kit (Applied Biosystems, USA) with an ABI PRISM<sup>®</sup> 3100 Genetic Analyzer (Applied Biosystems).

## **3.4 Development of a single-step multiplex PCR detection assay for five human *Plasmodium* species**

### **3.4.1 Multiplex primers design**

The primers for the hexaplex PCR were designed to amplify the specific region of highly conserved 18S small subunit ribosomal RNA (ssu rRNA) gene of the five human *Plasmodium* species, based on multiple alignments of sequences available in GenBank databases (<http://blast.ncbi.nlm.nih.gov/>) (Table 3.1). Basically, nucleotide sequences for all five human parasites were aligned and analyzed for their differences and conserved regions using CLUSTAL W program (Thompson, Higgins, & Gibson, 1994) and BioEdit version 7.0.9 software (Hall, 1999) to obtain the consensus sequences for primer design.

Overall, primers were designed by using Primer Premier Software 5.0 (PREMIER Biosoft International, CA). This software allows the secondary structure checking, e.g., the presence of hairpin and dimer structures, possible false-priming, as well as cross-dimers formations, which might affect the overall sensitivity and specificity of the multiplex PCR system. The primers with the secondary structure were re-designed with slight modification. Finally, five forward species-specific primers and a single reverse genus-specific primer of human malaria parasites were designed for this multiplex PCR system. The primers were then designed and checked through a Basic Local Alignment Tool (BLAST) (Altschul, Gish, Miller, Myers, & Lipman, 1990),

using Nucleotide BLAST (BLASTN) search (<http://www.ncbi.nlm.nih.gov/>) to ensure no non-specific amplification from non-target gene. The expected species-specific fragment sizes are shown in Table 3.1.

Table 3.1: *Plasmodium* species and GenBank accession numbers for the 18S ssu rRNA sequence.

<i>Plasmodium</i> species	Accession number	Base pair
<i>P. vivax</i>	X13926	~ 215
	U03079	
<i>P. knowlesi</i>	DQ350260	~ 284
	DQ350261	
	DQ350262	
	DQ350263	
<i>P. ovale curtisi</i>	AB182489	~ 304
	AB182490	
	AF145337	
	L48987	
<i>P. ovale wallikeri</i>	AB182491	
	AB182492	
<i>P. cf. malariae</i>	AF487999	~ 341
	AF488000	
<i>P. malariae</i>	AB489195	
	AB489196	
	AF145336	
<i>P. falciparum</i>	M19172	~ 453
	JQ627149	
	JQ627150	
	JQ627151	
	JQ627152	

### 3.4.2 *In silico* PCR

Multiple sequences of *Plasmodium* species 18S ssu rRNA available in GenBank and NCBI databases in FASTA format were exported to '*in silico*' database in txt format (up to five sequences in each assay). Together with designed primers pair, *in silico* PCR (<http://insilico.ehu.es/PCR/>) was performed for prediction of amplicons.

### 3.4.3 Multiplex PCR optimization

To develop a multiplex PCR, optimization in the concentration of MgCl<sub>2</sub>, dNTPs, primers, as well as PCR cycling parameters (especially primers annealing temperature) are important to avoid unspecific amplification and to ensure that each of the selected targets was correctly amplified at about equal intensity. Basically, the PCR parameters in the present study were optimized step by step as described by Henegariu and colleagues (Henegariu, Heerema, Dlouhy, Vance, & Vogt, 1997). Initially, the primer pair was optimized under monoplex conditions. Next, all primers were mixed together to perform subsequence multiplex PCR optimization for the detection of five human malaria parasites. PCR amplification was performed using TaKaRa PCR Thermal Cycler Dice<sup>TM</sup> (TAKARA BIO, Japan). Finally, a stable and consistent multiplex PCR condition was established.

#### 3.4.4 Positive control

Three sets of additional primers were designed, in which one of these primer set will subsequently be included into the optimized multiplex PCR system as positive control for the determination of successful DNA extraction procedure and PCR reaction in present multiplex system. The PCR condition of each of the primer set was experimental tested to validate the suitability as positive control in the present multiplex system.

In first control set, pGEX4T1 plasmid DNA, an external DNA together with a pair of targeted primers, i.e., pGEX (F) and pGEX (R) were included into optimized multiplex PCR system.

In the second control set, a single forward primer targeting both human and *Plasmodium* conserved region of 18S ssu rRNA genes as well as a single reverse primer targeting human conserved region of ssu rRNA gene were designed. The primers were able to amplify both human and *Plasmodium* ssu rRNA conserved gene, thus generated two additional amplicons for the system.

In the third control set, a pair of human housekeeping  $\beta$ -hemoglobin primers was designed. This primer set was finally included as an internal positive control for the present multiplex system.

### 3.4.5 Multiplex PCR amplification

Fifteen  $\mu\text{l}$  of PCR reagent mixture containing 20 mM of Tris-HCl, 20 mM of KCl, 5 mM of  $(\text{NH}_4)_2\text{SO}_4$ , 3.0 mM of  $\text{MgCl}_2$ , 0.2  $\mu\text{M}$  of each dNTP, the empirically determined concentration of primers (0.6  $\mu\text{M}$  of single reverse genus-specific, F<sub>453</sub>, M<sub>341</sub>, and O<sub>304</sub> primers, 0.5  $\mu\text{M}$  of K<sub>284</sub> primer, 0.4  $\mu\text{M}$  of V<sub>215</sub> primer, and 0.25  $\mu\text{M}$  of each  $\beta$ -hemoglobin primers), 1 U of Maxima<sup>®</sup> Hot Start Taq DNA polymerase (Fermentas, USA), and 1.5  $\mu\text{l}$  (~10 ng) of template DNA were used in the detection study. The reactions were subjected to initial denaturation at 95 °C for 5 min, 35 amplification cycles at 95 °C for 30 sec, 56 °C for 30 sec, 65 °C for 40 sec, followed by a final extension at 65 °C for 10 min using TaKaRa PCR Thermal Cycler Dice<sup>™</sup> (TAKARA BIO, Japan). The amplified products were visualized on 3 % (w/v) agarose gel (Promega) stained with ethidium bromide.



### 3.4.6 Nested PCR amplification

Nested PCR amplification was performed as a molecular gold standard method for the identification of human *Plasmodium* species (Singh, et al., 1999; Snounou, et al., 1993) (Appendix 3.1) to validate the sensitivity and specificity of the present multiplex PCR system. Nested PCR conditions with minor modification were done using TaKaRa PCR Thermal Cycler Dice<sup>TM</sup> (TAKARA BIO, Japan).

First nested PCR was performed in a final volume of 15 µl that consisted of 1× optimized Dream Taq<sup>TM</sup> buffer, 0.3 mM of each dNTP, 0.3 µM of each rPLU1 and rPLU5 primers (Snounou, et al., 1993), 2.0 mM of MgCl<sub>2</sub>, 1.5 µl of DNA template, 1.0 U Dream Taq<sup>TM</sup> DNA polymerase (Fermentas, USA). PCR amplifications were carried out with an initial denaturation step at 95 °C for 3 minutes; 30 repeated cycles of 95 °C for 30 seconds, 60 °C for 30 seconds, and 72 °C for 1 minute 30 seconds, followed by an extension step at 72 °C for 7 minutes.

Second nested PCR contained 10 mM of Tris-HCl, 50 mM of KCl, 0.08 (v/v) of Nonidet P40, 1.5 mM of MgCl<sub>2</sub>, 0.2 mM of each dNTP, 0.3 µM of each pair of primers i.e., rFAL1/2, rVIV1/2, rMAL1/2, rOVA1/2, and Pmk8/Pmk9 (Singh, et al., 1999; Singh, et al., 2004), 0.5 U of Taq DNA Polymerase (Fermentas, USA), as well as 0.5 µl of amplicons from first nested PCR was used as DNA template in a final volume of 15 µl. The OVA1/2 primer pair only targeting ssuRNA gene of *P. ovale curtisi* but not for *P. ovale wallikeri*, therefore an alternative primer pair targeting both *P. ovale curtisi* and *P. ovale wallikeri* from multiplex PCR was added to the second nested PCR (Padley, Moody, Chiodini, & Saldanha, 2003). The PCR thermal cycling was the same as the first nested PCR except that the temperature was changed to 72 °C for 30 seconds in the 30 repeated cycles.

First and second nested PCR products were visualized on 1 % and 2 % (w/v) agarose gel (Promega) stained with ethidium bromide respectively.

### 3.4.7 *Plasmodium* 18S ssu rRNA clones construction

Approximately 1.6-1.7 kb DNA fragment of 18S ssu rRNA gene of five human *Plasmodium* species, i.e., *P. falciparum*, *P. vivax*, *P. knowlesi*, *P. malariae*, and *P. ovale* clones were amplified using rPLU1 and rPLU5 primers (Snounou, et al., 1993) using nested PCR technique. The PCR products were further gel purified using QIAquick gel extraction kit prior to being cloned into the pCR<sup>®</sup>II-Topo TA cloning system (Invitrogen Life Technologies, USA) and transformed into Top10 chemically treated competent *E. coli* host cells, accordingly to the manufacturer's guidelines.

In general, 6 µl of ligation mixture containing 1 µl of salt (200 mM of NaCl; 10 mM MgCl<sub>2</sub>), 0.5 to 4.0 µl of purified PCR product, and 1 µl of pCR<sup>®</sup>II-TOPO vector [10 ng/µl plasmid DNA; 50 % (v/v) glycerol; 50 mM Tris-HCl, pH 7.4; 1mM EDTA; 1 mM DTT; 0.1 % (v/v) Triton X-100; 100 µg/ml BSA; phenol red). The ligation mixture was gently mixed and incubated for 30 minutes at room temperature (22-23 °C) and then placed on ice or kept overnight at -20 °C until transformation step was carried out. The amount of DNA needed for the ligation reaction was calculated, e.g.:

$$\frac{10 \text{ ng of vector} \times 1.7 \text{ kb of inserted DNA}}{3.9 \text{ kb of vector}} \times \frac{3}{1} = \sim 13 \text{ ng of insert DNA}$$

Two µl of the TOPO<sup>®</sup> cloning reaction was added into 100 µl of chemically competent TOP10 *E. coli* and mixed by gently swirling followed by incubation on ice for 30 minutes. Next, heat-shock transformation of the *E. coli* cells for 30 seconds at 42 °C was carried out and immediately transferred to the ice and incubated for 2 minutes. Then, 500 µl of S.O.C medium was added to the cells and shook horizontally (200 rpm) at 37 °C for 1 hour. Fifty and 100 µl of each transformation were spread onto the LB agar plates containing 100 µg/ml of ampicillin, 50 µg/ml IPTG and 40 µg/ml Xgal. The plates were incubated overnight at 37 °C.

### **3.4.7.1 Screening of positive clones by colony PCR**

In order to identify positive clones, approximately 20 white colonies were randomly picked from the master (transformation) plate and incubated overnight in 1 ml of LB broth containing 100 ug/ml of ampicillin. Putative transformations were further confirmed by colony PCR. The 15 µl reaction contained 1× Taq polymerase PCR buffer (10 mM Tris-HCl, 50 mM KCl, 0.08 (v/v) Nonidet P40), 1.5 mM of MgCl<sub>2</sub>, 0.2 mM of each dNTP, 0.1 µM of each pair of T7 promoter and SP6 primers, 0.5 U of Taq DNA Polymerase (Fermentas), and 5 µl of boiled supernatant as template (supernatant was prepared from 10 µl of culture boiled for 10 minutes and spun down at 14,000 ×g for 30 seconds). The cycling reaction was set as follows: an initial denaturation at 94 °C for 5 minutes, followed by 30 cycles of denaturation at 94 °C for 30 seconds, annealing at 60 °C for 30 seconds, extension at 72 °C for 90 seconds and a final extension incubation at 72 °C for 7 minutes. The PCR products were then analyzed on 1 % (w/v) agarose gel.

### 3.4.7.2 Screening of positive clones by DNA sequencing

The positive clone confirmed by colony PCR was further isolated from 1 ml of *E. coli* culture using HiYield Plasmid Mini Kit (Yestern Biotech, Taiwan), according to the manufacturer's instructions prior to subjected to sequencing. The nucleotide sequence of the selected plasmids was sequenced with T7 promoter (F) and SP6 (R) universal primers by using a Big Dye<sup>®</sup> Terminator (version 3.1) Cycle Sequencing Kit (Applied Biosystems, USA) with an ABI PRISM<sup>®</sup> 3100 Genetic Analyzer (Applied Biosystems) for subsequence clones confirmation. The gene sequence (electropherogram) obtained was then analyzed using BioEdit version 7.0.9 Software (Hall, 1999) and CLUSTAL-W program (Thompson, et al., 1994). The gene sequence of each of five constructs was then blast searched on NCBI (<http://www.ncbi.nih.gov>) for inter-species confirmation.

All five *Plasmodium* clones were used as templates in analytical sensitivity and specificity validation, as well as serve as positive controls in the subsequent PCR amplifications. Individual clones were long term stocked at -80 °C in LB broth containing 100 ug/ml of ampicillin and 15 % (v/v) glycerol.

### 3.4.8 Sensitivity and specificity tests

Sensitivity and specificity tests that were used to describe the value of assays, i.e., analytical sensitivity and specificity, diagnostic sensitivity and specificity, and random blind test were carried out in the present study.

#### 3.4.8.1 Analytical sensitivity test

The parasitemia of the five human *Plasmodium* species, i.e., *P. vivax*, *P. falciparum*, *P. knowlesi*, *P. malariae*, and *P. ovale* obtained from clinical samples were estimated (Session 3.3.2) and each of the DNA sample was extracted. The extracted DNA of each species was then 10-fold serially diluted ( $10^{-1}$  to  $10^{-7}$ ) with human DNA (10 ng/ $\mu$ l) and one  $\mu$ l of the DNA mixture was used in PCR reaction in the sensitivity validation assay. The sensitivity of the present hexaplex system to five human *Plasmodium* species were compared with the nested PCR as the molecular gold standard, whereas the microscopic results were used as the reference for the presence of the *Plasmodium* species.

In clinical mixed infections, the ratios between two or more parasite species can be vary substantially (Conway, 2007; Zimmerman, et al., 2004), therefore, the effect of DNA and primer competition was also tested for the present multiplex PCR system. Due to lack of natural mixed infections, three combinations of experimental mixtures, i.e., 100 pg/ $\mu$ l of *P. vivax* clone DNA and 1, 10 or 100 pg/ $\mu$ l of *P. falciparum* clone DNA were created to determine the sensitivity of this multiplex PCR. A total of 60 mixtures were test, i.e., make-up of 12 different simulated mixtures of DNA using two out of five human *Plasmodium* species for each set and three DNA concentrations. There were 10 possible combinations of two species simulated mixed infections. Besides, to test whether these primers would improve the detection of clinical mixed infections, a total of 30 experimental random mixed infections were created using

clinical samples and screened using the present multiplex PCR system and nested PCR as molecular gold standard for identifying mixed infections.

#### **3.4.8.2 Analytical specificity test**

Analytical specificity is the assay's ability to measure one *Plasmodium species*, rather than other organisms in the sample. To estimate the analytical specificity of the *Plasmodium* hexaplex assay, DNA samples of other non-*Plasmodium*, i.e., *Toxoplasma* species, *Giardia* species, *Aeromonas* species, *Serratia* species, *Vibrio* species, and hook worm were screened. Besides, DNA from 20 healthy individuals also tested for the specificity and possibility of unspecific fragment.

#### **3.4.8.3 Random blind test and clinical sample screening**

To validate the sensitivity and specificity of the present multiplex system in species determination, a random blind test on 50 DNA samples (randomly drawn from 211 microscopy confirmed clinical samples) followed by a detection study on 226 clinical samples were carried out together with nested PCR for comparison.

#### 3.4.8.4 Diagnostic sensitivity and specificity tests

The diagnostic sensitivity (true positive rate), specificity (true negative rate), positive predictive value (PPV) (probability that the diseases is present when the test is positive), and negative predictive value (NPV) (probability that the diseases is not present when the test is negative) of two species, i.e., *P. vivax* and *P. falciparum* were calculated as formulas stated below (Table 3.2), based on 226 microscopic-confirmed malaria samples collected from two medical centers as well as 20 healthy control donors, using nested PCR as the standard. The 95 % confidence interval (95 % CI) was also calculated using MedCalc-Diagnostic test evaluation ([http://www.medcalc.org/calc/diagnostic\\_test.php](http://www.medcalc.org/calc/diagnostic_test.php)). The calculations were expressed as percentage for ease of interpretation.

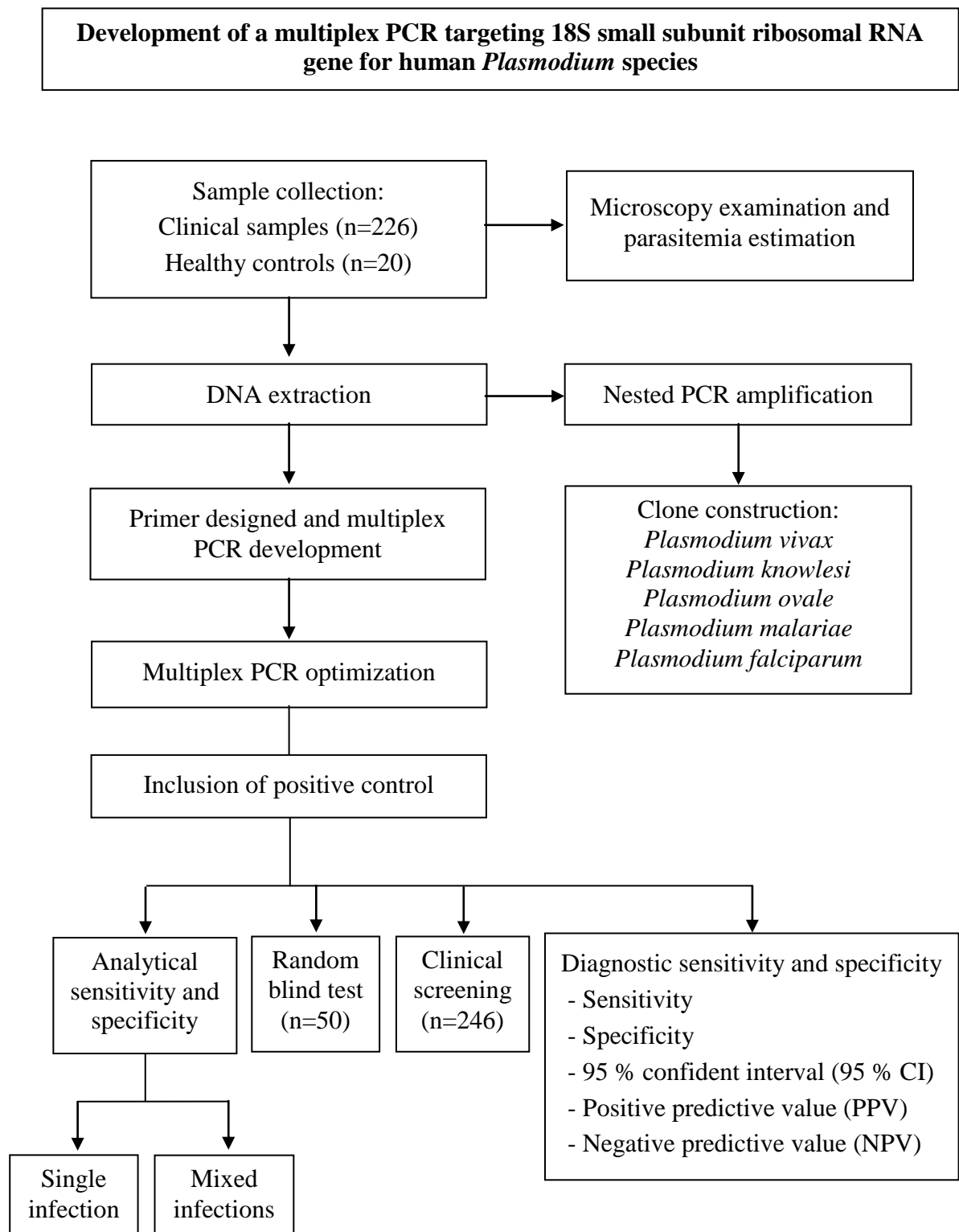
Table 3.2: Formulas used in diagnostic specificity and sensitivity tests.

Nested PCR Multiplex PCR	Positive	Negative
Positive	a	c
Negative	b	d
Sensitivity	$a/(a+b)$	
Specificity	$d/(c+d)$	
PPV	$a/(a+c)$	
NPV	$d/(b+d)$	

a = known positive; test result positive (true positive); b = known positive; test result negative (false negative); c = known negative; test result positive (false positive); d = known negative; test result negative (true negative).

$$95\% \text{ CI} = \exp \left[ \ln (\text{OR}) \pm 1.96 \sqrt{(1/a) + (1/b) + (1/c) + (1/d)} \right]$$

### 3.4.9 Overview of the development of a multiplex PCR detection system for human *Plasmodium* species





### **3.5 Identification of binding peptides for PkAMA1 and PvAMA1 using a phage display library**

#### **3.5.1 Heterologous protein expression in prokaryotic system**

Protein expression was carried out using Profinity eXact™ System (Bio-Rad) (Appendix 4), according to the manufacturer's instructions. The expression system was initiated with heterologous expression of target proteins in *E. coli*, which involved the construction and cloning of the target protein sequences into an expression vector, i.e., pPAL7 (size 5,901 bp) followed by further recombinant protein isolation as well as affinity purification using Profinity eXact Mini Spin Column (small scale purification) and 1 ml or 5 ml Bio-Scale Profinity eXact Mini Cartridges (large scale purification).

##### **3.5.1.1 Construction of PkAMA1 and PvAMA1 clones**

Specific forward and reverse primers were designed with appropriate RE recognition sites to adapt the *Plasmodium* AMA1 ectodomain gene for precise insertion into expression vector, i.e., pPAL7 based on the multiple cloning site provided by manufacturer (Appendix 4).

The currently available whole sequence of AMA1 of the *P. vivax* and *P. knowlesi* were blast searched using NCBI database, followed by subsequence multiple aligned using BioEdit and ClustalW softwares. Finally, two sets of PCR primers with 5' *SpeI* upstream (sense) and 5' *BamHI* downstream (anti-sense) RE sites were designed for the amplification of gene fragments encoding the whole ectodomain, i.e., domain I (DI), domain II (DII), and domain III (DIII) of AMA1 for *P. knowlesi* (PkAMA1) and *P. vivax* (PvAMA1) (Table 3.3). The compatibility of appropriate REs sites were confirmed by NEB cutter V2.0 (NEB; <http://tools.neb.com/NEBcutter2/>) to eliminate the possibility of RE digestion on the PCR amplicon.

Although all the apicomplexan parasites share a structural homology in AMA1 protein, the coding DNA of AMA1 gene is relatively polymorphic among *Plasmodium* species. As genetic variations were noted in the sequence of AMA 1 gene among intraspecies of *P. vivax* adopted from NCBI database, degenerate primers were designed as in Table 3.3. In each of the reverse primer, a stop codon (anticodon; +/-), either TTA (STOP<sub>TAA</sub>), CTA (STOP<sub>TAG</sub>), or TCA (STOP<sub>TGA</sub>) was included after RE recognition sequence to terminate the expression of target protein.

Table 3.3: Primer pairs used in protein expression of PkAMA1 and PvAMA1.

Name	Primer sequence (5'- 3')	REs sites
<b>PkAMA1</b>	AGCTATACTAGTGGGCCTATCATTGAGAGAAGT AGACAAGGATCCT <b><u>TTA</u></b> TAGTAGCATCTTCTTCTTATG	<i>SpeI</i> <i>BamHI</i>
<b>PvAMA1</b>	ATATATACTAGTGGGCCTACCGTTGAGAGRAGC AGACAAGGATCCT <b><u>TTA</u></b> TAGTAGCATCYGCTTGTTCTGA	<i>SpeI</i> <i>BamHI</i>

\* Bolded sequences indicate of the appropriate RE recognition site; underline-bolded sequences indicate a stop codon of the reverse primer.

DNA fragments of PkAMA1 and PvAMA1 were amplified using TaKaRa PCR Thermal Cycler Dice<sup>TM</sup> (TAKARA BIO, Japan) and KOD Hot Start DNA polymerase (Novagen, USA). The 30 µl reaction contained 1× optimized PCR buffer, 2.0 mM MgSO<sub>4</sub>, 0.3 mM of each dNTP, 0.5 mM of each forward and reverse primers, 1 U of KOD Hot Start DNA polymerase, as well as 3 µl (~ 20 ng) of template DNA. The cycling reaction was performed as follows: an initial denaturation step at 95 °C for 2 minutes, followed by 35 repeated cycles at 95 °C for 20 seconds, annealing temperature for 10 seconds, and 70 °C for 30 seconds, followed by a final extension step at 70 °C for 15 seconds. Annealing temperature of each of the primers set was differed with 48 °C and 50 °C for PkAMA1 and PvAMA1, respectively.

Both the PCR product (PkAMA 1 and PvAMA 1 fragments) and supercoiled pPAL7 plasmid (Bio-Rad) were double digested with two restriction enzymes, i.e., *SpeI* (5'- A/CTAGT-3') and *BamHI* (5'-G/GATCC-3') according to the manufacturer's instructions. In general, double digestion was performed at 37 °C for 5 minutes in PCR tube containing 1× FastDigest restriction buffer, 1 µl of each of FastDigest RE (Fermentas), and 200 ng of either PCR product or pPAL7 vector to a final reaction volume of 30 and 20 µl, respectively. The enzymatic digestion was inactivated by DNA gel purification (Session 3.3.9) prior to DNA ligation.

The gel purified RE digested-PCR product as well as pPAL7 vector were ligated using Ready-To-GO™ T4 DNA Ligase (Amersham Biosciences). The vector:insert molar ratio used here was 3:1 as described in Sambrook and Russell (2001) for optimal sticky end ligation. Generally, 100 ng of REs-digested pPAL7 vector and ~ 70 ng of REs-digested PCR product were added to the lyophilized Ready-To-GO™ T4 DNA Ligase tube, and was then reconstituted to a final volume of 20 µl solution, which contained 6 U of FPLCpure™ T4 DNA ligase, 66 mM Tris-HCl (pH 7.6), 6.6 mM MgCl<sub>2</sub>, 0.1 mM ATP, 0.1 mM spermidine, and 10 mM DTT. The ligation mixture was incubated at 16 °C for 45 minutes. The ligation reaction was heat inactivated by incubation at 70 °C for 10 minutes using heat block (Major Sciences).

Two µl of ligation mixture were added and mixed to each of the 100 µl aliquot of C-Max5α *E. coli* competent cells by stirring briefly using pipette tip and then incubated on ice for 30 minutes prior to heat shock transformation at 42 °C for 30 seconds. The *E. coli* was then incubated immediately on ice for another 2 minutes. One ml of SOC [2 % (w/v) Tryptone, 0.5 % (w/v) Yeast extract, 10 mM NaCl, 10 mM MgCl<sub>2</sub>, 20 mM glucose] media was added to the culture followed by incubation at 37 °C with 200 rpm agitation for 2 hours. One hundred µl of the culture was used for plating. Positive clones were selected onto LB agar supplemented with 100 ug/ml of ampicillin

---

and 0.5 % (w/v) glucose. The plates were incubated overnight at 37 °C.

Successful clones were then confirmed by colony PCR using forward T7 promoter and reverse T7 terminator universal primers as described in colony PCR (Session 3.4.7.1). A ~ 400 bp of PCR band indicative of negative insertion, while ~ 1.8 kb PCR band indicative of successful clone with insertion of ~ 1,350 bp target gene. Plasmids from successful clones were then isolated (Session 3.3.6) and sent for sequencing for the further correct insertion confirmation using pPAL7 internal forward primer (5'-GTGCTTCAAATATGTAGACGCA-3'; designed for sequencing) and T7 terminator reverse primers.

### 3.5.1.2 Subcloning of *Plasmodium* AMA 1 ectodomain

The *E. coli* culture that carries desired plasmid confirmed by sequencing was grown overnight and the plasmid was extracted (Session 3.3.6) and re-transformed into protein expression host, BL21-Codon Plus (DE3)-RIL *E. coli* cells (Stratagene) as manufacturer's instructions.

In general, an aliquot of competent cells (100  $\mu$ l) were thawed on ice and 2  $\mu$ l of 1:10 diluted XL10-Gold  $\beta$ -mercaptoethanol mixture provided by the kit was added to each of the 100  $\mu$ l of cells. The content of the tube was mixed gently by swirling and incubated on ice for 10 minutes with gentle swirling in every 2 minutes. Then, 50 ng of expression plasmid DNA containing the target gene was added to the tubes and swirled gently using pipette tip. The reaction mixture was incubated on ice for 30 minutes, followed by transformation of cell using heat shock method.

The successful clones were selected onto LB agar plates supplemented with 100  $\mu$ g/ml of ampicillin to select pPAL7 plasmid as well as 34  $\mu$ g/ml of chloramphenicol to select pACYC-based plasmid that confers chloramphenicol resistance. The plates were incubated overnight at 37 °C. Successful colonies were further confirmed by colony PCR using pPAL7 internal (F), T7 promoter (F), and T7 terminator (R).

Colony that carried positive clone was then streaked on a LB plate containing 100  $\mu$ g/ml ampicillin, 34  $\mu$ g/ml chloramphenicol and grown overnight at 37 °C. A loop full of colony was then inoculated in 5 ml of LB broth containing appropriate antibiotics and the log phase cells were then harvested by centrifugation at 4,000  $\times$ g. The cell pellet was then suspended in 2 ml of LB broth containing 100  $\mu$ g/ml ampicillin, 34  $\mu$ g/ml chloramphenicol and 15 % (v/v) glycerol and stored at -80 °C in two aliquots. The clone stocks acted as starter culture in subsequence recombinant protein expression.

### 3.5.2 Protein induction

Ten ml of LB agar supplemented with 100 µg/ml ampicillin and 34 µg/ml chloramphenicol was inoculated with 5 µl of frozen stock culture and grown to confluence overnight as seed culture.

One ml of overnight seed culture was added to 100 ml of 2× YT medium containing 100 µg/ml ampicillin and 34 µg/ml chloramphenicol and incubated at 37 °C with 225 rpm shaking for ~ 3 hours (till bacterial turbidity reached ~ 0.6 at OD<sub>600</sub>). The protein expression is under the transcriptional control of the *lac* operator, which cause the inhibition of the T7 promoter due to the *lac* repressor protein. The addition of IPTG leads to the inactivation of the repressor protein and subsequent protein expression. Therefore protein expression was induced by the addition of 0.5 mM IPTG to the culture and further incubation for another 3 hours at 25 °C with vigorous agitation at 250 rpm. The bacteria cells were harvested by the centrifugation at 4,000 ×g for 20 minutes at 4 °C. The cell pellet was lysed directly or kept at -80 °C for up to one week for further recombinant protein isolation.

### 3.5.3 SDS-PAGE solubility screening

Solubility and expression level of target protein were screened by SDS-PAGE prior to subsequence large scale purification. Basically, 1 ml of culture was centrifuged at  $16,000 \times g$  for 1 minute at 4 °C. Five hundred  $\mu$ l of lysis buffer (100 mM sodium phosphate, pH 7.2, 200  $\mu$ g/ml lysozyme) was added to the pellet and the cells were disrupted by vortexing for 1 minute. Twenty  $\mu$ l of lysate was collected in PCR tube and served as total sample (T) in SDS-PAGE analysis. The total lysate was then centrifuged at  $16,000 \times g$  for 5 minutes at 4 °C and the supernatant served as soluble sample (S). The insoluble pellet was then resuspended in 500  $\mu$ l of solubilization buffer (100 mM sodium phosphate, 4 M urea, pH 7.2), incubated for 1 hour at 4 °C, and then centrifuged at  $16,000 \times g$  for 5 minutes at 4 °C. The supernatant served as insoluble protein (I). Twenty  $\mu$ l of T, S, and I samples were analyzed by SDS-PAGE and visualized by Coomassie Blue staining.

### 3.5.4 Western hybridization and colorimetric detection

The expressed protein was further confirmed by colorimetric Western blotting assay using the anti-eXact monoclonal antibody (Bio-Rad).

Proteins on SDS-PAGE gel was transferred to a membrane by electroblotting using, i.e., TE70 ECL Semi-dry Transfer Unit (Amersham Biosciences). After completion of SDS-PAGE, stacking gel of the polyacrylamide gel was removed and discarded. Separating gel was equilibrated in the Towbin transfer buffer for 15 minutes prior to Western blotting.

For each gel, six pieces of blotting papers and 1 piece of Whatman Protran nitrocellulose transfer membrane (0.45  $\mu\text{m}$ ; Millipore) were cut to the same size as the gel or slightly smaller. The nitrocellulose membrane was soaked in  $\text{dH}_2\text{O}$  for 5 minutes, then transferred and soaked in Towbin transfer buffer [25 mM Tris, 192 mM glycine, 20 % (v/v) methanol, 0.1 % SDS; pH 8.3] for 5 minutes. Six pieces of blotting papers were also saturated in a dish filled with Towbin transfer buffer.

The electrode plates was rinsed with  $\text{dH}_2\text{O}$  and the transfer stack was assembled one by one in order from the lower plate (anode) to the upper plate (cathode) with three pieces of blotting paper, nitrocellulose membrane, gel, and followed by three pieces of blotting papers. Air pockets in each layer were removed by rolling a clean Falcon tube over the layer. After that, the lid of transfer unit was placed and the proteins were transferred at voltage limit to 30 V and current at  $0.8 \text{ mA/cm}^2$  for 1 hour.

After blotting, the membrane was pre-stained with NOVEX<sup>®</sup> Reversible membrane protein stain (Invitrogen) and then documented with ImageScanner III (GE Healthcare). The temporary stained was then removed according to the manufacturer's instructions followed by immunodetection of target protein, as well as chromogenic visualization with horseradish peroxidase (HRP) using Opti-4CN substrate kit (Bio-Rad).



All following steps were performed in a small plastic container on an orbital rocker. The membrane was air dried and washed twice with PBST for 5 minutes in each wash. After washing steps, the membrane was gently rocked in blocking buffer [PBST with 3 % (w/v) BSA] for 1 hour at room temperature, and then followed by two wash with PBST for 5 minutes each. After that, membrane was incubated with appropriate diluted primary antibody, i.e., anti-eXact monoclonal antibody (Bio-Rad) at dilution 1:5,000 in an antibody dilution buffer [PBST, 1 % (w/v) BSA] for 1 hour and then followed by two wash with PBST for 5 minutes each. Next, the membrane was incubated with goat-anti-mouse-HRP conjugated secondary antibody in dilution 1:5,000 for 1 hour at room temperature followed by another two washing steps with PBST for 5 minutes each.

Colorimetric reagent provided in Opti-4CN substrate kit was prepared according to the manufacturer's instructions. Basically, one part of 10× Opti-4CN diluent concentrate was added with nine parts of sdH<sub>2</sub>O and 0.2 ml of Opti-4CN substrate was added per 10 ml of diluent. The reagent was mixed well and poured onto a membrane followed by gentle agitation for up to 30 minutes or until the desired band intensity was observed. The membrane was then washed in sdH<sub>2</sub>O for 15 minutes and allowed to air dry followed by membrane documentation with ImageScanner III (GE Healthcare).

### 3.5.5 Recombinant protein extraction from *E. coli* and insoluble inclusion body purification

The cell pellet from the 100 ml of culture (Session 3.5.2) was resuspended in 5 ml of B-PER<sup>®</sup> in phosphate buffer (Pierce) in the presence of 1× Calbiochem<sup>®</sup> Protease Inhibitor Cocktail Set I (Novagen) and 200 µg/ml of lysozyme (Novagen). The cells were disrupted by 20 pass through a 25 Gauge syringe needle and followed by vortexed for a minute, and incubation at room temperature for 20 minutes with shaking at 40 rpm on an orbital rotary (Major Sciences). Ten U/ml of Benzonase (Novagen) was added after that and incubated for another 20 minutes to reduce the cell lysate viscosity. After incubation, 20 µl of total lysate was kept for SDS-PAGE analysis (labeled as T indicates of total lysate). The total lysate was centrifuged at  $16,000 \times g$  for 15 minutes at 4 °C. The supernatant containing the soluble protein was collected in clean Falcon tube and 20 µl of supernatant was kept for gel analysis (labeled as S).

The pellet containing insoluble proteins or known as inclusion body (IB) was resuspended in 5 ml of wash buffer 1 [B-PER buffer, 200 µg/ml lysozyme, 1 % (v/v) Triton X-100, 5 mM EDTA, 5 mM DTT, 1 M urea] by 20 pass through a 25 Gauge syringe needle followed by incubation at room temperature for another 20 minutes with shaking at 40 rpm on an orbital rotary (Major Sciences). Twenty µl of suspension was kept for gel analysis and labeled as insoluble protein (I). Generally, the IB was washed with 1 M urea and 1 % Triton X-100 to remove *E. coli* cellular materials. Higher concentration of urea (more than 4 M) may result in partial solubilization of the recombinant protein, whereas Triton X-100 will not solubilize IB proteins, it was included to help extract lipid and membrane-associated proteins. Then, a total 15 ml of pre-chilled IB wash buffer 2 [1:10 diluted B-PER, 1 % (v/v) Triton X-100, 5 mM EDTA, 5 mM DTT, 1 M urea] was added to the suspension and mixed by vortexing for 1 minute followed by centrifugation at  $16,000 \times g$  for 15 minutes at 4 °C. Twenty µl of

supernatant was kept for gel analysis and labeled as insoluble supernatant (IS). The pelleted IB was then resuspended and washed with 15 ml of IB wash buffer 3 (1:10 diluted B-PER) followed by centrifugation at  $16,000 \times g$  for 15 minutes at 4 °C to remove excess Triton X-100 from the pellet. The washed IB becomes whiter as the purity increased.

In every experiment, the protein fractions obtained during cells lysis and preparation of washed IB were analyzed with reduced SDS-PAGE. The purity of the IB can also be determined by comparing the intensities of the insoluble portion of total protein (I) as well as suspensions collected from each of the washing steps (W1 and W2). The suspension obtained from last washing step was designated as purified IB. Finally, the purified IB was then pelleted by centrifugation at  $16,000 \times g$  for 30 minutes at 4 °C, which can be either processed directly for protein purification or long term stored at -80 °C.

#### **3.5.5.1 Inclusion body solubilization**

Strong denaturant (urea) and reducing agent (DTT) were used to solubilize the purified IB. In general, purified IB was resuspended in IB solubilization buffer (100 mM sodium phosphate, pH 7.2, 4 M urea, 5 mM DTT, 1 mM EDTA) and incubated either for at least 1 hour at room temperature (~ 25 °C) or overnight at 4 °C. Suspension of protein was then centrifuged at  $15,000 \times g$  for 30 minutes at 4 °C. Supernatant containing denatured proteins was then collected and filtered through a 25 mm diameter 0.45  $\mu$ m pore size cellulose acetate membrane filter (Sartorius Stedim Biotech) prior to recombinant protein purification to prevent clotting of the Profinity eXact<sup>TM</sup> purification cartridge (Bio-Rad). The sample was then diluted to a final concentration of 2 M urea and then kept at 4 °C or on ice until further affinity purification.

### 3.5.6 Affinity protein purification under denatured conditions and fusion-tag removal

The solubilized pPAL7-PkAMA1 and pPAL7-rPvAMA1 proteins were purified using 1 ml or 5 ml Bio-Scale Mini Profinity eXact<sup>TM</sup> cartridges pre-packed with 1 or 5 column volumes (CV) settled resin (Bio-Rad), respectively, using low pressure peristaltic pump system (Heildolph, Germany). Generally, the denatured purification protocol was adapted from manufacturer's instructions that based on soluble protein purification, with inclusion of 4 M urea (denaturant) in both bind/wash and elution buffers along purification procedures.

Cartridge was equilibrated with 10 CV of 100 mM sodium phosphate (pH 7.2) buffer at 3 ml/min to remove storage buffer containing 0.02 % (w/v) sodium azide. Chilled and filtered protein sample (~ 10 ml) was loaded at 1 ml/min. The cartridge was then washed with 15 CV of pre-chilled bind/wash buffer (4 M urea, 100 mM sodium phosphate, pH 7.2) at 3 ml/min. Another 10 CV of stringency wash (4 M urea, 100 mM sodium phosphate, 200 mM sodium acetate, pH 7.2) was performed to reduce the nonspecific and electrostatic binding of fusion protein. After that, the cartridge was then pumped with 5 CV of elution buffer (4 M urea, 100 mM sodium phosphate, 100 mM sodium fluoride, pH 7.2) at 0.1 ml/min at room temperature and the eluted target protein was collected in clean microcentrifuge tubes (1 ml each). Purified protein was stored at -80 °C. The purity of the protein was determined using reduced SDS-PAGE and the concentration was estimated using Bradford Protein Assay (Bio-Rad).

### **3.5.7 Protein concentration determination using Bradford protein assay**

Concentration of the protein in solution was determined using Quick Start Bradford Protein Assay (Bio-Rad). The concentration of unknown protein was estimated using mean value of the triplicate readings obtained from the binding activity of Coomassie Brilliant Blue G250 dye to the protein standards, i.e., seven pre-diluted Bovine Serum Albumin (BSA) standard set (Bio-Rad) in final concentrations of 2,000 µg/ml, 1,500 µg/ml, 1,000 µg/ml, 750 µg/ml, 500 µg/ml, 250 µg/ml, and 125 µg/ml, respectively. A protein blank was included to the test.

Generally, an aliquot of well mixed 1× Bradford dye reagent (Coomassie Brilliant Blue G-250 dye containing methanol and phosphoric acid) was removed from 4 °C storage and was left to thaw to ambient temperature. Twenty µl of each standard as well as unknown sample were added and mixed well with 1 ml of the 1× dye reagent in microcentrifuge tubes. The protein mixture was incubated at room temperature for 5 minutes prior to spectrometrically determination at 595 nm (all reading must complete within 1 hour) using 1.5 ml disposable cuvette and NanoPhotometer<sup>TM</sup> (IMPLEN, Germany). A standard curve was plotted at the absorbance 595 nm values (y-axis) versus the concentration in µg/ml (x-axis) with the  $r^2$  equal or near to 1 using NanoPhotometer<sup>TM</sup>. The concentration of unknown protein sample was then determined based on the standard curve.

### **3.5.8 Precipitation of recombinant protein and buffer exchange**

The eluted Profinity eXact purified target protein in elution buffer (4 M urea, 100 mM sodium phosphate, 100 mM sodium fluoride, pH 7.2) was quite diluted, therefore sample collected from several purifications were pooled and concentrated, followed by buffer exchanged into refolding buffer (4 M urea, 50 mM Tris phosphate buffer, pH 8) using Vivaspin 20 concentrator fitted with 5,000 MWCO PES membrane (Sartorius Stedim Biotech). The buffer exchange steps were performed as manufacturer's instructions and the diluted target protein was then further concentrated into final concentration of approximately 2 mg/ml, confirmed by Bradford protein assay. The Vivaspin 20 enables concentration of solution in excess of 100×

Generally, concentrator was pre-rinsed with 15 ml of buffer solution or sdH<sub>2</sub>O to remove the trace amounts of glycerine and sodium azide on the membranes and decant the filtrate before sample processing. Samples collected from several small scale extractions were pooled and applied into the concentrator. The pooled sample was concentrated by centrifugation at 4,000 × g at 4 °C for 1 hour, and centrifugation repeated until final volume of ~ 500 µl. This was followed by three subsequence buffer exchanged steps with 15 ml concentrator exchange buffer (4 M urea, 50 mM Tris phosphate, pH 8). The centrifugation was continued until the concentration of contaminating microsolutes was sufficiently reduced (three wash cycles able to removed 99 % of initial salt content). Once the desired concentration was reached (~ 1.5 ml), the assembly was moved and the sample was collected using pipette tip. The final concentration of target protein was determined using Bradford Protein Assay (Bio-Rad) and diluted to ~ 1 mg/ml target protein. A 1× of Calbiochem® Protease Inhibitor Cocktail Set I (Novagen) was added to the concentrated sample solution and sample was aliquot into small volume (500 µl) in microcentrifuge tube to prevent several freeze-thaw cycles, and then stored at -80 °C.

### **3.5.9 Protein renaturation**

#### **3.5.9.1 Reduction of the target protein**

A 5 mM of DTT (reducing agent) was added to the concentrated protein solution (4 M urea, 50 mM Tris phosphate buffer, pH 8) prior to refolding to keep all cysteine residues in the reduced state and break all possible intramolecular disulfide bonds presented in entire ectodomain of *Plasmodium* AMA1 protein, and 1 mM of EDTA was added as the metal chelator. Generally, fresh prepared DTT was used to prevent air oxidation of the DTT stock solution, whereas EDTA was diluted from 0.5 M stock. The protein sample was then incubated at room temperature for 1 hour.

#### **3.5.9.2 Desalting and buffer exchange**

The reducing agent, DTT must be removed prior to refolding. The reduced protein sample (1 mM EDTA, 5 mM DTT, 4 M urea, 0.1 M Tris phosphate, pH 8) was buffer exchanged using 10 kDa MWCO Zeba Desalting Column (Pierces Thermo Scientific). Column was washed once with 5 ml of sdH<sub>2</sub>O to remove the trace amount of NaN<sub>3</sub> and then pre-equilibrated three times with desalting buffer (4 M urea, 50 mM Tris phosphate, pH 8) by centrifuged at  $1,780 \times g$  for 1 minute in each step. Two ml of protein sample was loaded onto the center of resin and centrifuged at  $1,780 \times g$  for 1 minute at 4 °C. The eluted protein was collected in a clean Falcon tube and the protein concentration was then determined using Bradford protein assay.

### 3.5.9.3 Protein refolding by dialysis

The native PkAMA1 and PvAMA1 contain eight disulfide bonds, therefore the refolding has to be supplemented with a redox system. The addition of a mixture of reduced and oxidized forms of low molecular weight thiol at a ratio of 4:1 usually provides the appropriate redox potential to allow formation and reshuffling of disulfide bonds. For instance, 1 mM reduced glutathione (GSH) and 0.25 mM oxidized glutathione (GSSG) were added to desalted rPkAMA1 and rPvAMA1.

In general, protein refolding was performed by dialysis method using 3 ml Slide-A-Lyzer Dialysis Cassettes with 10 kDa MWCO (Pierces Thermo Scientific). The membrane of the cassette was hydrated by immersing the cassette attached with a buoy into the dialysis buffer for 2 minutes prior to dialysis process. Then, the cassette was removed from buffer and excess liquid was removed by taping the edge of the cassette gently on paper towel.

Approximately 2 ml of the concentrated protein sample (1 mg/ml in 50 mM Tris phosphate, pH 8, 4 M urea, 1 mM EDTA, 1 mM GSH, 0.25 mM GSSG, and 1 × Calbiochem Protease Inhibitor Cocktail set 1) was loaded into the cassette using syringe fitted with 18-gauge needle by carefully penetrating the gasket through one of the syringe ports at the corner of the cassette with needle and the sample was then injected into the cassette cavity slowly to prevent the formation of bubble at high concentration. Next, the excess air was withdrawn by slightly pulling up the plunger. The syringe was then removed and the gasket was sealed automatically, and the membrane cavity has no air in direct contact with sample. The cassette was slipped into the groove of buoy and the assembly was floated in the dialysis solution and the sample was dialyzed at 4 °C with gentle stirring at the bottom using a magnetic stirrer (Eppendorf).

Protein sample in the cassette was dialyzed against two changes of 400 ml of dialysis buffer (50 mM Tris phosphate, 0.4 M L-arginine, 1 mM EDTA, pH 8) with



stepwise decreases of urea concentration, i.e., 2 M and 1 M at 4 °C with stirring for four hours in each change, which allows the protein to refold optimally. After the last change, the protein solution was further dialyzed (buffer exchanged) overnight at 4 °C against sample buffer without urea (25 mM Tris phosphate, 50 mM NaCl, pH 8), which is compatible to downstream application, i.e., biopanning.

To remove the refolded sample from cassette, the syringe fixed with needle was filled with a volume of air equal to sample volume. The gasket was penetrated with the needle through unused syringe guide port and the air was discharged into cassette cavity to separated membrane. Then, the unit was turned down so that needle was on the bottom, and the dialyzed sample was withdrawn and stored in clean microcentrifuge tube.

#### **3.5.9.4 Analysis of folding reactions**

Refolding screening was assessed by determining the turbidity of the solution where protein aggregation has occurred by visual inspection of aggregates formation and quantification of turbidity changes by measuring changes in absorbance at 390 nm. Generally, turbidity of the refolded rPkAMA1 and rPvAMA1 protein samples was assessed by measuring the OD at 390 nm using NanoPhotometer<sup>TM</sup> (IMPLEN) and the turbidity was determined by subtracting the apparent OD reading of the sample solution to the blank sample buffer (25 mM Tris phosphate, 50 mM NaCl, pH 8) and the protein was taken to be soluble at OD < 0.05. Refolded sample proteins were then further investigated using reduced and non-reduced SDS-PAGE (Session 3.3.8.2).

### **3.5.10 Protein identification by LC-MS/MS**

Recombinant PkAMA1 and PvAMA1 ectodomain were electrophoresed using 10 % SDS-PAGE under non-reduced conditions followed by staining with Coomassie Blue. The bands of interest were excised from the gel and sent for reduced (20 mM Tributylphosphine), alkylated (40 mM Iodoacetamine), in-gel trypsin digestion, and liquid chromatography tandem mass spectrometry (LC-MS/MS) analysis (Monash University Malaysia) for protein identification. The LC-MS/MS was performed using Agilent 6520 Accurate-Mass Q-TOF LC/MS system (Agilent Technologies, USA). Peptide ions were analyzed with GPS Explorer software (Applied Biosystems) using MASCOT<sup>TM</sup> Database.

### **3.5.11 Phage display and M13 general methods**

#### **3.5.11.1 Bacteria stain maintenance**

The ER2738 *E. coli* from the supplied glycerol culture was streaked out onto LB plate containing 20 µg/ml of tetracycline and incubated overnight at 37 °C. The cultured plate was then wrapped with parafilm and kept at 4 °C in the dark until needed for a maximum of one month. The *E. coli* culture for phages infection and propagation were prepared freshly by inoculating a single colony of ER2738 into LB broth containing 20 µg/ml of tetracycline and incubated at 37 °C with a vigorous shaking at 250 rpm until desired OD<sub>600</sub>.

### 3.5.11.2 Phage titering and plaques forming unit (pfu/ml) determination

Phage titering was performed to calculate the input and output of phage particles in biopanning. The measurement was determined experimentally by infecting *E. coli* (ER2738) in a petri dish and then evaluated by quantifying the number of plaque-forming units (cfu) left overnight on the bacterial lawn.

Ten ml of LB broth containing 20 µg/ml of tetracycline was inoculated with a single colony of ER2738 culture and incubated with a vigorous shaking at 250 rpm for 4-8 hours until OD<sub>600</sub> ~ 0.5 (mid-log phase). While cells were growing, Top agar was melted in microwave oven and the molten Top agar was kept at 50 °C until subsequent used. LB plates containing 40 µg/ml of Xgal as well as 50 µg/ml of IPTG (designated here as LB/IPTG/Xgal), which will be used in phage titering were pre-warmed at 37 °C for at least one hour prior to spreading of diluted phage. Basically, one LB/IPTG/Xgal plate per each dilution was prepared.

One µl of phage was serially diluted to appropriate dilutions in LB broth, ranging from 10 to 10<sup>4</sup>-fold for unamplified phages as well as 10<sup>8</sup> to 10<sup>11</sup> for amplified phages. To each dilution step, diluted phage was mixed by vigorous vortex for 10 seconds followed by brief spun before preceded to next dilution step. Two hundred µl of a mid-log phase *E. coli* culture was dispensed into microcentrifuge tubes and 10 µl of each diluted phage was then added into microcentrifuge tube (one tube/dilution). The phage infections was performed by brief vortexed of the mixture, followed by incubated at room temperature for 5 minutes. The infected cells were then transferred into 5 ml disposable sterile culture tube and 3 ml of pre-warmed (~ 50 °C) molten Top agar was then added to each of dilution tube. The samples were mixed and immediately poured onto a pre-warmed LB/IPTG/Xgal plate, and the plate was tilted gently to ensure even distribution. The plates were cooled for 5 minutes at room temperature and then incubated overnight at 37 °C.

Plaques on the plate that have ~ 100 plaques were calculated, then the number of plaques was multiplied with dilution factor to determine the plaque forming units (pfu) per 10  $\mu$ l. Usually, the titer of phage was expressed in unit of cfu/ml.

### **3.5.11.3 Phage amplification and precipitation**

A single colony of ER2738 was inoculated in 20 ml of LB broth using 250-ml Erlenmeyer flask and incubated at 37 °C with vigorous shaking. The growth of the culture was monitored carefully so that the culture did not grow beyond early log phase ( $OD_{600}$  0.01-0.05) or alternatively, an overnight culture of ER2738 was 1:100 diluted in 20 ml LB. Approximately 80  $\mu$ l of eluate phage (unamplified) from each of the biopanning step was added to the culture and incubated with vigorous shaking (250 rpm) for 4.5 hours at 37 °C.

Cell culture was then transferred to a 50-ml Falcon tube and centrifuged for 20 minutes at 4,000  $\times g$  at 4 °C. Supernatant was transferred to a new tube and re-spun, whereas the pellet was discarded. After that, 16 ml (80 %) of the upper supernatant was transferred to a fresh tube and 4 ml of 20 % (w/v) PEG/2.5 M NaCl was added. Subsequently, the amplified phages were allowed to precipitate at 4 °C for at least 2 hours, preferably overnight.

Subsequently, PEG precipitation was centrifuged at 12,000  $\times g$  for 15 minutes at 4 °C and the supernatant was discarded. Then, the tube was re-centrifuged briefly and the remaining residual supernatant was removed with a pipette. Phage pellet is likely a white finger print sized smear on the side of the tube. The pellet was suspended in 1 ml TBS and transferred to a microcentrifuge tube and spun at maximum speed (18,700  $\times g$ ) for 5 minutes at 4 °C to pellet residual cells. Supernatant was transferred to a fresh microcentrifuge tube and re-precipitated by adding 200  $\mu$ l of 20 % (w/v) PEG/2.5 M NaCl and then let it incubated on ice for 15-60 minutes. The sample solution was

centrifuged at  $18,700 \times g$  for 10 minutes at 4 °C. The supernatant was then discarded and the tube was re-spun briefly to remove the residual supernatant with a pipette. The pellet was resuspended in 200  $\mu$ l of TBS and incubated at room temperature for 1 hour. After that, the phage suspension was centrifuged at full speed for an additional 1 minute to pellet any remaining insoluble material and the supernatant (amplified phage) was then transferred to a fresh tube and can be stored for up to three weeks at 4 °C or long term storage at -20 °C under equal volume of glycerol.

#### **3.5.11.4 Storage of phage**

Eluted phage (in 0.2 M Glycine-HCl, pH 2.2 and neutralized with 1 M Tris-HCl, pH 9.1) as well as amplified phage (0.1 M TBS; either by adding of 0.02 % (w/v)  $\text{NaN}_3$  or incubated at 65 °C for 15 minutes to kill the residual of *E. coli*) can be kept for up to several weeks at 4 °C. For long term storage, phage stock was diluted 1:1 with sterile glycerol and 0.02 % (w/v)  $\text{NaN}_3$  and stored at -20 °C. The phage stored at -20 °C was recovered by re-amplification from phages stock prior to further experiments (e.g., biopanning, phage ELISA).

### 3.5.12 Biopanning of the phage display library

Biopanning was carried out using Costar high binding, flat bottom 96 well microtiter plate (Corning Incorporated, USA) accordingly to the direct target coating method described in Ph.D.<sup>TM</sup> Phage Display Libraries instruction manual. The following method can be used to immobilize target protein by hydrophobic adsorption on polystyrene plate whereby the target protein was coated onto the plate and then excess target was removed.

In general, 150  $\mu$ l of target solution (50  $\mu$ g target/ml of 0.1 M NaHCO<sub>3</sub>, pH 8.6) was added to each of the microtiter well and swirled repeatedly until the surface of each well was completely coated with the target solution. This was followed by incubation of the plate overnight at 4 °C in a humidified container.

On the following day, the coating solution from each well was poured off and firmly slapped face down onto a clean paper towel to remove residual solution. After that, each of the well was completely filled with 200  $\mu$ l of blocking buffer [0.5 mg/ml of BSA, 0.1 M NaHCO<sub>3</sub>, pH 8.6, 0.02 % (w/v) NaN<sub>3</sub>] and incubated at 4 °C for at least one hour. The blocking buffer was discarded as described in the above steps and washed with 300  $\mu$ l of TBST [TBS plus 0.1 % (v/v) Tween 20 for the first round of panning and TBS plus 0.5 % (v/v) Tween 20 for the subsequence rounds of panning experiment] with vigorous pipetting steps. The washing solution was poured off and the plate was slapped face down onto a clean paper each time. The washing steps were repeated for six times. Next, a total of 1  $\mu$ l of phage (original library) was diluted with 100  $\mu$ l of TBST [TBS plus 0.1 % (v/v) Tween 20] and dispensed into coated well and rocked gently at 15 rpm for 60 minutes at room temperature using a waver shaker (Major Sciences). The non-binding phage was then discarded and the plate was slapped face-down onto a clean paper towel. The well was washed thoroughly with PBST for 10 times as described before. The bound phages were eluted by pH shift with 0.2 M

glycine-HCl (pH 2.2) supplemented with 1 mg/ml BSA. The plate filled with elution buffer was rocked gently for 20 minutes and the eluate was aspirated into fresh microcentrifuge tube using pipette tip, and neutralized with 15  $\mu$ l of 1 M Tris-HCl, pH 9.1. One  $\mu$ l of the eluate was titered as described in general M13 phage titering protocol. The rest of the eluate was then amplified and precipitated as above protocol (Session 3.5.11.3).

Basically, the amplified eluates from previous round of biopanning were used for subsequent round of selection. In general, three biopanning were performed in typical epitopes mapping assay. Phage titering was carried out after each round of biopanning experiment not only to determine the concentration of bound/amplified phage but also used to calculate an appropriate input volume corresponding to the input titer in subsequent round of biopanning process. The input phage titer must be as little as  $10^9$  pfu for succeeding rounds of biopanning process.

Basically, after a third round of biopanning, a serial dilution ranging from  $10^1$  to  $10^5$  was carried on the unamplified eluate as described in general phage titering method and the diluted phages were then incubated overnight on LB/IPTG/Xgal plates at 37 °C no longer than 18 hours, as deletions may occur if plates were grown longer. Plaques from this titering were picked and amplified as following protocol for subsequence phage ELISA assay and sequencing.

### **3.5.13 Post panning protocols: Mini preparation of phage amplification for sequencing and peptide binding assays**

After third round of biopanning, 20 phage clones were randomly selected and identified by DNA sequencing. The binding specificity of phage can be confirmed by phage ELISA and Western blot binding assays. In both cases, it was necessary to amplify phage either from individual plaques or from the eluted pools, to obtain sufficient quantities to work with those assays.

An overnight ER2738 culture was 1:100 diluted in LB broth and dispensed 1 ml each into the 2 ml disposable culture tubes (one phage/tube). Approximately 10-20 of well separated form of blue colonies were randomly picked from a 1-3 days old, stored at 4 °C, and have less than 100 plaques titering plate using sterile pipette tip, and transferred to a tube containing 1 ml of diluted culture (one phage/tube). The tubes were then incubated at 37 °C with shaking at 250 rpm for 4.5 hours. The cultures were then spun at  $18,700 \times g$  for 30 seconds and the supernatant was then transferred to a fresh tube and re-spun. Using pipette, 800  $\mu$ l of the upper supernatant was transferred to a new tube and this was the amplified phage stock and can be stored at 4 °C for several weeks until further single stranded DNA isolation for sequencing or peptide binding assays.



### 3.5.13.1 Phage single-stranded DNA (ssDNA) isolation and sequencing

Single stranded bacteriophage M13 phagemid DNA was isolated from 500  $\mu$ l of amplified phage stock obtained from above amplification procedures. Generally, 200  $\mu$ l of 20 % (w/v) PEG/2.5 M NaCl was added to the 500  $\mu$ l of amplified phage stock and mixed by inverting the tube for several times, and let it to stand for 20 minutes at room temperature. After that, the precipitate phage solution was centrifuged at  $18,700 \times g$  for 10 minutes at 4 °C, and the supernatant was discarded. Basically, pellet may not be visible in such concentration. The remaining supernatant was re-centrifuged briefly and then aspirated carefully using pipette. The pellet was suspended thoroughly in 100  $\mu$ l of iodide buffer by vigorous tapping the tube. Then, 250  $\mu$ l of absolute ethanol was added to phage solution and was left to incubate for 20 minutes at room temperature. Short incubation at room temperature enhance the precipitated of phage ssDNA, while leaving most of phage protein in solution. After that, the microcentrifuge tube was centrifuged at  $18,700 \times g$  for 10 minutes at 4 °C and the supernatant was discarded. The pellet was then washed with 500  $\mu$ l of 70 % prechilled (-20 °C) ethanol, re-spun at  $18,700 \times g$  for 10 minutes at 4 °C. The supernatant was discarded and the pellet was air-dried overnight at room temperature. Finally, the pellet was suspended in 30  $\mu$ l of TE buffer and stored at -20 °C.

The concentration and purity of phage ssDNA were measured using NanoPhotometer<sup>TM</sup> (IMPLEN, Germany) as well as 1 % (w/v) agarose gel. In agarose gel electrophoresis, 5  $\mu$ l of phage ssDNA should give a band of comparable intensity to 0.5  $\mu$ g of purified single-stranded M13mp18 DNA ladder (NEB). Ten  $\mu$ l of ssDNA of each phage was sequenced using a -96gIII sequencing primer (5'-CCCTCATAGTTAGCGTAACG-3'). The nucleotide sequence of the phages were aligned with BioEdit version 7.0.9 Software (Hall, 1999) and a consensus sequences were compared to the sequence of original construct to obtain the translation

polypeptide sequence expressed by each of the individual phage.

### 3.5.13.2 Phage ELISA binding assay

The binding affinity of the selected phages to the target *Plasmodium* AMA1 ectodomain was determined using ELISA binding assay. This assay was essential to distinguish the true target binding from binding to the plastic support in the direct coating method of panning.

Each clone to be characterized after confirmation by sequencing was amplified as steps in phage amplification and precipitation (Session 3.5.11.3). In general, 5  $\mu$ l of each phage stock was added to the 20 ml of ER2738 culture ( $OD_{600}$  0.01 - 0.05) and incubated with vigorous aeration at 250 rpm for 4.5 hours at 37 °C. The amplified phage was finally suspended in 50  $\mu$ l of TBS and titer as general M13 method and the titer should be  $\sim 10^{14}$  pfu/ml. The phage stock can be either stored at 4 °C up to several weeks or long term stored at -20 °C in presence of 50 % (v/v) glycerol and 0.02 % (w/v)  $NaN_3$ .

The wells of the microtiter plate (every phage clone to be assayed per well) were coated (100  $\mu$ g/ml of *Plasmodium* AMA1 in 0.1 M  $NaHCO_3$ , pH 8.6) and blocked [0.1 M  $NaHCO_3$ , 0.5 mg/ml BSA, 0.02 % (w/v)  $NaN_3$ ] as biopanning step. Another row of uncoated wells per phage clone to be assayed were also blocked to test for binding of each selected sequence to BSA-coated plastic (background binding). One hundred  $\mu$ l of each of the phage ( $\sim 10^9$  in TBST) was filled respectively into one target-coated and one uncoated (blocked) wells and incubated at room temperature for 2 hour with agitation and washing similar to biopanning steps.

The HRP-conjugated anti-M13 monoclonal antibody (GE Healthcare) was 1:5,000 diluted in blocking buffer [0.1 M  $NaHCO_3$ , 0.5 mg/ml BSA, 0.02 % (w/v)  $NaN_3$ ]. Two hundred  $\mu$ l of diluted conjugate was added into each well and incubated at

---

room temperature for 1 hour with agitation. The diluted conjugate was shaken out and washed the plate 6 times with TBST. One hundred  $\mu\text{l}$  of ABTS<sup>™</sup> Chromophore substrate solution (Calbiochem) was added to each well and incubated at room temperature for up to 30 minutes. The reaction was stopped by adding 100  $\mu\text{l}$  of 0.5 M  $\text{H}_2\text{SO}_4$  to the wells and mixed properly, and the absorbance was read at 405 nm using ELISA iMark<sup>™</sup> microplate reader (BioRad). For each phage colony, the signals obtained with and without target protein were compared and the folds of binding were calculated by dividing the absorbance obtained from target protein to the absorbance obtained from BSA.

### 3.5.13.3 Western blot binding assay

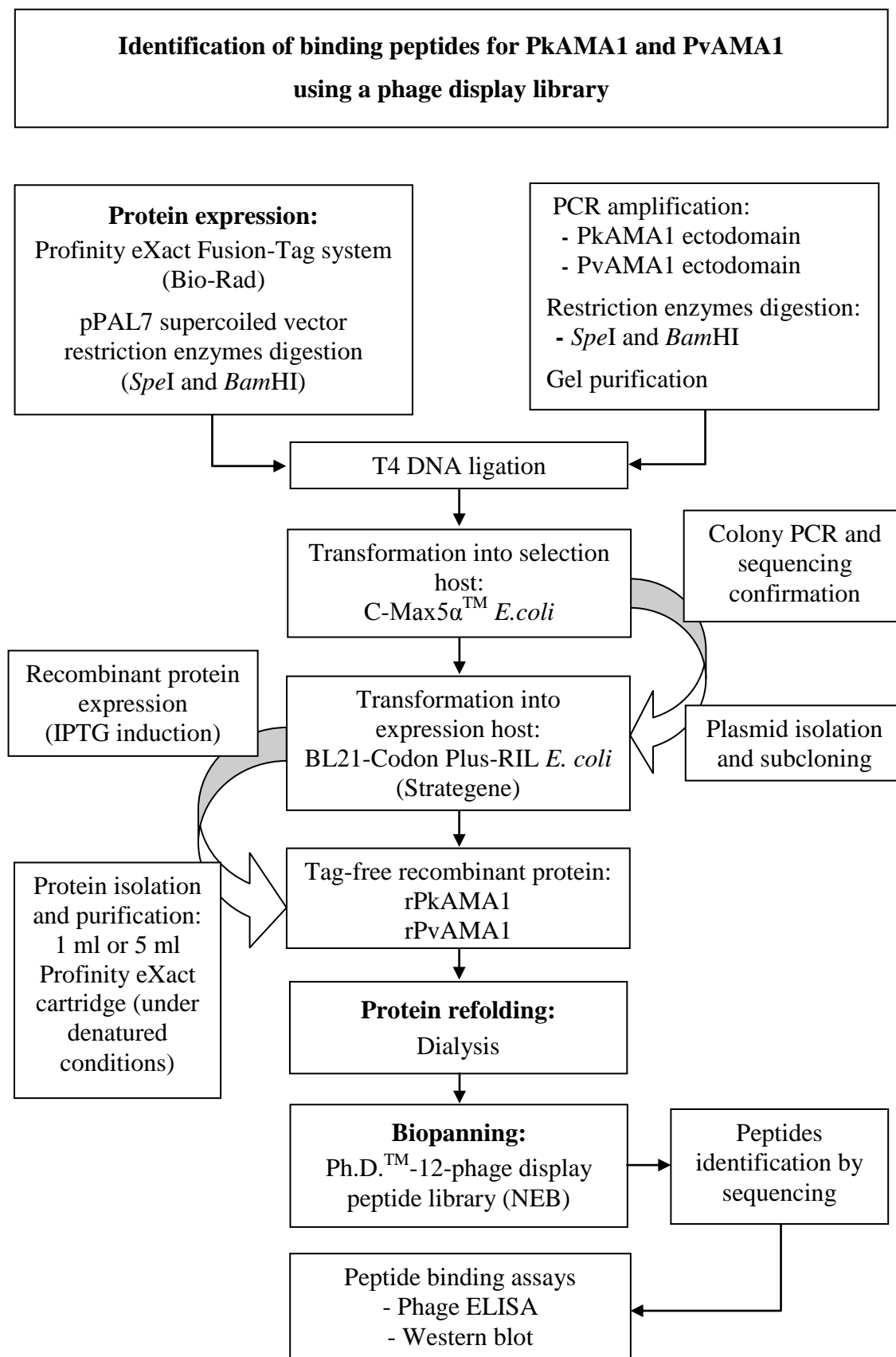
Binding phages were further confirmed by Western blot as described in Western hybridization (Session 3.5.4). In general, rPkAMA1 and rPvAMA1 proteins (10  $\mu\text{g}/\text{well}$ ) were electrophoresed on 12 % SDS-PAGE under non-reducing condition and then blotted onto a nitrocellulose membrane. The location of AMA1 protein was confirmed using NOVEX® Reversible membrane protein stain (Invitrogen). The blot was then cut into individual strips. The location of target protein was marked and then destained properly prior subjected to Western blot binding assay.

The membrane strips were air dried and blocked with 3 % (w/v) BSA for 1 hour at room temperature and then wash twice with PBST for 5 minutes in each wash. After that, protein strip was then incubated with each individual phage ( $10^9$  phage particles) for 1 hour at room temperature followed by two washing steps with PBST for 5 minutes each. The binding affinity of the each individual phage to rPkAMA1 and rPvAMA1 were determined using 1:2,500 HRP-conjugated anti-M13 monoclonal antibody (GE Healthcare) in antibody dilution buffer [PBST, 1 % (w/v) BSA] and Opti-4CN (Bio-Rad) as the substrate. The results obtained were captured with a digital camera.

### 3.5.14 Protein sequence and bioinformatic analysis

The whole genome of AMA1 of *P. knowlesi* and *P. vivax* were searched using BLASTN and aligned with BioEdit version 7.0.9 Software (Hall, 1999). Consensus motifs between the various peptide sequences were determined with ClustalW (Thompson, et al., 1994). The inserted coding frame of AMA1 ectodomain as well as phage displayed binding peptides was confirmed by Translate tool accessed via the ExPASy interface (<http://au.expasy.org>; Gasteiger, et al., 2003). Compute pI/MW tool ([http://web.expasy.org/compute\\_pi/](http://web.expasy.org/compute_pi/)) was used to determine the theoretical isoelectric point (pI) and molecular mass. The solubility of the *Plasmodium* AMA1 ectodomain recombinant proteins assuming the protein is being overexpressed in *E. coli* was predicted based on the amino acids composition using Recombinant Protein Solubility Prediction statistical tool (<http://biotech.ou.edu/>; Wilkinson & Harrison, 1991).

### 3.5.15 Overview of the identification of binding peptides for PkAMA1 and PvAMA1 using a phage display library



---

## CHAPTER FOUR: RESULTS

### 4.1 Clinical sample collection and DNA extraction

A total of 226 suspected malaria blood samples and 20 healthy control samples were collected during 2008 to 2010. In specificity validation of the multiplex PCR system, DNA from bacteria strains, i.e., *Aeromonas aquariorum*, *Aeromonas caviae*, *Aeromonas hydrophila*, *Aeromonas veronii*, *Vibrio harveyi*, *Vibrio parahaemolyticus*, and *Serratia* species were extracted. Besides that, DNA from other non-malaria parasites, i.e., *Toxoplasma gondii*, *Giardia duodenalis*, and hookworm (i.e., *Necator americanus* and *Ancylostoma duodenale*) were also obtained.

### 4.2 Identification of malaria by microscopic examination

A total of 211 malaria samples were positive by microscopic examination, in which 203 samples were single infection samples with 83, 63, 38, and 6 samples were identified as *P. vivax*, *P. falciparum*, *P. malariae*, and *P. knowlesi* respectively, whereas 13 samples were identified as either *P. malariae* or *P. knowlesi* samples. None of *P. ovale* infection was detected. Eight samples were examined as mixed infections, i.e., two were *P. vivax* mixed with *P. falciparum*, three were *P. vivax* mixed with *P. malariae*, one was *P. vivax* mixed with *P. knowlesi*, and two were *P. falciparum* mixed with *P. malariae*.

Of the positive samples, 91 cases (43 %) were scored as + category, 23 cases (11 %) were ++, 31 cases (15 %) were +++, and 66 cases (31 %) were +++. Whereas another 15 blood samples obtained from patients with clinical malaria symptoms and 20 healthy control samples were negative via microscopic examination.

Table 4.1 summarized the distribution of *Plasmodium* species by cases and parasitemia scores via microscopic examination.

Table 4.1: Distribution of *Plasmodium* species and parasitemia obtained from microscopic examination.

<div>Parasitemia</div> <div>Microscopy result</div>	Plus system (Parasites/μl)				Total (%)
	+	++	+++	++++	
	4-40	41-400	401-4,000	> 4,000	
<i>P. vivax</i>	38	7	13	25	<b>83 (39)</b>
<i>P. falciparum</i>	23	6	11	23	<b>63 (30)</b>
<i>P. malariae</i>	11	10	7	10	<b>38 (18)</b>
<i>P. knowlesi</i>	6	0	0	0	<b>6 (3)</b>
<i>P. malariae</i> or <i>P. knowlesi</i>	13	0	0	0	<b>13 (6)</b>
<i>P. ovale</i>	0	0	0	0	<b>0 (0)</b>
<i>P. vivax</i> & <i>P. falciparum</i>	0	0	0	2	<b>2 (1)</b>
<i>P. vivax</i> & <i>P. malariae</i>	0	0	0	3	<b>3 (1)</b>
<i>P. vivax</i> & <i>P. knowlesi</i>	0	0	0	1	<b>1 (1)</b>
<i>P. falciparum</i> & <i>P. malariae</i>	0	0	0	2	<b>2 (1)</b>
<b>Total (%)</b>	<b>91 (43)</b>	<b>23 (11)</b>	<b>31 (15)</b>	<b>66 (31)</b>	<b>211 (100)</b>
Suspected malaria case (microscopy negative)	15				
Healthy control (microscopy negative)	20				

### 4.3 Nested PCR

A primer pair of genus-specific, rPLU1 and rPLU5 for first nested PCR (Snounou, et al., 1993) as well as five pairs of species-specific primers for second nested PCR (Singh, et al., 1999; Singh, et al., 2004), targeting to 18S ssu rRNA gene of five of human *Plasmodium* species were synthesized (Appendix 3.1). Due to the inability of currently available nested PCR in identifying *P. ovale wallikeri* (variant type), which has some genetic differences with *P. ovale curtisi* (classic type), a primer pair targeting to both *P. ovale* subtypes (Padley, et al., 2003) was included into the nested PCR assay (Appendix 3.1). Hence, a total of seven separate monoplex PCR was performed in the identification of five human *Plasmodium* species.

DNA fragment of first nested PCR targeted to 18S ssu rRNA gene was approximately 1.7 kb. The second nested PCR DNA fragment with sizes of 117 bp for *P. vivax*, 144 bp for *P. malariae*, 153 bp for *P. knowlesi*, 205 bp for *P. falciparum*, and 787 bp and 375 bp (alternative primer pair) for *P. ovale*.

Figure 4.1 shows the positive clinical samples for five human *Plasmodium* species in nested PCR assay.



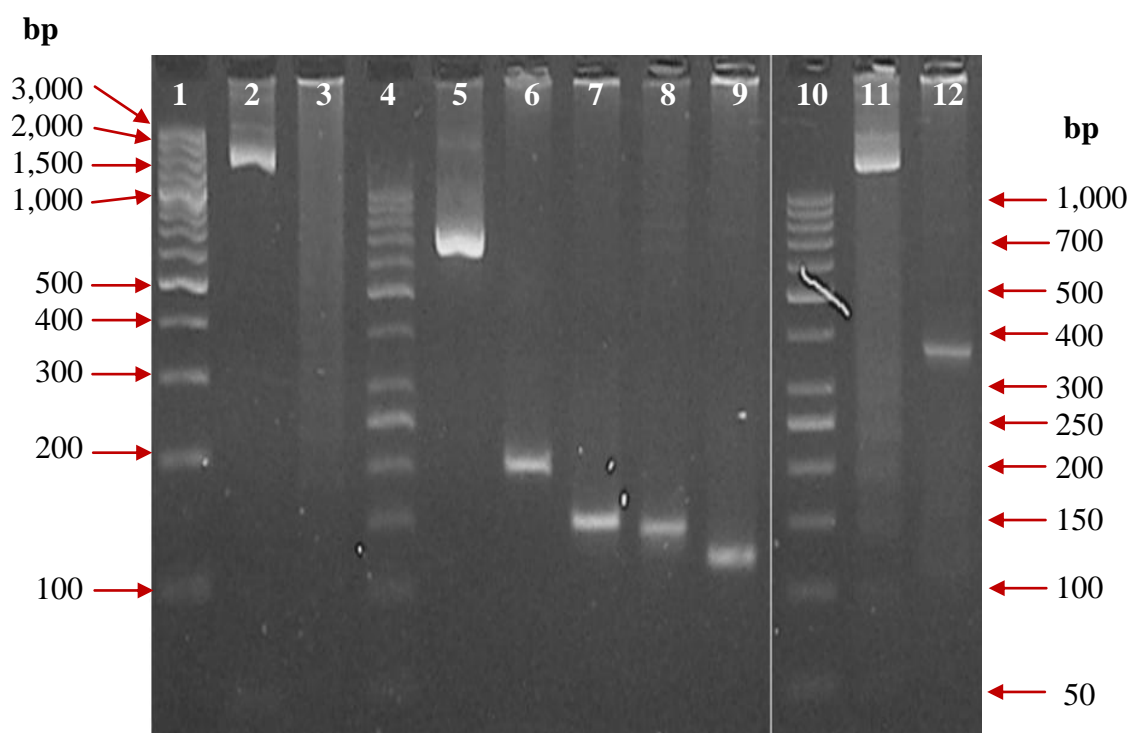


Figure 4.1: Nested PCR results. First nested PCR targeting genus conserved region of 18S ssu rRNA gene of *Plasmodium* species and second nested PCR targeting species conserved region were used in *Plasmodium* species determination.

Lanes,

- 1 : 100 bp plus DNA ladder (Fermentas)
- 2 & 11 : First nested PCR; sample with *Plasmodium* species infection (~ 1.7 kb)
- 3 : First nested PCR; sample absent of *Plasmodium* species infection
- 4 & 10 : 50 bp DNA ladder (Fermentas)
- 5 : *P. ovale curtisi* (787 bp)
- 6 : *P. falciparum* (205 bp)
- 7 : *P. knowlesi* (153 bp)
- 8 : *P. malariae* (144 bp)
- 9 : *P. vivax* (117 bp)
- 12 : *P. ovale* (375 bp) [Alternative primer pair from Padley, et al., 2003]

---

#### 4.4 18S ssu rRNA plasmids construction

A total of nine clones were constructed in the present study, i.e., two for each species, *P. vivax*, *P. knowlesi*, *P. malariae*, *P. falciparum*, and one for *P. ovale* based on availability of clinical samples. In general, PCR was performed using rPLU1 and rPLU5 primers as described in the first nested PCR that generated PCR amplicons with a size of ~ 1.7 kb. PCR product was then gel purified prior to cloning into pCR® II-TOPO vector (4.0 kb). *Escherichia coli* Top10 competent cells used here were prepared from stock culture to ensure that the transformation efficiencies in cloning experiments.

The putative positive clones were selected from white colonies from LB/IPTG/Xgal/ampicillin plates and then further confirmed by colony PCR and sequencing using T7 and SP6 promoter primers encompassing ~ 186 bp TA cloning site, which resulted in ~ 1.9 kb PCR amplicon, indicative of positive clone. The inserted DNA for each construct was sequenced and checked with BLASTN (<http://blast.ncbi.nlm.nih.gov/Blast.cgi>) for further clone confirmation. Finally, five human *Plasmodium* species clones were developed successfully and served as positive controls in the subsequent PCR amplifications as well as templates for sensitivity and specificity validation.

## 4.5 Development of a single step multiplex PCR detection assay for five human *Plasmodium* species

### 4.5.1 Multiplex PCR primers design and PCR optimization

The challenge of multiplex PCR development is to make the designed primers have similar annealing temperature while amplification products should be distinguishable in size in a single reaction when analysis is performed using agarose gel electrophoresis. For instance, primers in the present multiplex system is able to generate PCR fragments ranged between 200 to 500 bp, i.e., ~ 453 bp for *P. falciparum*, ~ 341 bp for *P. malariae*, ~ 304 bp for *P. ovale*, ~ 284 bp for *P. knowlesi*, and ~ 215 bp for *P. vivax*, after PCR (Figure 4.2).

The selected primers were tested through BLASTN search (<http://blast.ncbi.nlm.nih.gov/Blast.cgi>) and *in silico* PCR amplification (<http://insilico.ehu.es/PCR/index.php>) for the amplicon prediction. There was no any other nonspecific amplification from nontarget gene. Finally, single step multiplex PCR system utilizing five forward species-specific primers and a single reverse genus-specific primer targeting 18S ssu rRNA gene sequences from five human *Plasmodium* species was successful established.

PCR conditions and reaction mixture for each of the primer pairs were optimized individually and then mixed together to perform a multiplex PCR for the detection of five human malaria parasites. Regarding the PCR conditions, thermocycling conditions was initially optimized based on primer annealing temperatures ranging from 52 °C to 62 °C. The PCR bands of each primer pair in individual assay became invisible after 60 °C, therefore, the final multiplex PCR annealing temperature was set at 56 °C, which showed shaper and clearer bands in all five primer pairs. Due to relatively high AT-content in the *Plasmodium* DNA, lower extension temperature of 65 °C was selected and the extension time for 40 seconds was

sufficient to amplify all target genes.

Initially, equimolar primer concentration of 0.4  $\mu\text{M}$  each were used in the multiplex PCR, but there were inconsistent amplifications, with some of the larger fragments barely visible if compared to smaller fragments even after the reaction was optimized for the PCR conditions. To overcome this problem, the proportions of primers were changed, i.e., increase in the amount for the weak binding primers and a decrease in the amount for the strong binding primers. The final concentration of each primer (ranged between 0.4 to 0.6  $\mu\text{M}$ ) varied considerably was established empirically.

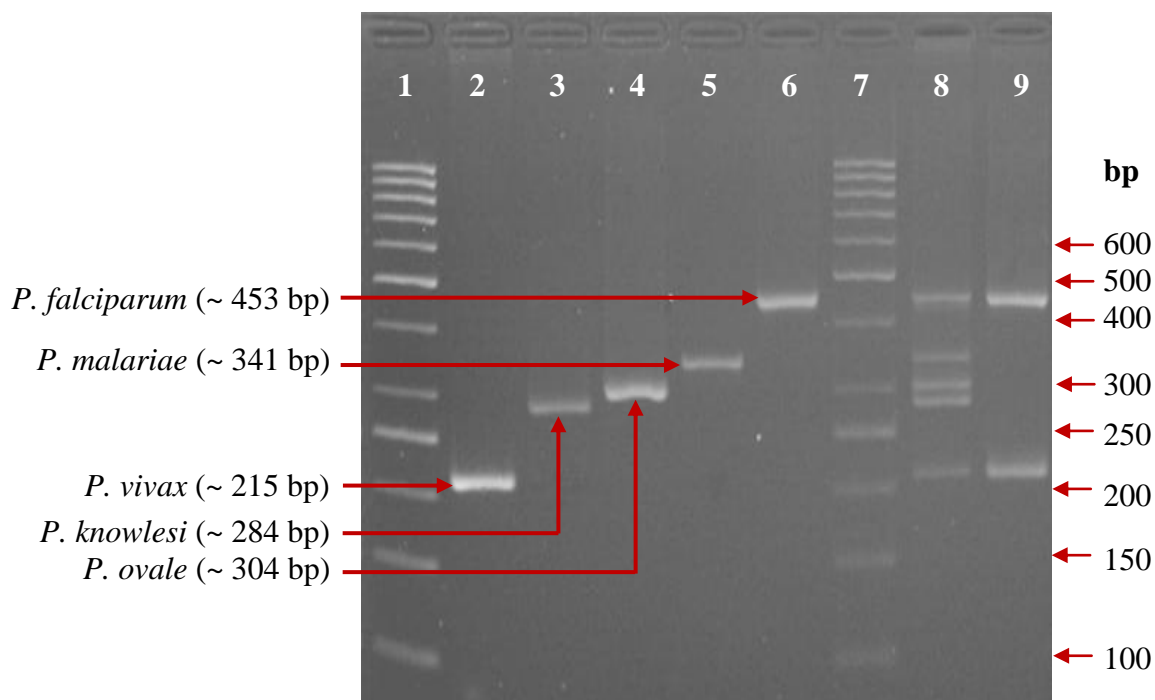


Figure 4.2: Pentaplex PCR results. All *Plasmodium* species primers target the 18S ssu rRNA gene of *Plasmodium* species resolved in 3 % (w/v) agarose gel stained with ethidium bromide.

Lanes,

1 & 7 : 50 bp DNA ladder (Fermentas, USA),

2 : *P. vivax* (~ 215 bp)

3 : *P. knowlesi* (~ 284 bp)

4 : *P. ovale* (~304 bp)

5 : *P. malariae* (~ 341 bp)

6 : *P. falciparum* (~ 453 bp)

8 : Ladder for five human *Plasmodium* species

9 : *P. vivax* mixed *P. falciparum*

### 4.5.2 Positive control

In the present multiplex PCR development, positive control was included as indicative of successful DNA extraction procedure as well as functionality of the PCR reaction mixture for amplification of the target DNA. Generally, three additional primer pairs were designed and tested individually on optimized pentaplex PCR system. The external positive control is an external DNA source spiked into test specimen, whereas an internal positive control is a nontarget DNA sequence occurring naturally in the test specimen, which is simultaneously extracted and co-amplified in the same tube together with the target DNA (Hoorfar, et al., 2004). The procedures of each of the positive control and the observations based on screening of 50 clinical samples were described.

#### 4.5.2.1 The pGEX4T1 plasmid DNA

Inclusion of pGEX4T-1 plasmid DNA as external positive control DNA as well as a pair of pGEX-targeted primers, i.e., pGEX 5' (5'-GGGCTGGCAAGCCACGTTT GGTG-3') and pGEX 3' (5'-CCGGGAGCTGCATGTGTCAGAGG-3') to primary optimized pentaplex PCR conditions generated a DNA fragment with a size of ~ 173 bp.

Due to high amount and integrity of the plasmid DNA compared to *Plasmodium* DNA, therefore the multiplex PCR system tends to favor the plasmid DNA amplification. This consequently led to the competition for PCR reagents and thus impairing the detection sensitivity in the present pentaplex system. The PCR selection phenomenon is referred to as competition inhibition. Even though the concentration of plasmid DNA was reduced to 50 pg and primers to 0.1  $\mu$ M, the competition effect still pose a problem, especially to samples with low parasitemia, thus limiting the applicability as positive control in the present multiplex PCR system. Figure 4.3 shows the PCR results with the inclusion of a pGEX4T1 plasmid DNA and its primer pair into clinical samples, which have a high parasitemia average.

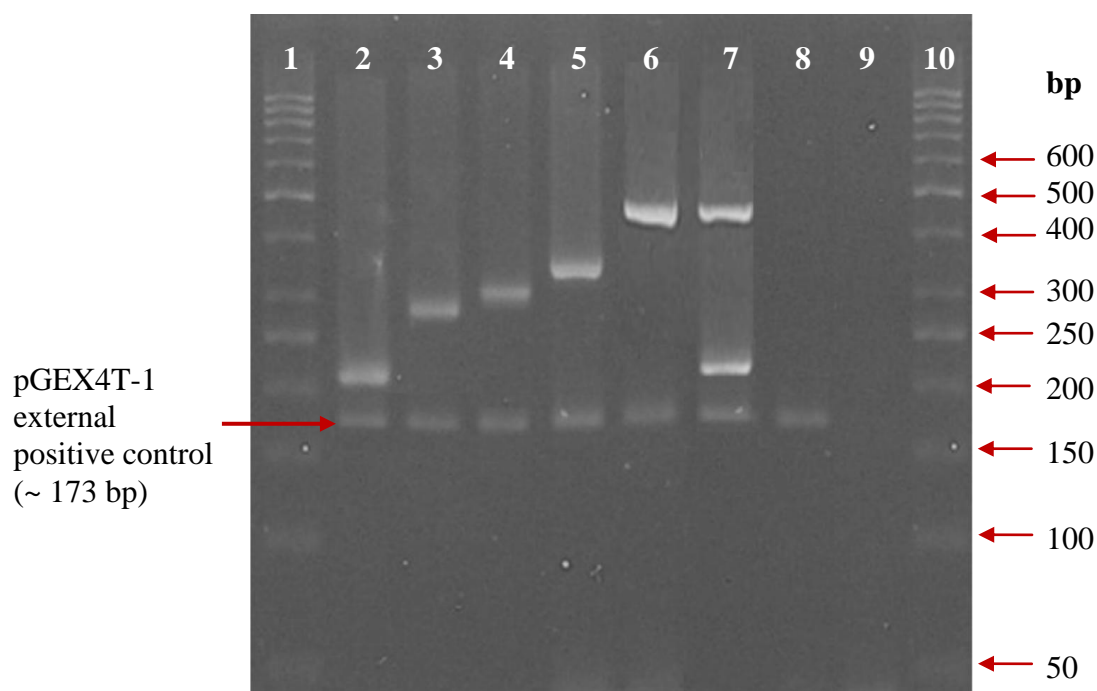


Figure 4.3: Multiplex PCR results with an external positive control, pGEX4T plasmid DNA.

Lanes,

1 & 10 : 50 bp DNA ladder (Fermentas, USA),

2 : *P. vivax*

3 : *P. knowlesi*

4 : *P. ovale*

5 : *P. malariae*

6 : *P. falciparum*

7 : *P. vivax* and *P. falciparum*

8 : pGEX4T-1, external positive control (~ 173 bp)

9 : DNA blank

---

#### 4.5.2.2 The human and *Plasmodium* 18S ssu rRNA genes

The inclusion of a human and *Plasmodium* 18S ssu rRNA conserved primer as forward primer (HP-F) and a human 18S ssu rRNA conserve reverse primer (HR155) to the pentaplex system generated two additional DNA fragments in pentaplex PCR system (Figure 4.4). Of which, the larger DNA fragment with a size range between 580 bp and 630 bp indicated the presence of *Plasmodium* species, whereas the smaller fragment DNA with a size of ~ 155 bp indicated human DNA that served as internal positive control of the multiplex PCR system. The human 18S ribosomal RNA gene is one of the common housekeeping genes in molecular studies and the primers designed in the present study was referred to the gene sequence deposited in GenBank (i.e., accession number NR\_003286.2).

Based on the screening results of 50 clinical samples, the human control band appeared consistently in all clinical samples; however, the appearance and intensity of *Plasmodium* genus-specific and species-specific bands were different. Some PCR intensities denoted favor either genus-specific amplification or species-specific amplification, whereas some other showed similar intensities. The reason for the biasness in the multiplex PCR was not further tested in the present study. The inconsistencies of results in species determination limit this format as an internal positive control.



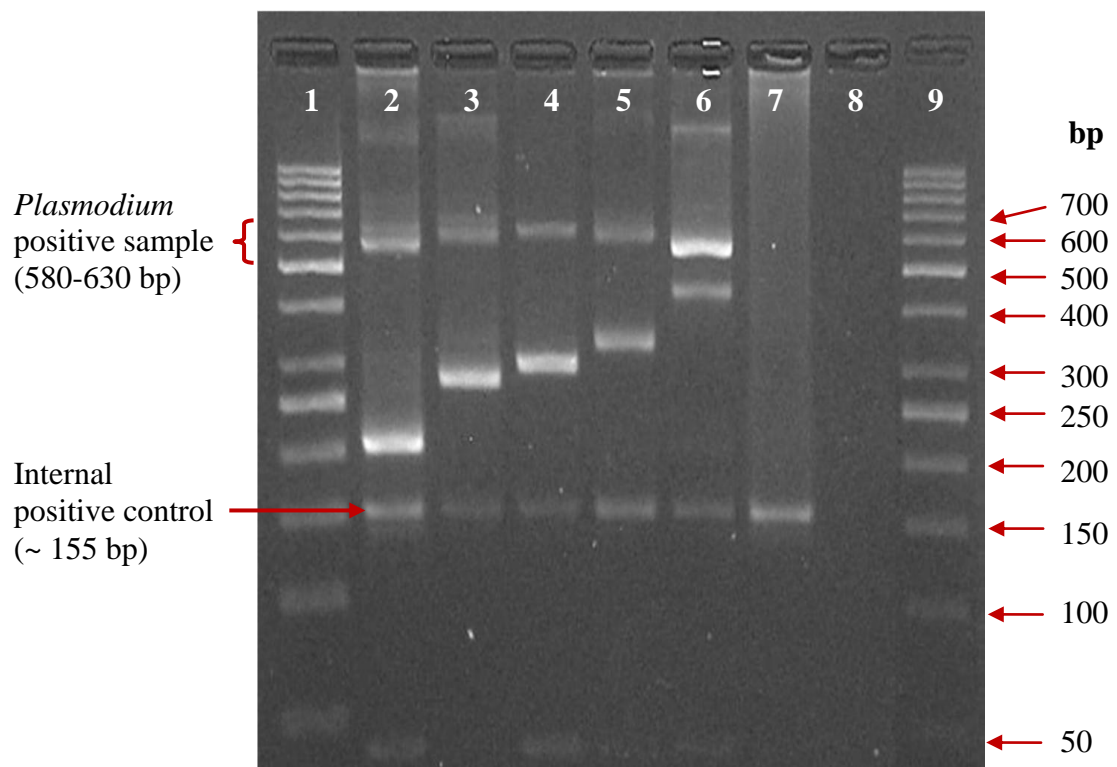


Figure 4.4: Multiplex PCR results with human internal positive control, *Plasmodium* genus-, and species-specific primers are both targeting 18S ssu rRNA gene.

Lanes,

1 & 10 : 50 bp DNA ladder (Fermentas, USA),

2 : *P. vivax*

3 : *P. knowlesi*

4 : *P. ovale*

5 : *P. malariae*

6 : *P. falciparum*

7 : *P. vivax* mixed *P. falciparum*

8 : Human internal positive control (~ 155 bp)

9 : DNA blank

#### 4.5.2.3 The human $\beta$ -hemoglobin gene

The inclusion of primer pair targeting human  $\beta$ -hemoglobin gene, i.e.,  $\beta$ -hemoglobin (F) (5'-CACAAGTGTGTTCACTAGC-3') and  $\beta$ -hemoglobin (R) (5'-CAACTTCATCCACGTTTCACC-3') into primary optimized pentaplex system generated an addition of PCR amplicon with a size of ~ 109 bp in all human samples. This human  $\beta$ -hemoglobin gene is a common human housekeeping gene in molecular studies. The primers design was referred to a gene sequence deposited as GenBank accession number of NM\_000518.4.

The concentration of primers used in PCR was fully optimized in present detection system, therefore no significant reduction of the sensitivity in the identification of five human *Plasmodium* species. The inclusion of this primer pair as internal positive control targeting heterologous gene gave a very consistence results in *Plasmodium* species determination that showed 100 % concordance to the results obtained from nested PCR. Finally, a hexaplex PCR detection system for identification of five human *Plasmodium* species together with a  $\beta$ -hemoglobin internal control was established. Figure 4.5 shows the hexaplex PCR results tested on six clinical samples.

The primers in this detection system were patented under reference no: PI 2010 003802 and currently is commercialized under Reszon Diagnostics International (<http://www.reszonics.com/product-Malaria.html>).

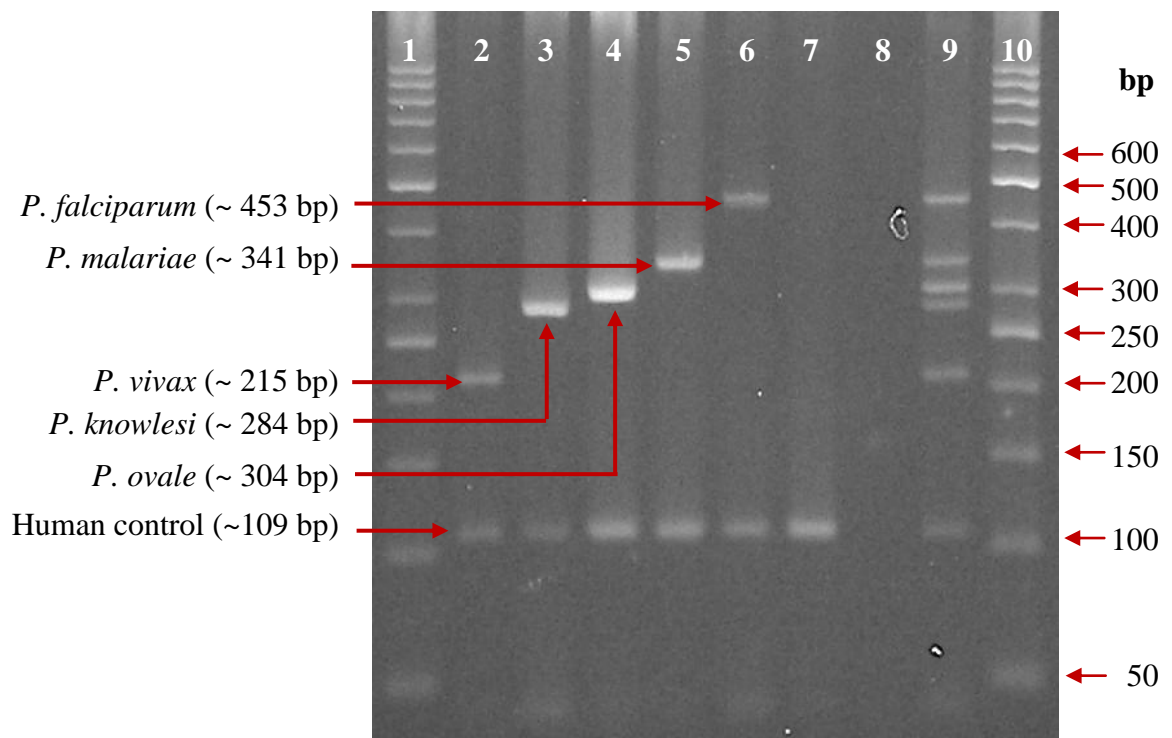


Figure 4.5: Hexaplex PCR results with a human internal positive control targeting  $\beta$ -hemoglobin gene. All *Plasmodium* species primers targeting 18S ssu rRNA gene of *Plasmodium* species.

Lanes,

1 & 10 : 50 bp DNA ladder (Fermentas)

2 : *P. vivax*

3 : *P. knowlesi*

4 : *P. ovale*

5 : *P. malariae*

6 : *P. falciparum*

7 : Healthy control sample

8 : DNA blank

9 : Hexaplex DNA ladder

### 4.5.3 Analytical sensitivity and specificity analyses

#### 4.5.3.1 Sensitivity in single infection

The starting parasitemia levels of the blood samples were 25,000 parasites/ $\mu$ l for *P. vivax*, 25,250 parasites/ $\mu$ l for *P. knowlesi*, 26,500 parasites/ $\mu$ l for *P. ovale*, 26,980 parasites/ $\mu$ l for *P. malariae*, as well as 15,000 parasites/ $\mu$ l for *P. falciparum*. The final detectable limit of the hexaplex PCR can be as low as 0.025 parasites/ $\mu$ l ( $10^{-6}$ ) for *P. vivax*, 0.25 parasites/ $\mu$ l ( $10^{-5}$ ) for *P. knowlesi*, 0.027 parasites/ $\mu$ l ( $10^{-6}$ ) for *P. ovale*, 0.27 parasites/ $\mu$ l ( $10^{-5}$ ) for *P. malariae*, and 0.15 parasites/ $\mu$ l ( $10^{-5}$ ) for *P. falciparum* (Figure 4.6).

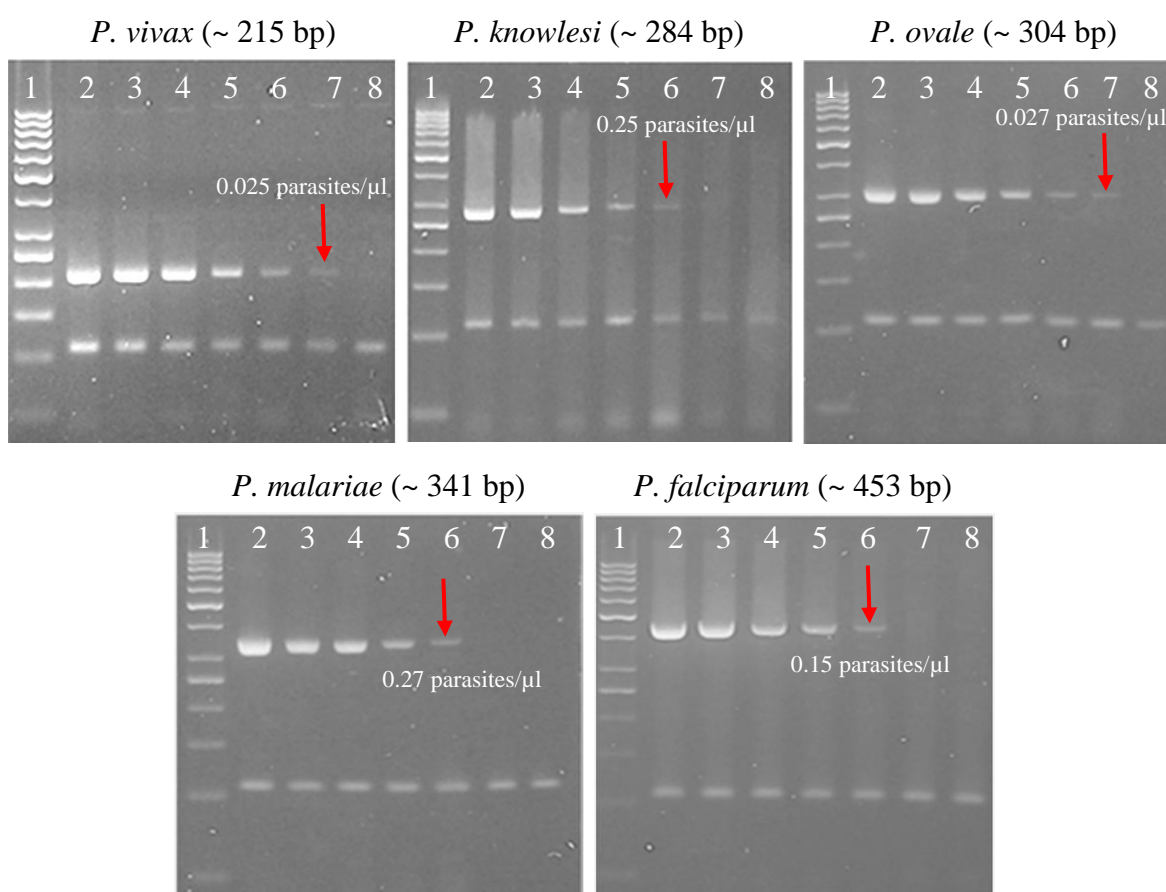


Figure 4.6: Detection limits of the hexaplex PCR system to five human *Plasmodium* species. Lane 1, 50 bp DNA ladder (Fermentas); Lanes 2-8, 10-fold dilutions of all five *Plasmodium* species DNA samples from malaria patients, using 10 ng/ $\mu$ l of human DNA. Dilution of *Plasmodium* DNA samples: lane 2,  $10^{-1}$ ; lane 3,  $10^{-2}$ ; lane 4,  $10^{-3}$ ; lane 5,  $10^{-4}$ ; lane 6,  $10^{-5}$ ; lane 7,  $10^{-6}$ ; lane 8:  $10^{-7}$ .

---

#### 4.5.3.2 Sensitivity in mixed infections

Sometimes, there is a possibility of more than one *Plasmodium* species infection occurring in a particular patient at the same time and this is recognized as mixed infections. In mixed infections, the ratios between the two or more parasite species can vary substantially in clinical samples (Conway, 2007; Mayxay, et al., 2004; Zimmerman, et al., 2004). Therefore, DNA and primer competition effects in mixed infections samples were also tested in the present study.

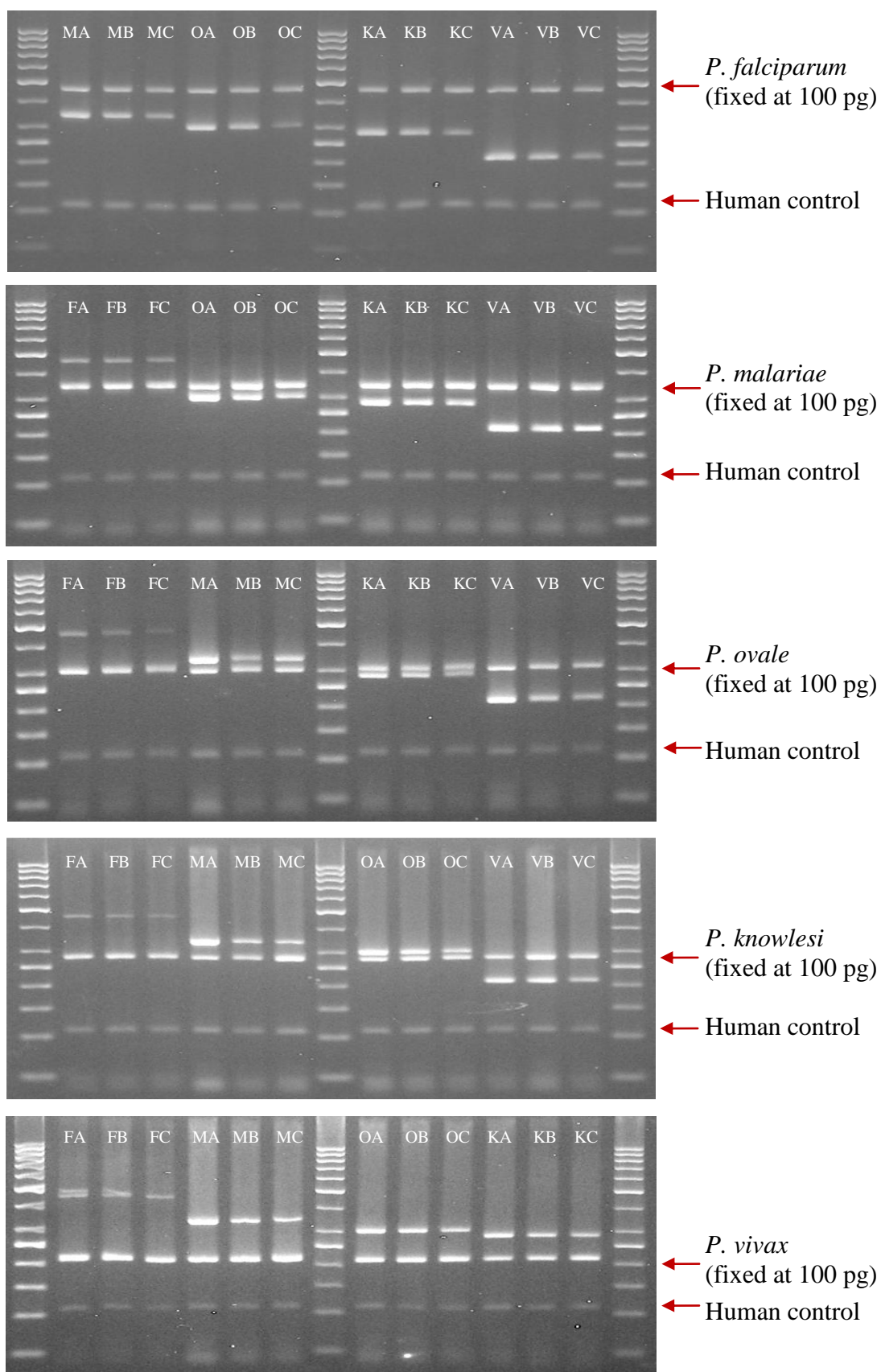
Due to the lack of natural acquired mixed infections during the study period, three simulated mixtures, i.e., 100 pg/μl of *P. vivax* clone DNA and 1, 10 or 100 pg/μl of *P. falciparum* clone DNA, were experimentally created to determine the sensitivity of this hexaplex PCR. A serial dilution of the DNA mixtures was performed using DNA solution containing 10 ng/μl human DNA. This was taken into consideration due to the presence of large amount of human DNA in the actual clinical samples. In addition, a pair of human housekeeping primers was included as internal positive control in the present detection system.

Subsequently, a sensitivity test with 12 different mixtures of DNA using two of the five human *Plasmodium* species for each set, together with another set of mixtures with all five *Plasmodium* species was performed as shown in Table 4.2. All mixed *Plasmodium* species DNA were successfully detected in the simulated mixtures (a total of 60 mixtures were tested) and the results are shown in Figure 4.7. A total of 10 possible combinations of DNA to create two-species-simulated mixed infections with equal clone DNA concentration (100 pg/μl) are shown in Figure 4.8.

Table 4.2: Validation of sensitivity in simulated mixed infections using clone DNA.

pg/ul	<i>P. falciparum</i>	<i>P. malariae</i>	<i>P. ovale</i>	<i>P. knowlesi</i>	<i>P. vivax</i>
<i>P. falciaprum</i>	100 (A)	100 (A)	100 (A)	100 (A)	100 (A)
		10 (B)	10 (B)	10 (B)	10 (B)
		1 (C)	1 (C)	1 (C)	1 (C)
<i>P. malariae</i>	100 (A)	100 (A)	100 (A)	100 (A)	100 (A)
	10 (B)		10 (B)	10 (B)	10 (B)
	1 (C)		1 (C)	1 (C)	1 (C)
<i>P. ovale</i>	100 (A)	100 (A)	100 (A)	100 (A)	100 (A)
	10 (B)	10 (B)		10 (B)	10 (B)
	1 (C)	1 (C)		1 (C)	1 (C)
<i>P. knowlesi</i>	100 (A)	100 (A)	100 (A)	100 (A)	100 (A)
	10 (B)	10 (B)	10 (B)		10 (B)
	1 (C)	1 (C)	1 (C)		1 (C)
<i>P. vivax</i>	100 (A)	100 (A)	100 (A)	100 (A)	100 (A)
	10 (B)	10 (B)	10 (B)	10 (B)	
	1 (C)	1 (C)	1 (C)	1 (C)	
Total	60 PCR samples				
	50 without repeat				
	10 mixed combinations				

Abbreviations: 100 (A), 10 (B), and 1 (C) indicate concentrations of clone DNA of 100 pg/μl, 10 pg/μl, and 1 pg/μl, respectively, in which A, B, and C were linked to the labeling in Figure 4.7.



Abbreviation: F = *P. falciparum*; M = *P. malariae*; O = *P. ovale*; K = *P. knowlesi*; V = *P. vivax*;  
A = 100 pg; B = 10 pg; C = 1 pg

Figure 4.7: Sensitivity assay of the hexaplex PCR system in two species mixed infections based on cloned DNA.

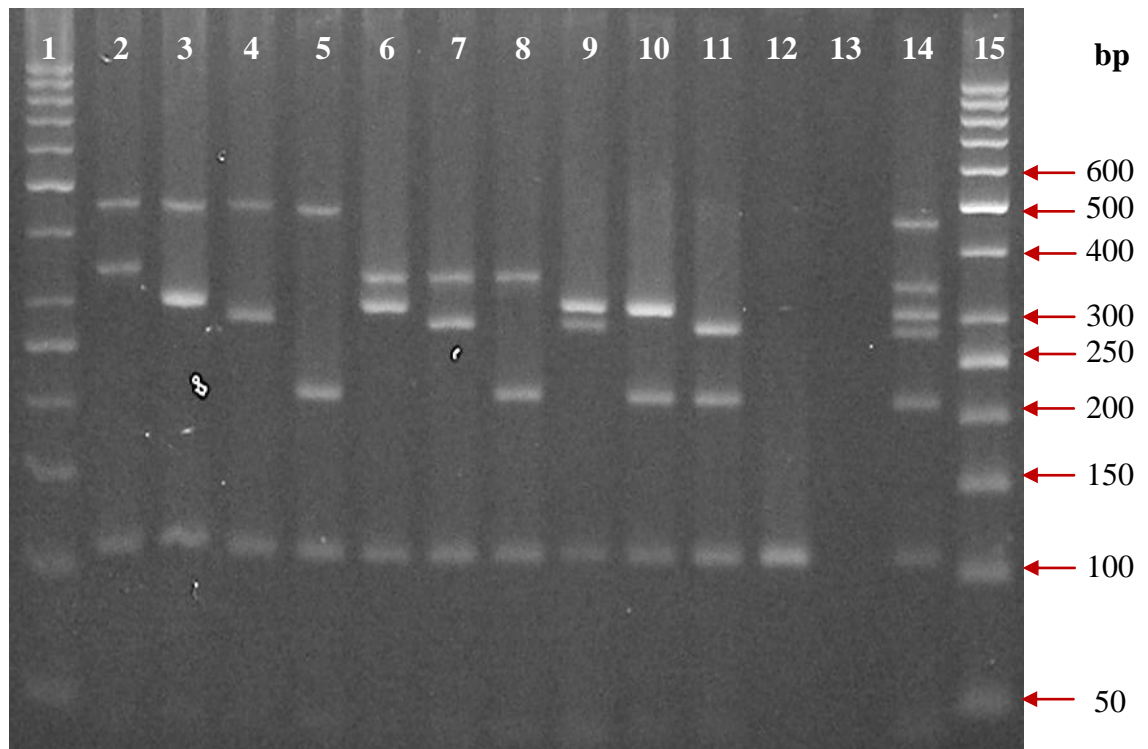


Figure 4.8: Hexaplex PCR results based on simulated mixture of clone DNAs. Ten possible combinations of two species mixed infections caused by five human *Plasmodium* species infection.

Lanes,

1 & 15 : 50 bp DNA ladder (Fermentas)	8 : <i>P. malariae</i> & <i>P. vivax</i>
2 : <i>P. falciparum</i> & <i>P. malariae</i>	9 : <i>P. ovale</i> & <i>P. knowlesi</i>
3 : <i>P. falciparum</i> & <i>P. ovale</i>	10 : <i>P. ovale</i> & <i>P. vivax</i>
4 : <i>P. falciparum</i> & <i>P. knowlesi</i>	11 : <i>P. knowlesi</i> & <i>P. vivax</i>
5 : <i>P. falciparum</i> & <i>P. vivax</i>	12 : Healthy control sample
6 : <i>P. malariae</i> & <i>P. ovale</i>	13 : DNA blank
7 : <i>P. malariae</i> & <i>P. knowlesi</i>	14 : Hexaplex DNA ladder



### 4.5.3.3 Simulated clinical mixed infections

To test whether these primers could improve the detection of clinical mixed infections, a total of 30 experimental random mixed infections (two to three *Plasmodium* species) were created using clinical samples, and these were screened using the present hexaplex PCR and a nested PCR, the molecular gold standard for comparison study. All mixed *Plasmodium* species infections were successfully detected in all the simulated clinical samples. Figure 4.9 shows the hexaplex PCR results based on simulated clinical mixed infections using three of the most prevalent *Plasmodium* species in our local scenario, i.e., *P. vivax*, *P. falciparum*, and *P. knowlesi*.

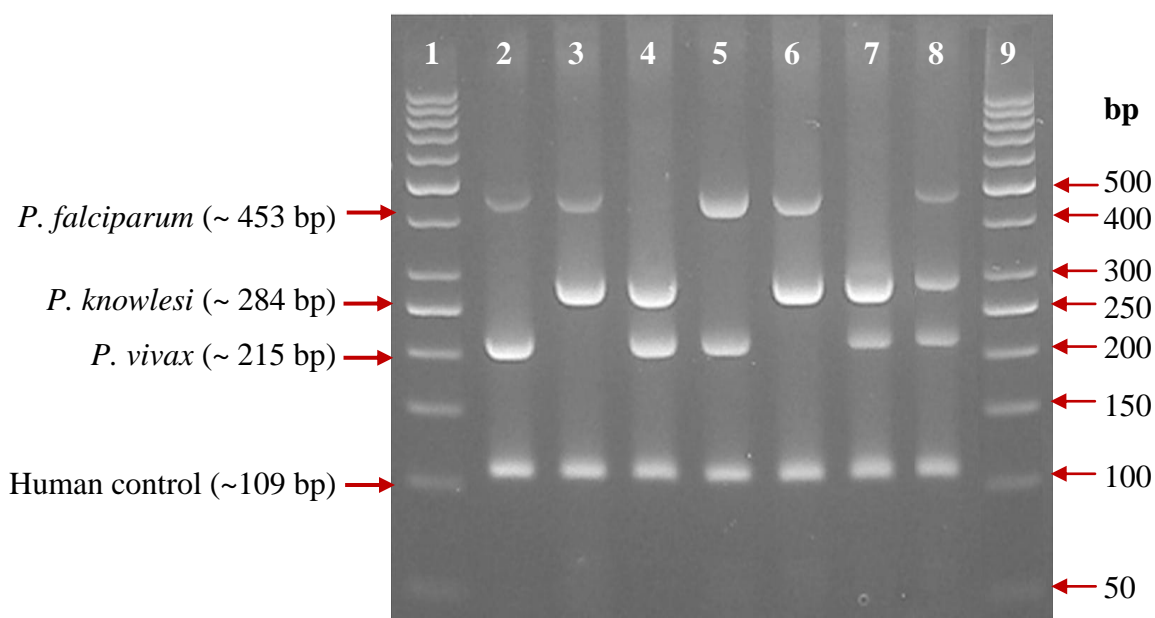


Figure 4.9: Hexaplex PCR results based on simulated clinical mixed infections. Lanes 1 and 9: 50 bp DNA ladder (Fermentas), Lane 2 to 7: Random mixed infections of two *Plasmodium* species. Lane 8: Random mixed infections of three *Plasmodium* species.

#### 4.5.3.4 Specificity analysis

To estimate the specificity of the *Plasmodium* hexaplex PCR assay, DNA samples obtained from two isolates of bacterial strains, i.e., *Aeromonas aquariorum*, *Aeromonas caviae*, *Aeromonas hydrophila*, *Aeromonas veronii*, *Vibrio harveyi*, *Vabrio parahaemolyticus*, and *Serratia* species, as well as non-malaria parasites, i.e., *Toxoplasma gondii*, *Giardia duodenalis*, and hook worms (*Necator americanus* and *Ancylostoma duodenale*) were screened. DNA samples from 20 healthy individuals were also tested for the specificity and possibility of non-specific fragments. None of the *Plasmodium* PCR product was detected by the hexaplex PCR assay when the DNA was obtained from all non-*Plasmodium* samples. Only an approximately 109 bp band that represented the human  $\beta$ -hemoglobin gene in human samples was visualized on the gel.

#### 4.5.4 Random blind test and clinical screening

The present hexaplex system demonstrated the specificity of the PCR primers to their target species. High sensitivity and specificity also were detected for at least two-species detection based on experimentally created mixed-infections without any significant diagnostic constrains. Both the hexaplex and nested PCR gave concordant results for species identification in all 50 samples in random blind test as well as 226 clinical samples suspected to have malaria.

Among the 211 microscopy confirmed malaria samples, the hexaplex PCR assays indicated that there were only two cases (1 %) of mixed infections (both caused by *P. falciparum* and *P. vivax* infections) another 201 (95 %) malaria samples showed single infection. PCR based species identification showed 39 % (83/211) of the samples were *P. vivax*, 28 % (60/211) were *P. falciparum*, 26 % (55/211) were *P. knowlesi*, 1 % (2/211) were *P. malariae*, as well as an imported *P. ovale* case, which was misdiagnosed as *P. vivax* by microscopy (Lim, et al, 2010) . The rest of the eight (4 %) malaria samples were negative by both nested and hexaplex PCR assays, with only the human positive control DNA amplicon observed.

Among 15 microscopy negative clinical malaria samples, five samples were diagnosed positive with single *Plasmodium* species, i.e., one *P. falciparum*, one *P. vivax*, and three *P. knowlesi* infections. The results were further confirmed by nested PCR with similar results obtained. Table 4.3 summarizes the results of hexaplex PCR and the comparison of results for the identification of *Plasmodium* species by hexaplex PCR and microscopy.

Table 4.3: Comparison of results for detection of *Plasmodium* species by hexaplex PCR and microscopy.

PCR results	No. of cases identified by microscopy									No. of cases identified by PCR	Microscopy negative
	<i>P. vivax</i>	<i>P. falciparum</i>	<i>P. malariae</i>	<i>P. knowlesi</i>	<i>P. malariae/ P. knowlesi</i>	<i>P. vivax &amp; P. falciparum</i>	<i>P. vivax &amp; P. malariae</i>	<i>P. vivax &amp; P. knowlesi</i>	<i>P. falciparum &amp; P. malariae</i>		
<i>P. vivax</i>	75	1	0	1	1	1	3	1	0	83 (39 %)	1 (7 %)
<i>P. falciparum</i>	1	57	2	0	0	0	0	0	0	60 (28 %)	1 (7 %)
<i>P. malariae</i>	0	0	1	0	1	0	0	0	0	2 (1 %)	0
<i>P. knowlesi</i>	3	1	35	4	10	0	0	0	2	55 (26 %)	3 (20 %)
<i>P. ovale</i>	1	0	0	0	0	0	0	0	0	1 (0 %)	0
<i>P. vivax &amp; P. falciparum</i>	1	0	0	0	0	1	0	0	0	2 (1 %)	0
Absent <i>Plasmodium</i>	2	4	0	1	1	0	0	0	0	8 (4 %)	10 (67 %)
	83 (39 %)	63 (30 %)	38 (18 %)	6 (3 %)	13 (6 %)	2 (1 %)	3 (1.5 %)	1 (0.5 %)	2 (1 %)	211 (100 %)	15

### 4.5.5 Diagnostic sensitivity and specificity

The sensitivity, specificity, positive predictive value (PPV), and negative predictive value (NPV) with 95 % confidence interval (95 % CI) of the microscopic examination as well as hexaplex PCR were evaluated using nested PCR as gold standard for all two modalities. The diagnostic sensitivity and specificity assays in *P. vivax* and *P. falciparum* determinations were calculated based on 246 samples (including two cases of *P. vivax* and *P. falciparum* mixed infections confirmed by PCR and 20 healthy controls) using MedCalc-Diagnostic test evaluation ([http://www.medcalc.org/calc/diagnostic\\_test.php](http://www.medcalc.org/calc/diagnostic_test.php)).

Table 4.4: The sensitivity, specificity, positive predictive value (PPV), and negative predictive value (NPV) of the hexaplex PCR and microscopy were compared to a standard nested PCR.

Nested PCR as gold standard					
Test \ Species		<i>P. vivax</i>		<i>P. falciparum</i>	
		Positive	Negative	Positive	Negative
Hexaplex PCR	Positive	86	0	63	0
	Negative	0	160	0	183
		Percentage (%)	95 % CI (%)	Percentage (%)	95 % CI (%)
	Sensitivity	100	95.76 to 100.00	100	94.26 to 100.00
	Specificity	100	97.70 to 100.00	100	97.98 to 100.00
	PPV	100	95.76 to 100.00	100	94.26 to 100.00
	NPV	100	97.70 to 100.00	100	97.98 to 100.00
Test \ Species		<i>P. vivax</i>		<i>P. falciparum</i>	
		Positive	Negative	Positive	Negative
Microscopy	Positive	82	7	58	8
	Negative	4	153	5	175
		Percentage (%)	95 % CI (%)	Percentage (%)	95 % CI (%)
	Sensitivity	95.35	88.51 to 98.69	92.06	82.43 to 97.34
	Specificity	95.62	91.19 to 98.22	95.63	91.57 to 98.09
	PPV	92.13	84.46 to 96.77	87.88	77.50 to 94.60
	NPV	97.45	93.60 to 99.29	97.22	93.63 to 99.08

## 4.6 Heterologous expression of PkAMA1 and PvAMA1 ectodomain proteins

### 4.6.1 *Plasmodium* strain used in plasmid construction

*Plasmodium knowlesi* strain H (GenBank accession no: DQ350263) as well as *P. vivax* strain Sal-1 (GenBank accession no: U03079) were selected for recombinant protein expression study.

### 4.6.2 Construction of pPAL7-PkAMA1 and pPAL7-PvAMA1 plasmids

The entire gene of PkAMA1 and PvAMA1 ectodomains were successfully amplified with the REs digestion sites, i.e., *SpeI* (upstream RE) and *BamHI* (downstream RE) to 5' and 3' of PCR amplicon (~ 1.34 kb), respectively allowed the creation of PCR amplicon with specific restriction sites for directional DNA ligation to the compatible multiple cloning sites of pPAL7 vector (~ 5.9 kb).

In general, both of the pPAL7 vector (~ 5.9 kb) and *Plasmodium* AMA1 PCR amplicon (~ 1.34 kb) were double digested with *SpeI* and *BamHI* and followed by gel purification prior to ligation step. The AMA1 coding DNA (cDNA) fragments of *P. knowlesi* and *P. vivax* were ligated in-frame respectively with the pPAL7 vector codes for a Profinity eXact tag on N-terminal end of the protein and generated DNA size with ~ 7.2 kb. The efficiency of REs digestion and DNA ligation were checked using 1 % (w/v) agarose gel (Figure 4.10A).

The pPAL7-PkAMA1 and pPAL7-PvAMA1 were initially transformed into C-Max5α *E. coli* (cloning host) and plated on LB agar containing 100 µg/ml of ampicillin to select the pPAL7 clones. The transformation efficiency of cloned DNA was confirmed by colony PCR using T7 promoter and T7 Terminator primers. Positive clone was indicated by a PCR fragment with ~ 1.75 kb. Bacterial colonies containing desired recombinant clone were picked and grown in LB broth and the plasmid of each clone was isolated and the inserted sequence was further confirmed by DNA sequencing

using T7 promoter, pPAL7 internal, and T7 Terminator primers.

Figure 4.10 shows the example of successful construction of pPAL7-PvAMA1 clone confirmed by RE digestions and colony PCR.

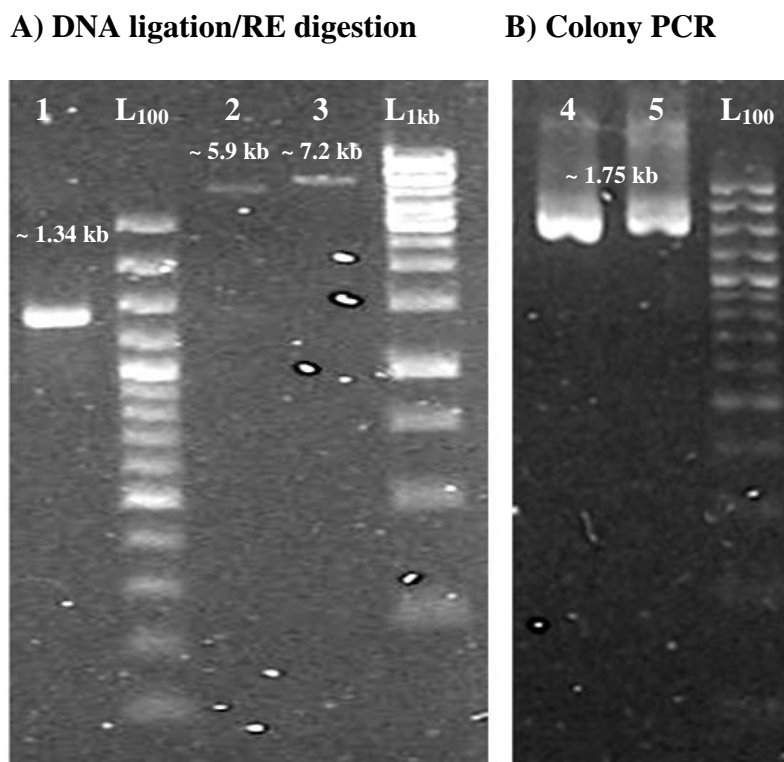


Figure 4.10: Confirmation of pPAL7-PvAMA1 construct by restriction enzyme digestion and colony PCR. (A) Increases of the size of pPAL7 vector indicated the successful of DNA ligation: Lane 1, Gel purified *Spe*I and *Bam*HI digested PvAMA1 PCR amplicon (~ 1.34 kb); Lane 2, *Spe*I digested pPAL7 DNA (~ 5.9 kb); and Lane 3, *Spe*I digested pPAL7-PvAMA1 (~ 7.2 kb). (B) Colony PCR with T7 promoter and T7 Terminator primers generated an ~ 1.75 kb DNA fragment indicating successful DNA transformation. L<sub>1kb</sub> is 1kb DNA ladder (Fermentas) and L<sub>100</sub> is 100 bp plus DNA ladder (Fermentas). Similar way was done for construction of pPAL7-PkAMA1. Due to similar in fragment size of PCR amplicon (~ 1.34 kb) for PkAMA1 and both of digested pPAL7 plasmid and pPAL7-PkAMA1 DNA, therefore, only the figure for construction of pPAL7-PvAMA1 clone is showed here.

### 4.6.3 Sequencing and BLAST search of PkAMA1 and PvAMA1

The sequencing results indicated that both of the pPAL7-PkAMA1 and pPAL7-PvAMA1 (Figure 4.11) constructed clones carried an inserted DNA of 1,338 bp length. The clones were 99 % concordance with the published mRNA of the AMA1 ectodomain gene of *P. knowlesi* (GenBank ref. no.: XM\_002259303; Appendix 5.1) as well as *P. vivax* (GenBank ref. no.: FJ785007; Appendix 5.2).

The nucleotide sequences were then translated into amino acid sequences (Figure 4.12) using ExPASy Translate tool (<http://web.expasy.org/translate/>) and then searched against the protein database using NCBI protein BLAST (BLASTP; <http://blast.ncbi.nlm.nih.gov/Blast.cgi>). The results indicated that both of the inserted coding sequences were in-frame with 446 amino acid residues of AMA1 ectodomain, encompassing entire region of domain I-II-III. The recombinant PkAMA1 (rPkAMA1) was 100 % identical with *P. knowlesi* H strain AMA1 protein (PKH\_093110) deposited in GenBank with accession number XP\_002259339 (corresponding to amino acids 42 to 487, number commencing from the first residue of the signal peptide; Appendix 5.3), whereas recombinant PvAMA1 (rPvAMA1) was identical with *P. vivax* AMA1 protein with accession number ACY68841 (corresponding to amino acids 42 to 487; Appendix 5.4).

Only *E. coli* carrying the clone with correct coding sequence and orientation (in-frame translation) confirmed by sequencing was further grown in LB broth and the plasmid was extracted and then re-transformed into BL21-CodonPlus (DE3)-RIL *E. coli*, a codon-optimized expression host, which carried an additional pACYC plasmid. This ColE1-compatible, pACYC-based plasmid containing extra copies of the *argU*, *ileY*, and *leuW* tRNA genes is suited for heterologous expression of recombinant protein consisted of AT-rich genome, i.e., *Plasmodium* DNA, as well as an additional chloramphenicol resistance (*Cam<sup>r</sup>*) gene to maintain the selection of pACYC plasmid.



Thus, only transformed *E. coli* colonies that carried recombinant clone were selected on LB plate containing 100 µg/ml of ampicillin and 34 µg/ml of chloramphenicol. Selected clones were further verified by colony PCR, REs digestion, and sequencing as mentioned above.

#### (A) Inserted PkAMA1 gene

```
GGGCCTATCATTGAGAGAAGTATACGAATGAGTAACCCATGGAAAGCCTTCATGGAAAAGTATGATT
TAGAGAGAGCACACAATTCCGGGATTAGAATTGATTTAGGGGAAGATGCAGAAGTGGGAAATTCCAA
GTATAGAATACCAGCTGGAAAATGTCCAGTTTTTGGAAAGGGTATCGTTATAGAAAATTCTAACGTT
AGCTTCTTAACACCCGTAGCTACAGGAGCTCAAAGGTTGAAGGAAGGAGGTTTCGCCTTCCCCAATG
CAGATGACCACATTTCCCTTATAACAATAGCAAACCTTAAAGAGAGGTATAAAGAAAATGCAGATTT
GATGAAATTAAATGATATAGCCTTGTGTAAAACGCATGCAGCCAGCTTTGTCATTGCAGAGGATCAA
AATACATCTTACAGACATCCAGCTGTTTATGACGAAAAGAATAAAACATGTTACATGTTGTATTTGT
CAGCGCAAGAAAATATGGGTCCACGATACTGTAGCCAGATTACAAAATAAAGACGCCATGTTTTG
CTTCAAGCCAGATAAAAAATGAAAAATTTGACAACCTGGTGTATTTAAGCAAAAACGTAAGTAATGAT
TGGGAAAACAAGTGCCCGCGTAAAAATTTAGGAAACGCAAAATTTGGATTATGGGTGGATGGGAACT
GTGAAGAAATACCATACGTTAATGAAGTGGAGGCAAGGAGCCTACGGGAATGCAACCGAATCGTTTT
CGAAGCTAGCGCTTCAGATCAACCACGTCAGTACGAAGAAGAACTGACAGATTATGAAAAATACAA
GAGGGATTAGACAAAATAATCGGGACATGATTAAGTGCCTTTCTTCCAGTGGGTGCATTTAACT
CAGACAATTTTAAAGAGTAAAGGAAGAGGATATAACTGGGCAAATTTTCGATTCTGTAAATAATAAGTG
TTACATTTTAAATACCAAACCTACGTGTCTCATTAATGACAAAAATTTTTTGCACAACAGCGTTA
TCTCACCTCAAGAAGTAGACAATGAATTTCCATGCAGCATATACAAAGATGAAATTGAAAGAGAAA
TTAAGAAACAGTCGAGAAAATATGAATCTGTACAGTGTGATAAGGAACGGATTGCTTTGCCAAGGAT
ATTTATCTCCACCGATAAGGAGAGTATCAAATGTCCATGTGAGCCTGAACACATTTCCAATAGTACC
TGCAACTTTTACGTTTGTAACTGTGTAGAGAAAGAGCAGAAAATTAAGGAAAATAACGAAGTTATCA
TAAAGGAAGAATTTAAGGAGGATTATGAAAATCCGGACGGCAAACATAAGAAGAAGATGCTACTA
```

#### (B) Inserted PvAMA1 gene

```
GGGCCTACCGTTGAGAGGAGCACACGAATGAGTAACCCCTGGAAAGCGTTTCATGGAAAATACGACA
TCGAAAGAACACACAGTTCTGGGGTTCGAGTGGATTTAGGGGAAGATGCAGAAGTGGAAAATGCAAA
GTACAGAAATCCAGCTGGAAGATGTCCTGTTTTTGGAAAGGGTATCGTCATAGAGAATTCGGCTGTT
AGCTTCTTAAAACCTGTGGCTACAGGAGATCAGAGGCTGAAGGATGGAGGTTTCGCCTTCCCCAATG
CGAATGACCATATCTCCCCATGACAATAGCGAACCTTAAGGCAAGGTATAAAGACAATGTAGAGAT
GATGAAGTTAAACGATATAGCTTTGTGCAGAACCCACGCAGCTAGCTTTGTCATGGCAGGGGATCAA
AATTCGTCTTACAGACACCCAGCTGTATACGACGAAAAGGAAAAACATGCCACATGTTGTATTTAT
CAGCGCAGGAAAAATATGGGTCCGAGGTACTGCAGCCAGATGCACAAAATAGAGATGCCGTGTTCTG
CTTCAAGCCAGATAAAAAATGAAAGCTTTGAAAACCTGGTGTATTTGAGCAAAAATGTGCGTAATGAT
TGGGATAAAAAATGCCCCGTAAAAATTTAGGAAACGCCAAGTTCGGATTATGGGTGGATGGGAACT
GCGAAGAAATTCATACGTTAAAGAAGTGGAGGCAAGGATCTGCGCAATGCAACCGAATCGTTTTT
CGAAGCGAGTGCCTCAGATCAACCAACTCAGTATGAAGAAGAAATGACGGATTATCAAAAATACAA
CAAGGGTTTAGACAAAACAACCGAGAGATGATTAAGTGCCTTTCTTCCAGTGGGTGCATTCAACT
CGGATAATTTCAAAAGTAAAGGAAGAGGATTTAACTGGGCAAATTTTCGATTCTGTAAAAAGAAGTG
TTACATCTTTAATACCAAACCGACTTGCCCTCATTAATGACAAAAATTTTATTGCAACAACGGCGTTA
TCTCACCCACAAGAAGTAGACCCGGAGTTCCCTGCAGCATATATAAAGACGAAATTGAAAGAGAAA
TTAAGAAACAATCGAGGAACATGAATCTGTACAGTGTGATGGGGAACGCATTGCTCTGCCGAGGAT
ATTTATCTCCAACGATAAGGAGAGTATCAAATGTCCCTGCGAACCTGAGCACATTTCCAACAGTACC
TGCAACTTTTACGTTTGTAACTGTGTAGAGAAAAGGGCGGAAATTAAGGAAAATAACCAAGTTGTTA
TAAAGGAAGAATTTAGGGATTATTACGAAAATGGGGAGGAAAAATCGAACAAGCAGATGCTACTA
```

Figure 4.11: *Plasmodium* AMA1 coding DNA inserted into pPAL7 vector. Both PkAMA1 (A) and PvAMA1 (B) clones consist of 1,338 bp inserted AMA1 ectodomain gene.

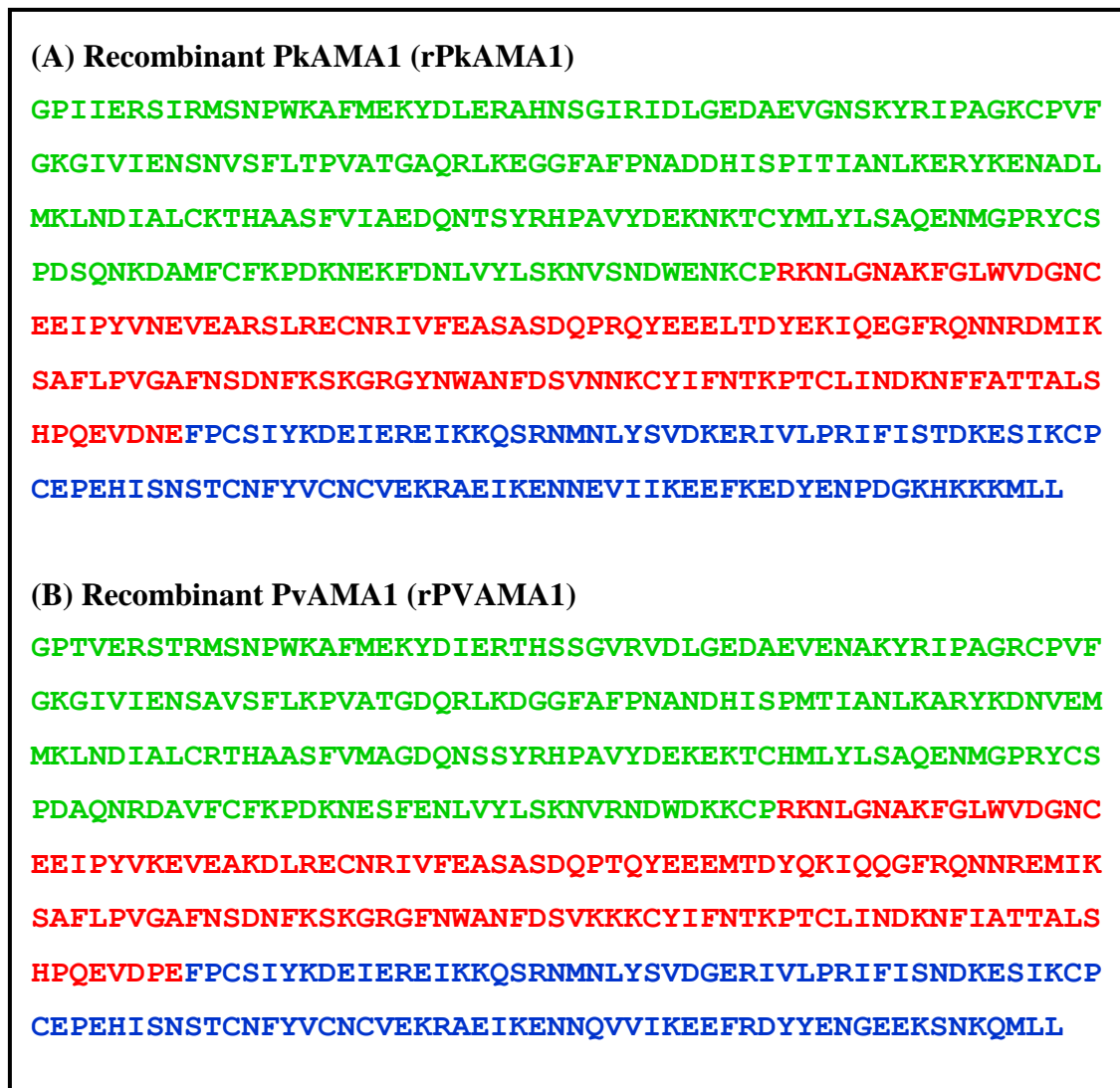


Figure 4.12: Protein sequences of the construct for rPkAMA1 and rPvAMA1 comprised 446 amino acids residues. The rPkAMA1 sequence was 100 % in concordance with *P. knowlesi* strain H (NCBI reference sequence: XP\_002259339), whereas rPvAMA1 sequence was 100 % in concordance with *P. vivax* strain Sal-1 (NCBI reference sequence: ACY68841). The *Plasmodium* AMA1 sequences are given the following domain colour coding: domain I in green, domain II in red, and domain III in blue.

#### 4.6.4 Protein sequence and bioinformatic analysis

The theoretical isoelectric point ( $pI$ ) and molecular weight (MW) of the rPkAMA1 and rPvAMA1 were estimated from their respective amino acids sequences using ExPASy interface, the Compute  $pI$ /MW tool ([http://web.expasy.org/compute\\_pi/](http://web.expasy.org/compute_pi/)). The theoretical  $pI$ /MW of rPkAMA1 and rPvAMA1 were 5.85/51343.86 and 6.28/51275.85, respectively. The Recombinant Protein Solubility Prediction tool (<http://biotech.ou.edu/>; Wilkinson & Harrison, 1991) estimated that 71.3 % of rPkAMA1 and 72.5 % of rPvAMA1 probably to be overexpressed in *E. coli* system in an insoluble form that mainly localized in an inclusion body (IB).

#### 4.6.5 Induction of protein expression

A fraction of pre- and post-induction crude culture samples were collected to check the expression level of the recombinant protein. In general, the expression level, protein purity, and solubility of fusion protein were analyzed using Coomassie-stained 12 % SDS-PAGE under reduced conditions (Session 4.6.5.1). The solubility of each fusion proteins was further confirmed using Western blot assay (Session 4.6.5.2).

##### 4.6.5.1 SDS-PAGE quick solubility screening

The AMA1 ectodomain of *P. knowlesi* and *P. vivax* were expressed in the form of fusion protein with N-terminal Profinity eXact-tag (8.2 kDa) and yielded a protein fragment with molecular weight of ~ 60 kDa from *E. coli* lysate after induction with IPTG. Generally, the solubility of recombinant protein was determined by analyzing fractions of the supernatant and pellet samples after centrifugation, on 12 % SDS-PAGE under reduced conditions. Reduced SDS-PAGE result shows that both the pPAL7-PkAMA1 and pPAL7-PvAMA1 proteins were found to be overexpressed as insoluble fraction of the cell lysate as IB by comparing the band of target protein at ~ 60 kDa in total, soluble, and insoluble fractions collected after 3 hour of induction (Figure 4.13).

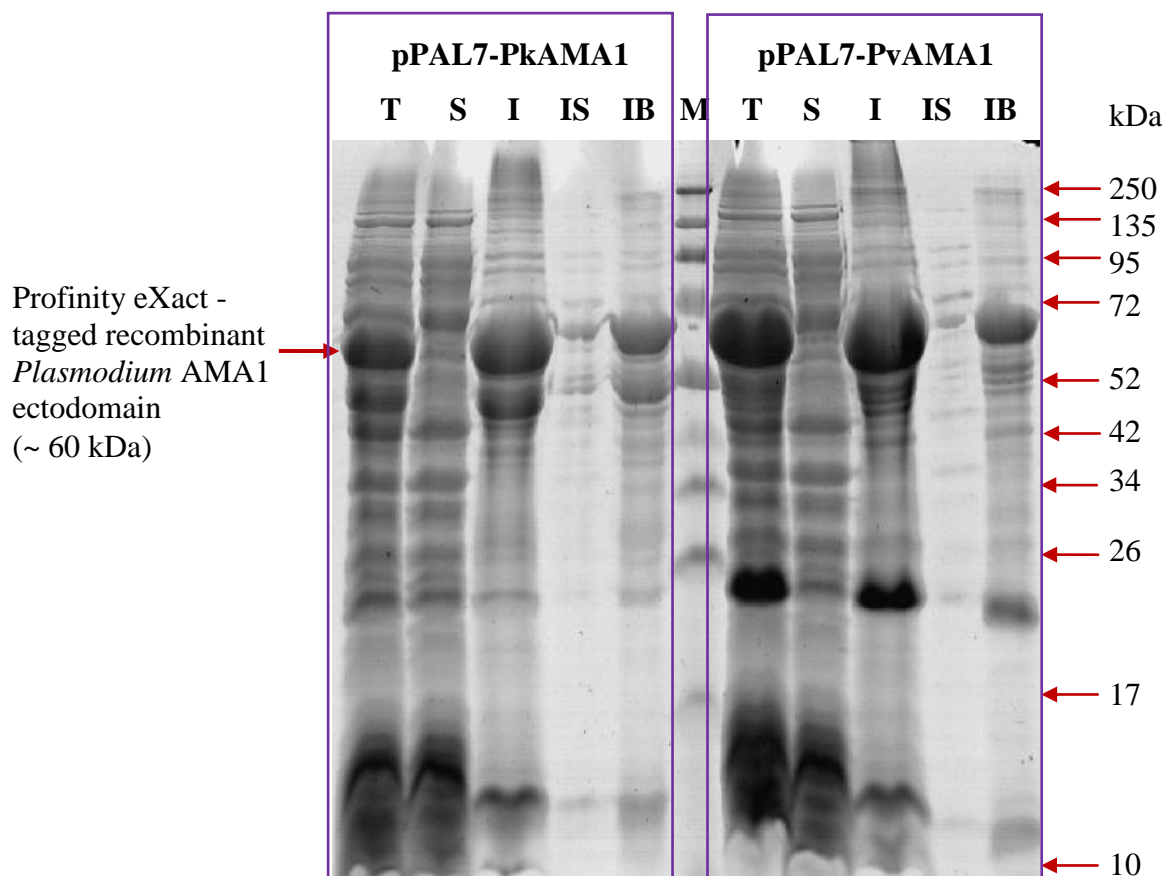


Figure 4.13: Fractionation profile of the supernatant and pellet after centrifugation, on reduced 12 % SDS-PAGE. SDS-PAGE analysis of *E. coli* produced recombinant PkAMA1 (left) and recombinant PvAMA1 (right) with N-terminal Profinity eXact-tag. The pPAL7-PkAMA1 and pPAL7-PvAMA1 proteins were expressed in molecular weight of ~ 60 kDa. Lanes T were total proteins contained of both soluble and insoluble proteins; Lanes S contained only soluble protein; Lanes I contained only insoluble protein; Lanes IS contained solubilized cellular contaminants after washed with W1 buffer containing additional treatment with 1 % (v/v) Triton X-100, 1 M urea, 1 mM EDTA, and 5 mM DTT; Lanes IB were purified inclusion bodies in W2 buffer; Lane M was protein marker (Fermentas).

#### 4.6.5.2 Detection of the expression by Western blot analysis

Western hybridization assay using anti-Profinity eXact monoclonal antibody (Bio-Rad) also showed that two of current expressed recombinant proteins, i.e., pPAL7-PkAMA1 and pPAL7-PvAMA1 were localized in an insoluble IB. None of these proteins was detected in a soluble form in Western blot assay (Figure 4.14).

Alterations in induction temperature (16 °C, 25 °C, and 37 °C), induction time (OD<sub>600</sub> to 0.6, 1.0, 1.5, and 2.0), as well as IPTG inducer concentration (0.1 mM, 0.5 mM, 1.0 mM, and 2.0 mM) did not improve the expression of soluble target protein. Therefore, both of the recombinant proteins used in phage display biopanning assay were isolated and purified from insoluble IBs.

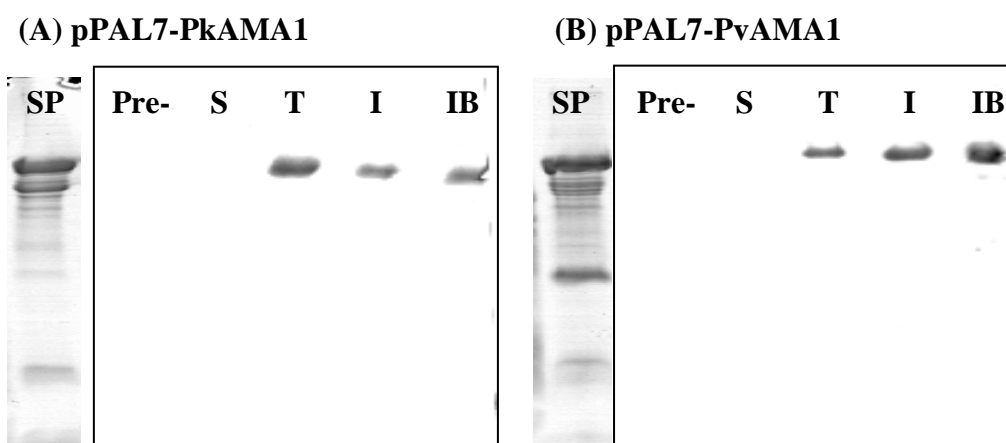


Figure 4.14: Western blot analyzed the expression level of pPAL7-PkAMA1 (A) and pPAL7-PvAMA1 (B) using anti-Profinity eXact monoclonal antibody (Bio-Rad).

Lanes,

SP : Induced protein on 12 % SDS-PAGE (Insoluble lysate)

Pre- : Pre-induce *E. coli* whole cell extract

S : Soluble protein lysate (S)

T : Total lysate (T)

I : Insoluble lysate (I)

IB : Purified inclusion body (IB)

#### **4.6.6 Recombinant protein extraction from *E. coli* and IB purification**

Basically, insoluble, unfolded, functional inactive IB is frequently formed upon overexpression of recombinant protein in transformed *E. coli*. The IB is accumulated in the cytoplasm of host cell, which contain the recombinant protein in high yield that can be isolated by solid/liquid separation, i.e., centrifugation.

##### **4.6.6.1 Cell lysis and IB purification**

Prior to protein isolation, *E. coli* cells were lysed so that the target protein can be purified from other cell components. In the present study, total proteins were extracted from bacterial cells with a combined disruption method to break down the cell walls or membranes, i.e., chemical and enzymatic disruptions (using B-PER<sup>®</sup> reagent and 200 µg/ml of lysozyme) as well as incorporation of mechanical disruption using 25 Gauge syringe needle followed by vigorous vortexing. After centrifugation, IB was settled down with bacteria debris to form a pellet. The pellet was washed twice with B-PER buffer containing low concentration of chaotropic agent (1 M urea) and detergent (1 % Triton X-100) to solubilize the protein contaminants, e.g., outer membranes and proteins (proteases) from *E. coli*. Finally, a purified IB was obtained.

Figure 4.15 and Figure 4.16 show the protein components isolated from *E. coli* crude culture collected during pre-induction and after 3 hours of post-induction (total, soluble, insoluble), as well as recombinant protein obtained from washed and purified IB.

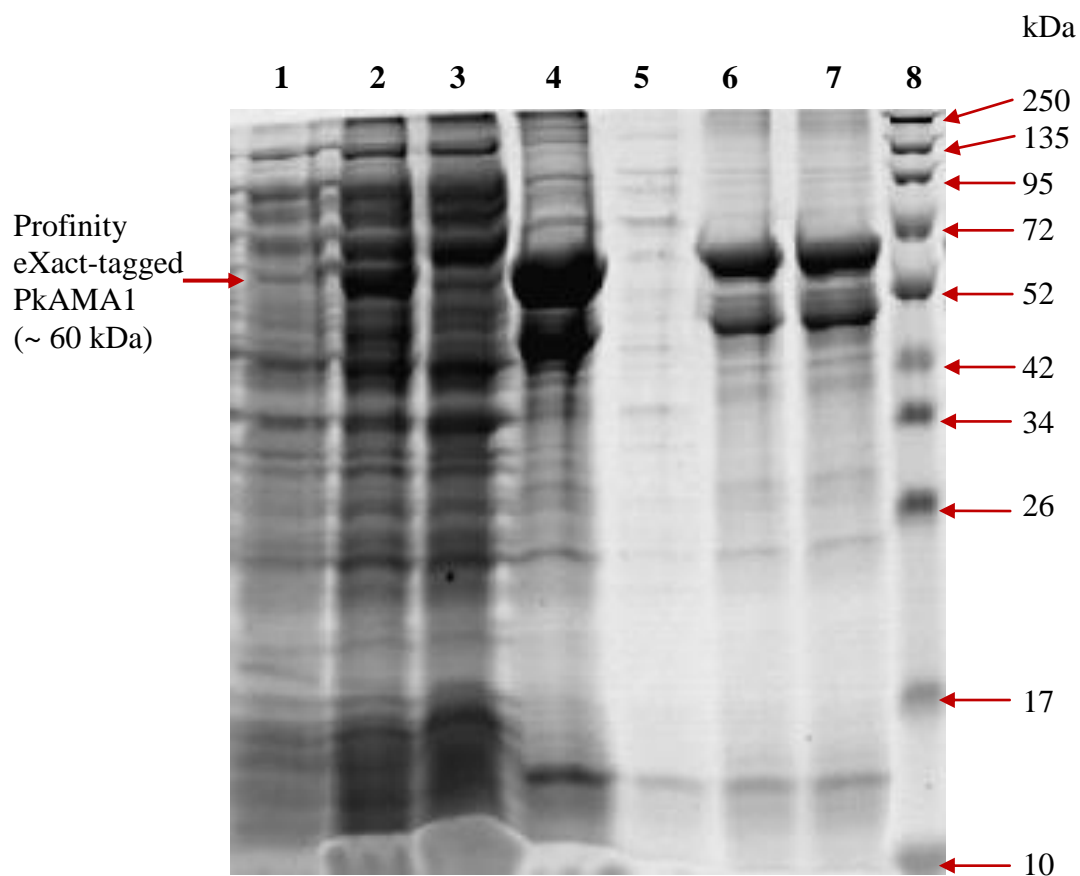


Figure 4.15: Profinity eXact-tagged PkAMA1 protein expression and IB purification.

Lanes,

- 1 : Pre-induced *E. coli* whole cell extract
- 2 : Induced *E. coli* whole cell extract- total lysate (T)
- 3 : Soluble (S) fraction
- 4 : Insoluble (I) fraction
- 5 : Insoluble supernatant (IS)
- 6 : Washed inclusion body (W1)
- 7 : Purified inclusion body (IB)
- 8 : Protein marker (Fermentas)

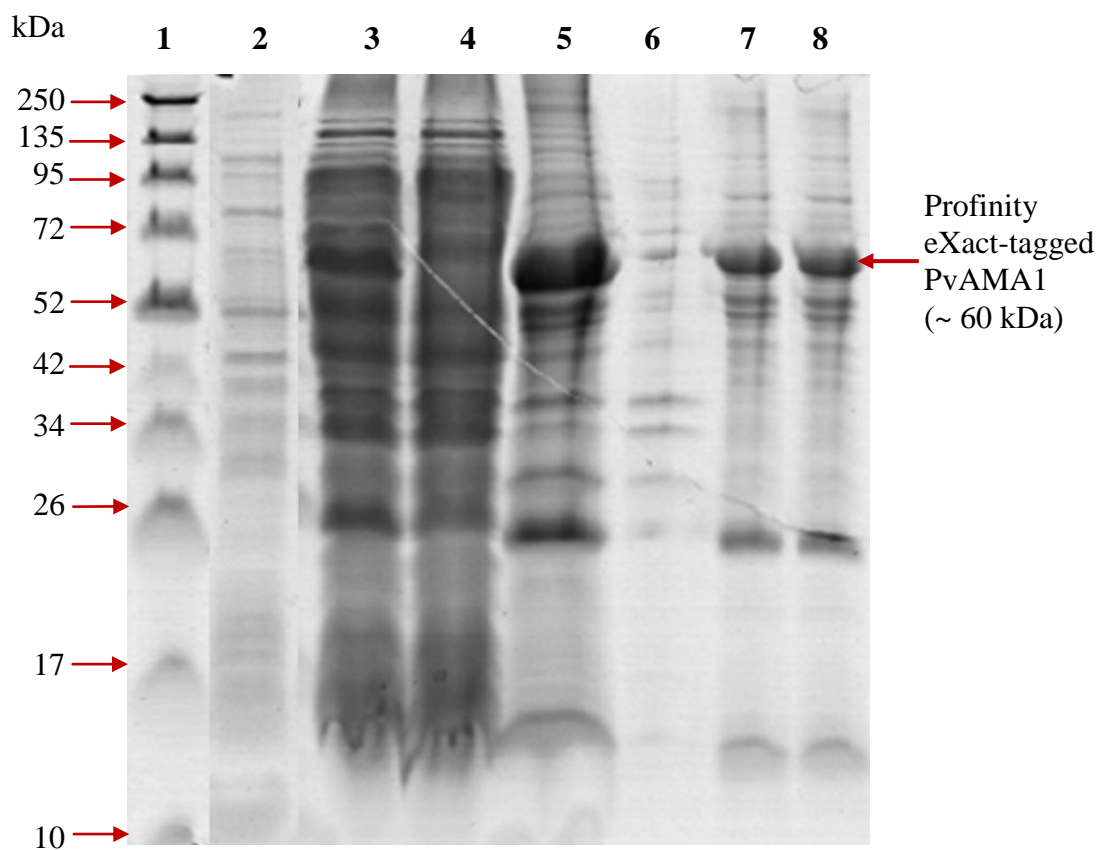


Figure 4.16: Profinity eXact-tagged PvAMA1 protein expression and IB purification.

Lanes,

- 1 : Protein marker (Fermentas)
- 2 : Pre-induced *E. coli* whole cell extract
- 3 : Induced *E. coli* whole cell extract- total lysate (T)
- 4 : Soluble (S) fraction
- 5 : Insoluble (I) fraction
- 6 : Insoluble supernatant (IS)
- 7 : Washed inclusion body (W1)
- 8 : Purified inclusion body (IB)



#### 4.6.6.2 Inclusion body solubilization

The IB is dense, insoluble aggregates of denature and unfolded proteins that need to be solubilized under denaturing condition using a high concentration of denaturant such as 4-8 M urea or 6 M guanidine-HCl. However, the ion  $\text{Cl}^-$  present in guanidine-HCl may trigger the cleavage of fusion protein therefore urea was chosen as denaturant for IB solubilization in this study. For some IB, very high concentration of denaturant, i.e., 8 M urea is required to facilitate the solubilization, otherwise protein might not be dissolve in a solution and keep deposited in insoluble pellet, which will inhibit further affinity purification procedure using column. Therefore the concentrations of minimal urea requirement for IB solubilization were empirically tested from range of 2 M to 8 M (Figure 4.17). Purification of target protein from IB with Profinity eXact resin can be run with urea concentration up to 2 M without affecting binding capacity or column performance, while protein solubilization with more than 4 M urea may lower the yield and affect the protein purity; therefore concentrations above 4 M are not recommended. IB solubilization buffer (0.1 M sodium phosphate, 5 mM DTT, 1 mM EDTA) with 4 M urea was sufficient to dissolve whole IB after incubation overnight at 4 °C.

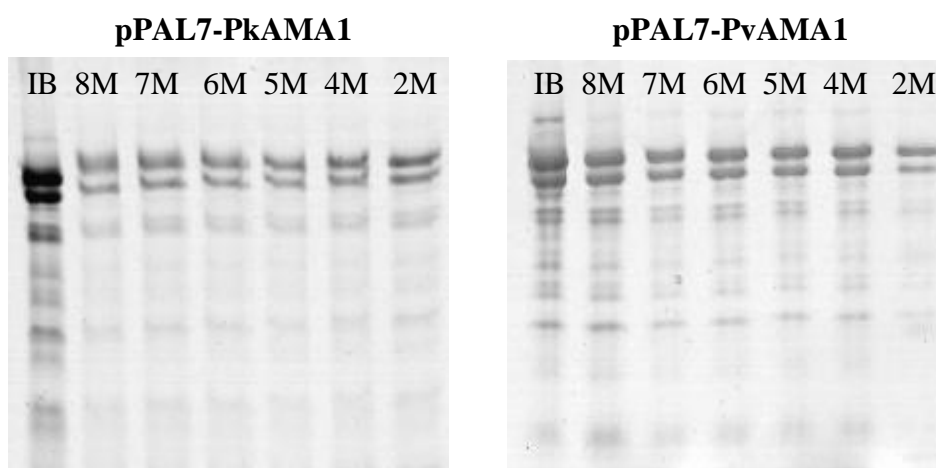


Figure 4.17: Optimization of concentrations of urea (2 M to 8 M) used in IB solubilization buffer. Loading samples were supernatant of solubilized protein centrifuged at  $15,000 \times g$  for 30 minute.

#### 4.6.7 Affinity protein purification and fusion-tag removal

The Profinity eXact technology enable a single step on-column affinity purification of fusion protein followed by cleavage release of purified recombinant protein with a native N-terminus triggered by 100 mM sodium fluoride (elution buffer). In general, solubilized IB protein sample was centrifuged and the supernatant was filtered and then diluted in 2 M urea prior to load into a Profinity eXact cartridge. The tagged recombinant protein was bound to the mutant subtilisin protease (S189), a ligand immobilized to the support matrix. The host protein contaminants and excessive unbound target protein were then collected in the flow-through fraction. After two subsequent column washes, a tag-free recombinant protein was collected into five elutions (0.1 ml/minute). The apparent molecular masses of two constructs were ~ 50 kDa, in accordance with theoretical mass calculated from their respective amino acid sequences. The Profinity eXact cartridge can be regenerated using 0.1 M phosphoric acid and the collected fraction contains an 8.2 kDa mass of Profinity eXact tag that has an apparent electrophoretic mass of ~ 12 kDa in SDS-PAGE as reported in product bulletin (Figure 4.18 and Figure 4.19, Lane 11).

SDS-PAGE results show that the Profinity eXact tag-free recombinant proteins, i.e., rPkAMA1 (Figure 4.18) and rPvAMA1 (Figure 4.19) were purified and eluted at the end of the affinity purification protocol under denatured conditions. The protein fractions along the isolation and purification procedures were analyzed by reduced SDS-PAGE.

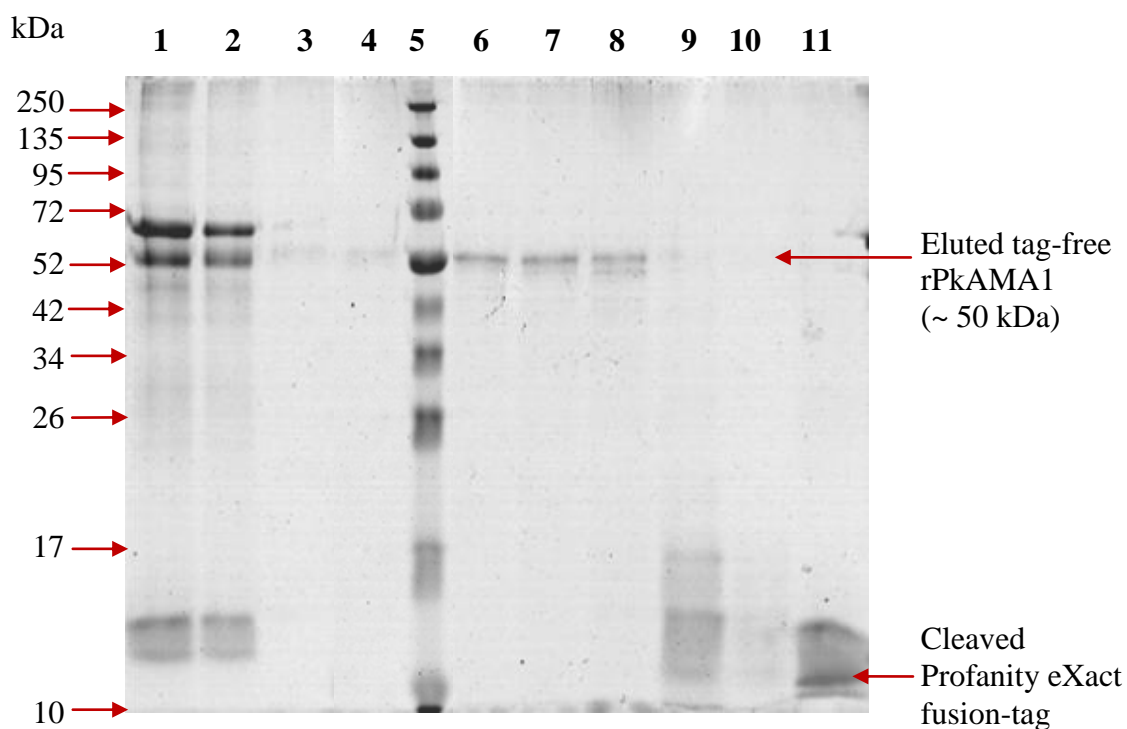


Figure 4.18: Profinity eXact tag-free rPkAMA1 purified and eluted using a 1 ml Bio-Scale Mini<sup>TM</sup> Profinity eXact cartridge under denatured and reduced conditions.

Lanes,

- 1 : Solubilized IB crude protein (centrifuged and filtered)
- 2 : Flow-through fraction (excessive target protein and host protein contaminants)
- 3 : Host protein contaminants from column wash
- 4 : Host protein contaminants from stringency wash
- 5 : Protein marker (Fermentas)
- 6 : Eluted tag-free rPkAMA1 (elution 1, 1 ml)
- 7 : Eluted tag-free rPkAMA1 (elution 2, 1 ml)
- 8 : Eluted tag-free rPkAMA1 (elution 3, 1 ml)
- 9 : Eluted tag-free rPkAMA1 (elution 4, 1 ml)
- 10 : Eluted tag-free rPkAMA1 (elution 5, 1 ml)
- 11 : Cleaved Profanity eXact fusion-tag (column regeneration)

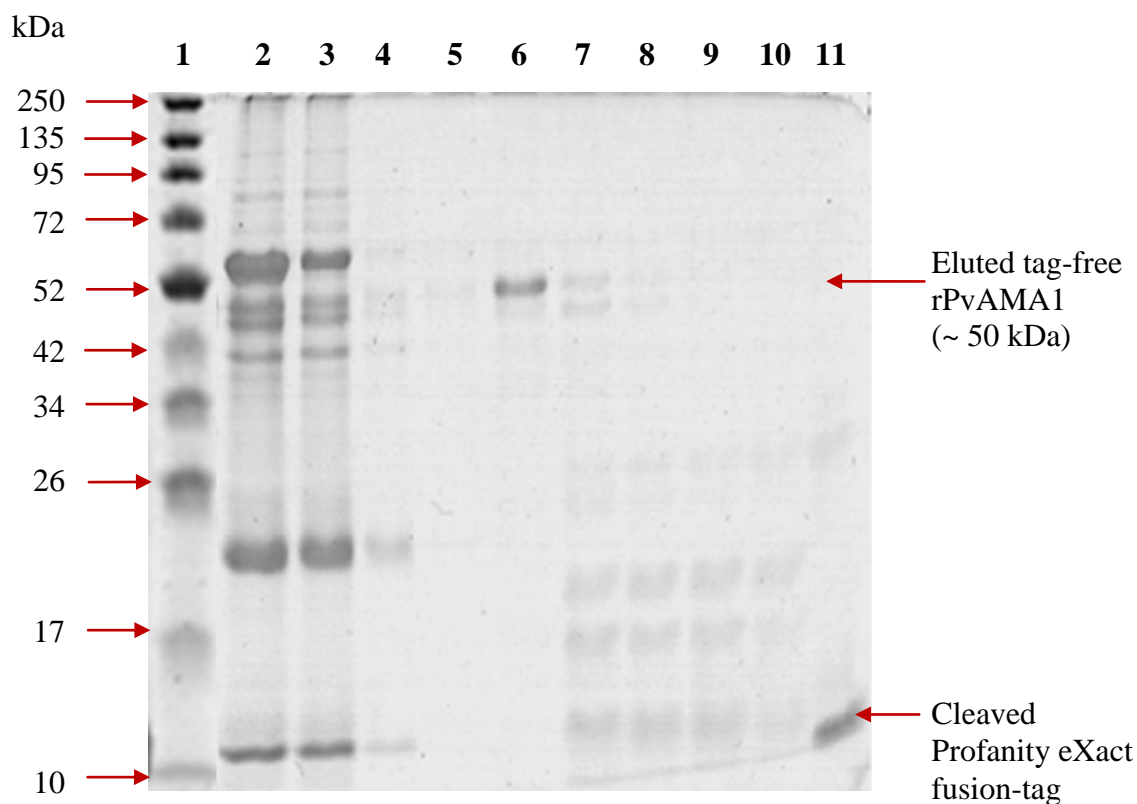


Figure 4.19: Profanity eXact tag-free rPvAMA1 purified and eluted using a 5 ml Bio-Scale Mini<sup>TM</sup> Profanity eXact cartridge under denatured and reduced conditions.

Lanes,

- 1 : Protein marker (Fermentas)
- 2 : Solubilized IB crude protein (centrifuged and filtered)
- 3 : Flow-through fraction (excessive target protein and host protein contaminants)
- 4 : Host protein contaminants from column wash
- 5 : Host protein contaminants from stringency wash
- 6 : Eluted tag-free rPvAMA1 (elution 1, 5 ml)
- 7 : Eluted tag-free rPvAMA1 (elution 2, 5 ml)
- 8 : Eluted tag-free rPvAMA1 (elution 3, 5 ml)
- 9 : Eluted tag-free rPvAMA1 (elution 4, 5 ml)
- 10 : Eluted tag-free rPvAMA1 (elution 5, 5 ml)
- 12 : Cleaved Profanity eXact fusion-tag (column regeneration)

#### **4.6.8 Analysis of folding reactions**

The efficiency of refolding conditions were monitored by measuring the protein aggregation by simple visual inspection and turbidity analysis (Session 4.6.8.1), as well as reduced/non-reduced SDS-PAGE (Session 4.6.8.2).

##### **4.6.8.1 Aggregation measurement**

Instant visual inspection is often used as the first line to monitor the refolding process. When refolding conditions are not optimized; the protein aggregation is clearly seen. In addition to visual inspection, the turbidity of the sample solution (aggregation) was further performed by measuring the optical density at 390 nm subtracted from the apparent absorbance readings due to solution turbidity without the protein sample. In the present study, the refolded rPkAMA1 and rPvAMA1 ectodomain proteins were taken to be soluble as both of the apparent OD reading for sample solution subtracted to blank sample buffer was less than 0.05. This solubility assay basically accounts for protein solubility and not for protein folding.

After completion of refolding, the sample solutions were then centrifuged at  $14,000 \times g$  for 1 hour. Neither of visually aggregates nor pellet was observed in both rPkAMA1 and rPvAMA1 sample solutions (non-denaturing buffer).

#### 4.6.8.2 Reduced and non-reduced SDS-PAGE

Evidence of successful protein refolding was further analyzed through SDS-PAGE under reducing and non-reducing conditions in the presence or absence of  $\beta$ -mercaptoethanol, respectively in the protein loading buffer.

Correctly folded (native) AMA1 protein is known to contain eight disulfide bonds (Hodder, et al., 1996). Generally, unsuccessful refolding results in an increased fraction of high molecular weight inter-molecular disulfide-linked multimeric AMA1 aggregates, i.e., dimers, trimers, and multimers. Refolding in some circumstances may also produce monomeric misfolded AMA1 that might co-migrate with refolded AMA1 on non-reduced SDS-PAGE. However, this monomeric misfolded AMA1 variants could be detected by the examination of band diffuseness on non-reducing SDS-PAGE. Under non-reducing conditions, the appearance of more fuzzy band or diffused band are due to differentially folded AMA1 variants (Gupta, et al., 2005).

For instance, the more diffuse and multimeric AMA1 aggregates were observed in pre-refold samples (Figure 4.20, Lanes 1 and 2). After refolding, both the refolded products (rPkAMA1 and rPvAMA1) were close to apparent homogeneity in a molecular mass of  $\sim 50$  kDa (Lanes 3 and 4). Furthermore, there were disappearance of most disulfide-bonded aggregates in post-refold samples and none of dimers, trimers, and multimers was observed in both of the post-refolded rPkAMA1 and rPvAMA1 (Figure 4.20, Lanes 3 and 4). Besides that, the resulting non-reduced bands (Lane 3) were not diffuse and virtually identical to the reduced bands (Lane 4) indicating most material was refolded successfully. Figure 4.20 also shows the refolding evidence of the rPkAMA1 and rPvAMA1, where the refolded and non-reduced proteins (Lane 3) exhibit a faster mobility than refolded and  $\beta$ -mercaptoethanol-treated proteins (Lane 4). Shift in mobility upon reduction showed that  $\beta$ -mercaptoethanol treatment reduced the expected intramolecular disulfide bonds in the refolded protein and thus

suggested that rPkAMA1 and rPvAMA1 produced in this study also contained reduction-sensitive, disulphide-bonded, tertiary structures.

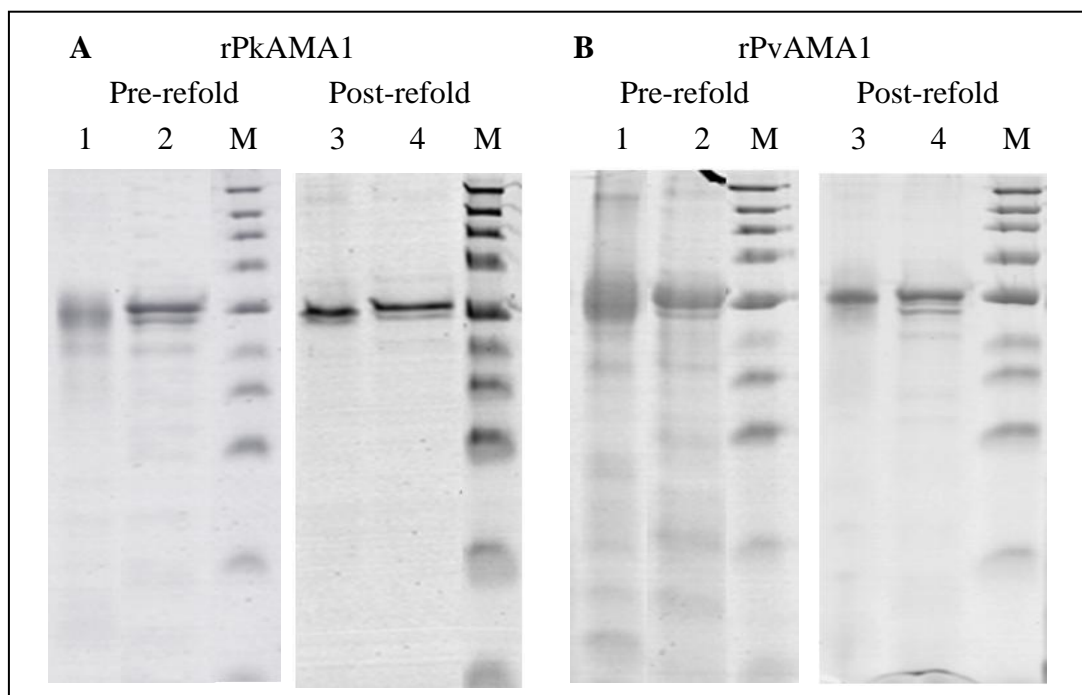


Figure 4.20: Reduced and non-reduced SDS-PAGE analysis of refolding of rPkAMA1 and rPvAMA1 ectodomain proteins. Pre-refold and post-refold fractions of rPkAMA1 (A) and rPvAMA1 (B) were analyzed under non-reducing (Lanes 1 and 3) and reducing (Lanes 2 and 4) conditions using 12 % SDS-PAGE. Non-reduced proteins exhibited overall a faster mobility than reduced proteins suggested that recombinant proteins produced in present study contained reduced-sensitive intramolecular disulfide bonds. More diffused and fuzzy band as indication of misfolded AMA1 variants were observed in both of the pre-refold rPkAMA1 and rPvAMA1 samples as compared to the post-refold samples, in both of the non-reduced and reduced conditions. The disappearance of most multimers and disulfide-bonded aggregates in post-refold showed that these proteins were successfully refolded.

#### 4.6.9 Protein identification by LC-MS/MS

The identity of rPKAMA1 and rPvAMA1 were further confirmed by LC-MS/MS (Table 4.5). Matched peptides are shown in Appendix 6.

Table 4.5: LC-MS/MS spectrum mill analysis of PkAMA1 and PvAMA1.

Spectra	Distinct peptides	MS/MS search score	% AA coverage*	Database accession	Protein ID
<b>Recombinant PkAMA1</b>					
47	25	426.00	38	P21303	Merozoite receptor PK66 OS= <i>Plasmodium knowlesi</i> (strain nuri) GN=PK66 PE=2 SV=2
<b>Recombinant PvAMA1</b>					
40	25	424.99	48	62738184 PDB: 1W81**	b 1W81 A Chain A, Crystal Structure Of Apical Membrane Antigen 1 From <i>Plasmodium vivax</i>
40	25	424.99	48	62738193 PDB: 1W8K**	b 1W8K A Chain A, Crystal Structure Of Apical Membrane Antigen 1 From <i>Plasmodium vivax</i>

\* Indicates the percentage of amino acids coverage in LC-MS/MS results compared with entire region of *Plasmodium* AMA1, including prosequence, ectodomain (domain I, II, and III), transmembrane region, and cytoplasmic domain deposited in reference database.

\*\* Protein Data Bank (PDB): <http://www.wwpdb.org/>



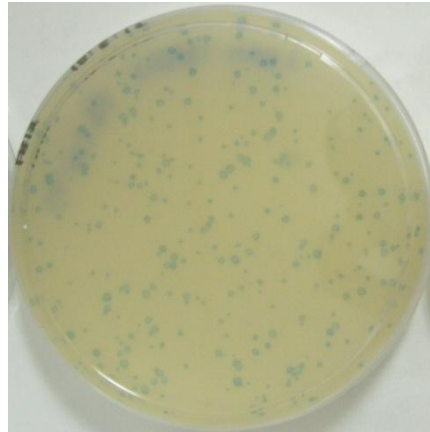
## 4.7 Identification of PkAMA1 and PvAMA1 binding peptides using a phage display library

In order to isolate phage that displayed peptides with specific to PkAMA1 and PvAMA1 proteins, a phage display peptide library with a diversity of  $\sim 2 \times 10^9$  phage particles was employed. This Ph.D.-12 phage display library was purchased from NEB. The rPkAMA1 and rPvAMA1 were used as target proteins conducted on two independent affinity selections. Three consecutive rounds of biopanning were carried out in order to identify the peptides binding to PkAMA1 as well as PvAMA1 proteins. The pool of selected phages that displayed polypeptides with high binding affinity towards the target protein was enriched prior to the subsequence round of biopanning.

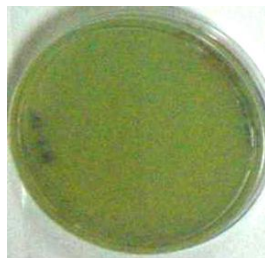
The titer of phage library was determined by infecting *E. coli* ER2738 with the ten-fold serial dilutions of phage in LB broth, i.e., with dilution ranging from  $10^0$  to  $10^4$  for unamplified biopanning eluates (Figure 4.21B) and  $10^8$  to  $10^{11}$  for amplified phage culture supernatants (Figure 4.21C).

In general, the blue plaques are recombinant phages from phage library that carried the *lacZ* gene, while the white plaques are due to wild-type phage contamination. During the three rounds of biopanning and phage amplification, none of white plaque was observed. This quality control was essential due to vanishingly small levels of contaminating wild-type phage will completely overtake the pool of phage library used in subsequent round of biopanning.

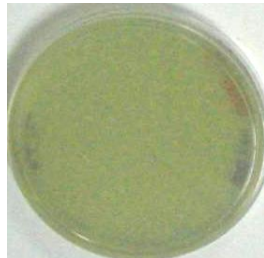
A) Titering plate with blue plaques resulted from the lysed of *E. coli* by phage



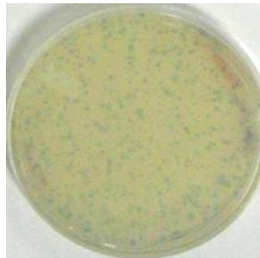
B) Serial dilutions of phage for unamplified biopanning eluates



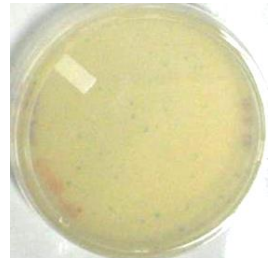
$10^{-1}$



$10^{-2}$

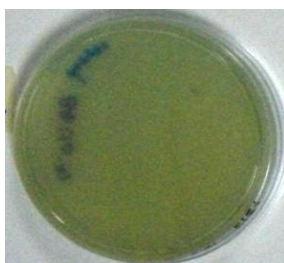


$10^{-3}$

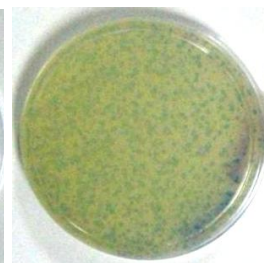


$10^{-4}$

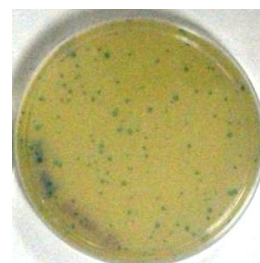
C) Serial dilutions of phage for amplified phage culture supernatants



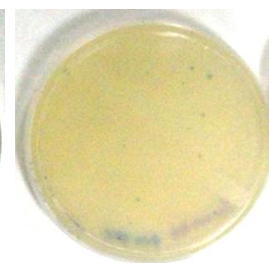
$10^{-8}$



$10^{-9}$



$10^{-10}$



$10^{-11}$

Figure 4.21: Phage titering. Example of typical results obtained from titering of phage sample. Serial dilutions of phage as indicated were mixed with *Escherichia coli* ER2738 cells and incubated on LB/IPTG/Xgal agar plates overnight at 37 °C.

### 4.7.1 Biopanning of phage library to PkAMA1 and PvAMA1

Generally,  $\sim 2 \times 10^{11}$  of the input phage library was used as initiation of biopanning. The titer of output phage was determined, amplified, and then diluted to the desired titer as the input for the subsequence round of biopanning procedure. The titer of input and output phage during three rounds of biopanning was listed in Table 4.6.

Table 4.6: Phage titers obtained following each round of biopanning of rPkAMA1 and rPvAMA1.

Number of phage particles			
<b>rPkAMA1</b>	<b>First</b>	<b>Second</b>	<b>Third</b>
Input	$2.0 \times 10^{11}$	$2.0 \times 10^{10}$	$4.0 \times 10^{10}$
Output	$4.5 \times 10^2$	$6.8 \times 10^2$	$2.2 \times 10^4$
<b>rPvAMA1</b>	<b>First</b>	<b>Second</b>	<b>Third</b>
Input	$2.0 \times 10^{11}$	$1.0 \times 10^{11}$	$4.0 \times 10^{10}$
Output	$2.8 \times 10^2$	$5.5 \times 10^2$	$2.0 \times 10^3$

### 4.7.2 Sequence analysis of phage clones selected from panning with PkAMA1 and PvAMA1

Peptides that bound to PkAMA1 and PvAMA1 have been identified from random peptide library expressed on the surface of phage. Twenty plaques were randomly selected and amplified from the third round of biopanning. Single-stranded DNA of each phage isolate was extracted and sequenced to determine the inserted coding DNA. The sequence of the inserted coding DNA was then translated into amino acid sequence using ExPASy Translate tool (<http://web.expasy.org/translate/>).

Figure 4.22 shows an example of the identification of a binding peptide selected from biopanning against PkAMA1.

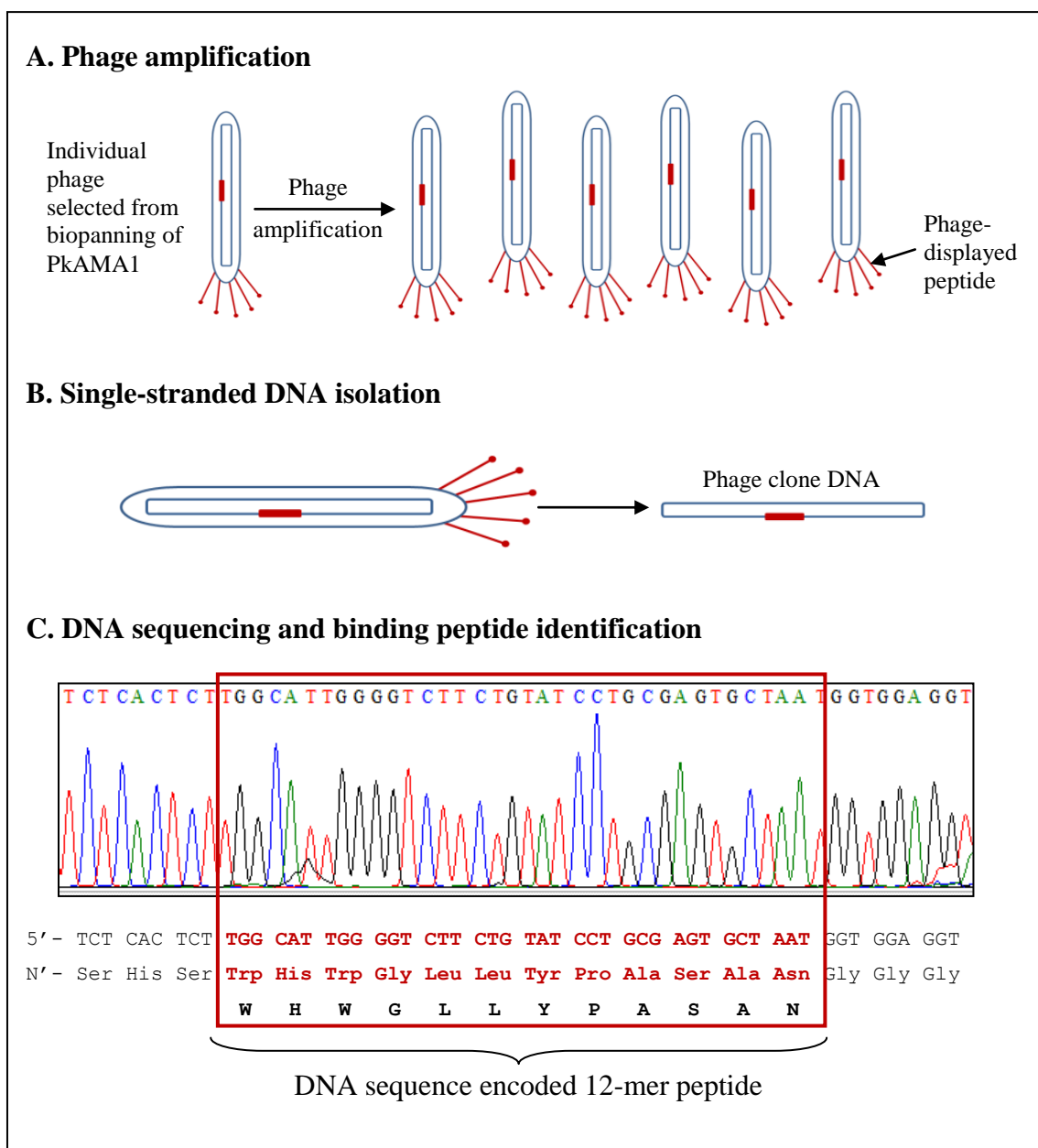


Figure 4.22: Amplification and sequencing of a phage clone selected from biopanning of rPkAMA1. Following elution of interacting peptides in phage display, the copy number can be increased by bacterial infection (phage amplification), as these peptides are displayed on M13 bacteriophage (A). Interacting phage displayed peptides can then be isolated and their sequence can be identified (B). In turn, these codons can be translated to determine the amino acid sequences of the interacting phage-derived peptides (C). Red box indicates a DNA sequence encoded for 12-mer peptide. The rest of binding peptides were identified in similar way (Appendix 8 and Appendix 9).

Overall, 4 and 3 phage peptide variants that bound to rPkAMA1 and rPvAMA1 respectively were identified from 20 random picked phage isolates in the third round of biopanning. Twenty sequences of the inserted DNA were obtained for rPkAMA1 while 16 were obtained for rPvAMA1, this was due to two clones were failed in sequencing and another two clones showed lack of inserted DNA. The overall results are listed in Table 4.7. Interesting, one of the peptide sequence, WHWSWWNPQLT (designated as PdK3 and PdV2) was identified in both of the biopanning against rPkAMA1 and rPvAMA1.

Table 4.7: Peptide sequences obtained in the third round of each biopanning against PkAMA1 and PvAMA1.

<b>Target protein: rPkAMA1</b>			
<b>Phage clone</b>	<b>Peptide sequences</b>	<b>Frequency (n=20)*</b>	<b>Percentage (%)</b>
PdK1	GGSIAASELEY	6	30
PdK2	WHWGLLYPASAN	10	50
PdK3	WHWSWWNPQLT	1	5
PdK4	HSQAMP SMLHQA	3	15
<b>Target protein: rPvAMA1</b>			
<b>Phage clone</b>	<b>Peptide sequences</b>	<b>Frequency (n=16)*</b>	<b>Percentage %</b>
PdV1	DLTFTVNPLSKA	8	50
PdV2	WHWSWWNPQLT	7	44
PdV3	TSVSYINNRHNL	1	6

\* Frequency and percentage indicate the total number of observations of a specified phage variants identified in third round of biopanning.

### 4.7.3 Consensus sequences determination

The presence of consensus motifs in the binding peptides with affinity to rPkAMA1 and rPvAMA1 were investigated using ClustalW (Thompson, et al., 1994) (Figure 4.23).

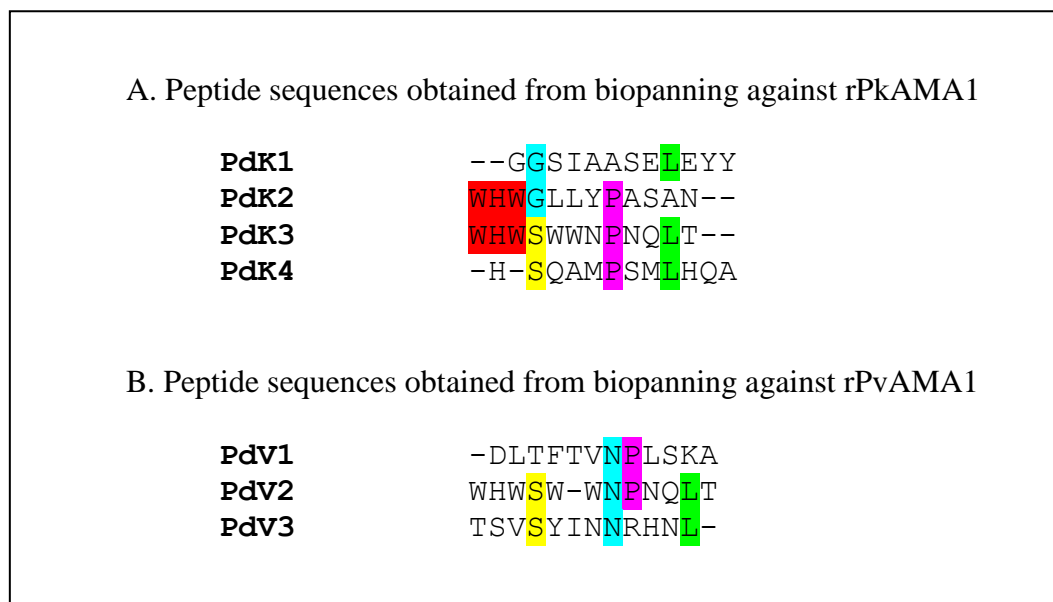


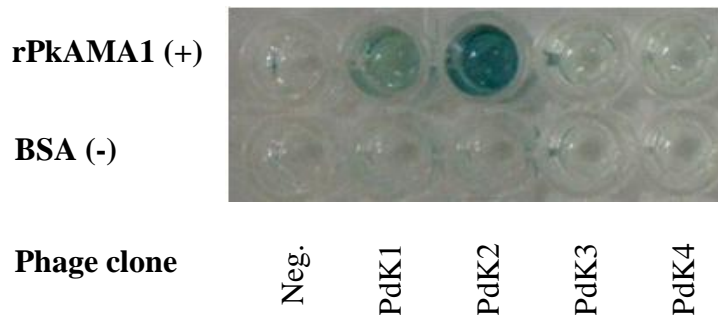
Figure 4.23: Amino acid sequences alignment of selected dodecapeptides obtained after three rounds of biopanning against rPkAMA1 (A) and rPvAMA1 (B). The color bar represented the consensus amino acids located at the same position of consensus motif.

#### 4.7.4 Analysis of binding affinity of selected peptides to PkAMA1 and PvAMA1

##### 4.7.4.1 Phage ELISA binding assay

The binding affinity of each selected peptide clone to rPkAMA1 as well as rPvAMA1 was validated using phage ELISA binding assay, a useful method for qualitative determination of relative binding affinities for a number of selected clones in parallel. The binding of respective phage with target protein, i.e., rPkAMA1 or rPvAMA1 and BSA as the negative control were determined and the binding signals of each of the individual phage with target protein and BSA were then compared. The bar charts in Figure 4.24 and Figure 4.25 show the comparative results obtained from phage ELISA binding assay with comparison of binding affinities of individual phage clone to the rPkAMA1 and rPvAMA1, respectively.

Finally, only two out of four of phage clones show strong binding signal to rPkAMA1, i.e., PdK1 (GGSIAASELEY) and PdK2 (WHWGLLYPASAN) with 8.3× and 22.6×, respectively, whereas PdK3 (WHWSWWNPQLT) and PdK4 (HSQAMPSMLHQA) peptides show weak binding signal with 2.1×. Three phage clones selected from biopanning on rPvAMA1, i.e., PdV1 (DLTFTVNPLSKA), PdV2 (WHWSWWNPQLT), and PdV3 (TSVSYINNRHNL) show positive binding signal with 12.1×, 3.5×, and 3.1×, respectively.



Phage clone	Absorbance 405 nm		Fold of binding
	BSA (-)	rPkAMA1 (+)	
Neg.	0.101	0.103	-
PdK1	0.094	0.779	8.3×
PdK2	0.093	2.106	22.6×
PdK3	0.106	0.225	2.1×
PdK4	0.106	0.224	2.1×

Figure 4.24: Phage ELISA binding assay for peptides selected from biopanning against rPkAMA1. Upper wells of microplate were coated with 100  $\mu\text{g/ml}$  of rPkAMA1, whereas lower wells were coated with BSA. Negative (Neg.) indicates none of phage clone was tested. Phage binding signals were determined using HRP-conjugated anti-M13 antibody and ABTS as the HRP-substrate. The folds of binding are shown in the table.



**rPvAMA1 (+)****BSA (-)****Phage clone**

Neg.

PdV1

PdV2

PdV3

Phage clone	Absorbance 405 nm		Fold of binding
	BSA (-)	rPvAMA1 (+)	
Neg.	0.141	0.141	-
PdV1	0.134	1.616	12.1×
PdV2	0.550	1.949	3.5×
PdV3	0.122	0.377	3.1×

Figure 4.25: Phage ELISA binding assay for peptides selected from biopanning against rPvAMA1. Upper wells of microplate were coated with 100 µg/ml of rPvAMA1, whereas lower wells were coated with BSA. Negative (Neg.) indicates none of phage clone was tested. Phage binding signals were determined using HRP-conjugated anti-M13 antibody and ABTS as the HRP-substrate. The folds of binding are shown in the table.

#### 4.7.4.2 Western blot binding assay

The binding characteristics of the phage peptides were further examined by Western blot analysis. The results obtained were captured with a digital camera (Figure 4.26).

The phage clones PdK1 and PdK2 showed positive signal to rPkAMA1, whereas no signals were being observed on strips PdK3 and PdK4. On the other hand, clear signal was observed in PdV1 to rPvAMA1, while weak binding signals were being observed in strips PdV2 and PdV3.

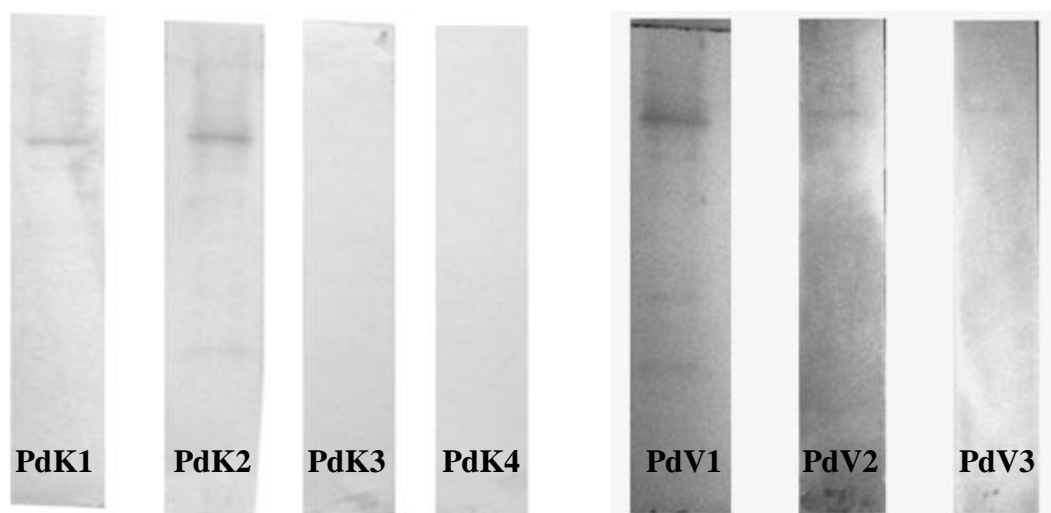


Figure 4.26: Western blot assay for peptides binding to rPkAMA1 and rPvAMA1.

## CHAPTER FIVE: DISCUSSION AND CONCLUSION

### 5.1 Diagnosis of malaria

Malaria is a serious global health challenge and the disease may turn severe if the patient is left untreated especially for *P. falciparum* and *P. knowlesi* infections. *Plasmodium vivax* is considered a benign infection and rarely causes death, however, there have been increasing severe vivax malaria reported elsewhere (Karyana, et al., 2008; Kochar, et al., 2005; Rogerson & Carter, 2008; Tjitra, et al., 2008). Severe vivax malaria was frequently reported in young children and debilitated patients after repeating infections (Mueller, et al., 2009; Rogerson & Carter, 2008). Furthermore, *P. vivax* gametocytes develop early in the infection and can be seen in the peripheral circulation before or at the beginning of clinical symptoms. The asymptomatic infection in yet untreated individual might serve as potential reservoir to transmit the infection to mosquitoes (Mueller, et al., 2009). Basically, most of the severe malaria may actually have been associated with mixed infections as well as multidrug resistance (Karyana, et al., 2008; Kochar, et al., 2005; Rogerson & Carter, 2008; Tjitra, et al., 2008).

Thus far, effective malaria vaccines are still unavailable (malERA Consultative Group on Vaccines; Richards & Beeson, 2009), therefore a rapid, accurate, species-sensitive/-specific and economically-efficient diagnostic tool is crucial to increase the effectiveness of targeted treatment for infected individuals and control management. Accurate diagnosis of malaria is necessary to prevent the disease from progressing and eliminating malaria death, besides avoiding the unnecessary use of antimalarial agents. The improper drug prescription not only may lead to drug-related adverse effects but also contribute to unnecessary drug pressure, thereby enhance the existence of drug resistance *Plasmodium* stains.

Most of the currently available malaria diagnostic tools are focused on parasites circulated in the erythrocytic cycle, which are responsible for the appearance of clinical

---

symptoms in human. To date, available diagnostic tools include microscopic examination of Giemsa stained thin and thick blood smears, immunochromatographic dipstick assay, and molecular PCR assays.

### 5.1.1 Microscopic examination

Giemsa stained blood smears are the most widely used approach for malaria diagnosis. Although this method is effective and inexpensive, it is laborious, time-consuming, and is challenging for *Plasmodium* species identification, especially when infections are at low parasitemia below the threshold of microscopy detection, i.e., below 40 parasites/ $\mu$ l of blood, as well as in mixed-species infection cases. Generally, the detection limit can vary among microscopists. The routine detection level usually exceed 50 parasites/ $\mu$ l (Mayxay, et al., 2004; Moody, 2002) and can be down to approximately 5-10 parasites/ $\mu$ l for an expert (Zimmerman, et al., 2004). Microscopic examination permits the determination of the infecting species as well as the stage of the circulating parasites. In addition, it also allows quantification of *Plasmodium* parasites, assessing the disease severity, as well as monitoring the response to antimalarial therapy. Moreover, malaria blood smears also provide a permanent record for quality assessment of the microscopy diagnosis.

Although microscopic examination has long served as a gold standard for routine malaria diagnosis, multiple morphological appearances of parasites remain the major concern in malaria diagnosis in both cases of the single- as well as in multiple-species infections. Morphological confusion in blood stages of some *Plasmodium* species to others is one of the major challenges in malaria diagnosis (Moody, 2002). For example, *P. knowlesi* morphologically resembles *P. falciparum* in the early ring trophozoite stage and to *P. malariae* in the later erythrocytic stages (mature trophozoite, schizont, and gametocyte). This has made it difficult for the speciation of *Plasmodium*

via microscopy (Lee, et al, 2009). Besides that, five human malaria parasites exhibit high morphological similarity in young ring-forms; therefore, species differentiation can also be difficult if the circulating stages are in immature erythrocytic stage, especially in mixed infections.

Unrecognized and underestimation of mixed infections are common in malaria cases diagnosed based on microscopy alone. The hallmark features of *P. falciparum* infection for severe malaria include mature parasites cytoadhere to a variety of receptors and become sequestered in the deep vasculature of various tissues and organs. Parasite sequestration could be the reasons for the absence of mature asexual blood stage forms of parasites in blood circulation, unless in severe cases with very high parasitemia (Zimmerman, et al., 2004). Other than sequestered parasite, undetectable of *P. vivax* and *P. ovale* parasites that exhibit hypnozoite forms (dormant stage) in the liver, as well as delayed appearance of one cryptic species might consequently lead to the difficulties in featuring the exact infectious species and parasitaemia in mixed infections (Mayxay, et al., 2004).

Mixed infections certainly have worst clinical outcome compared to single infection. Failure to detect mixed infections could result in inadequate or incorrect treatment. For example, missed diagnosis of *P. falciparum* and *P. knowlesi* within mixed infections could result in the risk of developing subsequent severe and possibly fatal disease; whereas, missed diagnosis of *P. vivax* and *P. ovale* infections could result in repeated debilitating relapses in the blood due to the reactivation of dormant liver-stage hypnozoite. Missed diagnosis of vivax malaria during pregnancy could also result in the birth of low-birth-weight infants that increases the risk death in newborn (Mayxay, et al., 2004; Desai, et al., 2007; Steketee, et al., 2001). Basically, the therapeutic regimens will differ in mixed infections and immediate drug treatment is priority recommended for treatment of *P. falciparum* infection in malaria cases with mixed

infections as the consideration of severe disease and even fatal complications in falciparum malaria (WHO, 2000).

### **5.1.2 Rapid diagnostic tests (RDTs)**

The RDTs offer the possibility of rapid (required 15-20 minutes assay time) and nonmicroscopic methods for malaria diagnosis based on the principle of immunochromatographic lateral-flow-strip technology. The dipstick format RDT enables the capture of the parasitic antigen from peripheral blood using *Plasmodium* specific monoclonal antibodies that are immobilized on the surface of a nitrocellulose membrane. Despite the low sensitivity (require > 100 parasites/μl of blood) and most of commercial available kits are only specific to *P. falciparum* detection, the RDTs have been implemented as an adjunct to microscopic examination in many diagnostic laboratories and also widely used in remote areas across the world, whereby lack of well-equipped diagnostic facilities is common (Moody, 2002; Murray, et al., 2008). However, antigenemia may persist in plasma a few weeks beyond the actual infection, leading to the possibility of false positive results (Moody, 2002).

### **5.1.3 Molecular PCR diagnosis**

In malaria epidemiological studies, correct estimates for the global burden of species-specific *Plasmodium* infections require better diagnostic methods. Therefore, a more sensitive and specific diagnostic assay is urgently needed. The detection of low level asymptomatic and mixed species infections with conventional light microscopy and RDTs are limited. Misdiagnosis of *Plasmodium* species, especially in overlooking lethal *Plasmodium* species will have a significant negative impact on the effectiveness of treatment, control measures and prognosis of patients (Moody, 2002; malERA Consultative Group on Diagnoses and Diagnostics, 2011). Essentially, this will

definitely stifle the global malaria eradication efforts.

The molecular detection for *Plasmodium* diagnosis using PCR has been proven to be relatively more sensitive and specific to detect asymptomatic carries, prepatent patients, and people recently exposed to *Plasmodium* infections. Conventional PCR assays, such as nested PCR (Singh, et al., 1999; Singh, et al., 2004; Snounou, et al., 1993), semi-nested PCR (Rubio, et al., 1999), and multiplex PCR (Padley, et al., 2003), as well as real-time PCR (Mangold, et al., 2005; Perandin, et al., 2004; Rougemont, et al., 2004; Safeukui, et al., 2008), have shown to improve the sensitivity and specificity over microscopic evaluations or RDTs in many cases, as they can detect parasitemia levels of < 5 parasites/μl, and as low as 0.004 parasites/μl for *P. ovale* (Padley, et al., 2003).

Real-time PCR is also known as a quantitative PCR (qPCR) due to its ability in quantifying the parasite DNA copy numbers, i.e., estimation of parasite densities in malaria. The real-time PCR is a rapid assay, and the result obtained is in a more straightforward format based on completion of amplification without any downstream analysis through gel electrophoresis such as in conventional PCR assays. Furthermore, the closed system can also minimize the probability of cross-contamination inherent in conventional PCR. However, the cost of reagents, consumables, and equipment are much higher than any conventional PCR assays.

Most recently, a simplest molecular method using loop-mediated isothermal amplification (LAMP) assay was first described by Han and colleagues in the diagnosis of four human malaria parasites (except *P. knowlesi*) (Han, et al., 2007). Generally, six distinct regions on a target gene (i.e., 18S rRNA gene) are amplified under constant temperature of 60 - 65 °C using either two to three sets of primers and a *Bst* DNA polymerase with high strand displacement activity in addition to a replication activity. The corresponding release and precipitation of magnesium pyrophosphate as by-product

---

of LAMP reaction will result in visible turbidity, which allows easy visualization by the naked eye or real-time turbidimeter (Han, et al., 2007). Although this method is rapid and simple, however further evaluation of this method is necessary to determine its utility for malaria diagnosis in the field.

Among the PCR assays, a single-step multiplex PCR seems to be the most ideal assay in the diagnosis of malaria in terms of costing and duration of time needed to obtain the results. The main advantage of multiplex PCR is the ability to simultaneously identify more than two targets in a single tube reaction; this is an attractive option for routine malaria diagnosis, since mixed infections can be detected in a single step. However, there are limited studies in this area due to the difficulties in primer design and the cumbersome optimization procedures that are needed to establish a highly sensitive and specific assay. The use of various couples of primers which have different characteristics, especially for primers annealing and melting temperatures are the main technical constraints in multiplex PCR development. Furthermore, there is no standard protocol in optimizing multiplex PCR, all primers designing and optimum reaction conditions need to be tested empirically.

To the best of our knowledge, only two multiplex PCR assays based on conventional PCR technology, i.e., a semi-nested PCR (Rubio, et al., 1999) and a single tube multiplex PCR (Padley, et al., 2003) that can detect up to four species, excluding *P. knowlesi*, have been described. In light of the emergence of the potentially fatal human infections with *P. knowlesi*, which was previously considered as a zoonotic parasite, a straightforward single-step multiplex PCR for simultaneously identification of five human malaria parasites was developed in the present study.



---

## 5.2 Multiplex PCR system for identification of five human *Plasmodium* species

Multiplex PCR is one of the research priorities for future malaria diagnosis (malERA Consultative Group on Diagnoses and Diagnostics, 2011). With the WHO malaria eradication programs back on the global health agenda, it is of paramount significance that a rapid, accurate, species-sensitive/species-specific, and economically efficient system be made available for the institution of effective treatment management and control. Essentially, with a highly effective diagnosis system, the ultimate aim is to increase the chances for patient recovery and survival, hence reducing morbidity and eliminating mortality due to malaria.

### 5.2.1 The significance of 18S ssu rRNA gene in species determination

18S ssu rRNA gene is a highly conserved and pivotal gene in the phylogenetic studies that universally existed in all eukaryotic cells. Thus far, most of the molecular characterization of different plasmodia has widely relied on sequencing and analyzing of 18S ssu rRNA genes (Leclerc, Hugot, Durand, & Renaud, 2004). The highly conserved and variable regions of 18S ssu rRNA gene not only provide important information for the relationship among species, it can also be used as the biological identification marker in PCR screening (Conway, 2007). In general, rRNA gene sequences are easy to be used as universal primers due to their highly conserved regions. Furthermore, the repetitive arrangement within the genome provides excessive amounts of template DNA for PCR. At least five copies of the 18S ssu rRNA gene are dispersed on separate chromosomes throughout the *Plasmodium* genome (Carlton, et al., 2008; Gardner, et al., 2002; Pain, et al., 2008), which certainly will enhance the sensitivity of PCR assay. Therefore, the 18S ssu rRNA gene of five human *Plasmodium* parasites was chosen as the target in the current multiplex PCR development.

### 5.2.2 Clinical samples and negative controls

In the present study, a total of 246 whole blood samples were collected in EDTA tubes, and further aliquot into three portions, i.e., for routine laboratory tests, such as microscopic examination and immunochromatographic test (ICT), DNA extraction for PCR assays, and the remaining portion was kept at -70 °C for long term storage. The 226 samples were from patients suspected with malaria, and 20 healthy controls were from volunteer group with no history of malaria and negative by microscopy. The DNA samples served as templates in specificity validation.

### 5.2.3 18S ssu rRNA plasmids construction

*Plasmodium* parasites have structurally and functionally different paralogous copies of the 18S ssu rRNA gene, which could be expressed during the different developmental stages. Thus far, three types of 18S ssu rRNA have been reported, they are asexual- (A-), sporozoite- (S-), and oocyst- (O-) types that are expressed in asexual, sporozoite, and oocyst stages, respectively (Leclerc, et al., 2004; Nishimoto, et al., 2008). However, based on the NCBI database records, the S-type of 18S ssu rRNA gene sequences of *P. knowlesi* are referred as putative sexually transcribed form, both of which were isolated from patient's blood samples reported in Malaysia Borneo (Singh, et al., 2004).

The primers used in nested PCR and DNA clone construction, i.e., rPLU1 (forward) and rPLU5 (reverse) are universally targeting genus-specific of all types of 18S ssu rRNA gene of *Plasmodium* species, based on the variably expressed during the parasite life cycle. The O-type gene expression is only restricted in oocyst stage in the mosquito, while the sporozoite-type gene is expressed during liver stage replication. Therefore, there are two possibilities of gene amplifications (either asexual- or sexual-types) and further randomly clone into *E. coli* cells when PCR using human blood

samples, due to unsynchronized stages of parasites in blood. In general, most of molecular studies, such as phylogenetic and molecular PCR analyses, are emphasizing only on the A-type gene (Leclerc, et al., 2004; Nishimoto, et al., 2008).

In the present study, the amplicon from the first nested PCR (~ 1.7 kb) was gel purified and further cloned into TOPO cloning vector, followed by transformation into competent cells. The successful clones were confirmed by colony PCR and sequencing. Only the clones carrying the representative gene types (either asexual- or sexual- types) were selected and kept as positive controls in multiplex PCR development. Generally, asexual-type primers were designed to identify four human *Plasmodium* species, excluding *P. knowlesi*. Given that the majority of human *P. knowlesi* 18S ssu rRNA gene sequences deposited in GenBank are in sexually transcribed form, therefore, a sexual-type primer was designed to identify *P. knowlesi*. The single reverse primer used in multiplex PCR system was conserved in both of the A-type and S-type genes.

#### 5.2.4 Primer design and multiplex PCR optimization

All the five species-specific forward primers as well as single reverse genus-specific primer were successfully designed with the aid of Primer Premier software (PREMIER Biosoft International). Basically, the primers were designed and selected based on the following parameters: homology of primers with their target nucleic acid sequences, primer length, product length, product location, minimal hairpin and dimer formations, the GC content, and annealing temperature. Ideally, all the primers in multiplex PCR should allow similar amplification efficiencies for respective target. This may be achieved through the utilization of primers with nearly identical optimum annealing temperatures. Furthermore, primers should not display significant homology either internally or to one another, to avoid the secondary structures (hairpin and dimer structures) and possibility of self-priming, false priming, and cross dimer formation.

In 2010, Sutherland and coworkers reported that there were two nonrecombining sympatric forms of *P. ovale* with dimorphism of genetic haplotypes, i.e., *P. ovale curtisi* (classic type) and *P. ovale wallikeri* (variant type), and only *P. ovale curtisi* can be identified by nested PCR based on the primers targeting ssu rRNA gene (Sutherland, et al., 2010). For this reason, an alternative PCR primer pair specific to both *P. ovale* subspecies (Padley, Heath, Sutherland, Chiodini, & Baylis, 2008) was also included to the second nested PCR (Figure 4.1). In the present study, this was taken into consideration by designing a degenerate *P. ovale* primer that covers both the classic and variant types of *P. ovale*. However, due to sample limitation, the detection of both *P. ovale* variants could only be tested through *in silico* PCR. In this study, the 18S ssu rRNA of the only *P. ovale* clinical sample was cloned and further confirmed as *P. ovale curtisi* through sequencing (Lim, et al., 2010).

The multiplex PCR conditions, such as, primers concentration, PCR reagent mixture, amplification conditions etc, were fully optimized using DNA extracted from

blood samples in this study.

### 5.2.5 Positive control

In a PCR without a positive control, a negative result obtained showing there was no target sequence present in the reaction, but it can also mean the reaction was inhibited due to malfunction of the thermal cycler, PCR mixture, or presence of inhibitory substances in the reaction mixture. Conversely, in a PCR with positive control, a control band should always be produced even though there is no target sequence present for disease specific primer pair. Therefore absent of control band can directly reveal the failure of a PCR.

In the present study, three types of positive controls targeting different sources of DNA (either external or internal control) as well as genes were tested on the pentaplex PCR system (Figure 5.1). The selection of positive control to be included in the multiplex PCR system was based on the observation of the PCR results from 50 malaria DNA samples.

In the first set of positive control (Figure 5.1A), inclusion of external positive control, pGEX4T1 plasmid DNA and pGEX4T1 primer pair (i.e, pGEX 5' and pGEX 3') posed a serious competition on *Plasmodium* PCR amplification, thus this set of control was excluded in the present multiplex PCR system. In contrast to external positive control, another two positive controls were considered as the internal amplification control, whereby control DNA sequence was present in the same specimen, which can be co-amplified simultaneously with the target sequence. Generally, internal positive control can be further subdivided into two formats in a diagnostic PCR assay, either to be used competitively or noncompetitively (Hoorfar, et al., 2004).

The inclusion of the second set of positive control, i.e., *Plasmodium* and human conserved primers to the multiplex PCR system is a typical type of competitive PCR,

where the target and control are amplified with a common set of primers under the same conditions in a PCR tube (Figure 5.1B). Simultaneous amplifications of two different *Plasmodium* DNA fragments flanked by the same primers sites can result in competition of both products as a phenomenon seen in the present study. The inconsistency in PCR amplifications could be explained by three possibilities. Firstly, primer-template competitions could have occurred in this multiplex PCR system, due to multiple forward primers to a single reverse primer. Secondly, there are variations in the binding affinity of each forward and reverse primer pairs targeting homologous gene. Thirdly, constrains of reaction mixture (dNTPs,  $Mg^{2+}$ , *Taq* polymerase, etc) due to at least three DNA fragments, i.e., human genus-specific, *Plasmodium* genus-specific, and *Plasmodium* species-specific 18 ssu rRNA genes must present in a single species infection case.

In the third design (Figure 5.1C), a noncompetitive primer pair targeting human  $\beta$ -hemoglobin gene was designed and finally selected, which served as an internal positive control, indicative of a successful DNA extraction procedure and PCR. There was no significant reduction of sensitivity and specificity of pentaplex PCR system with the inclusion of the  $\beta$ -hemoglobin primer pair. In contrast, PCR selection (competitive inhibition) was observed in another two positive control candidates. PCR selection is defined as a mechanism which inherently favors the amplification of certain templates due to the target concentrations or properties of the target. The amplification biasness may also be due to the primers itself, such as high or low amplification efficiency.

Finally, a rapid and single-step hexaplex PCR system for the identification of five human *Plasmodium* species with an internal positive control targeting  $\beta$ -hemoglobin gene was developed.

Figure 5.1 illustrates an overview of the three positive controls tested in the present multiplex PCR system.

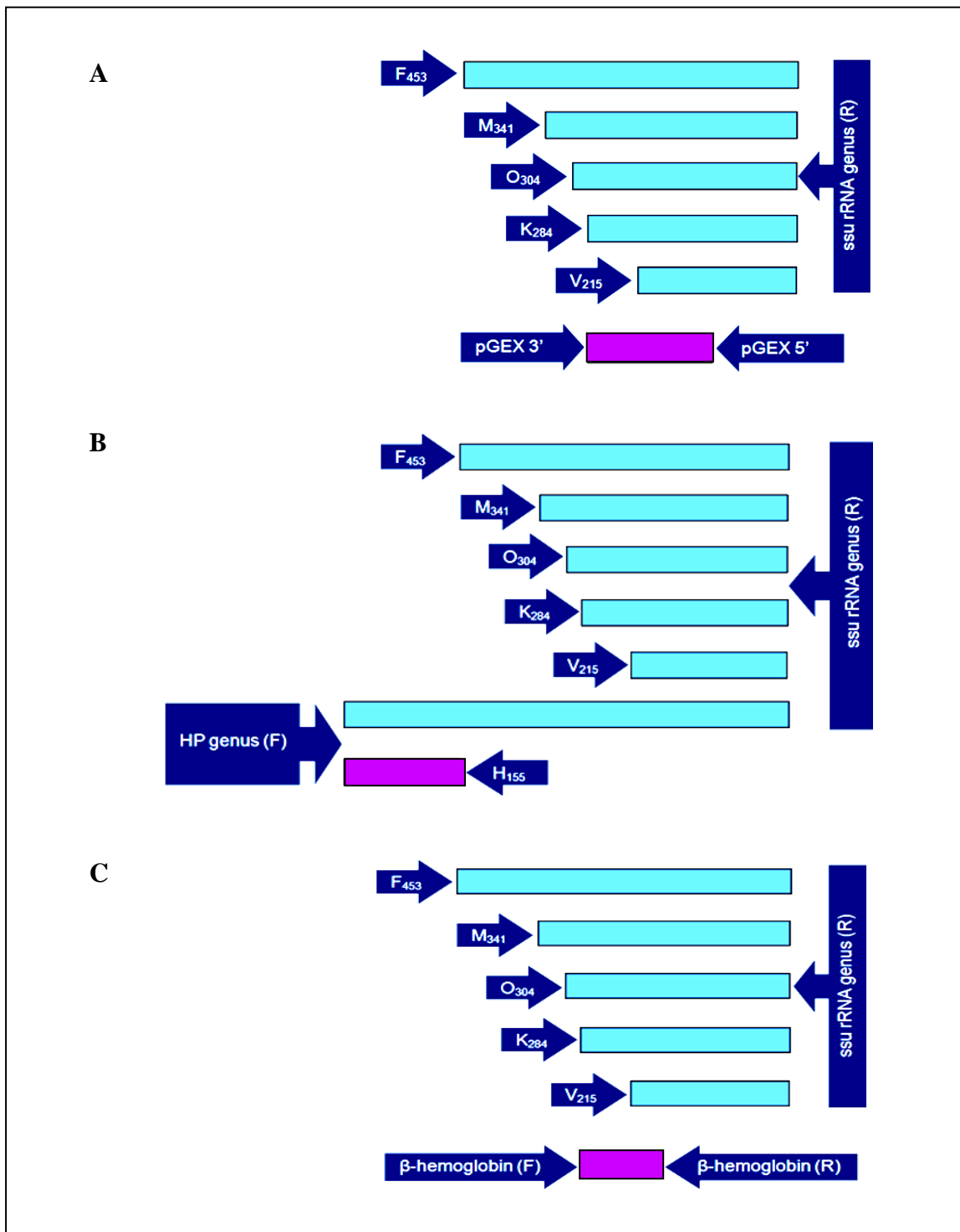


Figure 5.1: Schematic of the multiplex PCR amplification for identification of five human *Plasmodium* species with a positive control. (A) The pGEX4T-1 plasmid served as external positive control. (B) Both genus-specific of *Plasmodium* and human genes served as internal positive controls. (C)  $\beta$ -hemoglobin gene served as an internal positive control. The dark blue arrows represent the primers used in multiplex PCR; purple box represent positive control.

## 5.2.6 Sensitivity and specificity analyses

### 5.2.6.1 Sensitivity and specificity in single infection

The present hexaplex PCR revealed high sensitivity with all five human *Plasmodium* parasites detectable below 0.5 parasites/ $\mu$ l of blood sample in the sensitivity validation, i.e., 0.025 parasites/ $\mu$ l for *P. vivax*, 0.027 parasites/ $\mu$ l for *P. ovale*, 0.15 parasites/ $\mu$ l for *P. falciparum*, 0.25 parasites/ $\mu$ l for *P. knowlesi*, and 0.27 parasites/ $\mu$ l for *P. malariae*.

A study conducted on the validation and comparison of the detection limits of three conventional PCR detection systems, i.e., nested PCR (Singh, et al., 1999; Snounou, et al., 1993), semi-nested PCR (Rubio, et al., 1999), and multiplex PCR (Padley, et al., 2003) in the detection of four human *Plasmodium* species (excluding *P. knowlesi*), using a series of known parasitemia samples as well as experimentally mixed infections, noted that nested PCR was the only method that consistently and accurately diagnosed mixed infections and subclinical infections when compared with semi-nested PCR and multiplex PCR (Mixson-Hayden, Lucchi, & Udhayakumar, 2010).

Overall, optimized nested PCR in our laboratory was able to detect *Plasmodium* species at a low titer, with an average of 0.01 parasites/ $\mu$ l, which is more sensitive than nested PCR reported by Mixson-Hayden study, i.e., 0.4 parasites/ $\mu$ l (Mixson-Hayden, et al., 2010), semi-nested PCR, i.e., 0.1 parasites/ $\mu$ l (Rubio, et al., 1999), and the present hexaplex PCR system, i.e., less than 0.3 parasites/ $\mu$ l. However, this single-round hexaplex PCR results showed 100 % concordance with the results obtained through nested PCR. Furthermore, five missed malaria infections were successfully detected from 15 microscopy negative clinical samples. This may have been due to the fact that our tested samples had a parasitemia level above the detection limits of both approaches.

The only limitation of the present study was unable to further evaluate the sensitivity and specificity of *P. malariae* and *P. ovale* due to limited samples in this



study period. However, the current hexaplex PCR had been validated on sufficient numbers of clinical malaria samples, especially on three most prevalent malaria agents in our local area, i.e., *P. vivax*, *P. falciparum*, and *P. knowlesi*, which have multiple ranges of parasitemia counts. Most significantly, the system successfully and consistently picked up the two most potential fatal infectious agents, i.e., *P. falciparum* and *P. knowlesi*.

#### **5.2.6.2 Sensitivity and specificity in mixed infections**

In mixed infections, primer binding competition effect can contribute to result inconsistencies in most of the multiplex PCR assays. However, this problem did not exist in the present newly developed multiplex PCR. The only limitation in the evaluation of the present multiplex PCR is the lack of naturally acquired mixed infections. However, in the mixtures of two parasite species in the 60 experimentally simulated mixed infection tests using clones DNA with different DNA ratios (Figure 4.7) and 30 clinical samples, *Plasmodium* species were accurately identified in all the samples, confirming that this hexaplex PCR system is robust and capable of detecting mixed-infections at least up to two-species level without any diagnostic constrain. The triple-species mixed infections, i.e., *P. falciparum*, *P. vivax*, and *P. knowlesi* were also randomly created using clinical samples with various parasitemia scores, and all three mixed-species were successfully detected by multiplex PCR as shown in Figure 4.9 (Lane 8). Due to sample limitation, the simulated clinical mixed infections were not performed on *P. malariae* and *P. ovale*.

### 5.2.6.3 Random blind test and clinical screening

A random blind test based on 50 DNA samples was conducted, and no cross-reactions among the five species-specific primers were observed. This assay was further validated with 226 clinical samples, and the results demonstrated 100 % concordance with the results obtained through nested PCR, the current molecular gold standard. There were only two cases of *P. vivax*-*P. falciparum* mixed infections detected by PCR among 211 microscopy confirmed samples in the present study; one was microscopy identified to be mixed infections and one was microscopy identified as *P. vivax* single infection. Another 201 samples were single-species infections, including another seven samples identified by microscopy as mixed infections; one case of *P. vivax* mixed with *P. falciparum*, three cases of *P. vivax* mixed with *P. malariae*, as well as one case of *P. vivax* mixed with *P. knowlesi* (as identified by microscopy) were actually single infection of *P. vivax*, while another two cases of *P. falciparum* mixed with *P. knowlesi* were single infection of *P. knowlesi*. Neither *Plasmodium* species was detected in both nested PCR and multiplex PCR in the rest of the eight clinical samples. Only clear  $\beta$ -hemoglobin fragment (~ 109 bp) was visualized in multiplex PCR assay in these eight samples. Based on microscopy results, seven of these samples scored in the + category (two *P. vivax*, three *P. falciparum*, one *P. knowlesi*, and one *P. malariae/P. knowlesi*) and one *P. falciparum* was scored in the ++ category. Due to high sensitivity of molecular PCR detection assays (concordance results obtained in both nested PCR and multiplex PCR) over microscopy assay, the present study therefore postulated that these samples might be considered as false positive cases by microscopy. Furthermore, appearances of the internal positive control fragment in these cases are indicative of successful DNA extraction procedure and PCR.

Interesting, only two samples were PCR confirmed as *P. malariae* infection (4 %) among the 51 samples identified with microscopy as either *P. malariae* or *P.*

*malariae*/*P. knowlesi* infection. This finding was similar to the study done by Singh and colleagues in 2004, indicating that most microscopy-diagnosed *P. malariae* infections turned out to be *P. knowlesi* infections based on nested PCR assay (Singh, et al., 2004). Both findings further support the sensitivity and specificity of molecular PCR assays over microscopic examination for the diagnosis of malaria, especially for *P. knowlesi* cases.

#### **5.2.6.4 Diagnostic sensitivity and specificity**

Due to samples limitation in *P. ovale* and confusing results in microscopic examination between *P. malariae* and *P. knowlesi*, therefore only the sensitivity, specificity, PPV, and NPV of the present developed multiplex PCR system in diagnosis of both *P. falciparum* and *P. vivax* were estimated and there were 100 % concordance with the results of nested PCR as gold standard. While the overall decreases on these values were observed in microscopy assay. The present study can therefore propose that multiplex PCR is as reliable as nested PCR in clinical detection of these two species of malaria parasites, as reported here for *P. falciparum* and *P. vivax*.

### 5.2.7 Advantages of multiplex PCR over others molecular diagnostic assays

Some of the main advantages of the present novel hexaplex PCR over available semi-nested (Rubio, et al., 1999) and nested PCR (Singh, et al., 1999; Singh, et al., 2004; Snounou, et al., 1993) assays include the hexaplex PCR system being less labor-intensive and rapid (reduced hands-on time) due to its single-step PCR, compared to at least two and/or six PCRs which are need to be conducted for the semi-nested and nested-PCR assays, respectively, in the identification of all five *Plasmodium* species. The fewer steps reduce the usage of PCR reagents and disposable consumables. The time required for this single-step hexaplex PCR is only three hours, versus approximately six hours for semi-nested PCR and about twenty hours for nested PCR, including time for PCR preparation, conducting the PCR and agarose gel electrophoresis. Thus, the current hexaplex PCR significantly shorten the time for diagnosis. In addition, a single-tube reaction is also recommended, as it avoids the risk of carryover and possible external contamination during the transfer of PCR amplicons from primary to secondary PCR mixture and agarose gel electrophoresis for the detection of PCR products. However, this contamination can be avoided if good laboratory practice for molecular amplification techniques is followed.

Currently, ordinary multiplex PCR technique is widely applied in rapid diagnosis of many infectious diseases (Khamrin, et al., 2011; Padley, et al., 2003; Teh, Chua, & Thong, 2010; Thong, Lai, Teh, & Chua, 2011). With well-designed primers used under fully optimized conditions, most of the multiplex systems have shown high sensitivity and specificity. For instance, the results from the present hexaplex PCR and nested PCR assays were in agreement. Multiplex PCR is an ideal and affordable method in most of the laboratories or field settings, especially in developing countries or countries with lower economic resources, since the conventional PCR thermal cycler and agarose gel electrophoresis system remain the cheapest molecular assay if

compared with the real-time PCR assay, which utilizes expensive reagents (probes), consumables, and equipment. In addition, multiplex PCR assay also allows large-scale screening of samples within a short period, especially in malaria hyperendemic regions, where there is a lack of clinical personnel and experienced microscopists. The workflow in microscopic examination can be very burdensome and time-consuming when huge sample size must be handled.

Despite nested PCR assay being considered as molecular gold standard in the diagnosis of malaria, there are increasing issues that affect the usefulness of nested PCR in *Plasmodium* species discrimination recently. For instance, several studies carried out in different countries of Southeast Asia reported that the *P. knowlesi*-primers (i.e., Pmk8 and Pmk9) developed for nested PCR (Singh, et al., 2004), have been shown to give possible cross-hybridization with sequences of *P. vivax*, and thus lead to false positive results (Imwong, et al., 2009; Jiang, et al., 2010; Sulistyaningsih, et al., 2010; Van den Eede, et al., 2009). In addition, the *P. ovale wallikeri* (a variant type of *P. ovale*) was undetectable by current nested PCR (Sutherland, et al. 2010). This situation emphasizes a need to improve and establish a more reliable PCR-based method for routine diagnosis of malaria and the present multiplex offers a good option or alternative, which has been fully optimized for the identification of the five human *Plasmodium* species.

On the other hand, LAMP assay is claimed to be the simplest molecular approach for disease diagnosis, however only qualitative results can be obtained through LAMP and there is no specific indicator to determine whether it is a true-positive or false-positive result due to potential contamination. Furthermore, multiple primer pairs are required in the identification of a single species infection, therefore large scale screening efforts using LAMP are still under assessment. In addition, no reports have been published on multiplex-LAMP assays.

---

### 5.2.8 Future perspectives

As there were only one *P. ovale* and two *P. malariae* infections detected during the study period, more samples will be obtained in future from other countries (especially African countries) to carry out further sensitivity and specificity tests, especially for the case of *P. ovale wallikeri* infection.

The present hexaplex PCR have been validated with DNA extracted from whole blood samples, which gave 100 % concordance results with nested PCR. However, when handling with malaria disease, preserving the fingerprick blood sample by spotted on filter paper and/or in blood smear formats are the common practice, especially in field setting and rural areas that are lack of infrastructures and facilities. Therefore, hexaplex PCR system might be tested onto these two preserved formats as well.

The lack of consistency in the current standard operating procedures and diagnostic approaches among different laboratories is the major constrain in malaria epidemiology studies. This problem has made it difficult for results from distinct diagnostic approaches to be compared. To reconcile the differences between the management and the diagnosis of malaria, it is important to develop a diagnostic standard or parameter that facilitates inter-laboratories results comparisons. A good example is the development of the first WHO International Standard for *P. falciparum* DNA nucleic acid amplification technique (NAT)-based assay. This assay was calibrated in an international collaborative study involving 14 laboratories from 10 different countries and can be used to consistently access *P. falciparum* detection methods (Padley, et al., 2008). It is hoped that similar standard for other *Plasmodium* species will be developed in the near future to accommodate implementation of consistency for multiplex assays among laboratories.

### 5.2.9 Conclusion

Overall, the present hexaplex PCR system highlighted in the present study provides a set of primers which are sensitive and specific for simultaneous detection of single infection as well as mixed infections. Screening of *Plasmodium* species with this assay has proven to be rapid, beneficial and could significantly improve detection procedures. The availability of this system may indeed facilitate the efforts in the global malaria eradication programs. With a rapid and highly effective diagnostic system such as this, evaluation of malaria morbidity and mortality will be more accurate. In addition, this tool can also be used for future global molecular epidemiological studies to produce consistent and reliable data in malaria distribution, including asymptomatic and subclinical cases.

### **5.3 Identification of binding peptides for human *Plasmodium* species**

#### **5.3.1 Merozoite surface antigens and host cell invasion**

*Plasmodium* is an obligate intracellular parasite and the ability of this parasite to invade and replicate within host cells, i.e., hepatocyte and erythrocyte are thought to play critical role in pathogenesis of the malaria disease. Generally, the host cell invasion is rapid and thought to be a fundamental strategy in immune evasion of these parasites and the sequential mechanism is controlled exclusively by the parasite itself (Tyler, et al., 2011). The invasion of erythrocytes by *Plasmodium* parasites is highly complex and multi-steps involvement is dependent on a cascade of specific molecular interactions and mostly species-specific.

##### **5.3.1.1 AMA1 as invasion property of *Plasmodium* species**

Nowadays, numerous proteins have been implicated in the parasite invasion. AMA1 is the most prominent and best-characterized molecule among malarial surface antigens that is responsible for attachment and entry into host cells, i.e., sporozoite into hepatocyte (Silvie, et al., 2004) and merozoite into erythrocyte (Triglia, et al., 2000).

AMA1 is the first discovered invariant merozoite surface antigen in *P. knowlesi* (previously known as *Pk66*) (Deans, et al., 1982; Deans, Thomas, Alderson, & Cohen, 1984; Thomas, Deans, Mitchell, Alderson, & Cohen, 1984), and subsequently in *P. falciparum* (previously known as *Pf83*) (Peterson, et al., 1989), and then it was identified in all characterized *Plasmodium* species (Waters, et al., 1990). In general, AMA1 primary structure exhibits a conserved architecture throughout *Plasmodium* parasites, which is highly specialized for host cells invasion and maintaining parasite growth. The conservation of all 16 invariant cysteine residues within the ectodomain indicates that there is a structural constraint on the AMA1 molecule and underlying the importance of the disulfide bonds in defining the polypeptide fold (Chesne-Seck, et al.,



2005; Hodder, et al., 1996).

Although precise biological role of AMA1 in host cell invasion remain uncharacterized, much evidence have suggested a receptor-binding functions. The crystal structure indicates that DI and DII of AMA1 ectodomain exhibit the plasminogen-apple-nematode (PAN) folding motifs, which is generally found in an array of adhesive proteins that are involved in the binding to protein or carbohydrate receptors or ligands (Chesne-Seck, et al., 2005; Pizarro, et al., 2005). AMA1 is an essential component of moving junction (MJ), an irreversible multi-protein complex formed by tight interaction between a number of parasite receptors on the merozoite and host cell receptors on the erythrocyte membrane. The most recent study proved that binding of PfAMA1 with parasite rhoptry neck protein complex (RON2, RON4, and RON5) that spans the erythrocyte membrane, tight junction, and merozoites membrane triggers commitment to invasion (Richard, et al., 2010; Tyler, et al., 2011; Vulliez-Le Normand, et al., 2012).

#### **5.3.1.2 AMA1 as a potent antimalarial drug target and pivotal malaria vaccine candidate**

Although AMA1 is a low abundant malarial surface protein; it is thought to be the most prominent malarial surface antigen that has long served as a potent antimalarial drug target and pivotal malaria vaccine candidate (Macrailld, et al., 2011; Remarque, Faber, Kocken, & Thomas, 2008). AMA1 elicits strong immune responses and most individuals exposed to malaria develop anti-AMA1 antibodies after relatively few exposures (Rodrigues, et al., 2005; Wickramarachchi, et al., 2006). There is strong evidence to suggest that anti-AMA1 antibodies are the primary mediators for acquired immunity in human infection, as demonstrated by a decrease in parasite density in children following passive transfer of antibodies from immune adults (Hodder,

Crewther, & Anders, 2001). Moreover, active immunization of animal models, i.e., experimental rodents (Anders, et al., 1998; Crewther, Matthew, Flegg, & Anders, 1996; Deans, et al., 1982) and primates (Collins, et al., 1994; Deans, et al., 1988; Stowers, et al., 2002) with either native or recombinant forms of AMA1 proteins has been shown to induce parasite-inhibitory responses. In addition, passive immunization of anti-AMA1 antibodies can also facilitate protection (Anders, et al., 1998; Crewther, et al., 1996; Kennedy, et al., 2002; Narum, Ogun, Thomas, & Holder, 2000; Stowers, et al., 2002).

The role of AMA1 in invasion can be interfered with by antibodies. Both monoclonal (Deans, et al., 1982; Thomas, et al., 1984) and polyclonal (Hodder, et al., 2001) antibodies bind to AMA1 and block parasite invasion *in vitro* and thus reduce parasites multiplication substantially (Remarque, et al., 2008). Besides that, there is evidence of peptides derived from or with affinity for *Plasmodium* AMA1 can also inhibit invasion of erythrocyte by parasite *in vitro* (Harris, et al., 2005; Keizer, et al., 2003; Li, et al., 2002; Urquiza, et al., 2000).

Although there have been numerous AMA1-based vaccine approaches currently available (focused on *P. falciparum*), however none has yet been fully evaluated in clinical trials (mainly in phase I and few in phase II trials to date) and the efficacy of protective data are only available based on animal models and *in vitro* studies (Anders, et al., 2010; Remarque, et al., 2008; Richards & Beeson, 2009).

### 5.3.2 The significant of heterologous protein expression in *Plasmodium* studies

The critical constrain of molecular and functional studies on *Plasmodium* parasites is the inability to maintain large scale *in vitro* cultivation of parasites (excluded *P. falciparum*) that exhibits complex and multistage life cycle. Since the established continuous *in vitro* cultivation of *P. falciparum* by Trager and Jensen in 1976 (Trager, 1994; Trager & Jensen, 1976), the plasmodial proteome profiling across the life cycle that required high amounts of crude proteins is only focused on this species. Even though there are some progresses made in establishing cultivation methods of *P. vivax* (Golenda, Li, & Rosenberg, 1997) and *P. malariae* (Lingnau, Doeiring-Schwerdtfeger, & Maier, 1994) in the laboratory, the difficulty in long term reproducible and maintaining these pathogens *in vitro* is the major obstacle for further research manipulations. Furthermore, a specific protein of interest can only in rare instances be isolated in sufficient amounts from natural host cell for downstream applications that require highly homologous and pure material. Therefore, heterologous expression of the selected protein is of paramount importance for providing sufficient amounts of recombinant protein for further downstream analysis, such as biochemical, biophysical, and molecular functional studies, as well as in several immunological applications, such as the production of recombinant antigens for the generation of research antibodies and immunogens or subunit vaccine antigens for vaccination. Besides that, recombinant expression also enabled the development of serodiagnostic tools in malaria, e.g., HRP-2 and aldolase antigens in dipstick assays (Birkholtz et al., 2008; Fernandez-Robledo & Vasta, 2010).

---

### 5.3.2.1 Heterologous expression of plasmodial proteins in prokaryotic system

Generally, heterologous protein expression is referred to the production of protein of interest in an organism that is different from the organism source of target protein. Even though heterologous protein production has now become a relatively routine endeavor for most proteins of diverse origins, the functional expression of soluble plasmodial proteins is highly problematic and thus slows down the progress in the discoveries of novel antimalarial drugs and potential vaccine candidates. The performances of heterologous expression systems in production of recombinant proteins from protozoan parasites have been reviewed and compared (Birkholtz, et al., 2008; Fernandez-Robledo & Vasta, 2010).

If compared with other expression systems, the transfection and cultivation of *E. coli* is relatively more simple, rapid with high growth rate and high densities, and often inexpensive in fermentation processes. However, problems can arise when conformation and modification of recombinant proteins are important. This is because *E. coli* is a prokaryote and has different folding and modification patterns than eukaryotes, i.e., *Plasmodium*. Misfolding of recombinant protein can lead to solubility problems and the accumulation of heterologous proteins may also bring to toxicity effect on bacteria host cell and consequently reduce the level of expression.

Malaria antigens are among the most difficult proteins to be expressed with *in vitro* methods, as reflected by the paucity of plasmodial protein structures available in the Protein Data Bank (PDB) (~ 205 till mid of 2013), if compared to over 5,000 cDNA available in whole genomes sequencing data. Besides that, the lack of expression is always observed in heterologous expression efforts and the expression of soluble proteins is also a relatively difficult task in malarial studies. A study that attempted high-throughput expression of functional molecules of *P. falciparum* discovered that only nine soluble proteins (~ 9 %) were produced, out of 95 purified proteins (Aguiar, et

al., 2004). Similar observation also reported that of the expression of 1,000 genes of *P. falciparum*, only 337 (~ 34 %) target proteins were expressed successfully using heterologous system, with only 63 (~ 6 %) targets generating soluble proteins (Mehlin, et al., 2006). Additionally, most of potential antigens are highly polymorphic and expression and correct folding of recombinant proteins can be difficult to achieve (Beeson & Crabb, 2007). Besides that, increasing of molecular weight and isoelectric point (*pI*) of protein also correlated with the expression problems (Mehlin, et al., 2006).

During heterologous protein expression, low expression may attribute to the differences in synonymous codon usage between expression and natural hosts, which can be explained by codon bias. Codon bias is referred to the high frequency preferential use of a particular triplet codes for amino acids (codons, tRNA) within homologous organism. For instance, the genome of *Plasmodium* species have overall high AT content, i.e., 81 % in *P. falciparum* (Gardner, et al., 2002), 58 % in *P. vivax* (Carlton, et al., 2008), and 63 % in *P. knowlesi* (Pain, et al., 2008), whereas *E. coli* has only about 50 % (Baca & Hol, 2000). There is a high level of codon mismatch (difference in amino acid content) between the two organisms, particularly in *P. falciparum* and the codons that are preferentially used by *Plasmodium* in many instance are considered rarely used (definitely a low-usage codon) by *E. coli* for expression, thus it may impose a metabolic burden on the bacterial host during protein translation and consequently resulting in translation stalling and diminish the yields of recombinant protein (Baca & Hol, 2000; Birkholtz, et al., 2008; Chen & Texada, 2006). The codon usage of each organism can be referring to Codon usage database (<http://www.kazusa.or.jp/codon/>).

There are two strategies to overcome the expression problems caused by rare codon. One of the most common strategy is by expanding the intracellular tRNA pool using co-expressed plasmids, which encoded rare tRNAs used in host cell, i.e., *E. coli*

(Baca & Hol, 2000). Nowadays, there are many bacterial cell lines which have the advantage of rare tRNA supplementation; BL21-CodonPlus (Stratagene) used in the present study and Rosetta (Novagen) *E. coli* strains are the two most common examples. Second strategy refers to the codon optimization. Codon optimization is a kind of nucleotide substitution, whereby the rare (low frequency used) codons in the expression host are replaced by synonymous optimal or other major (frequently used) codons (Birkholtz, et al., 2008; Chen & Texada, 2006). Generally, in order to highly express a foreign gene in *E. coli*, either one or both of the two strategies may be adopted (Chen & Texada, 2006). There are several reported enhancements in heterologous expression of recombinant antimalarial candidate vaccine targets in *E. coli* by codon optimization so far (Narum, et al., 2001; Zhou, Schnake, Xiao, & Lal, 2004). However, in certain circumstance, some malaria proteins that have been synthesized with optimized codons could not be expressed in *E. coli* or either expressed as truncated forms or precipitated in IBs in bacterial cells (Aguiar, et al., 2004; Mehlin, et al., 2006).

Direct production of plasmodial proteins in prokaryotic expression system that is thought to be functionally active with the correct structural conformation is the most ideal for this study. However, proteins obtained in this way are frequently found to be insoluble, forming aggregates *in vivo* as IBs, especially during high levels expression of heterologous protein.

Despite protein expression in the form of IBs is often considered undesirable; their formation can be advantageous, as IBs are denser thus facilitating a straightforward purification of the protein of interest from the cell homogenate and cellular contaminants. Other advantages associated with formation of IBs include enable the high expression of recombinant protein, protect the expressed protein from proteolytic degradation, and also homogeneity of the protein of interest in IBs may reduce the purification steps to recover pure protein. Furthermore, formation of IBs also

offers the alternative to produce the protein which, when active can be toxic or lethal to the host cell (Clark, 1998; Singh & Panda, 2005).

### 5.3.3 Expression of recombinant PkAMA1 and PvAMA1 in *E.coli*

#### 5.3.3.1 Construction of PkAMA1 and PvAMA1 protein expression clones

In preparation to identify the potential binding peptides for AMA1 of *P. knowlesi* and *P. vivax* using phage display technology, two constructs for heterologous expression in *E. coli* were developed, designated as pPAL7-PkAMA1 and pPAL7-PvAMA1. The origin of cDNA was from clinical blood samples with confirmed malaria caused by *P. knowlesi* (strain H) and *P. vivax* (strain Sal-1), respectively. The strains of *Plasmodium* were determined based on the 18S ssu rRNA sequence in the first part of the study.

A novel Profinity eXact<sup>TM</sup> Fusion-Tag prokaryotic expression system (Bio-Rad) was applied in the present study in order to perform heterologous expression of recombinant *Plasmodium* AMA1 ectodomain, i.e., rPkAMA1 and rPvAMA1 in *E. coli*. The pPAL7 vector and Profinity eXact<sup>TM</sup> Fusion-Tag system is still new, there is no publication reported thus far since it was first launched in 2008. The unique feature of this system allows a single step affinity purification and fusion-tag cleavage of recombinant protein in less than one hour if compared with other expression system, as example, GST-tag protein purification and Thrombin cleavage in order to remove GST-tag from the target protein requires at least two days protocol.

Profinity eXact fusion-tag system is an affinity tag-based protein purification system that utilizes a modified form of the subtilisin protease, which is immobilized onto a chromatographic support and used to generate pure, tag-free target protein in a single step. The tag in this system is the prodomain of the subtilisin protease, a 75-amino acid sequence corresponding to ~ 8.2 kDa eXact tag domain that is fused to the N-terminus of a target protein of interest. Application of elution buffer triggers subtilisin's processing activity, which quickly and precisely cleaves the tag from the fusion protein and releases the purified target protein in elution fraction. At the end of



the purification process, the tag remains tightly bound to the resin and eluted protein contains only its native amino acid sequence (Appendix 4).

Generally, the cloning steps were followed exactly as manufacturer's recommendations, except the expression host used, i.e., BL21-CodonPlus (DE3)-RIL *E. coli* cells (Stratagene) was used in replacement of BL21(DE3) *E. coli* provided together with the kit. The BL21-CodonPlus (DE3)-RIL *E. coli* was selected in consideration to overcome the codon bias in plasmodial genome, which is AT richness. This *E. coli* host is co-transformed with an additional ColE1-compatible, pACYC-based plasmid carrying extra copies of the rare codon's cognate tRNA, i.e., *argU*, *ileY*, and *leuW* tRNA genes, suited for heterologous expression of recombinant protein consisted of AT-rich genome, as well as an additional chloramphenicol resistance (*Cam<sup>r</sup>*) gene to maintain the selection of pACYC plasmid.

Overall, DNA sequencing results indicated that whole ectodomain cDNA of PkAMA1 and PvAMA1 fragments with length of 1,338 bp were successfully cloned in-frame into pPAL7 expression vector. ExPASy Proteomics tools (<http://ca.expasy.org/tools/>) is an amalgamation of the most popular Web-based tools for *in silico* characterization of proteins based on their primary amino acids composition. The inserted cDNA was translated to protein sequence using ExPASy Translate tool (<http://web.expasy.org/translate/>). Both of the AMA1 of *P. knowlesi* and *P. vivax* cDNA encoded 446 amino acid residues, with DI extends from residues 42 to 248, DII from 249 to 385, followed by DIII from 386 to 487, and the residues are numbered from the first residue of the signal sequence (Figure 4.11 and Figure 4.12). BLASTP search indicated that rPkAMA1 was concordance with *P. knowlesi* H strain AMA1 protein (PKH\_093110) (GeneBank accession no: XP\_002259339; Appendix 5.3), and rPvAMA1 with *P. vivax* AMA1 strain Sal-1 (GeneBank accession no: ACY68841; Appendix 5.4).

LC-MS/MS data of rPkAMA1 hit the protein named merozoite receptor PK66 with UniProtKB/Swiss-Prot database accession number P21303, whereas rPvAMA1 hit two crystal structures of AMA1 from *P. vivax* with NCBI accession number 62738184 (PDB ID: 1W81\_A) and 62738193 (PDB ID: 1W8K\_A). The ExPASy Compute pI/MW tool ([http://web.expasy.org/compute\\_pi/](http://web.expasy.org/compute_pi/)) predicted that the theoretical isoelectric point (*pI*) of the rPkAMA1 and rPvAMA1 were 5.85 and 6.28, respectively, whereas the estimated molecular weight were ~ 51 kDa as concordance to both of present expressed rPkAMA1 and rPvAMA1.

### 5.3.3.2 Induction of protein expression

Soluble protein is thought to be native in structure and function, while insoluble aggregated protein reflects of improper fold and lack of functionality. To date, many studies attempt to optimize the culture conditions that favor for soluble expression. It has been suggested that factors such as culture pH, temperature, and protein amino acid composition might affect the solubility of a recombinant protein. It is well known that a reduced growth rate or rather rate of expression by lowering the growth temperature to between 20 °C and 30 °C with best aeration (250 rpm) usually leading to more soluble expression and hence reduced the tendency to form IBs. However, the drawback is that the overall yield of recombinant protein is also likely to decrease at lower temperature.

For protein that expressed under the control of an inducible promoter, the rate of expression can also be reduced by altering the induction conditions, such as induce for a shorter time, induce using a lower concentration of inducing agent (IPTG), and induce at lower cell densities ( $OD_{600} = 0.5$ ). However, a previous study attempted to optimize the various factors that influencing the expression, revealed that initiation of expression at post-log growth phase (with  $OD_{600}$  of ~ 2.0) instead of mid-log growth phase (with  $OD_{600}$  of ~ 0.5) significantly enhance the yield of soluble protein of high quality (Flick,

Ahuja, Chene, Bejarano, & Chen, 2004).

By referring to the above parameters, the present study tried to optimize the expression conditions performed in a small scale expression (15 ml), including the media used (typical 2× YT medium, MagicMedia<sup>TM</sup> from Invitrogen, and Overnight Express<sup>TM</sup> Instant LB media from Novagen) and induction conditions, such as temperature (16 °C, 25 °C, and 37 °C) and time point of inductions (OD<sub>600</sub> of 0.6, 1.0, 1.5, 2.0), as well as concentrations of inducer (0.1, 0.5, 1.0 mM of IPTG). However, there were no difference in terms of soluble protein expression; therefore the present study adopted the protocol to isolate and purified the rPkAMA1 and rPvAMA1 under denature conditions. Furthermore, the Recombinant Protein Solubility Prediction tool also estimation that 71.3 % of rPkAMA1 and 72.5 % of rPvAMA1 has a high propensity to form insoluble aggregate during overexpression in prokaryotic expression system based on their amino acid compositions data.

The eukaryotic proteins intracellularly expressed in *E. coli* system are frequently sequestered into insoluble IBs. The intramolecular associated to the hydrophobic domains during folding is believed to play a role in the formation of IBs. Furthermore, for protein with high cysteine residues like AMA1, improper formation of disulfide bonds in the reducing environment of *E. coli* cytoplasm may also contribute to incorrect folding and formation of IBs.

In the present study, cultures of pPAL7-PkAMA1 and pPAL7-PvAMA1 constructs were grown to OD<sub>600</sub> of ~ 0.6 at 37 °C and the protein expression was induced with 0.5 mM IPTG and incubated at 25 °C with vigorous shaking at 250 rpm for subsequent three hours. Overall, two recombinant proteins were successfully expressed in *E. coli* in a form of insoluble IB with high yield.

### 5.3.3.3 Protein isolation and inclusion body purification

Proteins expressed in recombinant manner may be soluble in the cytoplasm or insoluble as IBs, which may affect the subsequent protein extraction method to obtain the starting material for purification. Reducing SDS-PAGE (Figure 4.13) and Western blot (Figure 4.14) assays showed that both of the pPAL7-PkAMA1 and pPAL7-PvAMA1 were deposited in insoluble fraction with molecular weight appearance of ~ 60 kDa. This made it necessary to add an additional IB purification step after cell disruption prior to affinity purification. Western blot assays on both Profinity eXact tagged rPkAMA1 and rPvAMA1 also revealed that none of the soluble and truncated forms of protein were being observed.

Inclusion bodies are dense amorphous aggregates of misfolded protein contained within the insoluble fraction yielded from cell lysis and this make it easy to isolate from other cellular components in a fairly pure state by differential centrifugation. Generally, IBs often contain exclusively (40 % to 90 %) the overexpressed protein and successful in renaturation much depends on the purity of IBs (Cabrita & Bottomley, 2004).

To date, many protocols have been established to overcome the problems due to IB formation. Generally, three main steps are required to recover the functional active protein from IB: first step is the isolation and purification of IB from *E. coli* cells; second step is the solubilization of aggregated protein or purified IB, which causes denaturation; and finally the refolding of the solubilized protein.

Major contaminants of IB material after preparation are the outer membrane proteins, which are co-purified mainly as non-solubilized protein with IB fraction. The purity of IBs can be achieved by repeating the washing and centrifugation steps using different buffer cocktails containing low concentrations of denaturant such as urea and detergents such as Triton X-100 (Clark, 1998).

#### 5.3.3.4 Affinity protein purification and fusion-tag removal

Generally, handling of soluble recombinant protein is more straightforward and probably referred as purification under native conditions, whereas a more sophisticated protocol is required when handling IB as the IB must be purified and then solubilized using high concentration of denaturant such as 4-8 M urea or 4-6 M guanidine hydrochloride prior to affinity tag purification.

In the present study, the dissolved pPAL7-PkAMA1 and pPAL7-PvAMA1 were affinity purified under denatured and reduced conditions, which means all buffers used must keep the protein in the denatured reduced stage during the procedure. In general, this affinity purification and fusion-tag removal protocol utilized was modified from manufacturer's protocol based only on native conditions.

Solubilized IB proteins in general can be contaminated with varying levels of microbial contaminants, e.g., host proteins, nucleic acids, and cell membrane components, sometimes may induce aggregation during refolding. Thus the targeted recombinant proteins, i.e., rPkAMA1 and rPvAMA1 were isolated, purified, and in the meantime, fusion-tag was removed with a single affinity tag purification procedure prior to refolding, using 1 ml or 5 ml of Bio-Scale Mini<sup>TM</sup> Profinity eXact cartridge pre-packed with 1 or 5 column volume settled resin (Bio-Rad), respectively.

In the present study, two tag-free recombinant proteins were successfully isolated from purified and solubilized IB under denatured conditions. The removal of Profinity eXact tag with molecular mass of ~ 8.2 kDa generated two tag-free proteins, i.e., rPkAMA1 and rPvAMA1 of high purity and integrity with the molecular weight of ~ 51 kDa visualized in reduced SDS-PAGE (Figure 4.18 and Figure 4.19, respectively).

Established purification protocol under denatured conditions enhances the utilities of this protein expression system that allows rapid single affinity purification and tag-removal.

---

### 5.3.3.5 Renaturation of the rPkAMA1 and rPvAMA1

In general, extracellular domains of malaria antigens, such as AMA1 almost invariably contain disulfide linkages, thus production of this kind of proteins in the native conformation remains particularly difficult (Flick, et al., 2004). Disulfide bonds are derived by the coupling of two thiol groups (two cysteine residues) to form a covalent sulphur-sulphur (S-S) bond, which can be intra- or inter-molecular bridges. Native AMA1 ectodomain is high-cysteines protein, consists of 16 cysteine residues that are responsible for eight pairs of invariant intramolecular disulfide bonds, and this undoubtedly increase the difficulty in protein renaturation process. Previous work with *Plasmodium* AMA1 expression in *E. coli* showed that it was necessary to include an *in vitro* refolding step in the process in order to obtain correctly folded protein (Anders, et al., 1998; Dutta, et al., 2002; Gupta, et al., 2005; Hodder, et al., 2001; Lalitha, et al., 2004; Mufalo, et al., 2008). The renaturation process aims to remove the denaturant and allow the protein to fold (Cabrita & Bottomley, 2004). Dialysis, dilution, as well as chromatography refolding are the three most common strategies for protein renaturation.

Protein refolding is a common procedure to recover the target protein in a native condition, thus regaining full biological activity and functionality of denatured and unfolded proteins. The efficiency of refolding depends on the competition between correct folding and aggregation. The correct folding of AMA1 has been shown to be critical for its immunological activity, only the antibodies raised against refolded AMA1 inhibited parasite growth *in vitro*. In contrast, the reduced and alkylated AMA1 failed to induce protective immunity. Furthermore, this irreversible reduced AMA1 was not recognized by antibodies raised against the native antigen, and thus suggest that an effective immune response is much dependant on conformational epitopes maintained by a set of eight intramolecular disulfide bonds dispersed within an ectodomain (Anders, et al., 1998; Casey et al., 2004; Coley et al., 2001; Crewther, et al., 1996; Harris, et al.,

2005; Hodder, et al., 2001; Lalitha et al., 2004; Li, et al., 2002; Pizarro, et al., 2005).

Actually, there is no standard protocol for protein refolding, optimization of refolding conditions (e.g., buffer composition, temperature, redox agent, chemical additives etc.) is a cumbersome task and the precise conditions that give efficient refolding are different for each protein. In general, a more elaborate refolding procedure is needed in renaturation of the proteins that have multiple disulfide bonds, and usually a pair of oxidizing and reducing agents in the optimal concentrations are essential for the formation of disulfide bonds. For instance, a combination of reduced glutathione (GSH) and oxidized glutathione (GSSG) with molar ratio of 4:1 is commonly used as redox agents. The concentration of protein is also a critical factor, as high concentration (> 1 mg/ml) is prone to aggregation. Most refolding is done in the range of pH 5-9, with optimum level at about pH 8-8.5. Furthermore, addition of additives, mainly low molecular weight compounds, such as arginine, acetone, DMSO, PEG, etc. during refolding process often help in improving the yield of bioreactive proteins from IBs. These additives influence both the solubility and stability of the unfold protein, folding intermediate (molten globule), and the fully folded protein (Burgess, 2009; Cabrita & Bottomley, 2004; Singh & Panda, 2005). In the present study, the addition of 0.4 M L-arginine in dialysis buffer seems to diminish protein aggregation and thus improves the refolding yield of solubilized protein.

The refolding conditions utilized in present study was modified from the refolding parameters established by previous expression studies on recombinant *Plasmodium* AMA1 using prokaryotic system (Anders, et al., 1998; Dutta, et al., 2002; Gupta, et al., 2005; Hodder, et al., 2001; Lalitha, et al., 2004; Mufalo, et al., 2008). The present refolding protocol was performed by dialysis method, whereby the concentrated denatured proteins (1 mg/ml), i.e., rPkAMA1 and rPvAMA1 in 4 M urea were dialyzed against two changes of refolding buffer (at two progressive lower denaturant

concentrations, i.e., 2 M and 1 M urea). Such that, the concentration of denaturant decreases with buffer exchange under step-wise manner, followed by last changing to sample buffer with the absence of urea which is compatible for biopanning.

To date, there are many successful expression and refolding of *Plasmodium* AMA1 ectodomain which have been published elsewhere, of which most were recorded in *Plasmodium chabaudi*, a rodent parasite (Remarque, et al., 2008), PfAMA1 (Bai, et al., 2005; Dutta, et al., 2002; Feng, et al., 2005; Gupta, et al., 2005; Hodder, et al., 2001; Lalitha, et al., 2004; Nair, et al., 2002), and a few in PvAMA1 (Mufalo, et al., 2008; Pizarro, et al., 2005). The REFOLD database (<http://refold.med.monash.edu.au/>) is a good platform that summarizes all established refolding protocols, including AMA1 protein (Appendix 7) (Buckle, et al., 2005; Chow, et al., 2006).

In general, determination of correctly folded protein is commonly performed by evaluating the enzymatic activity. However, for those proteins that lack of enzymatic activity such as AMA1, the simple way to monitor the refolding condition is by direct visual inspection of the turbidity of solutions, where protein aggregation has occurred. The formation of insoluble aggregates is an indication of non-optimize in refolding protocol. The turbidity of the sample solution also can be assessed more accurately by measuring the optical density (OD) at 390 nm of the refolded protein solution (Tresaugues, et al., 2004; Vincentelli, et al., 2004). Generally, the solution is not absorbing the light, but rather the protein aggregates scatter light and thus decrease the amount of transmitted light measured. In other words, OD remains unchanged if the protein remains soluble, in contrast, the OD increases proportionally to the amount of precipitated produced.

After refolding, there is a total replacement of IB solubilization buffer that contains highly concentrated denaturant to the sample buffer that is free of denaturant. There were no insoluble aggregates being observed in both of the rPkAMA1 and



rPvAMA1 protein solutions after refolding. Furthermore, the protein OD<sub>390</sub> in the turbidity test was less than 0.05 in both of rPkAMA1 and rPvAMA1 protein solutions, thus suggesting that both of the refolded AMA1 proteins were considered to be soluble. The reduced and non-reduced SDS-PAGE results also supported that both of the rPkAMA1 and rPvAMA1 were refolded.

### 5.3.4 Phage display technology and applications in *Plasmodium* AMA1

Although AMA1 is long thought to be a target of natural immune response that can inhibit invasion, little is known about the molecular mechanisms by which immunologically relevant portions of AMA1 could facilitate the invasion process, therefore, characterization and identification of peptide ligands as well as ligand- or receptor-binding sites that specifically interact with, and block the function of AMA1 is essentially important.

To date, protective responses against the *Plasmodium* AMA1 have been investigated using various phage display libraries. For instance, four antibodies specific for *Plasmodium* AMA1 have been identified by mouse single chain variable fragment (scFv) antibodies library (derived by *P. chabaudi* immunized mouse) and were used for passive immunization against *P. falciparum* AMA1 (Fu, et al., 1997).

Most likely antigenic peptides were obtained from epitope mapping, in which direct antibody ELISA is used to affinity select antigenic peptides from very large libraries of peptides displayed on filamentous phage carries. If natural peptide library is used in selection, antigenic peptide is called epitope, while mimotope is selected from the random peptide library. Epitope mapping using PfAMA1 peptide library (Coley, et al., 2001; Coley, et al., 2006) as well as mimotopes mapping using random peptide library (Casey, et al., 2004; Sabo, et al., 2007) against monoclonal anti-AMA1 antibodies (e.g., MAb5G8, MAb4G2dc1, and MAb1F9) that blocks merozoite invasion by *P. falciparum* have facilitated greater understanding of immune responses against AMA1.

In addition to polyclonal and monoclonal antibodies that bind to AMA1 and block parasite invasion *in vitro*, several peptides that specifically bind to PfAMA1 and showed similar functionality to native anti-AMA1 have been isolated from random peptides libraries (Harris, et al., 2005; Keizer, et al., 2003; Li, et al., 2002). All of these

binding peptides and their analogues were synthesized and further validated with antibody competition ELISA assay as well as growth inhibition assay and immunofluorescence assay based on parasite cell culture (Harris, et al., 2009; Keizer, et al., 2003).

In some circumstances, peptides with high affinity to the target antigen can also be used in a drug-discovery process, although these peptides themselves do not generally make good drugs, they can provide a backbone for the peptidomimetic design of efficient drugs (Barbas, et al., 2001). As example, the structure of a phage displayed 15-residue peptide, F1 against PfAMA1 (Li, et al., 2002) provided a valuable starting point for the development of peptidomimetic as antimalarial antagonists directed at AMA1 (Keizer, et al., 2003). Most recently, one of the most prominent peptide inhibitor, a 20-residue peptide designated as R1 appears to target a site critical for PfAMA1 function and subsequently blocks the parasite invasion has been modified to be a potent leading compound for antimalarial drug development (Harris, et al., 2005; Harris, et al., 2009).

Nowadays, applications of both phage display technique together with the three dimensional structuring and/or protein docking techniques have speed up the studies on molecular binding interactions. For instance, the AMA1-binding molecules, i.e., monoclonal antibodies (both the epitopes and mimotopes) and peptides selected from phage display libraries, all of which block merozoite invasion of erythrocytes were successfully characterized and have been mapped to the location on AMA1 ectoplasmic region by nuclear magnetic resonance spectroscopy (Harris, et al., 2009; Keizer, et al., 2003; Sabo, et al., 2007) and X-ray crystallographic analysis (Bai, et al., 2005; Pizarro, et al., 2005).

Overall, all the studies described above focused on PfAMA1. This is the first study carried out on AMA1 protein of two other clinical significant *Plasmodium* species,

i.e., *P. vivax* and *P. knowlesi*.

### 5.3.5 Identification of peptides affinity for PkAMA1 and PvAMA1

Understanding of the parasites entry into their host cells is of great interest and this offers an attractive target for the development of novel therapeutics. From the successful and promising results obtained from the previous studies on the identification of binding peptides for PfAMA1 as mention above, the objective of the current study was to identify novel and potential binding peptides that have high binding affinity to PkAMA1 as well as PvAMA1. Differing from the previous studies, a ready-made library of random 12-residue peptides expressed as N-terminal fusion to protein III of filamentous phages M13 was used for identification of binding peptides for refolded rPkAMA1 and rPvAMA1 proteins.

In the present study, two set of peptides variants that have binding affinity to refolded rPkAMA1 (four dodecapeptide) and rPvAMA1 (three dodecapeptide) were identified through the Ph.D.-12 random peptide library (NEB) screening in separate biopanning experiments.

The biopanning process often generates peptides with conserved consensus sequences, which can then be chemically synthesized on the basic of consensus sequences and are evaluated by bioassay and structural analysis (Uchiyama, Tanaka, Minari, & Tokui, 2005). The selected peptides (synthetic forms) can be used to antagonize the interactions between two particular proteins, which may have an effect on the biological activities of the target protein. Alternatively, these peptides may also have an effect on of the activity of enzyme, either through active site inhibition or long-range interactions (Kay, Kasanov, & Yamabhai, 2001).

In the present study, the consensus sequences/motifs of binding peptides selected from biopanning against rPkAMA1 and rPvAMA1 respectively were

investigated using ClustalW (Thompson, Higgins, & Gibson, 1994). However, as shown in Figure 4.23A and Figure 5.2, there is no single consensus motif that could be seen in all the peptides identified from biopanning on rPkAMA1. If compared to PdK1 and PdK2 (positive binding sequences), only a single identical amino acid (Gly, G) was noticed with none of consensus motif being observed. If compared between two peptides, i.e., PdK2 versus PdK3 and PdK3 versus PdK4 respectively, consensus motifs with four and three conserved amino acids were observed. Two peptides, PdK3 and PdK4 selected from biopanning on rPkAMA1 showed weak binding signal with only  $2.1\times$  of binding activity when tested individually with phage ELISA binding assay although they shared a consensus motif.

When a consensus motif comparison was done on peptides identified from biopanning on rPvAMA1 (Figure 4.23B and Figure 5.2), there was a single amino acid, Asn (N) occurring among three positive binding peptides, i.e., PdV1, PdV2, and PdV3. Additional single amino acid, Pro (P) followed after Asn (N) amino acid was also found between PdV1 and PdV2. When compared between PdV2 and PdV3, there were three consensus amino acids, i.e., Ser (S), Asn (N), and Leu (L) noticed.

Overall, there were a lack of consensus sequence motif found among the two set of binding peptides selected from biopanning against rPkAMA1 (PdK1, PdK2, PdK3, and PdK4) and rPvAMA1 (PdV1, PdV2, and PdV3). The present observations were similar to two previous done biopanning against PfAMA1 that also aimed to identify the binding peptides (Harris, et al., 2005; Li, et al., 2002) (Table 5.1 and Figure 5.2). A follow up of these studies indicated that these binding peptides were mapped to different domains of PfAMA1 with different binding activities using NMR spectroscopy (Harris, et al., 2009; Keizer, et al., 2003) and it was reasonable to explain the lack of consensus sequence motif in such kind of study.

Table 5.1: Binding peptides for rPkAMA1 and rPvAMA1 in the present study and rPfAMA1 in the previous studies.

Target protein	Designation	Sequence of binding peptide	References
rPfAMA1	F1	GWRLLGFGPASSFSM	Li, et al., 2002
	F2	TRLFRVPVLPSGVTS	
	F3	PFARAPVEHHDVVGL	
rPfAMA1	R1	VFAEFLPLFSKFGSRMHILK	Harris, et al., 2005
	R3	PVLRSGRCAELIQIGFRCRA	
rPkAMA1	PdK1	GGSIAASELEY	Present study
	PdK2	WHWGLLYPASAN	
	PdK3	WHWSWWNPQNLT	
	PdK4	HSQAMP SMLHQA	
rPvAMA1	PdV1	DLTFTVNPLSKA	Present study
	PdV2	WHWSWWNPQNLT	
	PdV3	TSVSYINNRHNL	

<p><b>rPfAMA1 (15-mer peptide library)</b></p> <p><b>F1</b>      -GWRLLGFGPASSFSM *</p> <p><b>F2</b>      TRLFRVPVLPSGVTS-</p> <p><b>F3</b>      -PFARAPVEHHDVVGL</p>	Li, et al., 2002
<p><b>rPfAMA1 (20-mer peptide library)</b></p> <p><b>R1</b>      -VF-AEFLPLFSKFGSRMHILK *</p> <p><b>R3</b>      PVLRSGRCAELIQIGFRCRA-</p>	Harris, et al., 2005
<p><b>rPkAMA1 (12-mer peptide library)</b></p> <p><b>PdK1</b>    --GGSIAASELEY      (n=6)</p> <p><b>PdK2</b>    WHWGLLYPASAN--      (n=10)</p> <p><b>PdK3</b>    WHWSWWNPQNLT--      (n=1)</p> <p><b>PdK4</b>    -H-SQAMP SMLHQA      (n=3)</p> <p><b>rPvAMA1 (12-mer peptide library)</b></p> <p><b>PdV1</b>    -DLTFTVNPLSKA      (n=8)</p> <p><b>PdV2</b>    WHWSW-WNPQNLT      (n=7)</p> <p><b>PdV3</b>    TSVSYINNRHNL-      (n=1)</p>	Present study
<p>* Binding peptides F1 and R1 derived from phage display against PfAMA1, which exhibited strong invasion-inhibition effect, were modified as leading component for antimalarial drug development (Session 5.3.4).</p>	

Figure 5.2: Consensus motif aligned using ClustalW.

The binding affinity of each phage peptide variants to the target proteins, i.e., rPkAMA1 and rPvAMA1 was further determined using phage ELISA as well as Western blot binding assays. Only two out of four peptides, i.e., PdK1 (GGSIAASELEY) and PdK2 (WHWGLLYPASAN) selected from biopanning against rPkAMA1 showed strong signal in phage ELISA peptide binding assay, with 8.3-fold and 22.6-fold respectively and the rest of two peptides, PdK3 (WHWSWWNPQNLT) and PdK4 (HSQAMPMSMLHQA) showed 2.1-fold of binding signal. In the Western blot binding assay, similar results were obtained where PdK1 and PdK2 showed the strong binding signal to rPkAMA1, whereas no positive signal were being observed in PdK3 and PdK4. This might be due to weak interaction (below threshold of Western blot assay) between these two peptides to rPkAMA1, as reflected in the ELISA binding assay, which only showed 2.1 $\times$  binding signal, respectively.

Whereas three peptides, i.e., PdV1 (DLTFTVNPLSLA), PdV2 (WHWSWWNPQNLT), and PdV3 (TSVSYINNRHNL), identified from biopanning against rPvAMA1 showed 12.1-fold, 3.5-fold, and 3.1-fold respectively binding signal in phage ELISA binding assay. Even though, the peptide PdV2 showed the highest binding signal among three peptides, however the background binding was also quite high and thus lowered the fold of binding signal. In Western blot assay, sharp and clear binding signal was observed in PdV1, while weak binding signal observed in peptides PdV2 and PdV3.

Interestingly, a single identical peptide (WHWSWWNPQNLT) was selected from biopanning of rPkAMA1 as well as rPvAMA1 that performed in two separated experiments and time. When further tested on the binding affinity of individual peptides to two respective target proteins, positive binding signal only appeared toward rPvAMA1 in both peptide binding assays but weak binding signal and non-detectable toward rPkAMA1 in phage ELISA and Western blot binding assays, respectively.

Based on the preliminary data obtained from the present study, it was hard to make a complete conclusion on these individual peptides with affinity to rPkAMA1 and rPvAMA1. In depth investigation and characterization of the individual peptides in terms of molecular interactions and functionality, further antibody competitive binding assay and growth inhibition assay are proposed for future studies.

### 5.3.6 Future perspectives

Generally, the anti-AMA1 antibodies are essential material for immunological assays such as antibody competitive binding assay (competition ELISA), *in vitro* parasite growth inhibition assay, and immunofluorescence assay. As showed by previous studies on *P. falciparum*, antibodies raised against recombinant PfAMA1 ectoplasmic region were strain- and/or species-specific, there is lack of cross-reactive antibody currently available in targeting all five human *Plasmodium* parasites (Igonet, et al., 2007). Therefore, to enable further molecular characterization of these peptides derived from biopanning on rPkAMA1 and rPvAMA1, future study will need to produce antibodies raised against PkAMA1 and PvAMA1 ectoplasmic regions by immunizations of mice with the present expressed refolded and recombinant PkAMA1 and PvAMA1 proteins. Furthermore, in previous study, successful refolding of PfAMA1 can also be validated using anti-AMA1 antibodies, as the observation that monoclonal antibody raised against native PfAMA1 only reacted with the correctly folded recombinant PfAMA1 (Kocken, et al., 1998). Besides that, availability of anti-AMA1 antibodies of *P. knowlesi* and *P. vivax* may also allow the present study to proceed to epitopes/mimotopes mapping of their desired target proteins.

The interacting point (ligand), where the protein partners bind to rPkAMA1 and rPvAMA1 can be studied using combination of X-ray crystallography, NMR spectroscopy, and protein docking techniques.



Peptides with high binding affinity to rPkAMA1 and rPvAMA1 have potential bioactivity such as inhibiting merozoite invasion will aid in the discovery of new peptide-based drugs or subunit vaccines as what be done in anti-PfAMA1 (Harris, et al., 2009; Keizer, et al., 2003). Besides that, peptides with strong binding affinity to the target protein may also be modified and used as a protein binder or drug delivery compound. In addition, peptides that specifically recognize and reactive to PkAMA1 and PvAMA1 may also act as protein probes in the development of serodiagnostic assay for the detection of malaria parasites other than *P. falciparum*.

### 5.3.7 Conclusion

Malaria parasites have a complex life cycle during they infect humans. Basically, the successful completion of the parasite life cycle requires specific molecular interactions between the parasite and various host and vector tissues. A good understanding of the structure and function of *Plasmodium* proteins, particular those involved in host-cell adhesion and invasion will greatly facilitate the strategies in malaria controls and eradication. Thus far, there is a lot of work on the key surface antigens of merozoites, mainly focused on the most deadly *P. falciparum*, all of which is justified by the need to prevent and treat this fatalistic disease, but we must also be aware that *P. falciparum* is only one of the five human malaria species and thus, the eradication of all five species should be a priority. Among the malaria surface antigens, AMA1 is long thought to be the pivotal *Plasmodium* antigen that is responsible for parasite-host cell invasions. Investigation of molecular interactions that mediate invasion of hepatocytes by sporozoites and erythrocytes by merozoites may allow the development of strategies to target these key interactions and disrupt the parasite life cycle, thereby reducing parasites densities and provide protection against clinical disease.

Overall, the present study aimed to identify peptides that have binding affinity towards refolded recombinant *Plasmodium* AMA1 ectodomain proteins from *P. knowlesi* (rPkAMA1) and *P. vivax* (rPvAMA1) using a 12-mer peptide displaying phage library. Peptide phage display is a powerful method of mapping for protein-protein interactions based on a simple principle that a library of phage particles displaying peptides is used and the phage clones that bind to the rPkAMA1 as well as rPvAMA1 were selected, identified, and used for further research. Phage display is relatively fast and simple technique in mapping of protein-protein interactions if compare with other sophisticated laboratory technologies such as X-ray crystallography and NMR

spectroscopy. With the modest amount of time (two to three weeks), material (typically 100-500 µg), resources, and cost, peptides ligands have been isolated from a wide array of targets from phage display combinatorial peptide libraries.

Currently two dodecapeptides were selected from biopanning against rPkAMA1 and three dodecapeptides were selected from biopanning against rPvAMA1, all of which exhibited positive binding signal to target proteins in both direct phage assays. Further validations and characterizations of the individual phage peptides with antibody competitive binding assay and *in vitro* parasite growth inhibition assay can be carried out in future.

## REFERENCES

- Aguiar, J. C., LaBaer, J., Blair, P. L., Shamilova, V. Y., Koundinya, M., Russell, J. A., et al. (2004). High-throughput generation of *P. falciparum* functional molecules by recombinational cloning. *Genome Res*, 14(10B), 2076-2082.
- Alonso, P. L., Brown, G., Arevalo-Herrera, M., Binka, F., Chitnis, C., Collins, F., et al. (2011). A research agenda to underpin malaria eradication. *PLoS Med*, 8(1), e1000406.
- Altschul, S. F., Gish, W., Miller, W., Myers, E. W., & Lipman, D. J. (1990). Basic local alignment search tool. *J Mol Biol*, 215(3), 403-410.
- Anders, R. F., Adda, C. G., Foley, M., & Norton, R. S. (2010). Recombinant protein vaccines against the asexual blood stages of *Plasmodium falciparum*. *Hum Vaccin*, 6(1), 39-53.
- Anders, R. F., Crewther, P. E., Edwards, S., Margetts, M., Matthew, M. L., Pollock, B., et al. (1998). Immunisation with recombinant AMA-1 protects mice against infection with *Plasmodium chabaudi*. *Vaccine*, 16(2-3), 240-247.
- Antinori, S., Galimberti, L., Milazzo, L., & Corbellino, M. (2012). Biology of human malaria plasmodia including *Plasmodium knowlesi*. *Mediterr J Hematol Infect Dis*, 4(1), e2012013.
- Antinori, S., Galimberti, L., Milazzo, L., & Corbellino, M. (2013). *Plasmodium knowlesi*: the emerging zoonotic malaria parasite. *Acta Trop*, 125(2), 191-201.
- Arguin, P. M., & Mali, S. (2012) *Chapter 3: Infectious disease related to travel*. Atlanta, GA: Centers for Disease Control and Prevention. Retrieved 9 July 2013, from <http://wwwnc.cdc.gov/travel/yellowbook/2012/chapter-3-infectious-diseases-related-to-travel/malaria>.
- Baca, A. M., & Hol, W. G. (2000). Overcoming codon bias: a method for high-level overexpression of *Plasmodium* and other AT-rich parasite genes in *Escherichia coli*. *Int J Parasitol*, 30(2), 113-118.
- Bai, T., Becker, M., Gupta, A., Strike, P., Murphy, V. J., Anders, R. F., et al. (2005). Structure of AMA1 from *Plasmodium falciparum* reveals a clustering of polymorphisms that surround a conserved hydrophobic pocket. *Proc Natl Acad Sci U S A*, 102(36), 12736-12741.
- Barbas, C. F., Burton, D. R., Scott, J. K., Silverman, G. J. (2001). *Phage display: a laboratory manual*. Cold Spring Harbor, New York: Cold Spring Harbor Laboratory Press.
- Barber, B. E., William, T., Jikal, M., Jilip, J., Dhararaj, P., Menon, J., et al. (2011). *Plasmodium knowlesi* malaria in children. *Emerg Infect Dis*, 17(5), 814-820.
- Beeson, J. G., & Crabb, B. S. (2007). Towards a vaccine against *Plasmodium vivax* malaria. *PLoS Med*, 4(12), e350.

- Bentley, G. A. (2006). Functional and immunological insights from the three-dimensional structures of *Plasmodium* surface proteins. *Curr Opin Microbiol*, 9(4), 395-400.
- Berry, A., Iriart, X., Wilhelm, N., Valentin, A., Cassaing, S., Witkowski, B., et al. (2011). Imported *Plasmodium knowlesi* malaria in a French tourist returning from Thailand. *Am J Trop Med Hyg*, 84(4), 535-538.
- Birkholtz, L. M., Blatch, G., Coetzer, T. L., Hoppe, H. C., Human, E., Morris, E. J., et al. (2008). Heterologous expression of plasmodial proteins for structural studies and functional annotation. *Malar J*, 7, 197.
- Boyle, M. J., Wilson, D. W., Richards, J. S., Riglar, D. T., Tetteh, K. K., Conway, D. J., et al. (2010). Isolation of viable *Plasmodium falciparum* merozoites to define erythrocyte invasion events and advance vaccine and drug development. *Proc Natl Acad Sci U S A*, 107(32), 14378-14383.
- Bronner, U., Divis, P. C., Farnert, A., & Singh, B. (2009). Swedish traveller with *Plasmodium knowlesi* malaria after visiting Malaysian Borneo. *Malar J*, 8, 15.
- Buckle, A. M., Devlin, G. L., Jodun, R. A., Fulton, K. F., Faux, N., Whisstock, J. C., et al. (2005). The matrix refolded. *Nat Methods*, 2(1), 3.
- Burgess, R. R. (2009). Refolding solubilized inclusion body proteins. *Methods Enzymol*, 463, 259-282.
- Burns, J. M., Jr., Flaherty, P. R., Romero, M. M., & Weidanz, W. P. (2003). Immunization against *Plasmodium chabaudi* malaria using combined formulations of apical membrane antigen-1 and merozoite surface protein-1. *Vaccine*, 21(17-18), 1843-1852.
- Cabrita, L. D., & Bottomley, S. P. (2004). Protein expression and refolding-a practical guide to getting the most out of inclusion bodies. *Biotechnol Annu Rev*, 10, 31-50.
- Carlton, J. M., Adams, J. H., Silva, J. C., Bidwell, S. L., Lorenzi, H., Caler, E., et al. (2008). Comparative genomics of the neglected human malaria parasite *Plasmodium vivax*. *Nature*, 455(7214), 757-763.
- Casey, J. L., Coley, A. M., Anders, R. F., Murphy, V. J., Humberstone, K. S., Thomas, A. W., et al. (2004). Antibodies to malaria peptide mimics inhibit *Plasmodium falciparum* invasion of erythrocytes. *Infect Immun*, 72(2), 1126-1134.
- Centers for Disease Control and Prevention. (2009). *Diagnostic findings malaria: Comparison of Plasmodium species which cause malaria in humans*. Atlanta, GA: Centers for Disease Control and Prevention (Last modified: 20 July 2009). Retrieved 9 July 2013, from [http://www.dpd.cdc.gov/dpdx/HTML/Frames/M-R/Malaria/body\\_Malariadiagfind2.htm](http://www.dpd.cdc.gov/dpdx/HTML/Frames/M-R/Malaria/body_Malariadiagfind2.htm)
- Centers for Disease Control and Prevention. (2012). *Malaria: Anopheles mosquitoes*. Atlanta, GA: Centers for Disease Control and Prevention (Last reviewed: 9 November 2012). Retrieved 9 July 2013, from <http://www.cdc.gov/malaria/about/biology/mosquitoes/index.html>

- 
- Chappel, J. A., Rogers, W. O., Hoffman, S. L., & Kang, A. S. (2004). Molecular dissection of the human antibody response to the structural repeat epitope of *Plasmodium falciparum* sporozoite from a protected donor. *Malar J*, 3, 28.
- Chauhan, V., Negi, R. C., Verma, B., & Thakur, S. (2009). Transfusion transmitted malaria in a non-endemic area. *J Assoc Physicians India*, 57, 654-656.
- Chen, D., & Texada, D. E. (2006). Low-usage codons and rare codons of *Escherichia coli*. *Gene Therapy and Molecular Biology*, 10, 1-12.
- Chesne-Seck, M. L., Pizarro, J. C., Vulliez-Le Normand, B., Collins, C. R., Blackman, M. J., Faber, B. W., et al. (2005). Structural comparison of apical membrane antigen 1 orthologues and paralogues in apicomplexan parasites. *Mol Biochem Parasitol*, 144(1), 55-67.
- Chin, W., Contacos, P. G., Coatney, G. R., & Kimball, H. R. (1965). A naturally acquired quotidian-type malaria in man transferable to monkeys. *Science*, 149(3686), 865.
- Choochote, W., & Saeung, A. (2013). Systematic techniques for the recognition of *Anopheles* species complexes. In Manguin, S. (Ed.), *Anopheles mosquitoes - New insights into malaria vectors* (pp. 813): InTech.
- Chow, M. K., Amin, A. A., Fulton, K. F., Whisstock, J. C., Buckle, A. M., & Bottomley, S. P. (2006). REFOLD: an analytical database of protein refolding methods. *Protein Expr Purif*, 46(1), 166-171.
- Clark, E. D. B. (1998). Refolding of recombinant proteins. *Curr Opin Biotechnol*, 9(2), 157-163.
- Coatney, G. R., Collins, W. E., Warren, M. W., & Contacos, P. G. (1971). *The primate malarias*. Washington: U.S. Government Printing Office.
- Coley, A. M., Campanale, N. V., Casey, J. L., Hodder, A. N., Crewther, P. E., Anders, R. F., et al. (2001). Rapid and precise epitope mapping of monoclonal antibodies against *Plasmodium falciparum* AMA1 by combined phage display of fragments and random peptides. *Protein Eng*, 14(9), 691-698.
- Coley, A. M., Parisi, K., Masciantonio, R., Hoeck, J., Casey, J. L., Murphy, V. J., et al. (2006). The most polymorphic residue on *Plasmodium falciparum* apical membrane antigen 1 determines binding of an invasion-inhibitory antibody. *Infect Immun*, 74(5), 2628-2636.
- Collins, W. E., & Jeffery, G. M. (2005). *Plasmodium ovale*: parasite and disease. *Clin Microbiol Rev*, 18(3), 570-581.
- Collins, W. E., & Jeffery, G. M. (2007). *Plasmodium malariae*: parasite and disease. *Clin Microbiol Rev*, 20(4), 579-592.
- Collins, W. E., Pye, D., Crewther, P. E., Vandenberg, K. L., Galland, G. G., Sulzer, A. J., et al. (1994). Protective immunity induced in squirrel monkeys with recombinant apical membrane antigen-1 of *Plasmodium fragile*. *Am J Trop Med Hyg*, 51(6), 711-719.
-

- 
- Conway, D. J. (2007). Molecular epidemiology of malaria. *Clin Microbiol Rev*, 20(1), 188-204.
- Cowman, A. F., & Crabb, B. S. (2006). Invasion of red blood cells by malaria parasites. *Cell*, 124(4), 755-766.
- Cox-Singh, J., & Singh, B. (2008). Knowlesi malaria: newly emergent and of public health importance? *Trends Parasitol*, 24(9), 406-410.
- Cox-Singh, J., Davis, T. M., Lee, K. S., Shamsul, S. S., Matusop, A., Ratnam, S., et al. (2008). *Plasmodium knowlesi* malaria in humans is widely distributed and potentially life threatening. *Clin Infect Dis*, 46(2), 165-171.
- Cox-Singh, J., Hiu, J., Lucas, S. B., Divis, P. C., Zulkarnaen, M., Chandran, P., et al. (2010). Severe malaria - a case of fatal *Plasmodium knowlesi* infection with post-mortem findings: a case report. *Malar J*, 9, 10.
- Crewther, P. E., Matthew, M. L., Flegg, R. H., & Anders, R. F. (1996). Protective immune responses to apical membrane antigen 1 of *Plasmodium chabaudi* involve recognition of strain-specific epitopes. *Infect Immun*, 64(8), 3310-3317.
- Daneshvar, C., Davis, T. M., Cox-Singh, J., Rafa'ee, M. Z., Zakaria, S. K., Divis, P. C., et al. (2009). Clinical and laboratory features of human *Plasmodium knowlesi* infection. *Clin Infect Dis*, 49(6), 852-860.
- de Monbrison, F., Angei, C., Staal, A., Kaiser, K., & Picot, S. (2003). Simultaneous identification of the four human *Plasmodium* species and quantification of *Plasmodium* DNA load in human blood by real-time polymerase chain reaction. *Trans R Soc Trop Med Hyg*, 97(4), 387-390.
- Deans, J. A., Alderson, T., Thomas, A. W., Mitchell, G. H., Lennox, E. S., & Cohen, S. (1982). Rat monoclonal antibodies which inhibit the in vitro multiplication of *Plasmodium knowlesi*. *Clin Exp Immunol*, 49(2), 297-309.
- Deans, J. A., Knight, A. M., Jean, W. C., Waters, A. P., Cohen, S., & Mitchell, G. H. (1988). Vaccination trials in rhesus monkeys with a minor, invariant, *Plasmodium knowlesi* 66 kD merozoite antigen. *Parasite Immunol*, 10(5), 535-552.
- Deans, J. A., Thomas, A. W., Alderson, T., & Cohen, S. (1984). Biosynthesis of a putative protective *Plasmodium knowlesi* merozoite antigen. *Mol Biochem Parasitol*, 11, 189-204.
- Desai, M., ter Kuile, F. O., Nosten, F., McGready, R., Asamo, K., Brabin, B., et al. (2007). Epidemiology and burden of malaria in pregnancy. *Lancet Infect Dis*, 7(2), 93-104.
- Doolan, D. L., & Martinez-Alier, N. (2006). Immune response to pre-erythrocytic stages of malaria parasites. *Curr Mol Med*, 6(2), 169-185.
- Doolan, D. L., Dobano, C., & Baird, J. K. (2009). Acquired immunity to malaria. *Clin Microbiol Rev*, 22(1), 13-36, Table of Contents.
-

- Douradinha, B., & Doolan, D. L. (2011). Harnessing immune responses against *Plasmodium* for rational vaccine design. *Trends Parasitol*, 27(6), 274-283.
- Dutta, S., Lalitha, P. V., Ware, L. A., Barbosa, A., Moch, J. K., Vassell, M. A., et al. (2002). Purification, characterization, and immunogenicity of the refolded ectodomain of the *Plasmodium falciparum* apical membrane antigen 1 expressed in *Escherichia coli*. *Infect Immun*, 70(6), 3101-3110.
- Eda, K., Eda, S., & Sherman, I. W. (2004). Identification of peptides targeting the surface of *Plasmodium falciparum*-infected erythrocytes using a phage display peptide library. *Am J Trop Med Hyg*, 71(2), 190-195.
- Ennis, J., Teal, A., Habura, A., Madison-Antenucci, S., Keithly, J., Arguin, P., et al. (2009). Simian malaria in a US traveler-New York, 2008. *Morbidity and Mortality Weekly Report*, 58(9), 229-232.
- Erdman, L. K., & Kain, K. C. (2008). Molecular diagnostic and surveillance tools for global malaria control. *Travel Med Infect Dis*, 6(1-2), 82-99.
- Feng, Z. P., Keizer, D. W., Stevenson, R. A., Yao, S., Babon, J. J., Murphy, V. J., et al. (2005). Structure and inter-domain interactions of domain II from the blood-stage malarial protein, apical membrane antigen 1. *J Mol Biol*, 350(4), 641-656.
- Fernandez-Robledo, J. A., & Vasta, G. R. (2010). Production of recombinant proteins from protozoan parasites. *Trends Parasitol*, 26(5), 244-254.
- Figtree, M., Lee, R., Bain, L., Kennedy, T., Mackertich, S., Urban, M., et al. (2010). *Plasmodium knowlesi* in human, Indonesian Borneo. *Emerg Infect Dis*, 16(4), 672-674.
- Flick, K., Ahuja, S., Chene, A., Bejarano, M. T., & Chen, Q. (2004). Optimized expression of *Plasmodium falciparum* erythrocyte membrane protein 1 domains in *Escherichia coli*. *Malar J*, 3, 50.
- Florens, L., Washburn, M. P., Raine, J. D., Anthony, R. M., Grainger, M., Haynes, J. D., et al. (2002). A proteomic view of the *Plasmodium falciparum* life cycle. *Nature*, 419(6906), 520-526.
- Foy, B. D., Killeen, G. F., Frohn, R. H., Impoinvil, D., Williams, A., & Beier, J. C. (2002). Characterization of a unique human single-chain antibody isolated by phage-display selection on membrane-bound mosquito midgut antigens. *J Immunol Methods*, 261(1-2), 73-83.
- Fu, Y., Shearing, L. N., Haynes, S., Crewther, P., Tilley, L., Anders, R. F., et al. (1997). Isolation from phage display libraries of single chain variable fragment antibodies that recognize conformational epitopes in the malaria vaccine candidate, apical membrane antigen-1. *J Biol Chem*, 272(41), 25678-25684.
- Gallup, J. L., & Sachs, J. D. (2001). The economic burden of malaria. *Am J Trop Med Hyg*, 64(1-2 Suppl), 85-96.
- Gan, L. S., & Loh, J. P. (2010). Rapid identification of chloroquine and atovaquone drug resistance in *Plasmodium falciparum* using high-resolution melt polymerase chain reaction. *Malar J*, 9, 134.



- 
- Gardner, M. J., Hall, N., Fung, E., White, O., Berriman, M., Hyman, R. W., et al. (2002). Genome sequence of the human malaria parasite *Plasmodium falciparum*. *Nature*, 419(6906), 498-511.
- Gasteiger, E., Gattiker, A., Hoogland, C., Ivanyi, I., Appel, R. D., & Bairoch, A. (2003). ExPASy: The proteomics server for in-depth protein knowledge and analysis. *Nucleic Acids Res*, 31(13), 3784-3788.
- Gaur, D., Mayer, D. C., & Miller, L. H. (2004). Parasite ligand-host receptor interactions during invasion of erythrocytes by *Plasmodium* merozoites. *Int J Parasitol*, 34(13-14), 1413-1429.
- Ghosh, A. K., Moreira, L. A., & Jacobs-Lorena, M. (2002). *Plasmodium*-mosquito interactions, phage display libraries and transgenic mosquitoes impaired for malaria transmission. *Insect Biochem Mol Biol*, 32(10), 1325-1331.
- Ghosh, A. K., Ribolla, P. E., & Jacobs-Lorena, M. (2001). Targeting *Plasmodium* ligands on mosquito salivary glands and midgut with a phage display peptide library. *Proc Natl Acad Sci U S A*, 98(23), 13278-13281.
- Giersing, B., Miura, K., Shimp, R., Wang, J., Zhou, H., Orcutt, A., et al. (2005). posttranslational modification of recombinant *Plasmodium falciparum* apical membrane antigen 1: impact on functional immune responses to a malaria vaccine candidate. *Infect Immun*, 73(7), 3963-3970.
- Girard, M. P., Reed, Z. H., Friede, M., & Kieny, M. P. (2007). A review of human vaccine research and development: malaria. *Vaccine*, 25(9), 1567-1580.
- Golenda, C. F., Li, J., & Rosenberg, R. (1997). Continuous in vitro propagation of the malaria parasite *Plasmodium vivax*. *Proc Natl Acad Sci U S A*, 94(13), 6786-6791.
- Greenwood, B. M., Bojang, K., Whitty, C. J., & Targett, G. A. (2005). Malaria. *Lancet*, 365(9469), 1487-1498.
- Gupta, A., Bai, T., Murphy, V., Strike, P., Anders, R. F., & Batchelor, A. H. (2005). Refolding, purification, and crystallization of apical membrane antigen 1 from *Plasmodium falciparum*. *Protein Expr Purif*, 41(1), 186-198.
- Hall, T. A. (1999). *BioEdit: a user-friendly biological sequence alignment editor and analysis program for Windows 95/98/NT*. Paper presented at the Nucleic acids symposium series. <http://www.mbio.ncsu.edu/BioEdit/page2.html>
- Han, E. T., Watanabe, R., Sattabongkot, J., Khuntirat, B., Sirichaisinthop, J., Iriko, H., et al. (2007). Detection of four *Plasmodium* species by genus- and species-specific loop-mediated isothermal amplification for clinical diagnosis. *J Clin Microbiol*, 45(8), 2521-2528.
- Harris, K. S., Casey, J. L., Coley, A. M., Karas, J. A., Sabo, J. K., Tan, Y. Y., et al. (2009). Rapid optimization of a peptide inhibitor of malaria parasite invasion by comprehensive N-methyl scanning. *J Biol Chem*, 284(14), 9361-9371.
-

- Harris, K. S., Casey, J. L., Coley, A. M., Masciantonio, R., Sabo, J. K., Keizer, D. W., et al. (2005). Binding hot spot for invasion inhibitory molecules on *Plasmodium falciparum* apical membrane antigen 1. *Infect Immun*, 73(10), 6981-6989.
- Hay, S. I., Guerra, C. A., Gething, P. W., Patil, A. P., Tatem, A. J., Noor, A. M., et al. (2009). A world malaria map: *Plasmodium falciparum* endemicity in 2007. *PLoS Med*, 6(3), e1000048.
- Henegariu, O., Heerema, N. A., Dlouhy, S. R., Vance, G. H., & Vogt, P. H. (1997). Multiplex PCR: critical parameters and step-by-step protocol. *Biotechniques*, 23(3), 504-511.
- Hodder, A. N., Crewther, P. E., & Anders, R. F. (2001). Specificity of the protective antibody response to apical membrane antigen 1. *Infect Immun*, 69(5), 3286-3294.
- Hodder, A. N., Crewther, P. E., Matthew, M. L., Reid, G. E., Moritz, R. L., Simpson, R. J., et al. (1996). The disulfide bond structure of *Plasmodium* apical membrane antigen-1. *J Biol Chem*, 271(46), 29446-29452.
- Hoorfar, J., Malorny, B., Abdulmawjood, A., Cook, N., Wagner, M., & Fach, P. (2004). Practical considerations in design of internal amplification controls for diagnostic PCR assays. *J Clin Microbiol*, 42(5), 1863-1868.
- Hoosen, A., & Shaw, M. T. (2011). *Plasmodium knowlesi* in a traveller returning to New Zealand. *Travel Med Infect Dis*, 9(3), 144-148.
- Huang, J., Gutteridge, A., Honda, W., & Kanehisa, M. (2006). MIMOX: a web tool for phage display based epitope mapping. *BMC Bioinformatics*, 7, 451.
- Huang, J., Ru, B., Zhu, P., Nie, F., Yang, J., Wang, X., et al. (2012). MimoDB 2.0: a mimotope database and beyond. *Nucleic Acids Res*, 40(Database issue), D271-277.
- Igonet, S., Vulliez-Le Normand, B., Faure, G., Riottot, M. M., Kocken, C. H., Thomas, A. W., et al. (2007). Cross-reactivity studies of an anti-*Plasmodium vivax* apical membrane antigen 1 monoclonal antibody: binding and structural characterisation. *J Mol Biol*, 366(5), 1523-1537.
- Imwong, M., Tanomsing, N., Pukrittayakamee, S., Day, N. P., White, N. J., & Snounou, G. (2009). Spurious amplification of a *Plasmodium vivax* small-subunit RNA gene by use of primers currently used to detect *P. knowlesi*. *J Clin Microbiol*, 47(12), 4173-4175.
- Jeslyn, W. P., Huat, T. C., Vernon, L., Irene, L. M., Sung, L. K., Jarrod, L. P., et al. (2011). Molecular epidemiological investigation of *Plasmodium knowlesi* in humans and macaques in Singapore. *Vector Borne Zoonotic Dis*, 11(2), 131-135.
- Jiang, N., Chang, Q., Sun, X., Lu, H., Yin, J., Zhang, Z., et al. (2010). Co-infections with *Plasmodium knowlesi* and other malaria parasites, Myanmar. *Emerg Infect Dis*, 16(9), 1476-1478.

- Jongwutiwes, S., Putaporntip, C., Iwasaki, T., Sata, T., & Kanbara, H. (2004). Naturally acquired *Plasmodium knowlesi* malaria in human, Thailand. *Emerg Infect Dis*, 10(12), 2211-2213.
- Joveen-Neoh, W. F., Chong, K. L., Wong, C. M., & Lau, T. Y. (2011). Incidence of malaria in the interior division of sabah, malaysian borneo, based on nested PCR. *J Parasitol Res*, 2011, 104284.
- Kantele, A., & Jokiranta, T. S. (2011). Review of cases with the emerging fifth human malaria parasite, *Plasmodium knowlesi*. *Clin Infect Dis*, 52(11), 1356-1362.
- Kantele, A., Marti, H., Felger, I., Muller, D., & Jokiranta, T. S. (2008). Monkey malaria in a European traveler returning from Malaysia. *Emerg Infect Dis*, 14(9), 1434-1436.
- Kappe, S. H., Vaughan, A. M., Boddey, J. A., & Cowman, A. F. (2010). That was then but this is now: malaria research in the time of an eradication agenda. *Science*, 328(5980), 862-866.
- Karyana, M., Burdarm, L., Yeung, S., Kenangalem, E., Wariker, N., Maristela, R., et al. (2008). Malaria morbidity in Papua Indonesia, an area with multidrug resistant *Plasmodium vivax* and *Plasmodium falciparum*. *Malar J*, 7, 148.
- Kay, B. K., Kasanov, J., & Yamabhai, M. (2001). Screening phage-displayed combinatorial peptide libraries. *Methods*, 24(3), 240-246.
- Keizer, D. W., Miles, L. A., Li, F., Nair, M., Anders, R. F., Coley, A. M., et al. (2003). Structures of phage-display peptides that bind to the malarial surface protein, apical membrane antigen 1, and block erythrocyte invasion. *Biochemistry*, 42(33), 9915-9923.
- Kennedy, M. C., Wang, J., Zhang, Y., Miles, A. P., Chitsaz, F., Saul, A., et al. (2002). In vitro studies with recombinant *Plasmodium falciparum* apical membrane antigen 1 (AMA1): production and activity of an AMA1 vaccine and generation of a multiallelic response. *Infect Immun*, 70(12), 6948-6960.
- Khamrin, P., Okame, M., Thongprachum, A., Nantachit, N., Nishimura, S., Okitsu, S., et al. (2011). A single-tube multiplex PCR for rapid detection in feces of 10 viruses causing diarrhea. *J Virol Methods*, 173(2), 390-393.
- Kheong CC. (2010). *Country Updates Malaysia*. Asian Collaborative Training Network for Malaria (ACTMalaria) Executive Board Meeting, 15–17 March 2010. Luang Prabang, Lao PDR.
- Kho, W. G., Chung, J. Y., Sim, E. J., Kim, M. Y., Kim, D. W., Jongwutiwes, S., et al. (2003). A multiplex polymerase chain reaction for a differential diagnosis of *Plasmodium falciparum* and *Plasmodium vivax*. *Parasitol Int*, 52(3), 229-236.
- Kim, T. S., Kim, H. H., Lee, S. S., Na, B. K., Lin, K., Cho, S. H., et al. (2010). Prevalence of *Plasmodium vivax* VK210 and VK247 subtype in Myanmar. *Malar J*, 9, 195.
- Kochar, D. K., Saxena, V., Singh, N., Kochar, S. K., Kumar, S. V., & Das, A. (2005). *Plasmodium vivax* malaria. *Emerg Infect Dis*, 11(1), 132-134.

- Kocken, C. H., van der Wel, A. M., Dubbeld, M. A., Narum, D. L., van de Rijke, F. M., van Gemert, G. J., et al. (1998). Precise timing of expression of a *Plasmodium falciparum*-derived transgene in *Plasmodium berghei* is a critical determinant of subsequent subcellular localization. *J Biol Chem*, 273(24), 15119-15124.
- Kuo, M. C., Chiang, T. Y., Chan, C. W., Tsai, W. S., & Ji, D. D. (2009). A case report of simian malaria, *Plasmodium knowlesi*, in a Taiwanese traveler from Palawan Island, the Philippines. *Epidemiology Bulletin*, 25(3), 178-191.
- Lalitha, P. V., Ware, L. A., Barbosa, A., Dutta, S., Moch, J. K., Haynes, J. D., et al. (2004). Production of the subdomains of the *Plasmodium falciparum* apical membrane antigen 1 ectodomain and analysis of the immune response. *Infect Immun*, 72(8), 4464-4470.
- Lanzillotti, R., & Coetzer, T. L. (2008). Phage display: a useful tool for malaria research? *Trends Parasitol*, 24(1), 18-23.
- Lasonder, E., Ishihama, Y., Andersen, J. S., Vermunt, A. M., Pain, A., Sauerwein, R. W., et al. (2002). Analysis of the *Plasmodium falciparum* proteome by high-accuracy mass spectrometry. *Nature*, 419(6906), 537-542.
- Lauterbach, S. B., Lanzillotti, R., & Coetzer, T. L. (2003). Construction and use of *Plasmodium falciparum* phage display libraries to identify host parasite interactions. *Malar J*, 2(1), 47.
- Leclerc, M., Hugot, J., Durand, P., & Renaud, F. (2004). Evolutionary relationships between 15 *Plasmodium* species from New and Old World primates (including humans): a 18S rDNA cladistic analysis. *Parasitology*, 129(6), 677-684.
- Lee, C. E., Adeeba, K., & Freigang, G. (2010). Human *Plasmodium knowlesi* infections in Klang Valley, Peninsula Malaysia: a case series. *Med J Malaysia*, 65(1), 63-65.
- Lee, K. S., Cox-Singh, J., & Singh, B. (2009). Morphological features and differential counts of *Plasmodium knowlesi* parasites in naturally acquired human infections. *Malar J*, 8, 73.
- Li, F., Dluzewski, A., Coley, A. M., Thomas, A., Tilley, L., Anders, R. F., et al. (2002). Phage-displayed peptides bind to the malarial protein apical membrane antigen-1 and inhibit the merozoite invasion of host erythrocytes. *J Biol Chem*, 277(52), 50303-50310.
- Lim, Y. A., Mahmud, R., Chew, C. H., Thilaganathan, T., & Chua, K. H. (2010). *Plasmodium ovale* infection in Malaysia: first imported case. *Malar J*, 9, 272.
- Lingnau, A., Doehring-Schwerdtfeger, E., & Maier, W. A. (1994). Evidence for 6-day cultivation of human *Plasmodium malariae*. *Parasitol Res*, 80(3), 265-266.
- Link, L., Bart, A., Verhaar, N., van Gool, T., Pronk, M., & Scharnhorst, V. (2012). Molecular detection of *Plasmodium knowlesi* in a Dutch traveler by real-time PCR. *J Clin Microbiol*, 50(7), 2523-2524.

- Luchavez, J., Espino, F., Curameng, P., Espina, R., Bell, D., Chiodini, P., et al. (2008). Human Infections with *Plasmodium knowlesi*, the Philippines. *Emerg Infect Dis*, 14(5), 811-813.
- Macrauld, C. A., Anders, R. F., Foley, M., & Norton, R. S. (2011). Apical membrane antigen 1 as an anti-malarial drug target. *Curr Top Med Chem*, 11(16), 2039-2047.
- Malaria Site. (2012) *What is malaria?* Dr. B. S. Kakkilaya's Malaria Web Site (Last updated: 12 April 2012). Retrieved 9 July 2013, from <http://www.malariasite.com/malaria/WhatIsMalaria.htm>
- malERA Consultative Group on Diagnoses and Diagnostics. (2011). A research agenda for malaria eradication: diagnoses and diagnostics. *PLoS Med*, 8(1), e1000396.
- malERA Consultative Group on Vaccines. (2011). A research agenda for malaria eradication: vaccines. *PLoS Med*, 8(1), e1000398.
- Mangold, K. A., Manson, R. U., Koay, E. S., Stephens, L., Regner, M., Thomson, R. B., Jr., et al. (2005). Real-time PCR for detection and identification of *Plasmodium* spp. *J Clin Microbiol*, 43(5), 2435-2440.
- Manguin, S., Bangs, M. J., Pothikasikorn, J., & Chareonviriyaphap, T. (2010). Review on global co-transmission of human *Plasmodium* species and *Wuchereria bancrofti* by *Anopheles* mosquitoes. *Infect Genet Evol*, 10(2), 159-177.
- Manguin, S., Garros, C., Dusfour, I., Harbach, R. E., & Coosemans, M. (2008). Bionomics, taxonomy, and distribution of the major malaria vector taxa of *Anopheles* subgenus *Cellia* in Southeast Asia: an updated review. *Infect Genet Evol*, 8(4), 489-503.
- Masitah, M., Aini, N., & AyuSaid, M. (2008). Malaria among foreign workers in Selangor, Malaysia. *JUMMEC*, 11(2), 53-58.
- Matthews, L. J., Davis, R., & Smith, G. P. (2002). Immunogenically fit subunit vaccine components via epitope discovery from natural peptide libraries. *J Immunol*, 169(2), 837-846.
- Mayxay, M., Pukrittayakamee, S., Newton, P. N., & White, N. J. (2004). Mixed-species malaria infections in humans. *Trends Parasitol*, 20(5), 233-240.
- McFadden, G. I. (2012). Plasmodia - don't. *Trends Parasitol*, 28(8), 306.
- Mehlin, C., Boni, E., Buckner, F. S., Engel, L., Feist, T., Gelb, M. H., et al. (2006). Heterologous expression of proteins from *Plasmodium falciparum*: results from 1000 genes. *Mol Biochem Parasitol*, 148(2), 144-160.
- Ministry of Health Malaysia. (2012). *Country briefing: Eliminating malaria in Malaysia*. Retrieved 9 July 2013, from <http://apmen.org/storage/country-briefings/Malaysia.pdf>
- Mixson-Hayden, T., Lucchi, N. W., & Udhayakumar, V. (2010). Evaluation of three PCR-based diagnostic assays for detecting mixed *Plasmodium* infection. *BMC Res Notes*, 3, 88.

- 
- Moll, K., Ljungström, I., Perlmann, H., Scherf, A., & Wahlgren, M. (2008). *Methods in malaria research* (5<sup>th</sup> Edi.). Manassas, VA: Malaria Research and Reagent Resource Center (MR4), American Type Culture Collection (ATCC).
- Moody, A. (2002). Rapid diagnostic tests for malaria parasites. *Clin Microbiol Rev*, 15(1), 66-78.
- Mueller, I., Galinski, M. R., Baird, J. K., Carlton, J. M., Kochar, D. K., Alonso, P. L., et al. (2009). Key gaps in the knowledge of *Plasmodium vivax*, a neglected human malaria parasite. *Lancet Infect Dis*, 9(9), 555-566.
- Mufalo, B. C., Gentil, F., Bargieri, D. Y., Costa, F. T., Rodrigues, M. M., & Soares, I. S. (2008). *Plasmodium vivax* apical membrane antigen-1: comparative recognition of different domains by antibodies induced during natural human infection. *Microbes Infect*, 10(12-13), 1266-1273.
- Mullen, L. M., Nair, S. P., Ward, J. M., Rycroft, A. N., & Henderson, B. (2006). Phage display in the study of infectious diseases. *Trends Microbiol*, 14(3), 141-147.
- Murray, C. K., Gasser, R. A., Jr., Magill, A. J., & Miller, R. S. (2008). Update on rapid diagnostic testing for malaria. *Clin Microbiol Rev*, 21(1), 97-110.
- Nair, M., Hinds, M. G., Coley, A. M., Hodder, A. N., Foley, M., Anders, R. F., et al. (2002). Structure of domain III of the blood-stage malaria vaccine candidate, *Plasmodium falciparum* apical membrane antigen 1 (AMA1). *J Mol Biol*, 322(4), 741-753.
- Narum, D. L., & Thomas, A. W. (1994). Differential localization of full-length and processed forms of PF83/AMA-1 an apical membrane antigen of *Plasmodium falciparum* merozoites. *Mol Biochem Parasitol*, 67(1), 59-68.
- Narum, D. L., Kumar, S., Rogers, W. O., Fuhrmann, S. R., Liang, H., Oakley, M., et al. (2001). Codon optimization of gene fragments encoding *Plasmodium falciparum* merzoite proteins enhances DNA vaccine protein expression and immunogenicity in mice. *Infect Immun*, 69(12), 7250-7253.
- Narum, D. L., Ogun, S. A., Thomas, A. W., & Holder, A. A. (2000). Immunization with parasite-derived apical membrane antigen 1 or passive immunization with a specific monoclonal antibody protects BALB/c mice against lethal *Plasmodium yoelii yoelii* YM blood-stage infection. *Infect Immun*, 68(5), 2899-2906.
- Ng, O. T., Ooi, E. E., Lee, C. C., Lee, P. J., Ng, L. C., Pei, S. W., et al. (2008). Naturally acquired human *Plasmodium knowlesi* infection, Singapore. *Emerg Infect Dis*, 14(5), 814-816.
- Nishimoto, Y., Arisue, N., Kawai, S., Escalante, A. A., Horii, T., Tanabe, K., et al. (2008). Evolution and phylogeny of the heterogeneous cytosolic SSU rRNA genes in the genus *Plasmodium*. *Mol Phylogenet Evol*, 47(1), 45-53.
- Ong, C. W., Lee, S. Y., Koh, W. H., Ooi, E. E., & Tambyah, P. A. (2009). Monkey malaria in humans: a diagnostic dilemma with conflicting laboratory data. *Am J Trop Med Hyg*, 80(6), 927-928.
-

- Padley, D. J., Heath, A. B., Sutherland, C., Chiodini, P. L., & Baylis, S. A. (2008). Establishment of the 1st World Health Organization International Standard for *Plasmodium falciparum* DNA for nucleic acid amplification technique (NAT)-based assays. *Malar J*, 7, 139.
- Padley, D., Moody, A. H., Chiodini, P. L., & Saldanha, J. (2003). Use of a rapid, single-round, multiplex PCR to detect malarial parasites and identify the species present. *Ann Trop Med Parasitol*, 97(2), 131-137.
- Pain, A., Bohme, U., Berry, A. E., Mungall, K., Finn, R. D., Jackson, A. P., et al. (2008). The genome of the simian and human malaria parasite *Plasmodium knowlesi*. *Nature*, 455(7214), 799-803.
- Patsoula, E., Spanakos, G., Sofianatou, D., Parara, M., & Vakalis, N. C. (2003). A single-step, PCR-based method for the detection and differentiation of *Plasmodium vivax* and *P. falciparum*. *Ann Trop Med Parasitol*, 97(1), 15-21.
- Perandin, F., Manca, N., Calderaro, A., Piccolo, G., Galati, L., Ricci, L., et al. (2004). Development of a real-time PCR assay for detection of *Plasmodium falciparum*, *Plasmodium vivax*, and *Plasmodium ovale* for routine clinical diagnosis. *J Clin Microbiol*, 42(3), 1214-1219.
- Peterson, M. G., Marshall, V. M., Smythe, J. A., Crewther, P. E., Lew, A., Silva, A., et al. (1989). Integral membrane protein located in the apical complex of *Plasmodium falciparum*. *Mol Cell Biol*, 9(7), 3151-3154.
- Pizarro, J. C., Vulliez-Le Normand, B., Chesne-Seck, M. L., Collins, C. R., Withers-Martinez, C., Hackett, F., et al. (2005). Crystal structure of the malaria vaccine candidate apical membrane antigen 1. *Science*, 308(5720), 408-411.
- Putaporntip, C., Hongsriruang, T., Seethamchai, S., Kobasa, T., Limkittikul, K., Cui, L., et al. (2009). Differential prevalence of *Plasmodium* infections and cryptic *Plasmodium knowlesi* malaria in humans in Thailand. *J Infect Dis*, 199(8), 1143-1150.
- Rajahram, G. S., Barber, B. E., William, T., Menon, J., Anstey, N. M., & Yeo, T. W. (2012). Deaths due to *Plasmodium knowlesi* malaria in Sabah, Malaysia: association with reporting as *Plasmodium malariae* and delayed parenteral artesunate. *Malar J*, 11, 284.
- Remarque, E. J., Faber, B. W., Kocken, C. H., & Thomas, A. W. (2008). Apical membrane antigen 1: a malaria vaccine candidate in review. *Trends Parasitol*, 24(2), 74-84.
- Richard, D., MacRaild, C. A., Riglar, D. T., Chan, J. A., Foley, M., Baum, J., et al. (2010). Interaction between *Plasmodium falciparum* apical membrane antigen 1 and the rhoptry neck protein complex defines a key step in the erythrocyte invasion process of malaria parasites. *J Biol Chem*, 285(19), 14815-14822.
- Richards, J. S., & Beeson, J. G. (2009). The future for blood-stage vaccines against malaria. *Immunol Cell Biol*, 87(5), 377-390.

- Rodrigues, M. H., Rodrigues, K. M., Oliveira, T. R., Comodo, A. N., Rodrigues, M. M., Kocken, C. H., et al. (2005). Antibody response of naturally infected individuals to recombinant *Plasmodium vivax* apical membrane antigen-1. *Int J Parasitol*, 35(2), 185-192.
- Rogerson, S. J., & Carter, R. (2008). Severe vivax malaria: newly recognised or rediscovered? *PLoS Med*, 5(6), e136.
- Roobsoong, W., Roytrakul, S., Sattabongkot, J., Li, J., Udomsangpetch, R., & Cui, L. (2011). Determination of the *Plasmodium vivax* schizont stage proteome. *J Proteomics*, 74(9), 1701-1710.
- Rougemont, M., Van Saanen, M., Sahli, R., Hinrikson, H. P., Bille, J., & Jaton, K. (2004). Detection of four *Plasmodium* species in blood from humans by 18S rRNA gene subunit-based and species-specific real-time PCR assays. *J Clin Microbiol*, 42(12), 5636-5643.
- Rubio, J. M., Benito, A., Roche, J., Berzosa, P. J., Garcia, M. L., Mico, M., et al. (1999). Semi-nested, multiplex polymerase chain reaction for detection of human malaria parasites and evidence of *Plasmodium vivax* infection in Equatorial Guinea. *Am J Trop Med Hyg*, 60(2), 183-187.
- Rundi, C. (2011). *Malaria Elimination in Malaysia*. Third annual meeting of the Asia Pacific Malaria Elimination Network (APMEN), 9-12 May 2011. Kota Kinabalu, Sabah, Malaysia: Ministry of Health Malaysia. Retrieved 9 July 2013, from <http://apmen.org/storage/apmen-iii/Dr%20Christina%20Rundi.pdf>
- Sabo, J. K., Keizer, D. W., Feng, Z. P., Casey, J. L., Parisi, K., Coley, A. M., et al. (2007). Mimotopes of apical membrane antigen 1: Structures of phage-derived peptides recognized by the inhibitory monoclonal antibody 4G2dc1 and design of a more active analogue. *Infect Immun*, 75(1), 61-73.
- Sachs, J., & Malaney, P. (2002). The economic and social burden of malaria. *Nature*, 415(6872), 680-685.
- Safeukui, I., Millet, P., Boucher, S., Melinard, L., Fregeville, F., Receveur, M. C., et al. (2008). Evaluation of FRET real-time PCR assay for rapid detection and differentiation of *Plasmodium* species in returning travellers and migrants. *Malar J*, 7, 70.
- Sambrook, J., & Russell, D. W. (2001). *Molecular cloning: a laboratory manual*. Volume 1-3: Cold Spring Harbor, New York: Cold Spring Harbor Laboratory Press.
- Schreiber, A., Humbert, M., Benz, A., & Dietrich, U. (2005). 3D-Epitope-Explorer (3DEX): localization of conformational epitopes within three-dimensional structures of proteins. *J Comput Chem*, 26(9), 879-887.
- Sermwittayawong, N., Singh, B., Nishibuchi, M., Sawangjaroen, N., & Vuddhakul, V. (2012). Human *Plasmodium knowlesi* infection in Ranong province, southwestern border of Thailand. *Malar J*, 11, 36.
- Shetty, P. (2012). The numbers game. *Nature*, 484(7395), S14-15.



- Shokoples, S. E., Ndao, M., Kowalewska-Grochowska, K., & Yanow, S. K. (2009). Multiplexed real-time PCR assay for discrimination of *Plasmodium* species with improved sensitivity for mixed infections. *J Clin Microbiol*, 47(4), 975-980.
- Silvie, O., Franetich, J. F., Charrin, S., Mueller, M. S., Siau, A., Bodescot, M., et al. (2004). A role for apical membrane antigen 1 during invasion of hepatocytes by *Plasmodium falciparum* sporozoites. *J Biol Chem*, 279(10), 9490-9496.
- Singh, B (2011). *P. knowlesi and the Elimination Agenda*. Third annual meeting of the Asia Pacific Malaria Elimination Network (APMEN), 9-12 May 2011. Kota Kinabalu, Sabah, Malaysia: Ministry of Health Malaysia. Retrieved 9 July 2013, from <http://apmen.org/storage/apmen-iii/Prof%20Balbir%20Singh.pdf>
- Singh, B., Bobogare, A., Cox-Singh, J., Snounou, G., Abdullah, M. S., & Rahman, H. A. (1999). A genus- and species-specific nested polymerase chain reaction malaria detection assay for epidemiologic studies. *Am J Trop Med Hyg*, 60(4), 687-692.
- Singh, B., Kim Sung, L., Matusop, A., Radhakrishnan, A., Shamsul, S. S., Cox-Singh, J., et al. (2004). A large focus of naturally acquired *Plasmodium knowlesi* infections in human beings. *Lancet*, 363(9414), 1017-1024.
- Singh, S. M., & Panda, A. K. (2005). Solubilization and refolding of bacterial inclusion body proteins. *J Biosci Bioeng*, 99(4), 303-310.
- Smith, G. P. (1985). Filamentous fusion phage: novel expression vectors that display cloned antigens on the virion surface. *Science*, 228(4705), 1315-1317.
- Snounou, G., Viriyakosol, S., Zhu, X. P., Jarra, W., Pinheiro, L., do Rosario, V. E., et al. (1993). High sensitivity of detection of human malaria parasites by the use of nested polymerase chain reaction. *Mol Biochem Parasitol*, 61(2), 315-320.
- Sowa, K. M., Cavanagh, D. R., Creasey, A. M., Raats, J., McBride, J., Sauerwein, R., et al. (2001). Isolation of a monoclonal antibody from a malaria patient-derived phage display library recognising the Block 2 region of *Plasmodium falciparum* merozoite surface protein-1. *Mol Biochem Parasitol*, 112(1), 143-147.
- Steketee, R. W., Nahlen, B. L., Parise, M. E., & Menendez, C. (2001). The burden of malaria in pregnancy in malaria-endemic areas. *Am J Trop Med Hyg*, 64(1-2 Suppl), 28-35.
- Stowers, A. W., Kennedy, M. C., Keegan, B. P., Saul, A., Long, C. A., & Miller, L. H. (2002). Vaccination of monkeys with recombinant *Plasmodium falciparum* apical membrane antigen 1 confers protection against blood-stage malaria. *Infect Immun*, 70(12), 6961-6967.
- Sulistyaningsih, E., Fitri, L. E., Loscher, T., & Berens-Riha, N. (2010). Diagnostic difficulties with *Plasmodium knowlesi* infection in humans. *Emerg Infect Dis*, 16(6), 1033-1034.
- Sutherland, C. J., Tanomsing, N., Nolder, D., Oguike, M., Jennison, C., Pukrittayakamee, S., et al. (2010). Two nonrecombining sympatric forms of the human malaria parasite *Plasmodium ovale* occur globally. *J Infect Dis*, 201(10), 1544-1550.

- Ta, T. T., Salas, A., Ali-Tammam, M., Martinez Mdel, C., Lanza, M., Arroyo, E., et al. (2010). First case of detection of *Plasmodium knowlesi* in Spain by Real Time PCR in a traveller from Southeast Asia. *Malar J*, 9, 219.
- Tangpukdee, N., Duangdee, C., Wilairatana, P., & Krudsood, S. (2009). Malaria diagnosis: a brief review. *Korean J Parasitol*, 47(2), 93-102.
- Tanizaki, R., Ujiie, M., Kato, Y., Iwagami, M., Hashimoto, A., Kutsuna, S., et al. (2013). First case of *Plasmodium knowlesi* infection in a Japanese traveller returning from Malaysia. *Malar J*, 12, 128.
- Teh, C. S., Chua, K. H., & Thong, K. L. (2010). Simultaneous differential detection of human pathogenic and nonpathogenic *Vibrio* species using a multiplex PCR based on gyrB and pntA genes. *J Appl Microbiol*, 108(6), 1940-1945.
- Thomas, A. W., Deans, J. A., Mitchell, G. H., Alderson, T., & Cohen, S. (1984). The Fab fragments of monoclonal IgG to a merozoite surface antigen inhibit *Plasmodium knowlesi* invasion of erythrocytes. *Mol Biochem Parasitol*, 13(2), 187-199.
- Thompson, J. D., Higgins, D. G., & Gibson, T. J. (1994). CLUSTAL W: improving the sensitivity of progressive multiple sequence alignment through sequence weighting, position-specific gap penalties and weight matrix choice. *Nucleic Acids Res*, 22(22), 4673-4680. <http://www.ebi.ac.uk/Tools/msa/clustalw2/>
- Thong, K. L., Lai, M. Y., Teh, C. S., & Chua, K. H. (2011). Simultaneous detection of methicillin-resistant *Staphylococcus aureus*, *Acinetobacter baumannii*, *Escherichia coli*, *Klebsiella pneumoniae* and *Pseudomonas aeruginosa* by multiplex PCR. *Trop Biomed*, 28(1), 21-31.
- Tjitra, E., Anstey, N. M., Sugiarto, P., Warikar, N., Kenangalem, E., Karyana, M., et al. (2008). Multidrug-resistant *Plasmodium vivax* associated with severe and fatal malaria: a prospective study in Papua, Indonesia. *PLoS Med*, 5(6), e128.
- Todryk, S. M., & Hill, A. V. (2007). Malaria vaccines: the stage we are at. *Nat Rev Microbiol*, 5(7), 487-489.
- Trager, W. (1994). Cultivation of malaria parasites. *Methods Cell Biol*, 45, 7-26.
- Trager, W., & Jensen, J. B. (1976). Human malaria parasites in continuous culture. *Science*, 193(4254), 673-675.
- Tresaugues, L., Collinet, B., Minard, P., Henckes, G., Aufrere, R., Blondeau, K., et al. (2004). Refolding strategies from inclusion bodies in a structural genomics project. *J Struct Funct Genomics*, 5(3), 195-204.
- Triglia, T., Healer, J., Caruana, S. R., Hodder, A. N., Anders, R. F., Crabb, B. S., et al. (2000). Apical membrane antigen 1 plays a central role in erythrocyte invasion by Plasmodium species. *Mol Microbiol*, 38(4), 706-718.
- Tyler, J. S., Treeck, M., & Boothroyd, J. C. (2011). Focus on the ringleader: the role of AMA1 in apicomplexan invasion and replication. *Trends Parasitol*, 27(9), 410-420.

- Uchiyama, F., Tanaka, Y., Minari, Y., & Tokui, N. (2005). Designing scaffolds of peptides for phage display libraries. *J Biosci Bioeng*, 99(5), 448-456.
- Urquiza, M., Suarez, J. E., Cardenas, C., Lopez, R., Puentes, A., Chavez, F., et al. (2000). *Plasmodium falciparum* AMA-1 erythrocyte binding peptides implicate AMA-1 as erythrocyte binding protein. *Vaccine*, 19(4-5), 508-513.
- Van den Eede, P., Van, H. N., Van Overmeir, C., Vythilingam, I., Duc, T. N., Hung le, X., et al. (2009). Human *Plasmodium knowlesi* infections in young children in central Vietnam. *Malar J*, 8, 249.
- Van den Eede, P., Vythilingam, I., Ngo, D. T., Nguyen, V. H., Le, X. H., D'Alessandro, U., et al. (2010). *Plasmodium knowlesi* malaria in Vietnam: some clarifications. *Malar J*, 9, 20.
- Van Hellemond, J. J., Rutten, M., Koelewijn, R., Zeeman, A. M., Verweij, J. J., Wismans, P. J., et al. (2009). Human *Plasmodium knowlesi* infection detected by rapid diagnostic tests for malaria. *Emerging Infectious Diseases*, 15(9), 1478.
- Vaughan, A. M., & Kappe, S. H. (2012). Malaria vaccine development: persistent challenges. *Curr Opin Immunol*, 24(3), 324-331.
- Vincentelli, R., Canaan, S., Campanacci, V., Valencia, C., Maurin, D., Frassinetti, F., et al. (2004). High-throughput automated refolding screening of inclusion bodies. *Protein Sci*, 13(10), 2782-2792.
- Vulliez-Le Normand, B., Tonkin, M. L., Lamarque, M. H., Langer, S., Hoos, S., Roques, M., et al. (2012). Structural and functional insights into the malaria parasite moving junction complex. *PLoS Pathog*, 8(6), e1002755.
- Vythilingam, I., Noorazian, Y. M., Huat, T. C., Jiram, A. I., Yusri, Y. M., Azahari, A. H., et al. (2008). *Plasmodium knowlesi* in humans, macaques and mosquitoes in peninsular Malaysia. *Parasit Vectors*, 1(1), 26.
- Wajanarogana, S., Prasomrothanakul, T., Udomsangpetch, R., & Tungpradabkul, S. (2006). Construction of a human functional single-chain variable fragment (scFv) antibody recognizing the malaria parasite *Plasmodium falciparum*. *Biotechnol Appl Biochem*, 44(Pt 1), 55-61.
- Wang, L. F., & Yu, M. (2004). Epitope identification and discovery using phage display libraries: applications in vaccine development and diagnostics. *Curr Drug Targets*, 5(1), 1-15.
- Waters, A. P., Thomas, A. W., Deans, J. A., Mitchell, G. H., Hudson, D. E., Miller, L. H., et al. (1990). A merozoite receptor protein from *Plasmodium knowlesi* is highly conserved and distributed throughout *Plasmodium*. *J Biol Chem*, 265(29), 17974-17979.
- Wellems, T. E., Hayton, K., & Fairhurst, R. M. (2009). The impact of malaria parasitism: from corpuscles to communities. *J Clin Invest*, 119(9), 2496-2505.
- White, N. J. (2008). *Plasmodium knowlesi*: the fifth human malaria parasite. *Clin Infect Dis*, 46(2), 172-173.

- Wickramarachchi, T., Premaratne, P. H., Perera, K. L., Bandara, S., Kocken, C. H., Thomas, A. W., et al. (2006). Natural human antibody responses to *Plasmodium vivax* apical membrane antigen 1 under low transmission and unstable malaria conditions in Sri Lanka. *Infect Immun*, 74(1), 798-801.
- Wilkinson, D. L., & Harrison, R. G. (1991). Predicting the solubility of recombinant proteins in *Escherichia coli*. *Bio-Technology*, 9(5), 443-448.
- Willats, W. G. (2002). Phage display: practicalities and prospects. *Plant Mol Biol*, 50(6), 837-854.
- William, T., Menon, J., Rajahram, G., Chan, L., Ma, G., Donaldson, S., et al. (2011). Severe *Plasmodium knowlesi* malaria in a tertiary care hospital, Sabah, Malaysia. *Emerg Infect Dis*, 17(7), 1248-1255.
- World Health Organization. (2000). Severe falciparum malaria. *Trans R Soc Trop Med Hyg*, 94 Suppl 1, S1-90. Geneva, Switzerland: World Health Organization, Communicable Diseases Cluster.
- World Health Organization. (2008). *World malaria report 2008*. Geneva, Switzerland: World Health Organization Press. Retrieved 9 July 2013, from [http://whqlibdoc.who.int/publications/2008/9789241563697\\_eng.pdf](http://whqlibdoc.who.int/publications/2008/9789241563697_eng.pdf)
- World Health Organization. (2010a). *Guidelines for the treatment of malaria* (2<sup>nd</sup> edi.) (pp. 194). Geneva, Switzerland: World Health Organization Press.
- World Health Organization. (2010b). Routine examination of blood films for malaria parasites. In *Basic malaria microscopy. Part I: learner's guild* (2<sup>nd</sup> ed.) (pp. 69-76). Geneva, Switzerland: World Health Organization Press.
- World Health Organization. (2012). *World malaria report 2012*. Geneva, Switzerland: World Health Organization Press. Retrieved 9 July 2013, from [www.who.int/malaria/publications/world\\_malaria\\_report\\_2012/en/](http://www.who.int/malaria/publications/world_malaria_report_2012/en/)
- World Health Organization. (2013a). *Malaria fact sheet no. 94*. World Health Organization media centre (Reviewed March 2013). Retrieved 9 July 2013, from <http://www.who.int/mediacentre/factsheets/fs094/en/index.html>
- World Health Organization. (2013b). *The top 10 causes of death*. World Health Organization media centre (Last updated: July 2013). Retrieved 9 July 2013, from <http://www.who.int/mediacentre/factsheets/fs310/en/index.html>
- Zhou, Z., Schnake, P., Xiao, L., & Lal, A. A. (2004). Enhanced expression of a recombinant malaria candidate vaccine in *Escherichia coli* by codon optimization. *Protein Expr Purif*, 34(1), 87-94.
- Zhu, H. M., Li, J., & Zheng, H. (2006). [Human natural infection of *Plasmodium knowlesi*]. *Zhongguo Ji Sheng Chong Xue Yu Ji Sheng Chong Bing Za Zhi*, 24(1), 70-71.
- Zimmerman, P. A., Mehlotra, R. K., Kasehagen, L. J., & Kazura, J. W. (2004). Why do we need to know more about mixed *Plasmodium* species infections in humans? *Trends Parasitol*, 20(9), 440-447.

**ONLINE REFERENCES:**

[http://bioweb.uwlax.edu/bio203/s2007/augustin\\_laur/family\\_tree.htm](http://bioweb.uwlax.edu/bio203/s2007/augustin_laur/family_tree.htm)

<http://www.guardian.co.uk/news/datablog/2012/feb/03/malaria-deaths-mortality>

<http://www.malariavaccine.org/malvac-lifecycle.php>

<http://www.qiagen.com/products/genes%20and%20pathways/Pathway%20Details.aspx?pwid=423>

<http://www.qiagen.com/products/genes%20and%20pathways/Pathway%20Details.aspx?pwid=164>

**ONLINE DATABASES:**

BLASTN and BLASTP search (<http://blast.ncbi.nlm.nih.gov/Blast.cgi>)

Codon usage database (<http://www.kazusa.or.jp/codon/>)

Compute pI/MW tool ([http://web.expasy.org/compute\\_pi/](http://web.expasy.org/compute_pi/))

ExPASy Translate tool (<http://web.expasy.org/translate/>)

*In silico* PCR amplification (<http://insilico.ehu.es/PCR/index.php>)

MedCalc-Diagnostic test evaluation ([http://www.medcalc.org/calc/diagnostic\\_test.php](http://www.medcalc.org/calc/diagnostic_test.php))

NEB cutter V2.0 (<http://tools.neb.com/NEBcutter2/>)

Protein Data Bank (PDB) (<http://www.wwpdb.org/>)

Protein Solubility Prediction tool (<http://biotech.ou.edu/>)

**Appendix 1: Chemical agents and materials.****A. Chemical agents and materials used and their sources**

<b>Materials</b>	<b>Source</b>
<b>Chemical agents:</b>	
BSA Boric acid (H <sub>3</sub> BO <sub>3</sub> ) Ethylenediamine tetraacetate (EDTA) 85 % Phosphoric acid (14.7 M) Sodium chloride (NaCl) Sodium bicarbonate (NaHCO <sub>3</sub> ) Tris, free base Tris hydrochloride (Tris-HCl) Tween 20	Amresco, USA
ABT <sup>TM</sup> Chromophore substrate solution Ampicillin Chloramphenicol Oxidized glutathione (GSSG) Reduced glutathione (GSH) Glycerol Sodium acetate (NaOAc) Sodium azide (NaN <sub>3</sub> ) Sodium iodide (NaI) Sodium fluoride (NaF) Dibasic sodium phosphate (Na <sub>2</sub> HPO <sub>4</sub> ) Monobasic sodium phosphate (NaH <sub>2</sub> PO <sub>4</sub> ) 100× Protease inhibitor Cocktail Set 1 Triton X-100	Calbiochem, Merck Millipore, Germany
30 % Acrylamide/bis stock solution Ammonium persulfate (APS) Bio-Safe <sup>TM</sup> Coomassie G-250 stain Dithiothreitol (DTT) Glycine 2× Laemmli sample buffer Sodium dodecyl sulphate (SDS) N,N,N',N'-tetramethyl-ethylenediamine (TEMED)	Bio-Rad, California
Bromophenol blue β-mercaptoethanol Dimethyl formamide (DMF) Ethidium bromide (EtBr) Polyethylene glycol-8000 Tetracycline Xylene	Sigma-Aldrich, USA
Absolute ethanol 95 % Ethanol Giemsa stain Methanol	VWR International, UK
Agarose LE IPTG Xgal	Promega, USA

**A. Chemical agents and materials used and their sources (continued)**

Materials	Source
<b>Chemical agents:</b>	
L-arginine Calcium chloride (CaCl <sub>2</sub> ) Sucrose Urea	Nacalai Tesque, Japan
L-cysteine monohydrate B-PER bacterial protein extraction reagent (in phosphate buffer)	Pierces Thermo Scientific, USA
Dream <i>Taq</i> DNA polymerase <i>Taq</i> DNA polymerase (recombinant) Maxima <sup>TM</sup> Hot Start <i>Taq</i> polymerase 50 bp DNA ladder 100 bp plus DNA ladder 1 kb DNA ladder dNTP mix Spectra <sup>TM</sup> Multicolor Broad Range Protein Ladder Fast digest restriction enzymes: <i>Bam</i> H1, <i>Spe</i> I	Fermentas Thermo Scientific, USA
Benzonase KOD Hot Start DNA polymerase Lysozyme Overnight Express <sup>TM</sup> Instant LB media	Novagen, Merck Millipore, Germany
MagicMedia <sup>TM</sup> <i>E. coli</i> expression medium RNase	Invitrogen Life Technologies, USA
LB agar LB broth 2× YT medium SOC medium Top agar	BD, US
<b>Other materials:</b>	
Tips Centrifuge tubes PCR tubes Plastic wares Pasteur pipette	Axygen Scientific, California
0.22 µm syringe filter 0.45 µm syringe filter (cellulose acetate) Vivaspin 20 concentrator	Sartorius Stedim Biotech, US
Syringe with needle	BD, US
Zeba Desalting Column Slide-A-Lyzer Dialysis Cassettes	Pierces Thermo Scientific, USA
Costar 96 well plate 50 ml Falcon tube 15 ml Falcon tube	Corning Incorporated, USA
Whatman Protran nitrocellulose membrane, 0.45µm Blotting paper	Whatman GE Healthcare, USA

**Appendix 1: Chemical agents and materials** (continued).**B. Commercial kits and their sources**

Name	Source	Application
QIAamp DNA Mini Kit	Qiagen, Germany	DNA extraction
QIAquick gel extraction kit	Qiagen, Germany	DNA purification
pCR®II-Topo TA cloning kit	Invitrogen Life Technologies, USA	DNA cloning
HiYield Plasmid Mini Kit	Yestern Biotech, Taiwan	Plasmid isolation
Profinity eXact cloning and expression starter kit Profinity eXact affinity-tagged antibody	Bio-Rad, California	Protein expression
BL21 (DE3)-RIL codon plus <i>E. coli</i>	Stratagene, US	
Bradford Protein Assay BSA standard kit	Bio-Rad, California	Protein concentration determination
NOVEX® Reversible membrane protein stain	Invitrogen Life Technologies, USA	Western blot
Opti-4CN™ substrate kit	Bio-Rad, California	
Ph.D.™-12 phage display peptide library M13 DNA marker	New England Biolabs (NEB), USA	Phage display
HRP-conjugated anti-M13 monoclonal antibody	GE Healthcare, USA	

**C. Equipments used and their sources**

Name	Source
TaKaRa PCR Thermal Cycler Dice™	TAKARA BIO, Japan
Mini-PROTEAN II Electrophoresis cell iMark microplate reader	Bio-Rad, California
Heildolph pumpdrive 5001	Heildolph, Germany
Gel electrophoresis system UV gel documentation system MS waver shaker	Major Science, USA
NanoPhotometer™	IMPLEN, Germany
Shaker incubator	Kubota, Korea
Magnetic stirrer	Eppendorf, Germany
TE70 ECL Semi-dry Transfer Unit	Amersham Biosciences, GE Healthcare, USA
ImageScanner III	GE Healthcare, USA
CT15RE refrigerated microcentrifuge	Hitachi, Japan
Velocity 14R refrigerated centrifuge	Dynamica, UK
Universal 32R refrigerated centrifuge	Hettich Zentrifugen, Germany



---

## Appendix 2: Preparation of buffers, media, and stock solutions.

### A. Common used stock solutions

0.1 M Calcium chloride ( $\text{CaCl}_2$ )

1 M Dithiothreitol (DTT)

Ethanol ( $\text{EtOH}$ )

0.5 M Ethylenediamine tetraacetic acid (EDTA), pH 8

3 M Sodium acetate ( $\text{NaOAc}$ ), pH 7.2

5 % (w/v) Sodium azide ( $\text{NaN}_3$ )

5 M Sodium chloride ( $\text{NaCl}$ )

TE-buffer, pH 8

10× Phosphate-buffered saline (PBS), pH 7.2

10× Tris-buffered saline (TBS), pH 7.5

10 % (v/v) Tween 20

1× PBST plus or 1× TBST

#### **0.1 M Calcium chloride ( $\text{CaCl}_2$ )**

$\text{CaCl}_2$  (anhydrous) 10.6 g

sdH<sub>2</sub>O to 1,000 ml

Calcium chloride was dissolved in 1 L of sdH<sub>2</sub>O, autoclaved, and stored at 4 °C.

#### **1 M Dithiothreitol (DTT)**

DTT (154.25 MW) 0.1542 g

sdH<sub>2</sub>O to 1 ml

Dithiothreitol powder was dissolved in 1 ml of sdH<sub>2</sub>O and stored in 1 ml aliquots at -20 °C. Solution was prepared just before use.

**Ethanol (EtOH)**

Ethanol was used in various concentrations (v/v), i.e., 70 and 100 %. The stock of absolute EtOH was adjusted with sdH<sub>2</sub>O accordingly.

**0.5 M Ethylenediamine tetraacetic acid (EDTA), pH 8**

EDTA free acid 14.61 g

sdH<sub>2</sub>O to 100 ml

Ethylenediamine tetraacetic acid was dissolved in 70 ml of sdH<sub>2</sub>O and stirred vigorously with a magnetic stirrer. The pH was adjusted to 8.0 with 10 M NaOH (< 5 ml) and EDTA was only dissolved at pH between 7.0 and 8.0. The solution volume was then adjusted to 100 ml, filtered, and stored at 4 °C.

**3 M Sodium acetate, pH 7.2**

Sodium acetate (anhydrose) 24.61 g

sdH<sub>2</sub>O to 100 ml

Sodium acetate was fully dissolved in 80 ml of sdH<sub>2</sub>O and the pH was adjusted to 7.2 with glacial acetic acid. The final volume of the solution was then adjusted to 100 ml with sdH<sub>2</sub>O, autoclaved and stored at room temperature.

**5 % (w/v) Sodium azide (NaN<sub>3</sub>)**

NaN<sub>3</sub> 0.5 g

sdH<sub>2</sub>O to 10 ml

Sodium azide was fully dissolved in 10 ml of sdH<sub>2</sub>O, filter sterilized, and stored at room temperature.

**5 M Sodium chloride (NaCl)**

NaCl	14.61	g
sdH <sub>2</sub> O to	50	ml

Sodium chloride was fully dissolved in 50 ml of sdH<sub>2</sub>O by vigorous stirring using magnetic stirrer bar, autoclaved, and stored at room temperature.

**TE-buffer** (10 mM Tris-HCl, 1 mM EDTA, pH 8)

Tris base	0.121	g
0.5 M EDTA	0.2	ml
sdH <sub>2</sub> O to	100	ml

The above components were dissolved in 80 ml of sdH<sub>2</sub>O and the pH was adjusted to 8 with HCl. The volume of the solution was then adjusted to 100 ml, autoclaved, and stored at room temperature.

**10× Phosphate-buffered saline (PBS), pH 7.2**

NaCl	80.0	g	
KCl	2.0	g	
Na <sub>2</sub> HPO <sub>4</sub> ·2H <sub>2</sub> O	14.4	g	(81 mM of PO <sub>4</sub> <sup>3-</sup> )
KH <sub>2</sub> PO <sub>4</sub>	2.4	g	(19 mM of PO <sub>4</sub> <sup>3-</sup> )
sdH <sub>2</sub> O to	1,000	ml	

The above components were dissolved in 800 ml of sdH<sub>2</sub>O. The pH was adjusted to 7.2 using 1 N HCl and topped up to 1 L. The solution was then autoclaved and stored at room temperature. To prepare 1× working solution [0.9% (w/v) sodium chloride in 10 mM phosphate buffer, pH 7.4], 100 ml of 10× stock was combined with 900 ml sdH<sub>2</sub>O.

**10× Tris-buffered saline (TBS) (0.5 M Tris-HCl, 1.5 M NaCl, pH 7.5)**

		<u>10× working concentration</u>	
Tris base	60.56 g	0.5	M
NaCl	87.66 g	1.5	M
sdH <sub>2</sub> O to	1,000 ml		

The above components were dissolved in 800 ml of sdH<sub>2</sub>O, adjusted the pH to 7.5 and topped up to 1 L. The solution was then autoclaved and stored at room temperature. The 100 ml of 10× TBS buffer was then diluted in 900 ml of sdH<sub>2</sub>O into 1× working concentration.

**10 % (v/v) Tween-20 stock solution**

Ten ml of Tween-20 was added to 90 ml of sdH<sub>2</sub>O. Filter sterilized and stored at room temperature.

**1× PBS plus Tween 20 (PBST) or 1× TBS plus Tween 20 (TBST)**

<b>1× PBST/1× TBST</b>	<b>+ 0.1 % Tween-20</b>	<b>+ 0.5 % Tween-20</b>
10× PBST/10× TBST	100 ml	100 ml
10 % Tween 20 (v/v)	10 ml	50 ml
sdH <sub>2</sub> O to	1,000 ml	1,000 ml

To prepare 1× PBS or 1× TBS with 0.1 % (v/v) or 0.5 % (v/v) Tween 20, 10 or 50 ml of Tween 20, respectively, was added to 100 ml of 10× TBS. Then, topped up the solution to 1 L. Filter sterilized and stored at room temperature.

**B. Stock solutions and buffers used in Giemsa staining of blood films**

Giemsa stain solution (VWR International)

Methanol (Merck)

Giemsa phosphate buffer, pH 7.2

**Giemsa phosphate buffer, pH 7.2**

KH <sub>2</sub> PO <sub>4</sub>	0.7	g
Na <sub>2</sub> HPO <sub>4</sub>	1	g
sdH <sub>2</sub> O to	1,000	ml

Above components were dissolved in 1 L of sdH<sub>2</sub>O. Adjusted the pH to 7.2, autoclaved and stored at room temperature. The buffer can last for a month.

**C. Stock solution used in malarial DNA extraction****5 % (w/v) Saponin solution**

One g of saponin was dissolved in 20 ml of sdH<sub>2</sub>O. Filtered sterilization and stored at 4 °C (Moll, Ljungström, Perlmann, Scherf, & Wahlgren, 2008). The solution can last for two weeks.

---

**D. Stock solutions and buffers used in agarose gel electrophoresis**

6× Bromophenol blue loading dye

10× Tris-borate-EDTA (TBE) buffer

Ethidium bromide (EtBr) (10 mg/ml)

**6× Bromophenol blue loading dye**

Bromophenol blue	0.25	g
Xylene cyanol	0.25	g
Glycerol	50	ml
1 M Tris, pH 8.0	1	ml
Deionized H <sub>2</sub> O to	100	ml

The 100 ml stock solution was prepared by mixing all of the above components and stored at room temperature or -20 °C.

**10× Tris-borate-EDTA (TBE) buffer, pH 8.3**

Tris base	108	g
Boric acid	55	g
0.5 M EDTA	40	ml
sdH <sub>2</sub> O to	1,000	ml

The above components were dissolved and mixed well with sdH<sub>2</sub>O to a final volume of 1 L. The solution was stored at room temperature and used as soon as possible because precipitation occurred on extensive storage period. The 10× TBE stock solution was diluted to 1× strength for routine use in agarose gel electrophoresis.

**Ethidium bromide (EtBr) (10 mg/ml)**

EtBr	100	mg
sdH <sub>2</sub> O to	10	ml

The above solution was prepared and filtered through a 0.2 µm pore size cellulose acetate membrane filter, and stored in dark at room temperature. EtBr was used at a final concentration of 0.5 µg/ml, thus 0.5 µl of stock solution was added to 100 ml molten agarose in pre-stain protocol.

**E. Stock solutions and buffers used in SDS-PAGE**

The following buffers and solutions used in resolving SDS-PAGE were made as described in Laemmli SDS-PAGE system.

10 % (w/v) Ammonium persulfate (APS)

4× Tris/SDS resolving gel buffer

4× Tris/SDS stacking gel buffer

5× Tris-glycin-SDS running buffer

2× Laemmli sample buffer

Other chemical necessities were purchased directly from the related company:

30 % Acrylamide/bis stock solution (Bio-Rad)

Bio-Safe<sup>TM</sup> Coomassie G-250 stain (Bio-Rad)

N,N,N',N'-tetramethyl-ethylenediamine (TEMED) (Bio-Rad)

**10 % (w/v) Ammonium persulfate (APS)**

APS	20	mg
sdH <sub>2</sub> O to	200	µl

The above solution was prepared freshly prior to use.

---

**4× Tris/SDS resolving gel buffer** (1.5 M Tris-HCl, 4 % SDS, pH 8.8)

Tris base	36.3 g
SDS	0.8 g
sdH <sub>2</sub> O to	200 ml

Tris base was dissolved and mixed well in 150 ml sdH<sub>2</sub>O. The pH was then adjusted to 8.8 using 1 N HCl and sdH<sub>2</sub>O was added to a final volume of 200 ml. SDS was added and mixed well. The solution was filtered and stored up to 3 months at 4 °C in the dark.

**4× Tris/SDS staking gel buffer** (0.5 M Tris-HCl, 4 % SDS, pH 6.8)

Tris base	3 g
SDS	0.2 g
sdH <sub>2</sub> O to	50 ml

Tris base was dissolved and mixed well in 40 ml of sdH<sub>2</sub>O. The pH was then adjusted to 6.8 using 1 N HCl and sdH<sub>2</sub>O was added to a final volume of 50 ml. SDS was added and mixed well. The solution was filtered and stored up to 3 months at 4 °C in the dark.

**5× Tris-glycin-SDS running buffer** (25 mM Tris, 192 mM Glycine, 0.1 % SDS, pH 8.3)

Tris base	15.1 g
Glycine	72.0 g
SDS	5.0 g
sdH <sub>2</sub> O to	1,000 ml

The above components were dissolved and mixed well with sdH<sub>2</sub>O to a final volume of 1 L and stored at room temperature for up to 1 month. The pH was not adjusted (~ 8.3). To prepare a working solution, 200 ml of 5× stock solution was diluted with 800 ml of sdH<sub>2</sub>O.



---

**2× Laemmli sample buffer** (0.125 M Tris-HCl, 4 % SDS, 20 % Glycerol, 0.02 % Bromophenol blue, 5 %  $\beta$ -mercaptoethanol, pH 6.8)

0.5 M Tris-HCl, pH 6.8	2.5	ml
10 % (w/v) SDS	4	g
Glycerol	2	ml
Bromophenol blue	2	mg
$\beta$ -mercaptoethanol	0.5	ml
sdH <sub>2</sub> O to	10	ml

The above components were dissolved and mixed well with sdH<sub>2</sub>O to a final volume of 10 ml. The solution was then dispensed into 1 ml aliquots, covered tightly and stored at -20 °C for up to 6 months. For best result,  $\beta$ -mercaptoethanol was added prior to use. Fifty  $\mu$ l of  $\beta$ -mercaptoethanol was added to the 950  $\mu$ l of sample buffer for a final concentration of 5 %  $\beta$ -mercaptoethanol.

---

**F. Stock solutions, buffers, and materials used in Western blot**

Towbin transfer buffer

1× PBST [0.1 % (v/v) Tween 20]

3 % (w/v) Blocker (BSA)

Antibody dilution buffer [1 % (w/v) BSA in PBST]

**Towbin transfer buffer** (25 mM Tris, 192 mM Glycine, 20 % Methanol, 0.1 % SDS)

Tris base	30.3	g
Glycine	144.1	g
SDS	10.0	g
Methanol	2	L
sdH <sub>2</sub> O to	10	L

Tris, glycine, and SDS were dissolved in 8 L sdH<sub>2</sub>O and the pH was measured but was not adjusted (it should be ~ 8.2-8.4). Two L of methanol was added to the solution and brought up to a final volume of 10 L with sdH<sub>2</sub>O.

**3 % (w/v) Blocker**

Twenty g of BSA powder was added slowly, a little bit at a time over a period of 30-45 minutes into 665 ml of PBST under vigorously stirring. The solution was kept on stirring for another 60 minutes after all powder had been added and warmed slowly to 55 °C to fully dissolved the BSA and then stored at 4 °C. The blocker was warmed to room temperature before use.

**Antibody dilution buffer** [1 % (w/v) BSA in PBST]

A weight of 0.75 g of BSA was dissolved in 75 ml rapidly stirring PBST. The buffer was used for dilution of primary and secondary antibodies.

---

**G. Stock solutions and buffers used in recombinant protein extraction and inclusion body (IB) purification and solubilization**

8M Urea stock, pH 8

100 mg/ml Lysozyme in B-PER reagent, -20 °C

B-PER protein extraction reagent in phosphate buffer (Pierce Biotechnology)

100× Calbiochem<sup>®</sup> Protease Inhibitor Cocktail Set I (Novagen)

The compositions of the reagents and buffers were prepared from stock solution as follows:

Bacterial lysis and extraction reagent:

B-PER, 0.2 mg/ml lysozyme, 1× protease inhibitor

IB wash 1:

B-PER, 0.2 mg/ml lysozyme, 1 % (v/v) Triton X-100, 1 M urea, 1 mM EDTA, 5 mM DTT

IB wash 2:

1:10 dilution of B-PER

IB solubilization buffer:

0.1 M Sodium phosphate, 4 M urea, 1 mM EDTA, 5 mM DTT, pH 8

**8 M Urea stock, pH 8**

Tris base	1.21	g
Urea	240.24	g
sdH <sub>2</sub> O to	500	ml

Above components were dissolved in 500 ml of sdH<sub>2</sub>O and adjusted to pH 7.2 or 8.0 with concentrated phosphoric acid. The solution was filter sterilized and stored at room temperature. The solution was prepared freshly to prevent cyanate formation.

---

**IB solubilization buffer**

			<u>Final concentration</u>	
0.2 M Sodium phosphate, pH 7.2	25	ml	100	mM
8 M Urea	25	ml	4	M
0.5 M EDTA, pH 8*	100	μl	1	mM
1 M DTT*	250	μl	5	mM
Final volume	50	ml		

Twenty five ml of each 0.2 M sodium phosphate (v/v) and 8 M urea (v/v) were mixed well. The EDTA and DTT were then added freshly to solution prior used.

---

## **H. Stock solutions and buffers used in tag-free recombinant protein isolation and purification**

The following stock solution and buffers used in Profinity exact<sup>TM</sup> purification system were made according to the manufacturer's instructions.

0.2 M Sodium phosphate, pH 7.2

0.2 M Sodium fluoride, pH 7.2

0.1 M Phosphoric acid, pH 1.8

All the working reagents and buffers used were prepared from stock solution and the compositions were as follows:

### Bind/wash buffer:

4 M Urea, 0.1 M Sodium phosphate, pH 7.2

### Stringency wash:

0.3 M Sodium acetate, 4 M urea, 0.1 M Sodium phosphate, pH 7.2

### Elution buffer:

0.1 M Sodium fluoride, 4 M urea, 0.1 M Sodium phosphate, pH 7.2

### Column regeneration buffer:

0.1 M Phosphoric acid, pH 1.8

### Column wash buffer:

0.1 M Sodium phosphate, pH 7.2

### Column storage buffer:

0.1 M Sodium phosphate, 0.02 % (w/v) Sodium azide, pH 7.2

**0.2 M Sodium phosphate, pH 7.2****0.2 M Dibasic sodium phosphate (stock solution)**

Na <sub>2</sub> HPO <sub>4</sub>	28.4	g
sdH <sub>2</sub> O to	1,000	ml

**0.2 M Monobasic sodium phosphate (stock solution)**

NaH <sub>2</sub> PO <sub>4</sub> ·H <sub>2</sub> O	13.8	g
sdH <sub>2</sub> O to	500	mL

The above sodium phosphate solutions were prepared and the pH was adjusted to 7.2 using phosphoric acid. To prepare 1 L of 0.2 M of sodium phosphate at pH 7.2, 720 ml of 0.2 M dibasic sodium phosphate was mixed with 280 ml of 0.2 M monobasic sodium phosphate, autoclaved and stored at room temperature.

**0.2 M Sodium fluoride, pH 7.2**

NaF	0.84	g
sdH <sub>2</sub> O to	100	ml

Sodium fluoride was dissolved in 100 ml of sdH<sub>2</sub>O and the pH was adjusted to 7.2 using phosphoric acid, autoclaved, and stored at room temperature.

**0.1 M Phosphoric acid, pH 1.8**

Column regeneration buffer was prepared by diluting the 0.68 ml of 85 % (14.7 M) concentrated phosphoric acid into 99.32 ml of sdH<sub>2</sub>O.

**I. Stock solutions and buffers used in protein renaturation**

1 M Sodium phosphate, pH 8

1 M Tris phosphate, pH 8

8 M Urea

5× Dialysis buffer stock (250 mM Tris phosphate, 2 M L-arginine, pH 8)

All the buffers used were prepared from stock solution and the compositions were as follows:

**Buffer exchange:**

50 mM Tris phosphate, 4 M urea, pH 8

**Refolding sample buffer:**

1 mg/ml recombinant protein in 50 mM Tris Phosphate, 4 M urea, 1 mM EDTA, 1 mM reduced glutathione (GSH), 0.25 mM oxidized glutathione (GSSG), 1× protease inhibitor cocktail

**Dialysis buffers:**

50 mM Tris phosphate, 0.4 M L-arginine, 1 mM EDTA, 2 M urea, pH 8

50 mM Tris phosphate, 0.4 M L-arginine, 1 mM EDTA, 1 M urea, pH 8

25 mM Tris phosphate, 50 mM NaCl, pH 8

**1 M Tris phosphate, pH 8**

Tris base	60.56 g
-----------	---------

sdH <sub>2</sub> O to	500 ml
-----------------------	--------

Tris base was dissolved in 500 ml of sdH<sub>2</sub>O and pH was adjusted with concentrated phosphoric acid, then filter sterilized and stored at room temperature.

**200 mM reduced glutathione (GSH)**

A total of 61.4 mg of GSH (307.33 MW) powder was dissolved in 1 ml of sdH<sub>2</sub>O. The solution was freshly prepared before use.

**100 mM oxidized glutathione (GSSG)**

A total of 61.2 mg of GSSG (612.64 MW) powder was dissolved in 1 ml of sdH<sub>2</sub>O. The solution was freshly prepared before use.

**5× Dialysis buffer stock (250 mM Tris phosphate, 2 M L-arginine, pH 8)**

Tris base	15.14 g
L-arginine	174.2 g
sdH <sub>2</sub> O to	500 ml

Above components were dissolved in 400 ml of sdH<sub>2</sub>O with vigorous stirring. The pH was adjusted to 8.0 with concentrated phosphoric acid. The solution was then topped up to 500 ml, autoclaved and stored at 4 °C. The 5× dialysis buffer stock solution was diluted to 1× strength for the first and second rounds of dialysis.



---

## **J. Stock solutions and buffers used in biopanning**

All the buffers used in biopanning were prepared as described (Barbas, et al., 2001).

### **Immobilized buffer:**

0.1 M Sodium bicarbonate ( $\text{NaHCO}_3$ ), pH 8.6

### **Blocking buffer:**

5 mg/ml of BSA in  $\text{NaHCO}_3$ , pH 8.6

### **Biopanning and washing buffer:**

TBST

### **Glycine elution buffer:**

1 mg/ml BSA, 0.2 M Glycine-HCl, pH 2.2

### **Neutralization Buffer:**

1 M Tris-HCl, pH 9.1

## **0.1 M Sodium bicarbonate ( $\text{NaHCO}_3$ ), pH 8.6**

$\text{NaHCO}_3$	0.84	g
------------------	------	---

sdH <sub>2</sub> O	100	ml
--------------------	-----	----

Sodium bicarbonate was dissolved in 100 ml of sdH<sub>2</sub>O. The pH was adjusted to 8.6 and filter sterilized and stored at room temperature.

## **Blocking buffer**

The blocking buffer was freshly prepared by dissolving 5 mg/ml of bovine serum albumin (BSA) (Amresco) in immobilized buffer and 0.02 %  $\text{NaN}_3$  was then added to the solution, filter sterilized and stored at 4 °C.

**1 mg/ml of BSA, 0.2 M Glycine-HCl, pH 2.2**

Glycine	0.75	g
BSA	0.05	g
sdH <sub>2</sub> O to	50	ml

The above component was dissolved in 50 ml of sdH<sub>2</sub>O and the pH was adjusted to 2.2 with concentrated HCl. Filter sterilized and stored at 4°C.

**1 M Tris-HCl, pH 9.1**

Tris base	6.06	g
sdH <sub>2</sub> O to	50	ml

Tris base was dissolved in 50 ml of sdH<sub>2</sub>O and the pH was adjusted to 9.1 with concentrated HCl, filter sterilized and stored at room temperature.

**K. Stock solution used in phage precipitation****20 % (w/v) PEG/2.5 M NaCl**

Polyethylene glycol-8000	40	g
NaCl	29.22	g
sdH <sub>2</sub> O to	200	ml

The above components were dissolved in sdH<sub>2</sub>O by vigorous stirring using magnetic stirrer and then autoclaved. The two separated layers of solution were mixed by vigorous stirring while still in warm after autoclave and the mixture was stored at room temperature.

---

**L. Buffer used in single-strand M13 phage DNA extraction**
**Iodide buffer**

		<u>Final concentration</u>
1 M Tris base	0.121 g	10 mM
Sodium iodide (NaI)	59.96 g	4 M
0.5 M EDTA	0.2 ml	1 mM
sdH <sub>2</sub> O to	100 ml	

The above components were dissolved in 100 ml of sdH<sub>2</sub>O, filter sterilized and stored at room temperature in the dark. The solution was discarded if color is evident.

**M. Stock solutions and buffers used in phage ELISA**

All the buffers used were prepared from stock solution and the compositions were as follows:

Blocking buffer:

0.5 mg/ml BSA, 0.1 M NaHCO<sub>3</sub>, pH 8.6, 0.02 % (w/v) NaN<sub>3</sub>

Wash buffer:

TBST [TBS plus 0.5 % (v/v) Tween 20]

Secondary antibody:

1:5000 HRP-conjugated anti-M13 antibody (GE Healthcare) in blocking buffer

HRP substrate:

ABTS<sup>Tm</sup> Chromophore substrate solution (Calbiochem)

ABTS stop solution:

0.5 M Sulfuric acid

**0.5 M Sulfuric acid**

Sulfuric acid solution was prepared by adding 2.8 ml of 96 % concentrated H<sub>2</sub>SO<sub>4</sub> (18 M) into 97.2 ml of sdH<sub>2</sub>O.

---

---

**N. Media, antibiotics, and stock solutions used in bacteria cultivation and phage amplification**

LB broth

LB agar

SOC broth

Top agar

2× Yeast Extract Tryptone (YT) broth

100 mg/ml Ampicilin stock

34 mg/ml Chloramphenicol stock

20 mg/ml Tetracycline stock

100 mg/ml IPTG stock

50 mg/ml Xgal stock

**LB broth**

Bacto-Tryptone	10	g
Yeast extract	5	g
NaCl	5	g
sdH <sub>2</sub> O to	1	L

The above components were dissolved and mixed well with sdH<sub>2</sub>O to a final volume of 1 L, autoclaved, and stored at 4 °C. Appropriate antibiotics were added freshly to the broth prior to use.

---

**LB agar**

Fifteen g of Bacto agar was added to LB medium components and then dissolved in 1 L of sdH<sub>2</sub>O, and autoclaved. Autoclaved media was cooled to 55 °C before antibiotic or enzyme was added. The solution was mixed by gentle swirling and ~ 20 ml of molten agar was poured into Petri dish, and allowed to solidify at room temperature. Agar plates can store up to a month at 4 °C.

**SOC broth**

Bacto-Tryptone	2	g
Yeast extract	0.5	g
NaCl	0.05	g
sdH <sub>2</sub> O to	100	ml

The above components were dissolved in 100 ml of sdH<sub>2</sub>O, then autoclaved, and stored at 4 °C. Prior to use, 0.5 ml of 2 M of MgCl<sub>2</sub> and 2 ml of 1 M glucose (both sterilized) were added to the broth.

**Top agar**

Bacto-Tryptone	1	g
Yeast extract	0.5	g
NaCl	0.5	g
Bacto agar	0.7	g
sdH <sub>2</sub> O to	100	ml

The above components were dissolved in 100 ml of sdH<sub>2</sub>O, autoclaved, and stored solid at room temperature. The solidified agar was then melted in microwave as needed.

**2× YT broth**

Tryptone	16	g
Yeast extract	10	g
Sodium chloride	5	g
sdH <sub>2</sub> O to	1000	ml

The above components were dissolved in 1L of sdH<sub>2</sub>O, autoclaved, and stored at 4 °C.

Appropriate antibiotics were added freshly to broth prior use.

**100 mg/ml Ampicillin stock**

One g of ampicillin was dissolved with sterilized sdH<sub>2</sub>O to a final volume of 10 ml. The solution was filter sterilized and dispensed into 1.0 ml aliquots, and stored at -20 °C.

**34 mg/ml Chloramphenicol stock**

Thirty four mg of chloramphenicol was dissolved in 1 ml of ethanol and stored at -20 °C.

**20 mg/ml Tetracycline stock**

Twenty mg of tetracycline was dissolved in 1:1 of ethanol:water and stored at -20 °C.

The stock solution was mixed well by vortex before each use.

**100 mg/ml IPTG stock**

One g of IPTG (isopropyl-β-D-thiogalactoside) was dissolved in 10 ml of sdH<sub>2</sub>O, filter sterilized, and dispensed into 1 ml aliquots, before being stored at -20 °C.

**40 mg/ml Xgal stock**

One g of Xgal (5-bromo-4-chloro-3-β-D-galactoside) was dissolved in 25 ml DMF (dimethyl formamide) and stored at -20 °C.

### Appendix 3: PCR reagents and oligonucleotide primers.

#### A. PCR reagents

PCR reagents	Storage buffer	Supplements	Applications
Dream™ <i>Taq</i> DNA polymerase (5 U/μl)	20 mM Tris-HCl (pH 8), 1 mM DTT, 0.1 mM EDTA, 100 mM KCl, stabilizing agent, 50 % (v/v) glycerol	✓ 10× Dream buffer (containing 15 mM MgCl <sub>2</sub> ) ✓ 25 mM MgCl <sub>2</sub>	First nested PCR DNA cloning
Recombinant <i>Taq</i> DNA polymerase (5 U/μl)	20 mM Tris-HCl (pH 8), 1 mM DTT, 0.1 mM EDTA, 100 mM KCl, 0.5 % (v/v) Nonidet P40, 0.5 % (v/v) Tween 20, 50 % (v/v) glycerol	✓ 10× <i>Taq</i> buffer [100 mM Tris-HCl (pH 8.8), 500 mM KCl, 0.8 (v/v) Nonidet P40] ✓ 25 mM MgCl <sub>2</sub>	Second nested PCR Colony PCR
Maxima™ Hot Start <i>Taq</i> DNA polymerase (5 U/μl)	20 mM Tris-HCl (pH 9.0), 1 mM DTT, 0.1 mM EDTA, 100 mM KCl, 0.5 % (v/v) Tween 20, 0.5 % (v/v) Nonidet P40, 50 % (v/v) glycerol	✓ 10× Hot Start buffer [200 mM Tris-HCl (pH 8.3), 200 mM KCl, 50 mM (NH <sub>4</sub> ) <sub>2</sub> SO <sub>4</sub> ] ✓ 25 mM MgCl <sub>2</sub>	Multiplex PCR assay
KOD Hot Start DNA polymerase (1 U/μl)	50 mM Tris-HCl, 1 mM DTT, 0.1 mM EDTA, 50 % (v/v) glycerol, 0.001 % (v/v) Nonidet P-40, 0.001 % (v/v) Tween 20, pH 8	✓ 10× KOD PCR buffer ✓ 25 mM MgSO <sub>4</sub> ✓ 2 mM dNTP mix	Recombinant protein expression
10 mM dNTP mix	-	-	PCR reagent

\*Proper thaw and well mixed of the 10× PCR buffer and Mg<sup>2+</sup> stock solution were required to avoid formation of concentration gradients in master mixture preparation.

**Appendix 3: PCR reagents and oligonucleotide primers (continued).****B. Primers used in nested PCR**

Primer	Primer sequence (5' - 3')	Size (bp)	References
rPLU1	TCAAAGATTAAGCCATGCAAGTGA	1,600-1,700	Snounou, et al., 1993; Singh, et al., 1999
rPLU5	CCT GTTGTTGCCTTAAACTCC		
rFAL1	TTAAACTGGTTTGGGAAAACCAAATATATT	205	
rFAL2	ACACAATGAACTCAATCATGACTACCCGTC		
rVIV1	CGCTTCTAGCTTAATCCACATAACTGATAC	117	
rVIV2	ACTTCCAAGCCGAAGCAAAGAAAGTCCTTA		
rMAL1	ATAACATAGTTGTACGTTAAGAATAACCGC	144	
rMAL2	AAAATTCCCATGCATAAAAAATTATACAAA		
rOVA1	ATCTCT TTTGCTATTTTTTAGTATTGGAGA	787	Singh, et al., 1999
rOVA2	GGAAAAGGACACATTAATTGTATCCTAGTG		
rPO (F)	CGTTAAGAATAAACGCCAAGCG	375	Padley, et al., 2003
Conserve	GTATCTGATCGTCTTCACTCCC		
Pmk8	GTTAGCGAGAGCCACAAAAAAGCG	153	Singh, et al., 2004
Pmrk9	ACTCAAAGTAACAAAATCTTCC		

**C. Primers used in colony PCR and DNA sequencing**

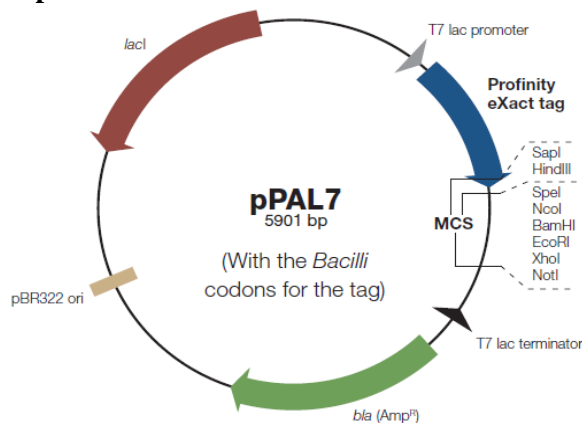
Primer	Primer sequence (5'- 3')	Application
M13 (-20)-F	GTAAAACGACGGCCAG	Colony PCR and sequencing
M13-R	CAGGAAACAGCTATGAC	
SP6	TATTTAGGTGACACTATAG	
T7 promoter	TAATACGACTCACTATAGGG	
T7 terminator	GCTAGTTATTGCTCAGCGG	
pPAL7 internal	GTGCTTCAAATATGTAGACGCA	
-96 gIII	CCCTCATAGTTAGCGTAACG	Phage sequencing



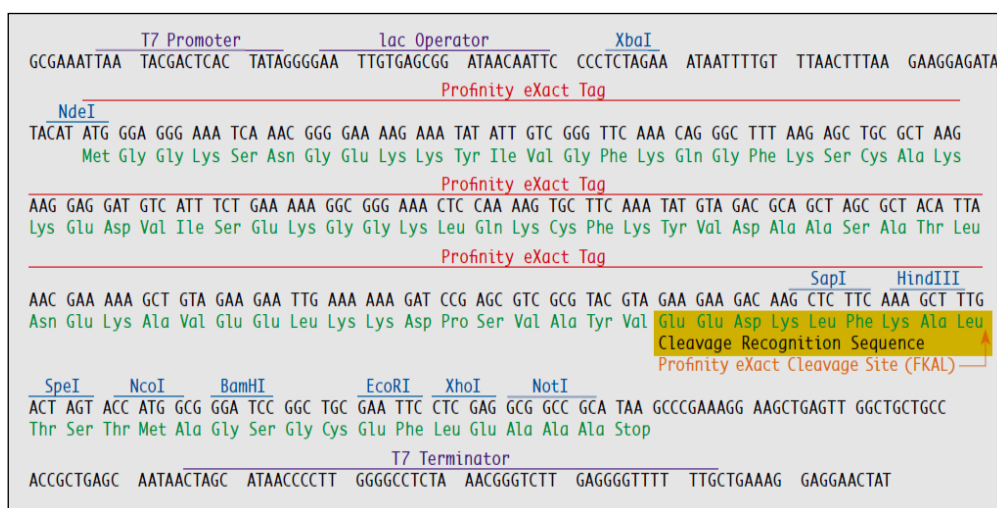
## Appendix 4: Overview of recombinant protein production using Profinity eXact™ System.

(A) The pPAL7 vector with Profinity eXact tag; (B) Multiple cloning sites (MCS) and Profinity eXact cleavage site (FKAL); (C) Single step affinity purification and tag cleavage of recombinant protein.

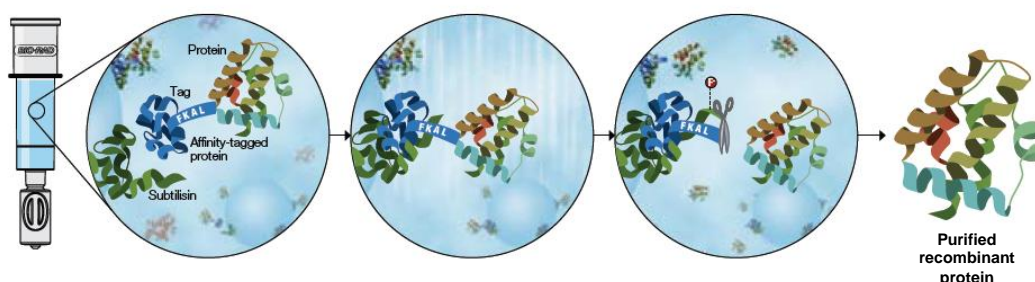
### A. Profinity eXact pPAL7 vector



### B. Cloning and expression region



### C. Single step on-column purification and tag removal



## Appendix 5.1: BLASTN search of recombinant PkAMA1.

*Plasmodium knowlesi* strain H apical merozoite antigen 1 (PKH\_093110) mRNA, complete cds  
Sequence ID: ref|XM\_002259303.1|  
Length: 1692  
Number of Matches: 1

Score	Expect	Identities	Gaps	Strand
2460 bits (1332)	0.0	1336/1338 (99%)	0/1338 (0%)	Plus/Plus
Query 1	GGGCCTATCATTGAGAGAAGTATACGAATGAGTAACCCATGGAAAGCCTTCATGGAAAAAG	60		
Sbjct 124	GGGCCTATCATTGAGAGAAGTATACGAATGAGTAACCCATGGAAAGCCTTCATGGAAAAAG	183		
Query 61	TATGATTTAGAGAGACACACAATTCGGGATTAGAATTGATTAGGGGAAGATGCAGAA	120		
Sbjct 184	TATGATTTAGAAAGAGCACACAATTCGGGATTAGAATTGATTAGGGGAAGATGCAGAA	243		
Query 121	GTGGGAAATTCGAAGTATAGAATACCAAGCTGGAAAAATGTCCAGTTTTTGGAAAGGGTATC	180		
Sbjct 244	GTGGGAAATTCGAAGTATAGAATACCAAGCTGGAAAAATGTCCAGTTTTTGGAAAGGGTATC	303		
Query 181	GTTATAGAAAAATCTAACGTTAGCTTCTTAACACCCGTAGCTACAGGAGCTCAAAGGTTG	240		
Sbjct 304	GTTATAGAAAAATCTAACGTTAGCTTCTTAACACCCGTAGCTACAGGAGCTCAGAGGTTG	363		
Query 241	AAGGAAGGAGGTTTCGCCCTTCCCAATGCAGATGACCACATTTCCCTATAACAATAGCA	300		
Sbjct 364	AAGGAAGGAGGTTTCGCCCTTCCCAATGCAGATGACCACATTTCCCTATAACAATAGCA	423		
Query 301	AACCTTAAGAGAGGTATAAAGAAAAATGCAGATTGATGAAATTAATGATATAGCCTTG	360		
Sbjct 424	AACCTTAAGAGAGGTATAAAGAAAAATGCAGATTGATGAAATTAATGATATAGCCTTG	483		
Query 361	TGTAAAACGCATGCAGCCAGCTTTGTCTATGCAGAGGATCAAAATACATCTTACAGACAT	420		
Sbjct 484	TGTAAAACGCATGCAGCCAGCTTTGTCTATGCAGAGGATCAAAATACATCTTACAGACAT	543		
Query 421	CCAGCTGTTTATGACGAAAAGAATAAAACATGTTACATGTTGTATTGTCAGCGCAAGAA	480		
Sbjct 544	CCAGCTGTTTATGACGAAAAGAATAAAACATGTTACATGTTGTATTGTCAGCGCAAGAA	603		
Query 481	AATATGGGTCCACGATACTGTAGCCAGATTACAAAAATAAGACGCCATGTTTGTCTTC	540		
Sbjct 604	AATATGGGTCCACGATACTGTAGCCAGATTACAAAAATAAGACGCCATGTTTGTCTTC	663		
Query 541	AAGCCAGATAAAAAATGAAAAATTTGACAACCTGGTGTATTTAAGCAAAAACGTAAGTAAT	600		
Sbjct 664	AAGCCAGATAAAAAATGAAAAATTTGACAACCTGGTGTATTTAAGCAAAAACGTAAGTAAT	723		
Query 601	GATTGGGAAAAACAAGTGCCCGCGTAAAAATTTAGGAAACGCAAAATTTGGATTATGGGTG	660		
Sbjct 724	GATTGGGAAAAACAAGTGCCCGCGTAAAAATTTAGGAAACGCAAAATTTGGATTATGGGTG	783		
Query 661	GATGGGAACGTGAAGAAATACCATACGTTAATGAAGTGGAGGCAAGGAGCCTACGGGAA	720		
Sbjct 784	GATGGGAACGTGAAGAAATACCATACGTTAATGAAGTGGAGGCAAGGAGCCTACGGGAA	843		
Query 721	TGCAACCGAATCGTTTTTCGAAGCTAGCGCTTCAGATCAACCACGTCAGTACGAAGAAGAA	780		
Sbjct 844	TGCAACCGAATCGTTTTTCGAAGCTAGCGCTTCAGATCAACCACGTCAGTACGAAGAAGAA	903		
Query 781	CTGACAGATTATGAAAAAATACAAGAGGGATTAGACAAAATAATCGGGACATGATTAAA	840		
Sbjct 904	CTGACAGATTATGAAAAAATACAAGAGGGATTAGACAAAATAATCGGGACATGATTAAA	963		
Query 841	AGTGCCTTTCTTCCAGTGGGTGCATTTAACTCAGACAATTTTAAGAGTAAAGGAAGAGGA	900		
Sbjct 964	AGTGCCTTTCTTCCAGTGGGTGCATTTAACTCAGACAATTTTAAGAGTAAAGGAAGAGGA	1023		
Query 901	TATAACTGGGCAAAATTCGATTCTGTAATAATAAGTGTTACATTTTTAATACCAAACT	960		
Sbjct 1024	TATAACTGGGCAAAATTCGATTCTGTAATAATAAGTGTTACATTTTTAATACCAAACT	1083		
Query 961	ACGTGCTCATTAAATGACAAAAATTTTTTGCAACAACAGCGTTATCTCACCCCTCAAGAA	1020		
Sbjct 1084	ACGTGCTCATTAAATGACAAAAATTTTTTGCAACAACAGCGTTATCTCACCCCTCAAGAA	1143		
Query 1021	GTAGACAATGAATTTCCATGCAGCATATACAAAGATGAAATTGAAAGAGAAATTAAGAAA	1080		
Sbjct 1144	GTAGACAATGAATTTCCATGCAGCATATACAAAGATGAAATTGAAAGAGAAATTAAGAAA	1203		
Query 1081	CAGTCGAGAAATATGAATCTGTACAGTGTGATAAGGAACGGATTGCTTGCCAAGGATA	1140		
Sbjct 1204	CAGTCGAGAAATATGAATCTGTACAGTGTGATAAGGAACGGATTGCTTGCCAAGGATA	1263		
Query 1141	TTTATCTCCACCGATAAGGAGAGTATCAAATGCCATGTGAGCCTGAACACATTTCCAAT	1200		
Sbjct 1264	TTTATCTCCACCGATAAGGAGAGTATCAAATGCCATGTGAGCCTGAACACATTTCCAAT	1323		
Query 1201	AGTACCTGCAACTTTTACGTTTGTAAGTGTGTAGAGAAGAGAGCAGAAATTAAGGAAAAAT	1260		
Sbjct 1324	AGTACCTGCAACTTTTACGTTTGTAAGTGTGTAGAGAAGAGAGCAGAAATTAAGGAAAAAT	1383		
Query 1261	AACGAAGTTATCATAAAGGAAGAATTTAAGGAGGATTATGAAAAATCCGGACGGCAAAACAT	1320		
Sbjct 1384	AACGAAGTTATCATAAAGGAAGAATTTAAGGAGGATTATGAAAAATCCGGACGGCAAAACAT	1443		
Query 1321	AAGAAGAAGATGCTACTA	1338		
Sbjct 1444	AAGAAGAAGATGCTACTA	1461		

## Appendix 5.2: BLASTN search of recombinant PvAMA1.

*Plasmodium vivax* isolate CTra26 apical membrane protein-1 (AMA-1) gene, complete cds  
Sequence ID: gb|FJ785007.1|  
Length: 1689  
Number of Matches: 1

Score	Expect	Identities	Gaps	Strand
2466 bits (1335)	0.0	1337/1338 (99%)	0/1338 (0%)	Plus/Plus
Query 1	GGGCCTACCGTTGAGAGGAGCACACGAATGAGTAACCCCTGGAAAGCGTTCATGGAAAAA	60		
Sbjct 124	GGGCCTACCGTTGAGAGGAGCACACGAATGAGTAACCCCTGGAAAGCGTTCATGGAAAAA	183		
Query 61	TACGACATCGAAAGAACACACAGTTCTGGGGTTCGAGTGGATTAGGGGAAGATGCAGAA	120		
Sbjct 184	TACGACATCGAAAGAACACACAGTTCTGGGGTTCGAGTGGATTAGGGGAAGATGCAGAA	243		
Query 121	GTGGAAATGCAAAGTACAGAATCCAGCTGGAAGATGTCCTGTTTTGGAAAGGGTATC	180		
Sbjct 244	GTGGAAATGCAAAGTACAGAATCCAGCTGGAAGATGTCCTGTTTTGGAAAGGGTATC	303		
Query 181	GTCATAGAGAATTCCGCTGTTAGCTTCTTAAACCTGTGGCTACAGGAGATCAGAGGCTG	240		
Sbjct 304	GTCATAGAGAATTCCGCTGTTAGCTTCTTAAACCTGTGGCTACAGGAGATCAGAGGCTG	363		
Query 241	AAGGATGGAGGTTTCGCCCTTCCCAATGCGAATGACCATATCTCCCCATGACAATAGCG	300		
Sbjct 364	AAGGATGGAGGTTTCGCCCTTCCCAATGCGAATGACCATATCTCCCCATGACAATAGCG	423		
Query 301	AACCTTAAGGCAAGGTATAAAGACAATGTAGAGATGATGAAGTTAAACGATATAGCTTTG	360		
Sbjct 424	AACCTTAAGGCAAGGTATAAAGACAATGTAGAGATGATGAAGTTAAACGATATAGCTTTG	483		
Query 361	TGCAGAACCCACGCGCTAGCTTTGTCATGGCAGGGGATCAAAATTCGTCCTACAGACAC	420		
Sbjct 484	TGCAGAACCCACGCGCTAGCTTTGTCATGGCAGGGGATCAAAATTCGTCCTACAGACAC	543		
Query 421	CCAGCTGTATACGACGAAAAGGAAAAACATGCCACATGTTGTATTTATCAGCGCAGGAA	480		
Sbjct 544	CCAGCTGTATACGACGAAAAGGAAAAACATGCCACATGTTGTATTTATCAGCGCAGGAA	603		
Query 481	AATATGGGTCCGAGGTACTGCAGCCAGATGCACAAATAGAGATGCCGTGTTCTGCTTC	540		
Sbjct 604	AATATGGGTCCGAGGTACTGCAGCCAGATGCACAAATAGAGATGCCGTGTTCTGCTTC	663		
Query 541	AAGCCAGATAAAAAATGAAAGCTTTGAAAACCTGGTGTATTTGAGCAAAAATGTGCGTAAT	600		
Sbjct 664	AAGCCAGATAAAAAATGAAAGCTTTGAAAACCTGGTGTATTTGAGCAAAAATGTGCGTAAT	723		
Query 601	GATTGGGATAAAAAATGCCCCCGTAAAAATTTAGGAAACGCCAAGTTCGGATTATGGGTG	660		
Sbjct 724	GATTGGGATAAAAAATGCCCCCGTAAAAATTTAGGAAACGCCAAGTTCGGATTATGGGTG	783		
Query 661	GATGGGAACGCGAAGAAATTCATACGTTAAAGAAGTGGAGGCAAGGATCTGCGCGAA	720		
Sbjct 784	GATGGGAACGCGAAGAAATTCATACGTTAAAGAAGTGGAGGCAAGGATCTGCGCGAA	843		
Query 721	TGCAACCGAATCGTTTTTCGAAGCGAGTGCCTCAGATCAACCAACTCAGTATGAAGAAGAA	780		
Sbjct 844	TGCAACCGAATCGTTTTTCGAAGCGAGTGCCTCAGATCAACCAACTCAGTATGAAGAAGAA	903		
Query 781	ATGACGGATTATCAAAAAATACAACAAGGGTTTAGACAAAACAACCGAGAGATGATTAAT	840		
Sbjct 904	ATGACGGATTATCAAAAAATACAACAAGGGTTTAGACAAAACAACCGAGAGATGATTAAT	963		
Query 841	AGTGCCTTTCTTCCAGTGGGTGCATTCAACTCGGATAATTTCAAAGTAAAGGAAGAGGA	900		
Sbjct 964	AGTGCCTTTCTTCCAGTGGGTGCATTCAACTCGGATAATTTCAAAGTAAAGGAAGAGGA	1023		
Query 901	TTTAAGTGGGCAAAATTCGATTCTGTAAAAAAGAAGTGTACATCTTTAATACCAACCG	960		
Sbjct 1024	TTTAAGTGGGCAAAATTCGATTCTGTAAAAAAGAAGTGTACATCTTTAATACCAACCG	1083		
Query 961	ACTTGCCCTCATTAATGACAAAAATTTTATTGCAACAACGGCGTTATCTCACCACAAGAA	1020		
Sbjct 1084	ACTTGCCCTCATTAATGACAAAAATTTTATTGCAACAACGGCGTTATCTCACCACAAGAA	1143		
Query 1021	GTAGACCCGGAGTCCCGCTGCAGCATATATAAGACGAAATTGAAAGAGAAATTAAGAAA	1080		
Sbjct 1144	GTAGACCCGGAGTCCCGCTGCAGCATATATAAGACGAAATTGAAAGAGAAATTAAGAAA	1203		
Query 1081	CAATCGAGGAACATGAATCTGTACAGTGTGATGGGGAACGCATTGTCCTGCCGAGGATA	1140		
Sbjct 1204	CAATCGAGGAACATGAATCTGTACAGTGTGATGGGGAACGCATTGTCCTGCCGAGGATA	1263		
Query 1141	TTTATCTCCAACGATAAGGAGAGTATCAAATGTCCTGCGAACCTGAGCACATTTCCAAC	1200		
Sbjct 1264	TTTATCTCCAACGATAAGGAGAGTATCAAATGTCCTGCGAACCTGAGCACATTTCCAAC	1323		
Query 1201	AGTACCTGCAACTTTTACGTTTGTAAGTGTGTAGAGAAAAGGGCGGAAATTAAGGAAAT	1260		
Sbjct 1324	AGTACCTGCAACTTTTACGTTTGTAAGTGTGTAGAGAAAAGGGCGGAAATTAAGGAAAT	1383		
Query 1261	AACCAAGTTGTTATAAAGGAAGAATTTAGGGATTATTACGAAAAATGGGAGGAAAAATCG	1320		
Sbjct 1384	AACCAAGTTGTTATAAAGGAAGAATTTAGGGATTATTACGAAAAATGGGAGGAAAAATCG	1443		
Query 1321	AACAAGCAGATGCTACTA	1338		
Sbjct 1444	AACAAGCAGATGCTACTA	1461		

### Appendix 5.3: BLASTP search of recombinant PkAMA1.

Apical merozoite antigen 1 [*Plasmodium knowlesi* strain H]

Sequence ID: ref|XP\_002259339.1|

Length: 563

Number of Matches: 1

Score	Expect	Method	Identities	Positives	Gaps
929 bits (2401)	0.0	Compositional matrix adjust.	446/446 (100%)	446/446 (100%)	0/446 (0%)
Query 1	GPIIERSIRMSNPWKAFMEKYDLERAHNSGIRIDLGEDAEVGNISKYRIPAGKCPVFGKGI				60
Sbjct 42	GPIIERSIRMSNPWKAFMEKYDLERAHNSGIRIDLGEDAEVGNISKYRIPAGKCPVFGKGI				101
Query 61	VIENSNVSFLTPVATGAQRLKEGGFAFPNADDHISPITIANLKERYKENADLMKLNIDIAL				120
Sbjct 102	VIENSNVSFLTPVATGAQRLKEGGFAFPNADDHISPITIANLKERYKENADLMKLNIDIAL				161
Query 121	CKTHAASFVIAEDQNTSYRHPAVYDEKNKTCYMLYLSAQENMGPRYCSFDSQNKDAMFCF				180
Sbjct 162	CKTHAASFVIAEDQNTSYRHPAVYDEKNKTCYMLYLSAQENMGPRYCSFDSQNKDAMFCF				221
Query 181	KPKNEKFDNLVYLSKNVSNWENKCPKRNKLGNAKFGWVDGNCEEIPYVNEVEARSLRE				240
Sbjct 222	KPKNEKFDNLVYLSKNVSNWENKCPKRNKLGNAKFGWVDGNCEEIPYVNEVEARSLRE				281
Query 241	CNRIVFEASASDQPRQYEEELTDYEKIQEGFRQNNRDMIKSAFLPVGAFNSDNFKSKGRG				300
Sbjct 282	CNRIVFEASASDQPRQYEEELTDYEKIQEGFRQNNRDMIKSAFLPVGAFNSDNFKSKGRG				341
Query 301	YNWANFDSVNNKCYIFNTKPTCLINDKNFFATTALSHPQEVDFNEFPCSIYKDEIEREIKK				360
Sbjct 342	YNWANFDSVNNKCYIFNTKPTCLINDKNFFATTALSHPQEVDFNEFPCSIYKDEIEREIKK				401
Query 361	QSRNMNLYSVDKERIVLPRIFISTDKESIKCPCEPEHISNSTCNFYVCNCVEKRAEIKEN				420
Sbjct 402	QSRNMNLYSVDKERIVLPRIFISTDKESIKCPCEPEHISNSTCNFYVCNCVEKRAEIKEN				461
Query 421	NEVIIKEEFKEDYENPDGKHKKKMLL				446
Sbjct 462	NEVIIKEEFKEDYENPDGKHKKKMLL				487

## Appendix 5.4: BLASTP search of recombinant PvAMA1.

Apical membrane protein-1 [*Plasmodium vivax*]

Sequence ID: gb|ACY68841.1|

Length: 562

Number of Matches: 1

Score	Expect	Method	Identities	Positives	Gaps
932 bits (2410)	0.0	Compositional matrix adjust.	446/446 (100%)	446/446 (100%)	0/446 (0%)
Query 1	GPTVERSTRMSNPWKAFMEKYDIERTHSSGVRVDLGEDAEVENAKYRIPAGRCPVFGKGI				60
Sbjct 42	GPTVERSTRMSNPWKAFMEKYDIERTHSSGVRVDLGEDAEVENAKYRIPAGRCPVFGKGI				101
Query 61	VIENSAVSFLKPVATGDQRLKDGGFAFPNANDHISPMTIANLKARYKDNVEMMKLNDIAL				120
Sbjct 102	VIENSAVSFLKPVATGDQRLKDGGFAFPNANDHISPMTIANLKARYKDNVEMMKLNDIAL				161
Query 121	CRTHAASFVMAGDQNSSYRHPAVYDEKEKTCHMLYLSAQENMGPRYCSFDAQNRDAVFCF				180
Sbjct 162	CRTHAASFVMAGDQNSSYRHPAVYDEKEKTCHMLYLSAQENMGPRYCSFDAQNRDAVFCF				221
Query 181	KPDKNESFENLVYLSKNVRNDWDKKCPRKNLGNKAFGLWVDGNCEEIPYVKEVEAKDLRE				240
Sbjct 222	KPDKNESFENLVYLSKNVRNDWDKKCPRKNLGNKAFGLWVDGNCEEIPYVKEVEAKDLRE				281
Query 241	CNRIVFEASASDQPTQYEEEMTDYQKIQQGFRQNNREMIKSAFLPVGAFNSDNFKSKGRG				300
Sbjct 282	CNRIVFEASASDQPTQYEEEMTDYQKIQQGFRQNNREMIKSAFLPVGAFNSDNFKSKGRG				341
Query 301	FNWANFDSVKKKCYIFNTKPTCLINDKNFIATTALSHPQEVDPFPCSIYKDEIEREIKK				360
Sbjct 342	FNWANFDSVKKKCYIFNTKPTCLINDKNFIATTALSHPQEVDPFPCSIYKDEIEREIKK				401
Query 361	QSRNMNLYSVDGERIVLPRIFISNDKESIKCPCEPEHISNSTCNFYVCNCVEKRAEIKEN				420
Sbjct 402	QSRNMNLYSVDGERIVLPRIFISNDKESIKCPCEPEHISNSTCNFYVCNCVEKRAEIKEN				461
Query 421	NQVVIKEEFRDYYENGEEKSNKQMLL		446		
Sbjct 462	NQVVIKEEFRDYYENGEEKSNKQMLL		487		

## Appendix 6: LC-MS/MS results and analysis.

Matched peptides were indicated in green for the rPkAMA1 (A) and rPvAMA1 (B).

### **(A) rPkAMA1**

GPIIERSI**RMSNPWKAFMEKYDLERA**HNSGI**RIDLGEDAEVGN**SKYRI**PAGKC**PVF  
**GKGIVIENS**NVS**FLTPVATGAQRLKEGGFAFPNADDHIS**PITIAN**LKERYKENADL**  
**MKLNDIALCKTHAASFVIAEDQNTSYRHPAVYDEKN**KTCYMLYLSAQENMGPRYCS  
PDSQNKDAMFCFKPDKNEKFDNLVYLS**KNVSNDWENKC**PRKNLGNAKFGLWVDGNC  
EEIPYVNEVEARS**LRECNRIVFEASASDQPRQYEEELTDYEKIQEGFRQNNRDMIK**  
**SAFLPVGAFN**SDNF**SKGRGYNWANFDSVNNKCYIFNTKPTCLINDKNFFATTALS**  
HPQEVDFEFPCSIYKDEIEREIKKQS**RNMNLYSVDKERIVLPRI**FIST**DKESIKCP**  
CEPEHISNSTCNFYVCNCVEKRAEI**KENNEVIKEEFKEDYENPDGKHKKKMLL**

### **(B) rPvAMA1**

GPTVERST**RMSNPWKAFMEKYDIERTHSSGV**RVDLGEDAEVENAKYRI**PAGRC**PVF  
**GKGIVIENS**AVS**FLKPVATGDQRLKDGGFAFPNANDHIS**PMTIAN**LKARYKDNVEM**  
**MKLNDIALCRTHAASFVMAGDQNSSYRHPAVYDEKEKTCHMLYLSAQENMGPRYCS**  
**PDAQNRD**AVFCFKPD**KNESFENLVYLSKNVRNDWDK**KCPRKNLGNAKFGLWVDGNC  
EEIPYVKEVEAKDLREC**NRIVFEASASDQPTQYEEEMTDYQKIQQGFRQNNREMIK**  
**SAFLPVGAFN**SDNF**SKGRGFNWANFDSVKKKCYIFNTKPTCLINDKNFIATTALS**  
HPQEVDPFPCSIYKDEIEREIKKQS**RNMNLYSVDGERIVLPRI**FIS**NDKESIKCP**  
**CEPEHISNSTCNFYVCNCVEKRAEIKENNQVVIKEEFRDYYENGEEKSNKQMLL**

## Appendix 7: Protein expression and refolding records for *Plasmodium* AMA1 deposited in REFOLD database.

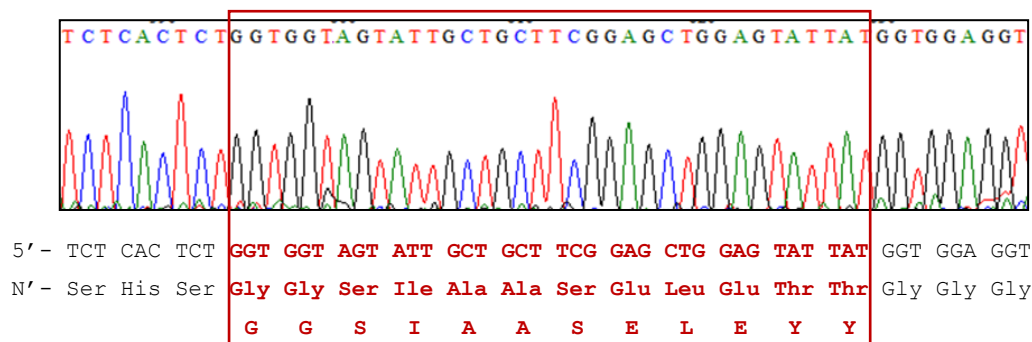
Refolding Records (18) for Protein: Apical membrane antigen 1 (modified from <http://refold.med.monash.edu.au/>).

Class/UniProt Accession No.	Organism	Family/ Domain	Molecularity	MW (Da)	Refolding Method	Redox Agent	Reference
Small Proteins/ P16445	<i>Plasmodium chabaudi</i>	AMA1/ NA	Monomer	73876.1	Column refolding: Nickel-chelating chromatography	None	Burns, et al., 2003
Small Proteins/ Q7KQK5	<i>Plasmodium falciparum</i>	AMA1/ NA	Monomer	54634.3	Dilution	GSH/GSSG	Dutta, et al., 2002
Small Proteins/ P16445	<i>Plasmodium chabaudi</i>	AMA1/ NA	Monomer	53371.1	Dilution	GSH/GSSG	Anders, et al., 1998
Small Proteins/ O00784	<i>Plasmodium falciparum</i>	AMA1/ NA	Monomer	72622.2	Dilution	GSH/GSSG	Hodder, et al., 2001
Small Proteins/ P50492	<i>Plasmodium falciparum</i>	AMA1/ NA	Unknown	51425.7	Dilution	GSH/GSSG	Dutta, et al., 2002
Small Proteins/ P50492	<i>Plasmodium falciparum</i>	AMA1/ NA	Unknown	69135.1	Dilution	NA	Gupta, et al., 2005
Small Proteins/ A3F8A6	<i>Plasmodium falciparum</i>	AMA1/ NA	Unknown	14471.3	Dilution	GSH/GSSG	Feng, et al., 2005
Small Proteins/ A3F8A6	<i>Plasmodium falciparum</i>	AMA1/ DII	Unknown	14471.3	Dilution	GSH/GSSG	Feng, et al., 2005
Small Proteins/ P22621	<i>Plasmodium falciparum</i>	AMA1/ DI	Unknown	26972.3	Dilution	GSH/GSSG	Lalitha, et al., 2004
Small Proteins/ P22621	<i>Plasmodium falciparum</i>	AMA1/ DII	Unknown	12499.1	Dilution	GSH/GSSG	Lalitha, et al., 2004
Small Proteins/ P22621	<i>Plasmodium falciparum</i>	AMA1/ DIII	Unknown	12887.5	Dilution	GSH/GSSG	Lalitha, et al., 2004
Small Proteins/ P22621	<i>Plasmodium falciparum</i>	AMA1/ DI+DII	Unknown	41081.1	Dilution	GSH/GSSG	Lalitha, et al., 2004.
Small Proteins/ P22621	<i>Plasmodium falciparum</i>	AMA1/ DII+DIII	Unknown	26244.5	Dilution	GSH/GSSG	Lalitha, et al., 2004
Small Proteins/ P22621	<i>Plasmodium falciparum</i>	AMA1/ DI+DII	Unknown	41081.1	Dilution	GSH/GSSG	Lalitha, et al., 2004
Small Proteins/ P22621	<i>Plasmodium falciparum</i>	AMA1/ DI+DII	Unknown	41081.1	Dilution	GSH/GSSG	Lalitha, et al., 2004
Small Proteins/ P22621	<i>Plasmodium falciparum</i>	AMA1/ DIII	Unknown	12887.5	Dilution	GSH/GSSG	Lalitha, et al., 2004
Small Proteins/ P22621	<i>Plasmodium falciparum</i>	AMA1/ DI+DIII	Unknown	38696.5	Dilution	GSH/GSSG	Lalitha, et al., 2004
Small Proteins/ Q9GVB7	<i>Plasmodium falciparum</i>	AMA1/ 	Unknown	69896.9	Dilution	DTT/cystamine	Giersing, et al., 2005

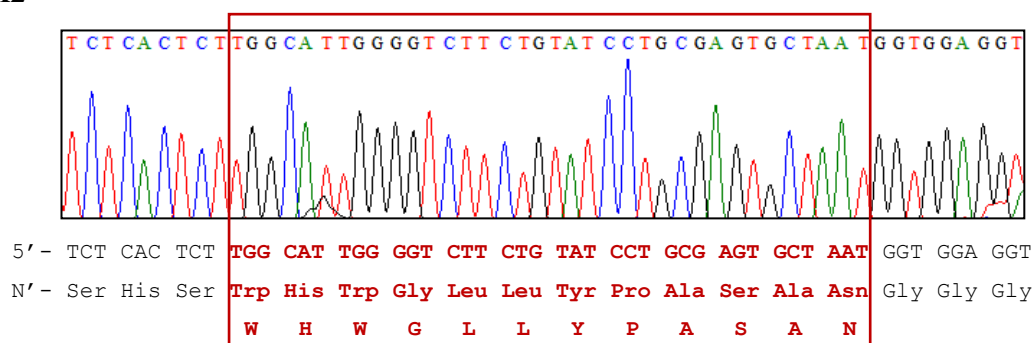
NA indicates not available. DI indicates domain I, DII indicates domain II, and DIII indicates domain III.

## Appendix 8: Identification of binding peptides for PkAMA1.

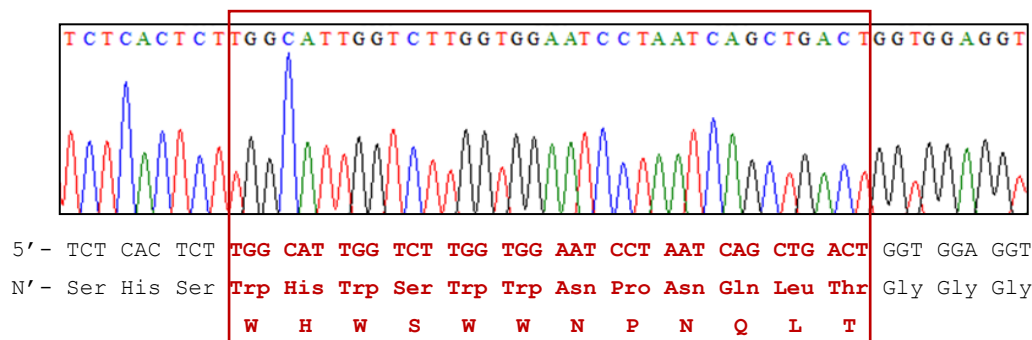
### PdK1



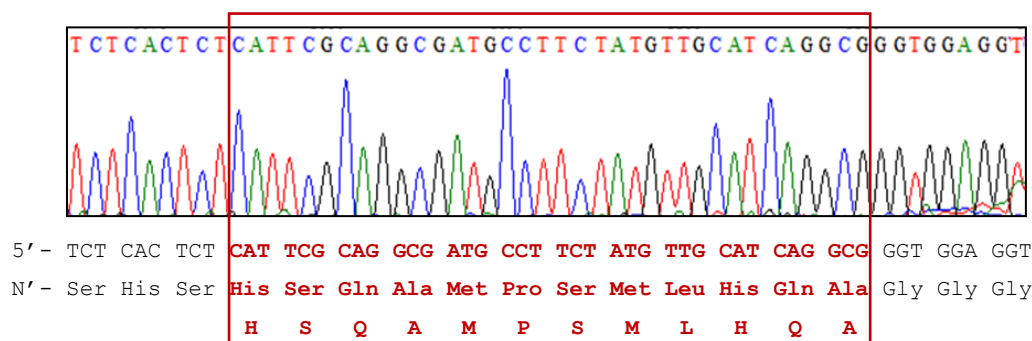
### PdK2



### PdK3



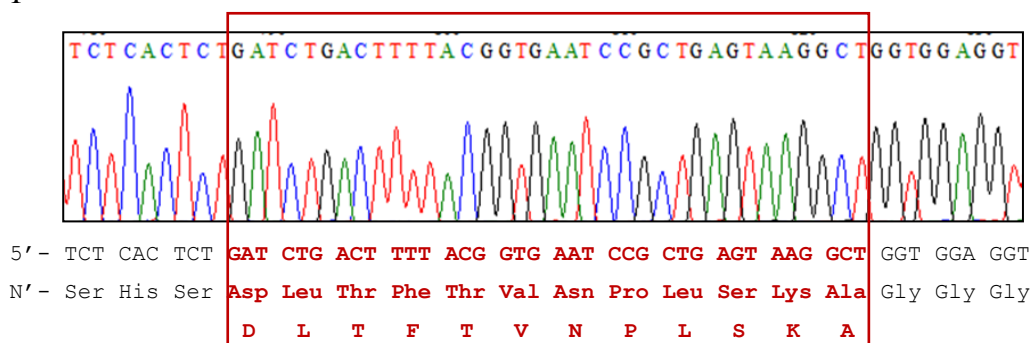
### PdK4



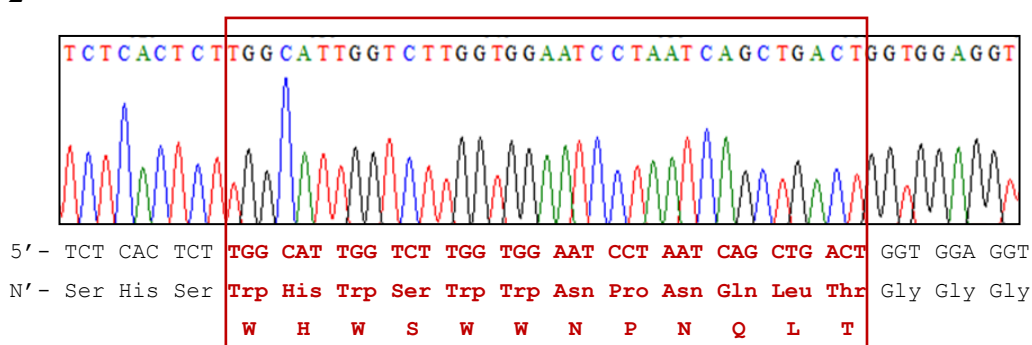


## Appendix 9: Identification of binding peptides for PvAMA1.

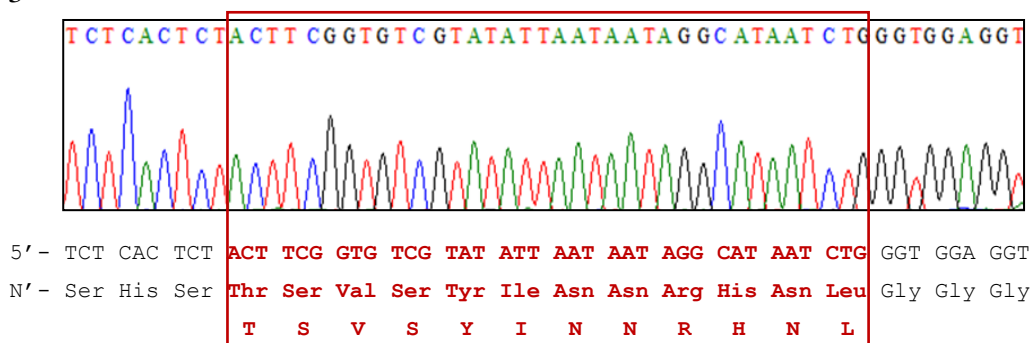
### PdV1




### PdV2



### PdV3



## Appendix 10: Ethics approval letter.

 <b>UNIVERSITI MALAYA</b> KUALA LUMPUR <b>PUSAT PERUBATAN UM</b>		<b>JAWATANKUASA ETIKA PERUBATAN PUSAT PERUBATAN UNIVERSITI MALAYA</b> ALAMAT: LEMBAH PANTAI, 59100 KUALA LUMPUR, MALAYSIA TELEFON: 03-79494422 samb. 3209 FAKSIMILI: 03-79494638	
<b>NAME OF ETHICS COMMITTEE/IRB:</b> Medical Ethics Committee, University Malaya Medical Centre  <b>ADDRESS:</b> LEMBAH PANTAI 59100 KUALA LUMPUR		<b>ETHICS COMMITTEE/IRB REFERENCE NUMBER:</b>  709.2	
<b>PROTOCOL NO:</b>  <b>TITLE:</b> Development Of Malaria Detection System Through Genomic And Proteomic Approaches			
<b>PRINCIPAL INVESTIGATOR:</b> Dr. Chua Kek Heng  <b>TELEPHONE:</b> <b>KOMTEL:</b>		<b>SPONSOR:</b>	

The following item ☒ have been received and reviewed in connection with the above study to be conducted by the above investigator.

<input checked="" type="checkbox"/> Borang Permohonan Penyelidikan	Ver date: 21 Jan 09
<input checked="" type="checkbox"/> Study Protocol	Ver date:
<input type="checkbox"/> Investigator Brochure	Ver date:
<input checked="" type="checkbox"/> Patient Information Sheet	Ver date:
<input checked="" type="checkbox"/> Consent Form	Ver date:
<input type="checkbox"/> Questionnaire	
<input checked="" type="checkbox"/> Investigator(s) CV's (Dr. Chua Kek Heng)	

and have been ☒

☒ Approved  
☐ Conditionally approved (identify item and specify modification below or in accompanying letter)  
☐ Rejected (identify item and specify reasons below or in accompanying letter)

Comments:

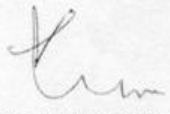
i. *Investigator is required to follow instructions, guidelines and requirements of the Medical Ethics Committee.*  
 ii. *Investigator is required to report any protocol deviations/violations through the Clinical Investigation Centre and provide annual/closure reports to the Medical Ethics Committee.*

Date of approval: 18<sup>th</sup> MAC 2009

s.k Ketua  
 Jabatan Perubatan Molekul

Timbalan Dekan (Penyelidikan)  
 Fakulti Perubatan, Universiti Malaya

Setiausaha  
 Jawatankuasa Penyelidikan Pusat Perubatan  
 Fakulti Perubatan, Universiti Malaya

  
**PROF. LOOI LAI MENG**  
 Chairman  
 Medical Ethics Committee

**Appendix 11: Inform consent form.**

UNIVERSITY MALAYA MEDICAL CENTRE

**CONSENT BY PATIENT FOR CLINICAL RESEARCH**

I, ..... Identity Card No. ....  
(Name of Patient)

of .....  
(Address)

hereby agree to take part in the clinical research (clinical study/questionnaire study/drug trial) specified below:

**Title of Study:** Development of malaria detection system through genomic and proteomic approaches.

the nature and purpose of which has been explained to me by Dr. ....  
(Name & Designation of Doctor)

..... and interpreted by .....  
(Name & Designation of Interpreter)

..... to the best of his/her ability in ..... language/dialect.

I have been told about the nature of the clinical research in terms of methodology, possible adverse effects and complications (as per patient information sheet). After knowing and understanding all the possible advantages and disadvantages of this clinical research, I voluntarily consent of my own free will to participate in the clinical research specified above.

I understand that I can withdraw from this clinical research at any time without assigning any reason whatsoever and in such a situation shall not be denied the benefits of usual treatment by the attending doctors.

Date: ..... Signature or Thumbprint .....  
(Patient)

**IN THE PRESENCE OF**

Name ..... )  
Identity Card No. .... )  
Designation ..... )

Signature .....  
(Witness for Signature of Patient)

I confirm that I have explained to the patient the nature and purpose of the above-mentioned clinical research.

Date ..... Signature .....  
(Attending Doctor)

**CONSENT BY PATIENT  
FOR  
CLINICAL RESEARCH**

R.N.  
Name  
Sex  
Age  
Unit

FPU-DOF-BK-012-05-R01

## RESEARCH OUTCOMES

### Patent:

A multiplex PCR assay for human malaria parasites was patented in November 2010 with reference number: PI 2010 003802 (Malaysia) and June 2011 with reference number: PCT/2011/000158 (International).

### Human malaria detection assay:

This hexaplex PCR assay (PlasmoNex™) is currently commercialized under Reszon Diagnostics International (<http://www.reszonics.com/product-Malaria.html>).

### Publications:

Lim, Y. A. L., Mahmud, R., **Chew, C. H.**, Thilaganathan, T., & Chua, K. H. (2010). *Plasmodium ovale* infection in Malaysia: first imported case. *Malar J*, 9, 272.

**Chew, C. H.**, Lim, Y. A. L., Lee, P. C., Mahmud, R., & Chua, K. H. (2012). Hexaplex PCR detection system for identification of five human *Plasmodium* species with an internal control. *J Clin Microbiol*, 50(12), 4012-4019.

Goh, X. T., Lim, Y. A. L., Vythilingam, I., **Chew, C. H.**, Lee, P. C., Ngui, R., Tan, T. C., Yap, N. J., Nissapatorn, V., & Chua, K. H. (2013). Increased detection of *Plasmodium knowlesi* in Sandakan division, Sabah as revealed by PlasmoNex™. *Malar J*, 12, 264.

### Presentations/ Awards:

**Chew, C. H.**, Lim, Y. A. L., Lee, P. C., Mahmud, R., and Chua, K. H. (2009). Development of multiplex polymerase chain reaction (PCR) for detection of human *Plasmodium* spp infection in malaria disease. In *14th Biological Sciences Graduate Congress* (10 - 12 December 2009), Chulalongkorn University, Bangkok, Thailand. p.195.

---

**Presentations/ Awards (continued):**

- Chua, K. H., Mahmud, R., Lim, Y. A. L., Lee, P. C., and **Chew, C. H.** (2010). PlasmoNex - One step multiplex PCR detection system for malaria parasites. In *Bio Malaysia 2010* (1 - 3 November 2010), Kuala Lumpur Convention Centre, Malaysia. (BioInno Award 2010 - Gold Medal).
- Chua, K. H., Mahmud, R., Lim, Y. A. L., Lee, P. C., and **Chew, C. H.** (2011). PlasmoNex - Advanced detection system for malaria parasites. In *Malaysia Technology Expo 2011* (17 - 19 February 2011), Kuala Lumpur Convention Centre, Malaysia. (Malaysian Association of Research Scientist Award - Silver Medal).
- Chua, K. H., Mahmud, R., Lim, Y. A. L., Lee, P. C., and **Chew, C. H.** (2011). PlasmoNex II - A PCR system for detection of general and human malaria parasites. In *22<sup>nd</sup> International Invention, Innovation and Technology Exhibition (ITEX)* (20 - 22 May 2011), Kuala Lumpur Convention Centre, Malaysia. (ITEX 2011 Award - Silver Medal).
- Chua, K. H., Mahmud, R., Lim, Y. A. L., Lee, P. C., and **Chew, C. H.** (2011). PlasmoNex – A single step multiplex PCR detection system for human malaria parasites. In *Pecipta 2011 Malaysia* (13 - 15 September 2011), Kuala Lumpur Convention Centre, Malaysia. (PECIPTA 2011 Award - Silver Medal).
- Chua, K. H., Mahmud, R., Lim, Y. A. L., Lee, P. C., and **Chew, C. H.** (2011). PlasmoNex™ - Ultimate identification of malaria parasites. In *Bio Malaysia 2011* (21 - 23 November 2011), Kuala Lumpur Convention Centre, Malaysia. (BioInnovation Award 2011 - Gold Medal).
- Chua, K. H., Mahmud, R., Lim, Y. A. L., Lee, P. C., and **Chew, C. H.** (2012). PlasmoNex - A detection system for human malaria parasites. In *National Innovation Conference and Exhibition* (5 - 7 November 2012), Kuala Lumpur Convention Centre, Malaysia.
- Chua, K. H., Mahmud, R., Lim, Y. A. L., Lee, P. C., and **Chew, C. H.** (2012). PlasmoNex™ – A detection kit for human malaria parasites. In *Seoul International Invention Fair 2012* (22 November - 2 December 2012), Seoul, Korea. (SIIF 2012 - Gold Medal).
-